

# MATHEMATICAL MODELLING AND SIMULATION IN PULP MILL OPERATIONS

## A THESIS

*Submitted in partial fulfilment of the  
requirements for the award of the degree*

*of*

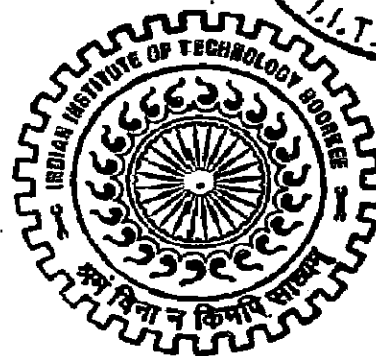
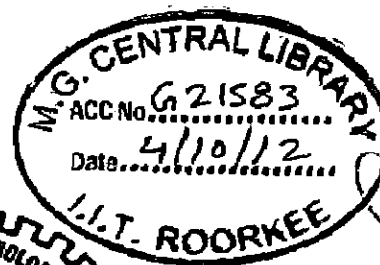
DOCTOR OF PHILOSOPHY

*in*

APPLIED MATHEMATICS

*by*

**DEEPAK KUMAR**



DEPARTMENT OF PAPER TECHNOLOGY  
INDIAN INSTITUTE OF TECHNOLOGY ROORKEE  
ROORKEE-247 667 (INDIA)

APRIL, 2011

**©INDIAN INSTITUTE OF TECHNOLOGY ROORKEE, ROORKEE, 2011  
ALL RIGHTS RESERVED**



# INDIAN INSTITUTE OF TECHNOLOGY ROORKEE ROORKEE


## CANDIDATE'S DECLARATION

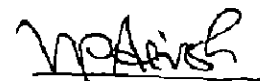
I hereby certify that the work which is being presented in the thesis entitled **MATHEMATICAL MODLLING AND SIMULATION IN PULP MILL OPERATIONS** in partial fulfilment of the requirement and for the award of the Degree of Doctor of Philosophy and submitted in the Department of Paper Technology of the Indian Institute of Technology Roorkee, Roorkee, is an authentic record of my own work carried out during a period from January, 2006 to April, 2011, under the supervision of Dr. V.P. Singh, Professor, and Dr. Vivek Kumar, Assistant Professor, Department of Paper Technology, Indian Institute of Technology Roorkee, Roorkee.

The matter presented in the thesis has not been submitted by me for the award of any other degree of this or any other Institute.

  
(Deepak Kumar)

This is to certify that the above statement made by the candidate is correct to the best of our knowledge.

  
(Vivek Kumar)  
Supervisor

  
(V.P. Singh)  
Supervisor

Date ~~26/11/2011~~ 6/4/11

The Ph.D. Viva-Voce Examination of Mr. **Deepak Kumar**, Research Scholar, has been held on.....

Signature of Supervisors

Signature of External Examiner

## Abstract

---

Pulp and paper industry is an energy intensive industry. Huge amount of raw material, chemical, energy and water are consumed in the process of paper manufacturing. Some energy intensive subsystems of the integrated pulp mill that are the focus of present study are brown stock washing, multi-effect evaporation, and multi-stage bleaching which significantly affect the economy as well as environment. In the present study the dynamic model has been developed by using material & energy balance and various other parametric equations reported in the literature in last five decades. Dynamic model helps us in better understanding of the process and behavior of its variables, thereby helps in determining a better control system.

The work presented on the washing subsystem is based on dynamic simulation of single and multi stage brown stock washing (BSW) system. Mathematical model for pulp washing was described by using basic material balance equation (Transport Equation) and including the relevant mathematical equations for adsorption-desorption isotherms (linear as well as non-linear). To validate the solution technique the transport equation is solved by using 'pdepe' solver in MATLAB source code and compared with the results of analytical given by Brenner (1962) as well as results of Grahs (1974) obtained through numerical methods. The results show the good agreement. After the validation of the solution technique ('pdepe' solver) the solution of single stage washing is obtained by using different adsorption-desorption isotherms to show the suitability of the isotherm coupled with the washing model. Rate of mass accumulation in the solid phase due to adsorption-desorption is taken into consideration for evaluation of the solute concentration in the fiber by the linear isotherms given by [Lapidus and Amundson (1952), Perron and Lebeau (1977) and Sherman (1964)] and non linear Langmuir isotherm. Linear isotherm based model gives satisfactory profile, although the model with isotherm given by Sherman (1964) gives the erratic values of the solute concentration. However, non linear Langmuir isotherm is the best suitable for the satisfactory model performance. Further for the simulation of washing model for multistage washing non linear Langmuir isotherm is used with various boundary conditions. The system of simultaneous differential equations (i.e. transport equation and adsorption isotherm) is solved by using 'pdepe' solver in MATLAB source code with various boundary conditions for the sodium ion specie. Data obtained by Grahs (1974) for the species sodium ( $\text{Na}^+$ ) by using softwood (pine) sulphate pulp is used for simulation. On the basis of the solution, three dimensional (3-D) graphs of the behavior of solute concentration with respect to time as well as cake thickness are

obtained for single stage and for each washer of multistage washing system. For the optimal control of the multistage washing system the parametric effect of various parameters namely (i) Peclet number, (ii) kappa number and (iii) porosity also studied for the individual washer. The breakthrough curves are also plotted for exit solute concentration versus time and cake thickness for each washer of the four stage washing system.

The transport equation is given by

$$D_L \left( \frac{\partial^2 c}{\partial z^2} \right) = u \left( \frac{\partial c}{\partial z} \right) + \left( \frac{\partial c}{\partial t} \right) + \mu \left( \frac{\partial n}{\partial t} \right)$$

The 'pdepe' solver used in the present investigation is simple, elegant and convenient for solving two point boundary value problems with varying range of parameters and show a comparable performance with average numerical errors. The use of MATLAB for the simulation of such type of complex system is a good alternative to the available techniques.

The work presented on the evaporation subsystem is based on the dynamic simulation of multi-effect evaporation system. The dynamic behavior of multi-effect evaporator system of a paper industry is obtained by disturbing the feed flow rate, feed concentration, live steam temperature and feed temperature. For this purpose an unsteady-state model for the multi-effect evaporator system is developed for backward, mixed and split feed sequence respectively. Each effect in the process is represented by a number of variables which are related by the energy and material balance equations for the feed, product and vapor flow. In this study a generalized mathematical model is proposed which could be applied to any number of effects and all kinds of feeding arrangements like forward feed, backward feed, mixed feed and spilt feed in the MEE system with simple modifications. The model developed is based on the work proposed by Aly and Marwan (1997). To study the dynamic response of any chemical process initial values of the process variables are needed. For this purpose steady state solution of the system is obtained first. Data for simulation purpose is taken from literature given by Gupta (2001). The range of operating parameters is also taken from the literature and duly modified values are considered according to Indian Paper mill evaporation conditions. The steady state solution of the dynamic model is obtained by taking the accumulation terms equal to zero and using 'fsolve' solver in MATLAB source code for the solution of simultaneous nonlinear algebraic equations. To predict the system time-dependent parameters under various transient conditions the solution of the system of simultaneous ordinary differential equations is obtained by using 'ode45' solver in MATLAB source code. To study the dynamic response of outgoing liquor

and steam characteristics (Concentration of outgoing liquor and steam temperature) disturbances is applied on various input variables such as feed flow rate, feed concentration, steam temperature and feed temperature.

The parametric influences of various input parameters on output parameters steam consumption (SC), steam economy (SE) and area requirement (A) for backward, mixed and split feed sequences is studied by obtaining the steady state solution by varying the range of input parameters and find that in all cases the mixed feed sequence is optimal.

As no dynamic data are available for further validation, further comparisons could not be made at this time. However, the steady-state validation together with the fact that the observed responses follow the same nature of the dynamic responses of the fundamental distributed parameter model, based on first-principles knowledge about the fluid dynamics and heat transfer processes. The dynamic behavior of each effect's temperature and product concentration was studied by disturbing the liquor flow rate, feed concentration, steam and feed temperatures by  $\pm 10\%$  step input for backward, mixed and split feed sequences. The disturbance in feed temperature does not bring noticeable change in the temperature and product concentration of each effect. Temperature of each effect is changed significantly while no significant change in the product concentration is observed with disturbance in feed temperature and steam temperature. The dynamic behavior of effect's temperature with respect to disturbances in feed concentration shows slight change in temperature, but change in product concentration is significant. The transient study shows that the steady state is reached more quickly for temperature in comparison of the solid concentration and all of the responses converge in a smooth fashion for all the feed sequences.

The work presented on the bleaching subsystem is based on the modelling and simulation of multi-stage bleach plant. Steady state model is described for DED bleach plant based on the work presented by Dogan and Guruz (2004). In the steady state modelling, model equations related to mixer are simple mass balance equations and are easy to solve. Study of the pulp washing operation is already done in the present study. So the main focus is on the modelling of retention tower. The most important parameter in the modelling of retention tower is the bleaching reaction kinetics. In the literature different kinetic models are proposed. Most of the delignification models are based on the kinetic study conducted by Ackert et al. (1975). Ackert (1973) presented chlorination kinetics model comprising by two parallel reactions, identified as fast substitution and slow oxidation. Based on this slow fast combination of the reaction Tessier

and Savoie (1997) presented a kinetic model for 100% chlorine dioxide delignification based on experimental data. Bleaching reaction kinetics for chlorine dioxide substitution were also studied by Chandranupap and Nguyen (2000), Barroca et al. (2001), Barroca and Castro (2003), Gu and Edwards (2003) and Jain et al. (2007, 2009). An attempt has been made to study the kinetic models for chlorine dioxide and extraction stages reported in literature and evaluate their suitability for indigenous raw material. For the purpose laboratory experiment is done for the chlorine dioxide and extraction stages and studied the kappa number reduction with respect to different times as well as temperatures. For suitability of kinetic models given by some earlier researchers, the solutions of the kinetic models are fitted with the experimental results. It is found by comparison that the kinetic models given by Jain et al. (2009) fitted well and can be used for the modelling purpose. However, the experiment should be carried out to get the exact value of the kinetic parameters i.e. activation energy and frequency factor.

## ACKNOWLEDGEMENT

---

I wish to express my deep sense of gratitude towards my Supervisors Prof. V.P. Singh and Dr. Vivek Kumar (Assistant Professor), Department of Paper Technology, for inspiring, guiding and supporting me to enhance my knowledge by pursuing the innovative and challenging area of my thesis "**Mathematical Modelling and Simulation in Pulp Mill Operations**". I feel myself very lucky to get a chance to work under them and will remain indebted towards them for my life. I am very thankful to my SRC members Prof. A.K. Ray, Prof. A.K. Singh and Dr. S.P. Yadav (Associate Professor, Department of Mathematics, IIT Roorkee) for their invaluable suggestions and encouragement throughout my work. It has been a great pleasure and honor to work in the prestigious institute like IIT Roorkee.

I convey my sincere thanks to Prof. J.S. Upadhyaya, former Head, Department of Paper Technology, Prof. Satish Kumar, present H.O.D, for their encouragement and belief that they showered on me, and for providing the necessary facilities to carry out this work. I would like to express my sincere thanks to Dr. Millie Pant and Dr. Rajan Arora for their support to me time to time. I am also indebted to all the faculty members of DPT for their support and help to carry out this work.

I wish to express my sincere thanks to my friends (Research Scholars DPT) Mr. Sudheer Kumar Shukla for his valuable suggestions and Mr. Yashwat Reddy Dodla and Mr. Praveen Kumar for helping me in experimental work. I would like to extend to my thanks to my colleagues and friends Dr. Ramakrishna Malkapuram, Mr. Shiv Kumar, Mr. Mussarat Ali, Mr. Amit Tomar, Mr. Pravesh Tomar, Mr. Junaid Siddiqui, Mr. Sushil Kumar and Mr. Samit Kumar for their support and encouragement.

I am highly obliged and wish to express my thanks to academic, accounts and library staff of the Department of Paper Technology for their support during my research work.

I am extremely thankful to Mrs. Vimlesh Singh and Mrs. Shikha Kumar for their continuous encouragement and support throughout the work.

Now, I wish to pay my utmost gratitude to my mother Smt. Bala Devi, Father Shri Tejram Singh for their invaluable blessings and delightful love.



I also, want to express my sincere thanks to my brothers Mr. Neeraj Kumar, Mr. Rajkumar, Mr. Mukesh Kumar, sisters in law Mrs. Neeraj Kumari and Mrs. Neeraj Bala and sister Kiran and brother in law Mr. Mukul Kumar, and my Nephews, Niece, for their patience and unceasing support throughout my research work.

Last, but not least my beloved wife Mrs. Charul Kumar for her sacrifice, love, motivation, inspiration, patience and constant support and a lot of love to my pretty son Pranav Kumar.

I also want to express my sincere thanks to all those who directly and indirectly helped me at various stage of the work but I would not mention their name due to shortage of the space.

The financial support provided by Ministry of Human Resource Development, Govt. of India is greatly acknowledged.

Finally I am always thankful to the omnipresent, GOD, without whose elegance even this world does not exist.

IIT Roorkee

Date 06/11/2011



DEEPAK KUMAR

## LIST OF PUBLICATIONS

---

### PUBLISHED IN REFERED JOURNALS

1. **Kumar, Deepak., Kumar, Vivek. and Singh, V.P.,** "Mathematical Modeling of Brown Stock Washing Problems and their Numerical Solution using MATLAB". *Computers and Chemical Engineering*, (Elsevier Publication), ISSN: 0098-1354, 34, 9-16, (2010).
2. **Kumar, Deepak., Kumar, Vivek. and Singh, V.P.,** "To study the parametric effect on optimality of various feeding sequences of a multi-effect evaporators in Paper industry using Mathematical modeling and simulation with MATLAB". *International Journal of Chemical and Biological Engineering*, ISSN: 1307-6892, 3(3), 129-136, (2010).
3. **Kumar, Deepak., Kumar, Vivek. and Singh, V.P.,** "Mathematical modeling of pulp washing on rotary drums and their numerical solution for various adsorption isotherms". *World Journal of Modeling and Simulation*, ISSN: 1746-7233, 6(3), 214-222, (2010).
4. **Kumar, Deepak., Kumar, Vivek. and Singh, V.P.,** "To Study the parametric effects on the performance of brown stock washer in Paper Industry using MATLAB". *World Journal of Modeling and Simulation*. ISSN: 1746-7233, 5(1), 30-37, (2009).
5. Singh, V.P., Kumar, Vivek. and **Kumar, Deepak.,** "Mathematical Model for Waste Minimization of a bleach Plant in paper industry" *Wiley InterScience Journals, PAMM*, ISSN: 1617-7061, 7(1), 2150045-2150046, (2007).

### PUBLISHED IN REFERED CONFERENCE PROCEEDINGS

6. **Kumar, Deepak., Kumar, Vivek. and Singh, V.P.,** "Analysis of parametric effect on efficiency of the brown stock washer in Paper Industry using MATLAB", *American Institute of Physics Conference Proceeding*, 1146, 390-399, (2009).
7. Singh, V.P, Kumar, Vivek. and **Kumar, Deepak.,** "Numerical Solution of diffusion model of Brown Stock washing beds of finite length Using MATLAB" *Proceeding of "Second UKSIM European Symposium on Computer Modeling and Simulation"*, *IEEE Digital Library*, 295-300, (2008).
8. **Kumar, Deepak., Kumar, Vivek. and Singh, V.P.,** "Numerical solution of brown stock washer problems in Paper Industry", *11<sup>th</sup> Punjab Science Congress, Thapar University Patiala, Feb 7-9, Abstract No. BC-64, 37, (2008).*

## LIST OF CONTENTS

Subject	Page No.
Candidate declaration	
Abstract	i
Acknowledgement	v
List of Publications	vii
List of Contents	viii
List of Figures	xii
List of tables	xvi
Nomenclature	xviii
<b>Chapter 1 Introduction</b>	1
<b>Chapter 2 Modelling and Simulation of Pulp Washing System</b>	9
2.1. Introduction	9
2.2. Modelling and Simulation of Pulp Washing: A Review	11
2.2.1. Mathematical Model of Pulp Washing	22
2.3. Description of Mathematical Model of Pulp Washing	22
2.3.1. Model attributed to axial dispersion	22
2.3.2. Model attributed to axial dispersion as well as particle diffusion	24
2.3.3. Adsorption-desorption isotherm for various species of black liquor	25
2.3.4. Initial and boundary conditions	27
2.3.5. Conversion into dimensionless form	27
2.4. Solution Technique	30
2.5. Validation of the Solution Technique	31
2.6. Solution of the Washing Models for Single Stage	33
2.7. Multistage Pulp Washing	37
2.8. Solution of Pulp Washing Models for Multistage	38
2.9. Analysis of Parametric Effects on Efficiency of Multistage Brown Stock Washers	44
2.9.1. Effects of pecllet number on exit solute concentration	45
2.9.2. Effects of kappa number on exit solute concentration	50
2.9.3. Effects of porosity on exit solute concentration	55
2.10. Conclusion	60

<b>Chapter 3 Modelling and Simulation of Multi-effect Evaporation System</b>	<b>62</b>
3.1. Introduction	62
3.2. Modelling and Simulation of Multi-effect Evaporation: A Review	66
3.3. Physico-thermal/Chemical Properties of Black Liquor and Water	74
3.3.1. Density of black liquor ( $\rho$ )	74
3.3.2. Specific heat of black liquor ( $C_p$ )	76
3.3.3. Specific heat of water ( $C_{pw}$ )	76
3.3.4. Boiling point rise (BPR)	76
3.3.5. Latent heat of vaporization of water ( $\lambda$ )	77
3.3.6. Enthalpy of saturated water	78
3.3.7. Enthalpy of saturated steam/ vapor	78
3.4. Modelling and Simulation of MEE System	80
3.4.1. System description	80
3.5. Development of Mathematical Model	81
3.5.1. Mathematical modelling for sextuple effect evaporators using backward feed sequence	82
3.5.2. Mathematical modelling for sextuple effect evaporators using mixed feed sequence	85
3.5.3. Mathematical modelling for sextuple effect evaporators using split feed sequence	87
3.6. Simulation Studies	89
3.6.1. Solution technique	90
3.6.2. Steady state simulation	90
3.6.3. Model validation	91
3.7. Model Application	93
3.8. Parametric Effect on the Performance of Various Feeding Sequences	94
3.8.1. Effect of feed temperature on steam economy	94
3.8.2. Effect of steam temperature on steam economy	95
3.8.3. Effect of feed flow rate on steam economy	95
3.8.4. Effect of feed concentration on steam economy	95
3.8.5. Effect of product concentration on steam economy	97
3.8.6. Effect of last body temperature on steam economy	97
3.9. Dynamic simulation	98
3.10. Dynamic Response of MEE System for Various Feed Sequences	98

3.10.1. Time constant ( $\tau$ )	99
3.10.2. Dynamic response of sextuple effect evaporator for the backward feed	99
3.10.2.1. Effect of varying feed flow rate	100
3.10.2.2. Effect of varying feed concentration	102
3.10.2.3. Effect of varying steam temperature	105
3.10.2.4. Effect of varying feed temperature	108
3.10.3. Dynamic response of sextuple effect evaporator for the mixed feed	111
3.10.3.1. Effect of varying feed flow rate	111
3.10.3.2. Effect of varying feed concentration	114
3.10.3.3. Effect of varying steam temperature	116
3.10.3.4. Effect of varying feed temperature	119
3.10.4. Dynamic response of sextuple effect evaporator for the split feed	122
3.10.4.1. Effect of varying feed flow rate	122
3.10.4.2. Effect of varying feed concentration	125
3.10.4.3. Effect of varying steam temperature	127
3.10.4.4. Effect of varying feed temperature	130
3.11. Conclusion	133
<b>Chapter 4 Modelling and Simulation of Pulp Bleaching System</b>	<b>136</b>
4.1. Introduction	136
4.1.1. Bleaching sequences	137
4.2. Modelling and Simulation of Bleaching Plant: A Review	138
4.2.1. Bleaching reaction kinetics: A review	140
4.3. Mathematical Modelling of the Bleach Plant	148
4.4. Experimental Study	150
4.4.1. Materials	150
4.4.2. Experimental procedure	151
4.4.2.1. Chlorine dioxide bleaching stage ( $D_0$ )	151
4.4.2.2. Alkaline extraction (E)	151
4.4.3. Standard test procedure	152
4.4.3.1. Analysis of $\text{NaClO}_2$ bleach liquor	152
(a) Disintegration of pulp	152
(b) Preparation of sheets for kappa number determination	153

4.5. Experimental Results	153
4.6. Solution of Kinetic Models	155
4.7. Results and Discussion	156
4.7.1. Chlorine dioxide stage	156
4.7.2. Extraction stage	161
4.8. Conclusion	164
<b>5. Conclusions and Recommendations</b>	<b>165</b>
5.1. Pulp Washing	165
5.2. Multi-effect Evaporation	167
5.3. Pulp Bleaching	170
5.4. Recommendations for Future Work	171
5.4.1. Pulp washing	171
5.4.2. Multi-effect evaporation	171
5.4.3. Pulp bleaching	172
<b>Bibliography</b>	<b>173</b>

## LIST OF FIGURES

Figure No.	Title of the Figure	Page No.
2.1	A simple shell balance	22
2.2	C vs. Z & T profile for model 1	32
2.3	Comparison of the solutions of model 1 for $Pe = 100$	32
2.4	C vs. Z & T profile for model-2	35
2.5	C vs. Z & T profile for model-3	35
2.6	C vs. Z & T profile for model-4	35
2.7	C vs. Z & T profile for model-5	35
2.8	C vs. Z & T profile for model-6	36
2.9	C vs. Z & T profile for model-7	36
2.10	C vs. Z & T profile for model-8	36
2.11	C vs. Z & T profile for model-9	36
2.12	Flow diagram of a counter current washing system with four drums washers	38
2.13	Solution of different stages (washers) for model-8 (a) C vs. Z & T profile for washer No. 1 (b) C vs. Z & T profile for washer No. 2 (c) C vs. Z & T profile for washer No. 3 (d) C vs. Z & T profile for washer No. 4	42
2.14	Solution of different stages (washers) for model-9 (a) C vs. Z & T profile for washer No. 1 (b) C vs. Z & T profile for washer No. 2 (c) C vs. Z & T profile for washer No. 3 (d) C vs. Z & T profile for washer No. 4	43
2.15	C vs. T profile for various values of $Pe$ at bed exit of washer-1 for model-8	46
2.16	C vs. T profile for various values of $Pe$ at bed exit of washer-1 for model-9	46
2.17	C vs. T profile for various values of $Pe$ at bed exit of washer-2 for model-8	47
2.18	C vs. T profile for various values of $Pe$ at bed exit of washer-2 for model-9	47

2.19	C vs. T profile for various values of $P_e$ at bed exit of washer-3 for model-8	48
2.20	C vs. T profile for various values of $P_e$ at bed exit of washer-3 for model-9	48
2.21	C vs. T profile for various values of $P_c$ at bed exit of washer-4 for model-8	49
2.22	C vs. T profile for various values of $P_e$ at bed exit of washer-4 for model-9	49
2.23	C vs. T profile for various values of K. No. at bed exit of washer-1 for model-8	51
2.24	C vs. T profile for various values of K. No. at bed exit of washer-1 for model-9	51
2.25	C vs. T profile for various values of K. No. at bed exit of washer-2 for model-8	52
2.26	C vs. T profile for various values of K. No. at bed exit of washer-2 for model-9	52
2.27	C vs. T profile for various values of K. No. at bed exit of washer-3 for model-8	53
2.28	C vs. T profile for various values of K. No. at bed exit of washer-3 for model-9	53
2.29	C vs. T profile for various values of K. No. at bed exit of washer-4 for model-8	54
2.30	C vs. T profile for various values of K. No. at bed exit of washer-4 for model-9	54
2.31	C vs. T profile for various values of porosity at bed exit of washer-1 for model-8	56
2.32	C vs. T profile for various values of porosity at bed exit of washer-1 for model-9	56
2.33	C vs. T profile for various values of porosity at bed exit of washer-2 for model-8	57
2.34	C vs. T profile for various values of porosity at bed exit of washer-2 for model-9	57
2.35	C vs. T profile for various values of porosity at bed exit of washer-3	58



	for model-8	
2.36	C vs. T profile for various values of porosity at bed exit of washer-3 for model-9	58
2.37	C vs. T profile for various values of porosity at bed exit of washer-4 for model-8	59
2.38	C vs. T profile for various values of porosity at bed exit of washer-4 for model-9	59
3.1	Block diagram of a pulp mill	63
3.2	Schematic diagram of multiple effect evaporator	80
3.3	Block diagram with variables used for the $i^{\text{th}}$ effect	81
3.4	Flow diagram of Sextuple backward feed evaporator ( $\rightarrow 6 \rightarrow 5 \rightarrow 4 \rightarrow 3 \rightarrow 2 \rightarrow 1$ )	82
3.5	Flow diagram of Sextuple mixed feed evaporator ( $\rightarrow 5 \rightarrow 6 \rightarrow 4 \rightarrow 3 \rightarrow 2 \rightarrow 1$ )	86
3.6	Flow diagram of Sextuple Split feed evaporator $\rightarrow 5 \searrow$ $4 \rightarrow 3 \rightarrow 2 \rightarrow 1$ $\rightarrow 6 \nearrow$	88
3.7	Effect of feed temperature on steam economy	94
3.8	Effect of steam temperature on steam economy	95
3.9	Effect of feed flow rate on steam economy	96
3.10	Effect of feed concentration on steam economy	96
3.11	Effect of product concentration on steam economy	97
3.12	Effect of last body temperature on steam economy	98
3.13	Response of $6^{\text{th}}$ effect by disturbing $\pm 10\%$ in the feed flow rate	101
3.14	Response of $1^{\text{st}}$ effect by disturbing $\pm 10\%$ in the feed flow rate	102
3.15	Response of $6^{\text{th}}$ effect by disturbing $\pm 10\%$ in the feed concentration	104
3.16	Response of $1^{\text{st}}$ effect by disturbing $\pm 10\%$ in the feed concentration	105
3.17	Response of $6^{\text{th}}$ effect by disturbing $\pm 10\%$ in the steam temperature	106
3.18	Response of $1^{\text{st}}$ effect by disturbing $\pm 10\%$ in the steam temperature	107
3.19	Response of $6^{\text{th}}$ effect by disturbing $\pm 10\%$ in the feed temperature	109
3.20	Response of $1^{\text{st}}$ effect by disturbing $\pm 10\%$ in the feed temperature	110
3.21	Response of $6^{\text{th}}$ effect by disturbing $\pm 10\%$ in the feed flow rate	112

3.22	Response of 1 <sup>st</sup> effect by disturbing $\pm 10\%$ in the feed flow rate	113
3.23	Response of 6 <sup>th</sup> effect by disturbing $\pm 10\%$ in the feed concentration	115
3.24	Response of 1 <sup>st</sup> effect by disturbing $\pm 10\%$ in the feed concentration	116
3.25	Response of 6 <sup>th</sup> effect by disturbing $\pm 10\%$ in the steam temperature	117
3.26	Response of 1 <sup>st</sup> effect by disturbing $\pm 10\%$ in the steam temperature	118
3.27	Response of 6 <sup>th</sup> effect by disturbing $\pm 10\%$ in the feed temperature	120
3.28	Response of 1 <sup>st</sup> effect by disturbing $\pm 10\%$ in the feed temperature	121
3.29	Response of 6 <sup>th</sup> effect by disturbing $\pm 10\%$ in the feed flow rate	123
3.30	Response of 1 <sup>st</sup> effect by disturbing $\pm 10\%$ in the feed flow rate	124
3.31	Response of 6 <sup>th</sup> effect by disturbing $\pm 10\%$ in the feed concentration	126
3.32	Response of 1 <sup>st</sup> effect by disturbing $\pm 10\%$ in the feed concentration	127
3.33	Response of 6 <sup>th</sup> effect by disturbing $\pm 10\%$ in the steam temperature	128
3.34	Response of 1 <sup>st</sup> effect by disturbing $\pm 10\%$ in the steam temperature	129
3.35	Response of 6 <sup>th</sup> effect by disturbing $\pm 10\%$ in the feed temperature	131
3.36	Response of 1 <sup>st</sup> effect by disturbing $\pm 10\%$ in the feed temperature	132
4.1	Process units and variables of the bleach plant	140
4.2	Process flow diagram of a DED bleach plant	149
4.3	Experimental data ( $D_0$ ) and models prediction at 50 °C for mix hardwood	157
4.4	Experimental data ( $D_0$ ) and models prediction at 60 °C for mix hardwood	157
4.5	Experimental data ( $D_0$ ) and models prediction at 70 °C for mix hardwood	158
4.6	Experimental data ( $D_0$ ) and models prediction at 80 °C for mix hardwood	158
4.7	Experimental data ( $D_0$ ) and models prediction at 50 °C for bagasse	159
4.8	Experimental data ( $D_0$ ) and models prediction at 60 °C for bagasse	160
4.9	Experimental data ( $D_0$ ) and models prediction at 70 °C for bagasse	160
4.10	Experimental data ( $D_0$ ) and models prediction at 80 °C for bagasse	161
4.11	Experimental data ( $E_0$ ) and models prediction at 50 °C for bagasse	162
4.12	Experimental data ( $E_0$ ) and models prediction at 60 °C for bagasse	162
4.13	Experimental data ( $E_0$ ) and models prediction at 70 °C for bagasse	163
4.14	Experimental data ( $E_0$ ) and models prediction at 80 °C for bagasse	163

## LIST OF TABLES

Table No.	Title of the Table	Page No.
2.1	Mathematical models for pulp washing used by previous investigators	14
2.2	Dimensionless parameters	28
2.3	Existing mathematical models for washing zone used in present investigation	29
2.4	Comparison of solutions at same $Pe = 100$ for different solution techniques	33
2.5	Data for Simulation for sodium species	34
2.6	Solutions of the models 2 to 9 for single stage washing	34
2.7	Process data of four stage brown stock washing system	39
2.8	Solutions of the models 8 & 9 for four washers (stages)	40
2.9	Peclet Number ( $Pe$ ), $N_0$ and $\mu'$ for all four washers	41
2.10	Peclet Number for all four washers	50
3.1	Weak kraft black liquor constituents	64
3.2	Physico-thermal properties of black liquor, saturated steam and condensate	79
3.3	Range of operational parameters	89
3.4	Steady state solution of sextuple effect evaporator for backward feed	91
3.5	Steady state solution of sextuple effect evaporator for mixed feed	92
3.6	Steady state solution of sextuple effect evaporator for split feed	93
3.7	Time constant for dynamic response due to 10% step input change in various input variables for backward feed sequence	99
3.8	Time constant for dynamic response due to 10% step input change in various input variables for mixed feed sequence	111
3.9	Time constant for dynamic response due to 10% step input change in various input variables for split feed sequence	122
4.1	Commonly applied chemical treatments and their shorthand designations	138

4.2	Activation energies and frequency factors for 100% chlorine dioxide and extraction stages	147
4.3	Mathematical models of a bleach plant	150
4.4	Bleaching conditions for D <sub>0</sub> and E stages of D <sub>0</sub> E D <sub>1</sub> bleaching sequence	152
4.5	Standard test methods followed for analysis	153
4.6	Kappa number at different temperatures and times for D <sub>0</sub> stage for mix hardwood	154
4.7	Kappa number at different temperatures and times for D <sub>0</sub> stage for bagasse pulp	154
4.8	Kappa number at different temperatures and times for E <sub>0</sub> stage for Bagasse pulp	155

## NOMENCLATURE

A	: Shell area of the evaporator body, (m <sup>2</sup> )
A'	: Surface area of pulp bed, (m <sup>2</sup> )
A, B	: Langmuir constants, (m <sup>3</sup> /kg)
A <sub>c</sub>	: Area of cross section of washing zone, (m <sup>2</sup> )
BPR	: Boiling point rise, (°C)
BSW	: Brown stock washer
[ClO <sub>2</sub> ]	: Concentration in chlorine dioxide, (mol/L)
c	: Concentration of the solute in the liquor, (kg/m <sup>3</sup> )
C	: Dimensionless concentration of solute in the liquor
C <sub>0</sub>	: Concentration of solute inside the vat, (kg/m <sup>3</sup> )
C1 to C9	: Constants
C <sub>F</sub>	: Fiber consistency, (kg/m <sup>3</sup> )
C <sub>i</sub>	: Condensate from i <sup>th</sup> effect evaporator
COD	: Chemical oxygen demand
C <sub>p</sub>	: Specific heat of black liquor at constant pressure, (kJ/kg °C)
C <sub>pW</sub>	: Specific heat of water at constant pressure, (kJ/kg °C)
C <sub>s</sub>	: Concentration of solute in the wash liquor, (kg/m <sup>3</sup> )
CSTR	: Continuous stirred tank reactor
C <sub>y</sub>	: Fiber consistency, (% on slurry)
C <sub>yd</sub>	: Discharged consistency of the pulp, (kg of fiber/kg of liquor)
C <sub>yi</sub>	: Inlet vat consistency of the pulp, (kg of fiber/kg of liquor)
D <sub>L</sub>	: Longitudinal dispersion coefficient, (m <sup>2</sup> /s)
D <sub>v</sub>	: Molecular diffusion coefficient, (m <sup>2</sup> /s)
E <sub>af</sub>	: Activation energy for the fast delignification reaction, (kJ/mol)
E <sub>as</sub>	: Activation energy for the slow delignification reaction, (kJ/mol)
E <sub>N</sub>	: Norden efficiency factor
F	: Initial Feed flow rate, (kg/s) (In Chapter 3)
F	: Flow rate of liquor in pulp stream, (kg/min) (In Chapter 4)
h <sub>c</sub>	: Enthalpy of the condensate, (kJ/kg)
h <sub>l</sub>	: Enthalpy of the liquor, (kJ/kg)
h <sub>v</sub>	: Enthalpy of the vapor, (kJ/kg)
K	: Dimensionless mass transfer coefficient (In Chapter 2)

K	: Content of chromophores, expressed as Kappa number in delignification stages (C and E) , ml 0.1 N KMnO <sub>4</sub> /g fibre or light absorption coefficient in brightening stage (H <sub>1</sub> , H <sub>2</sub> ) (m <sup>2</sup> / kg) . (In Chapter 4)
K <sub>0</sub>	: Initial kappa number
k <sub>1</sub> , k <sub>2</sub> , k	: Mass transfer coefficients, (1/s)
K <sub>Eto</sub>	: The content of the initial fast reactive lignin in extraction stage
K <sub>Eso</sub>	: The content of the initial slow reactive lignin in extraction stage
K <sub>f</sub>	: Kappa number associated to fast lignin, (ml 0.1 N KMnO <sub>4</sub> /g fibre)
k <sub>f</sub>	: Rate constant of the fast delignification reaction, (L/mol.s)
K <sub>F</sub>	: Kappa factor, (% of active chlorine on O.D pulp/Unbleach kappa number)
k <sub>fo</sub>	: Frequency factor of the fast delignification reaction, (L/mol.s)
K <sub>f0</sub>	: Floor kappa number
K <sub>s</sub>	: Kappa number associated to slow lignin, (ml 0.1 N KMnO <sub>4</sub> /g fibre)
k <sub>s</sub>	: Rate constant of the slow delignification reaction, (L/mol.s)
k <sub>so</sub>	: Frequency factor of the slow delignification reaction, (L/mol.s)
L	: Cake thickness, (m) In chapter 2)
L	: Liquor level, (m) (In Chapter 3)
L	: Dissolved solids or bleaching chemical content of the pulp stream, (%) (In Chapter 4)
L <sub>d</sub>	: Amount of liquor in discharge pulp, (kg of liquor/kg of pulp)
L <sub>f</sub>	: Amount of filtrate, (kg of liquor/kg of pulp)
L <sub>i</sub>	: Amount of liquor inside the vat, (kg of liquor/kg of pulp)
L <sub>r</sub>	: Amount of liquor recycled to previous washer, (kg of liquor/kg of pulp)
L <sub>s</sub>	: Amount of wash water, (kg of water/kg of pulp)
M	: Mass, (kg) (In Chapter 3)
M	: Dissolved solids or bleaching chemical content of the non-pulp stream, (%) (In Chapter 4)
MEE	: Multi effect evaporator
N	: Dimensionless concentration of solute in the fiber
n, q, w	: Concentration of solute on fibers, (kg/m <sup>3</sup> )
N <sub>0</sub>	: Amount of solute accumulated on the fiber surface at the inlet, (kg/m <sup>3</sup> )
Pe	: Peclet number
PFR	: Plug flow reactor
Q	: Heat transfer rate, (kJ)

R	: Ideal gas constant, (8.314 kJ/mol. <sup>0</sup> K)
r <sub>f</sub>	: Reaction rate of the fast delignification reaction, (Kappa number/s)
r <sub>s</sub>	: Reaction rate of the slow delignification reaction, (Kappa number/s)
RW	: Wash liquor ratio
t	: Time, (sec) (In Chapter 3)
t	: Mean residence time in PFR, (min) (In Chapter 4)
T	: Dimensionless time (In Chapter 1)
T	: Temperature, (°C) (In Chapter 3)
T	: Temperature, ( <sup>0</sup> K) (In Chapter 4)
TC	: Time constant, (sec)
u	: Liquor speed in cake pores, (m/s)
U	: Overall heat transfer coefficient (OHTC), (kJ/sec.m <sup>2</sup> .°C)
V <sub>w</sub>	: Filtrate flow rate through cake washing zone, (kg/s)
W	: Flow rate of liquor in non-pulp stream, (kg/min)
W <sub>l</sub>	: Mass flow rate of the liquor, (kg/s)
W <sub>v</sub>	: Mass flow rate of the vapor, (kg/s)
X or TS	: Solid content, (%)
x <sub>d</sub>	: Dissolved solids in discharged pulp, (%)
x <sub>f</sub>	: Dissolved solids in the filtrate, (%)
x <sub>i</sub>	: Dissolved solids inside the vat, (%)
x <sub>r</sub>	: Dissolved solids in recycle liquor, (%)
x <sub>s</sub>	: Dissolved solids in washing water, (%)
Z	: Dimensionless cake thickness
z	: Variable cake thickness, (m)
Δz	: Small increment in cake thickness, (m)

#### Subscripts

c	: Chlorination stage
d	: Drum filter stream
DS	: Dissolved solids
E	: Extraction stage
f	: Fast
H	: Hypo chlorination stage
i	: Into process unit
j	: Bleaching liquor components Cl <sub>2</sub> , H, OH <sup>-</sup> and DS

- o : Off process unit
- r : Recycle stream
- s : Slow
- v : Dilution vat stream

**Greek Symbols**

- $\mu, \mu'$  : Constant in terms of porosity
- $\epsilon_d$  : Interfiber porosity of the cake, dimensionless
- $\epsilon_s$  : Intrafiber porosity of the cake, dimensionless
- $\epsilon_t$  : Total porosity of the cake, dimensionless
- $\lambda$  : Latent heat of vaporization, (kJ/kg)
- $\rho$  : Black liquor density, (kg/m<sup>3</sup>)
- $\tau$  : Time constant, (sec)



## Chapter-1

### Introduction

---

Manufacturing of quality product at competitive prices, environmental degradation, acute shortages of raw material and energy, increasing prices of all basic inputs and environmental considerations have forced the engineers to adopt design of process, plant and equipment in a most quantized or deterministic way. For the purpose Mathematical modelling and simulation is becoming a very popular tool. Mathematical models are developed through interaction of Mathematics, Engineering, and Physical Science.

Mathematical modelling and simulation are used in several areas of systems engineering. In Chemical processes Mathematical models of complex operations are developed using various process phenomena like flow mixing, reactions, heat and mass transfer, etc. to gain a thorough understanding of what is really going on inside the process. Analysis of such models is used further to optimize process inputs, research and development and new product/process development. In product design, models are used in defining effects of variables on product quality and amount. In process design, modelling, simulation and optimization methods [Mohan and Deep (2009)] are nowadays used in studying alternatives for process equipment and connections to optimize process operation and to find best ways to utilize raw materials and energy. Equipment sizing also utilize modelling and simulation. In control engineering, modelling and simulation are utilized in determining control strategies for the process. Simulation is also an interesting tool for process operation. It is employed in disturbance and alarm analysis, in start-up and shut-down planning, in real time control, optimization, and in operator training. The word simulation is then not restricted to the solution of the model equations but it is thought to encompass the whole process of model construction, model validation and model use. In pulp and paper industry simulation is used on four typical levels forest sector (regional, national and international), corporate, mill and process. In the present study the main attention is directed to process level.

Pulp and paper industry is an energy intensive industry. Huge amount of raw material, chemical, energy and water are consumed in the process of paper manufacturing with the requirement of large labor force. Some energy intensive subsystems that are the focus of present study are brown stock washing, multi-effect evaporation and bleaching, which significantly affect the economy as

well as environment. Mathematical approach to quantify the optimal parameters will be of immense potential to alleviate many problems faced by the paper industry. Systematic Mathematical modelling of each subsystem is therefore an imperative necessity to solve the above issues one after another. Mathematical models of these sections have been proposed in the literature for last five decades and details with reference are discussed in the chapters of the respective sections.

The basic mechanism of pulp washing consists of dilution, agitation, extraction and displacement. Generally, the pulp slurry is diluted and mixed thoroughly with weak wash liquor or clean water in the vat and the fibers are extracted from the slurry due to vacuum inside the drum. In displacement washing the wash liquor or water passes through the pulp bed in a piston like manner, pushing out the liquor which is associated with the pulp. Ideally, it is possible to displace one volume of the liquor in the pulp with the same amount of clean water. Practically it is impossible due to the porous structure of the pulp fibers.

As a first step towards improved pulp washing, the mill must be able to quantify the performance of their existing washers. This can lead to improvements in the existing system and define benchmark for evaluating new equipment, systems and technology. The rotary drum vacuum washer is the most common pulp washing device in use today. Rotary vacuum multistage washer containing 3-4 stages is a widely preferred piece of equipment around the globe because of its simplicity in design and flexibility in operation.

If one goes through the study of the models developed by some earlier researchers, it is observed that majority of the investigators have followed the axial dispersion model in one or the other form. Further the investigators had followed either the linear or finite rate adsorption isotherm to correlate the concentration of the solute in the liquor and concentration of the solute on the fibers. Most of the researchers have developed mathematical model and solved for single stage washing to reduce the Mathematical complexities. In the present study an up-to date review of mathematical models relating to pulp washing or similar systems with or without adsorption is made. Kuo (1960) was the first to introduce the concept of film resistance in the washing of pulp fibers. After that Pretneiks (1972) have followed the micro and macroscopic study of the washing process by combining the models for particle phase and the bulk fluid phase. There are various other investigators who have contributed a large to the study of the washing of pulp fibers. Brenner

(1962), Potucek (2001, 2005) has followed the linear one dimensional axial dispersion model to study the washing behavior of pulp fibers and granular particles. Al Jabari et al. (1994), Kukreja et al. (1995, 1998), Kumar (2002) have considered the linear along with the dispersion diffusion based transport equations. However, Fogelberg and Fugleberg (1963), Hartler and Rydin (1975), Ohlsson and Rydin (1975), Grahs (1976), Gullichsen and Ostman (1976), Eriksson and Gren (1996), Arora et al. (2006a, b) used non linear Langmuir adsorption isotherm and obtain the solution of washing model by using different solution techniques for single stage washing. Tervola and Rasanen [2005] used the Donnan equilibrium and overall cation transfer model to correlate the concentration between two phases.

No work found in the literature on the dynamic simulation of multistage washing system by using linear or nonlinear adsorption isotherm with the transport equation. The effects of various parameters on performance of single stage brown stock washer in paper industry were studied for different species of black liquor by some earlier researchers like Grahs (1974), Kukreja (1996), Kumar (2002), Arora et al. (2006a, b) and Kumar et al. (2009a, b) but no parametric studies were found in the literature for multistage washing.

Evaporators are widely used in the chemical industry to concentrate weak solution and recover solvents. It is used in industries like paper, sugar and caustic soda to concentrate black liquor, sugar cane juice and caustic soda solutions respectively. The Pulp and Paper industry, which is the focus of the present investigation, predominantly uses the Kraft Process in which black liquor is generated as spent liquor. This liquor is concentrated in multiple effect evaporator (MEE) house for further processing. Rao and Kumar (1985) pointed out that the Multi-effect evaporator system alone consumes around 24-30% of the total steam consumed in a large Indian paper mill. Therefore, it calls for a thorough investigation into its analysis and various energy reduction schemes.

A wide range of mathematical models for multiple effect evaporators (MEE) in process industry including paper industry are well reported in the literature. These Mathematical models are differentiated on the basis of the heuristic knowledge, which is incorporated in their development and the technique used for simulation. For the steady state analysis of MEE system, mathematical models and design of single as well as multi-stage evaporation have been reported in the literature since last five decades. A few of these were developed by Rao and Kumar (1985), Lambert et al.

(1987), Ray (1995), Patel and Babu (1996), Cadet et al. (1999), Ugrin and Urbicain (1999), Ray and Singh (2000), Ray and Sharma (2004), Bakker et al. (2006), Kaya and Sarac (2007), Karimi et al. (2007), Bhargava et al. (2008a, b), and Khanam and Mohanty (2010). For the modelling of multi-effect evaporation process majority of the investigators have discussed the steady state model in terms of nonlinear equations and obtain the solution after converting the nonlinear equations into linear and then solved by various numerical techniques.

Dynamic modelling is a powerful tool for predicting the changes in the system variables under transient condition. Nowadays, dynamic programming is considered a must in designing control systems of various processes. This help into better insight into the working of the process assists in the design of the control system for optimum operation. Efficiency and Energy conservation are among the most important factors considered, while designing the system. A way of achieving these objectives is the design of the better control system as well as the knowledge of the various system parameters under different conditions. This could be done in a better way by the knowledge of the dynamic behavior of the system.

Although the methods of design and steady state operation of single and multi-effect evaporators are well documented in the literature but not so extensive work on the dynamic behavior of MEE system is available in the literature. The dynamic behavior of two or three effect MEE systems in process industries like sugar, food and desalination etc. are studied by few researchers such as Andre and Ritter (1968), Bolmstedt (1977), El-Nashar and Qamhiyeh (1990), Tonelli et al. (1990), and Miranda and Simpson (2005).

No more work presented on the dynamic response of MEE system in Paper industry except Stefanov and Hoo (2003, 2004). They developed a fundamental dynamic model, based on first principles knowledge about the fluid dynamics and heat transfer processes for evaporation side of angle plate (lamella) of a falling film evaporator that accounted for the condensation side of the plate, the heating/flashing at the evaporator entrance, the evaporator inventory, mixing and recirculation flows but neglecting the effect of BPR.

Chemical pulps are bleached by the addition of chemicals such as chlorine, chlorine dioxide or hypochlorite. The bleaching process removes lignin from the pulp, which reduces the yield of a pulp produced from a given initial quantity of wood. Bleached pulps generally give stable high-

brightness pulps. The concern about the environmental effects of chlorinated organic in bleach plant effluents is steadily increasing. In the interest of reducing environmental impact of pulp mill effluents, many companies are examining ways to modify effluent composition and reduce effluent volume. In the extreme, reduced effluent volume means a closed effluent-free pulp mill operation.

In modelling of pulp bleaching most of the investigators discussed the modelling of various delignification as well as brightening stages. In the modelling of the retention tower of a bleach plant the most important parameter is the bleaching reaction kinetics. In the literature different kinetic models are proposed such as Ackert (1973), Ackert et al. (1975), Singh et al. (1975), Axegard (1979), Ni et al. (1995), Tessier and Savoie (1997), Chandranupap and Nguyen (2000), Barroca et al. (2001), Barroca et al. (2003), Gu and Edwards (2003), Jain et al. (2007, 2009). Most of the delignification models are based on the kinetic study conducted by Ackert et al. (1975). The kinetic models discussed in the literature try to describe and/or explain the chemical and physical interactions between the bleaching agent and the pulp fibers. No standard kinetic model is presented in the literature.

Mathematical models of aforesaid sections for multistage systems generate a number of linear, non-linear, homogeneous, non-homogeneous, algebraic, ordinary, and partial differential equations, the solutions of which are sometimes cumbersome, intricate and bewildered. For the solution of the mathematical models various methods are used like analytical techniques, numerical methods and optimization procedures. MATLAB is well-known among the control community. It offers excellent performance qualities for designing regulation algorithms. This makes it the best candidate for accomplishing the objective of fostering interdisciplinary integration if thermo hydraulic models can be implemented.

The transport equation describing the pulp washing model is a non homogeneous, linear, first degree, second order, parabolic, partial differential equation. Further the transport equation is combined with the adsorption isotherm which is in the form of first order partial differential equation. The solution of the transport model with adsorption isotherm simultaneously is very typical task and practically appears to be unsolvable for multistage washing system, even by using any sophisticated numerical techniques. The problem for single washer with its simplified version has been solved analytically by Brenner (1962), Kukreja (1996) using Laplace transform and numerically using Orthogonal Collocation by Grahs (1975) and Arora et al. (2006a, b). Al-Jabari et

al. (1994) used Galerkin finite element method with the predictor-corrector time integration technique for the forward-backward Euler type. Arora et al. (2006a, b) first discretized the partial differential equations into differential algebraic equations, which are then solved using ode15s solver separately. Kumar (2002) attempted to solve the washing model using Finite difference method. Solution of such type transient convection-diffusion-reaction problems are also obtained by Liu and Bhatia (2001) by Petrov-Galerkin method and Alhumaizi (2006) by moving collocation method. While Tervola (2006) developed a Fourier series solution method for solving a multistage countercurrent cake washing problem by using the advection-dispersion model presented by Brenner (1962) in a segregated and a non-segregated wash effluent circulation. To reduce the mathematical complication Tervola (2006) did not include the adsorption isotherm with the transport equation. All these methods are very complex and time consuming. Application of such solution techniques in control systems is not possible due to the more processing time and involvement of high mathematical skills at operator level. Using these techniques the parametric study for multistage washing is very typical task. Thus for the solution of washing model use of a different numerical technique like pdepe solver in MATLAB can be a good idea, which is easy to use, more efficient in processing time and gives the results with accuracy. Pdepe solver solves initial-boundary value problems for systems of parabolic and elliptic partial differential equations in the one space variable  $x$  and time  $t$ . Pdepe solver first discretized the partial differential equations into ordinary differential algebraic equations. The ordinary differential algebraic equations (ODEs) resulting from the discretization in space are integrated to obtain the solutions, for the given values of time.

The evaporator governing equations are, as usual, the overall mass balance and the solute mass balance, the enthalpy balance, and the heat transfer rate equations around each effect. These equations are nonlinear due to the dependence of the coefficients on temperature and composition, these being unknowns, and solution is feasible only by either linearizing the equations or using nonlinear techniques [Koko and Joye (1987)], which have proved to be not always successful. The multiple effect evaporator arrangements are quite cumbersome to perform calculations because the steady state model of MEE system contains the system of nonlinear equations. Solution of the steady state model was obtained by various researchers by using different solution techniques. Lambert et al. (1987) presented a calculation procedure in which the series of nonlinear algebraic equations that govern the evaporator system reduces into linear form and solves them iteratively by

linear technique, e.g. Gaussian Elimination. Koko and Joye (1987) solved the system as fully nonlinear simultaneous equations, governing the MEE system by using nonlinear equation solver IMSL-ZSCNT. The ISLM packaged software routine ZSCNT uses a secant method in the solution of sets of non linear algebraic equations. Ray and Singh (2000), Ray and Sharma (2004) and Ray et al. (2004) first convert the equations into linear form and then used Newton Raphson method with Jacobian matrix method and method of Gauss elimination with partial pivoting supplemented with LU decomposition with the aid of Hilbert norm and program was developed in FORTRAN-77 language. Bhargava et al. (2008a, b), and Khanam and Mohanty (2010) developed a computer program in FORTRAN 90 and run on Pentium IV machine, using Microsoft FORTRAN Power Station 4.0 compiler, to solve such type of models. All these methods are lengthy and so much time and programming skills is required for the development of the program in FORTRAN or in any other languages.

The dynamic model developed in the present investigations contains a number of simultaneous non linear ordinary differential equations. For the solution of ordinary differential equations (ODEs) initial values of the variables are needed. To fulfill the requirement of initial values the steady state solution of the model is obtained first by putting the accumulation terms is equal to zero. Thus by using these methods the solution of dynamic model of MEE system is very tough task. Thus for the solution of models in steady state conditions, 'fsolve' solver in MATLAB can be used, which is an equation solver used to solve nonlinear equations by the least squares method. For solution of the unsteady state (ODEs) model and to predict the dynamic behavior of the system 'ode45' solver in MATLAB can be used, which solves initial value problems for ordinary differential equations (ODEs). Ode45 is based on an explicit Runge-Kutta (4, 5) formula. It is a one-step solver - in computing  $y(t_n)$ , it needs only the solution at the immediately preceding time point,  $y(t_{n-1})$ .

The model described for the waste minimization of DED bleach plant are in the form of linear equations and also contains the chemical reaction kinetics in the form of ordinary differential equations. Dogan and Guruz (2004) used FORTRAN source code and subroutines for the simulation of whole bleach plant. Jain et al. (2009) used Visual Studio 2005 (Visual Basic for interface) and C++ for simulations, the differential equations was solved by using finite difference combined with explicit Euler method. Sarwar et al. (2010) deals with  $D_0E_pD_1$ , bleaching of *Trema orientalis* (Nalita) soda-AQ pulp with kappa number 17.8. The effects of kappa factor, bleaching

temperature and consistency in the  $D_0$  stage on final pulp properties were studied. Responses of bleached pulp properties to the process were analyzed using statistical software (SPSS 15). In the present investigation a much easier technique is investigated for the solution of such type of linear equations and kinetic models. Thus for the solution of linear equations of models is obtained directly by MATLAB or may be used 'fsolve' solver and for the solution of the system of ODE equations 'ode45' solvers in MATLAB source code is used.

Thus in the present investigation MATLAB is used for simulation of such energy subsystems. The major objectives of the study are

**Objectives:**

- Dynamic simulation of single and multi stage brown stock washing (BSW) system by using linear and non linear adsorption isotherms.
- Dynamic simulation of multi effect evaporator (MEE) system by considering equal heating surface areas in evaporator bodies.
- Modelling and simulation of DED bleach plant.



#### 2.1 Introduction

Pulp washing is a key unit operation in pulp and paper mills which significantly affects the economy as well as the environment. Chemical pulps are produced by digesting wood chips in chemical liquor. The output from a digester is a high consistency stock of fibers suspended in a solution containing dissolved lignin and digesting liquids often containing alkaline chemicals. Before further processes can be performed on the fibers separated from the wood chips, the dissolved lignin and digesting chemicals referred to as black liquor must be separated from the fibers. To minimize downstream problems and the production of undesirable waste products, the better than 99 % of the black liquor must be separated from the fibers. The process of separating the dissolved lignin and digesting chemicals is referred to as the washing process.

The objective of the pulp washing is to remove the soluble undesired products i.e. black liquor containing organic solids (lignin), inorganic solids (Na, Mg, Ca and K ions). Removal of these undesired products reduces the consumption of chemicals in subsequent sections, which in turn produce less pollutant. Ideally pulp should be washed using less amount of wash water and with maximum removal of black liquor solids. Dilution must be minimized because after separation of the fiber the black liquor and all wash water is evaporated and the residue is burnt to produce energy and ash. The ash referred to as smelt, contains an alkaline residue which is processed to create the digesting liquor thus completing the digestion cycle by recycling the chemicals used to digest the lignin in the wood chips [Gallagher (1999)].

The basic mechanism of pulp washing consists of dilution, agitation, extraction and displacement. Generally, the pulp slurry is diluted and mixed thoroughly with weak wash liquor or clean water in the vat and the fibers are extracted from the slurry due to vacuum inside the drum. In displacement washing the wash liquor or water passes through the pulp bed in a piston like manner, pushing out the liquor which is associated with the pulp. Ideally it is possible to displace one volume of the liquor in the pulp with the same amount of clean water. Although, practically it is impossible due to the porous structure of the fibers. The phenomenon of diffusion and dispersion dominates the washing theory.

Several types of washing devices have been introduced in recent years, most notably the pressure washer. There has also been renewed interest in wash press. Several configurations of multiphase washers are available. Both atmospheric and pressure diffusers are used in a variety of applications. However, conventional rotary drum vacuum washer is by far the most common pulp washing device in use today. Rotary vacuum multistage washer containing 3-4 stages is a widely preferred piece of equipment around the globe because of its simplicity in design and flexibility in operation. Conventionally vacuum washer systems are operated by back end analysis, soda loss or conductivity is measured of the last washing stage and there is little, if any information on the washing performance of the individual stages. As a first step towards improved washing the mill must be able to quantify the performance of their existing washers. This can lead to improvements in the existing system and define benchmarks for evaluating new equipment, systems and technology [Leddy (1998)].

Rotary vacuum washer consists of a wire mesh covered cylinder which rotates in a vat containing slurry. During each rotation of drum, various zones are formed. These are: cake formation, dewatering, washing, drying, blow and discharge, and dead zone. Overall performance of the washer depends critically upon cake formation and washing zones. For a typical rotary vacuum washer working for brown stock and bleach washing, total area combining these two zones may be around 70-75% of the area of drum.

Cake formation and washing zones contribute to maximum amount of filtrate. During the cake formation zone vat consistency and fractional submergence play an important role whereas in cake washing zone porosity, cake thickness, time of washing, liquor speed in cake pores are the key factors. The cake formation, dewatering and cake drying zone are affected by the saturation due to the simultaneous flow of the liquor and air. Hence, it is clear that the parameters and mechanism involved in each zone are different and therefore a single mathematical model cannot be used to predict the functioning of each zone. A major amount of air is extracted in dewatering and drying zones along with the filtrate, exhibiting a two-phase flow system. Thus their contribution towards air displacement of black liquor is not much significant. Therefore, the solute removal efficiency is confined mainly to the washing zone alone. In fact, efficiency of a washer is highly dependent on the design and area coverage of the washing zone.

The present study is mainly concentrated on the washing zone. The mechanism of pulp washing involves fluid mechanics associated with mass transport phenomenon related to diffusion and dispersion. This is further complicated by the adsorption, desorption, foaming and channeling. Various studies have shown that diffusion and dispersion significantly affect the washing operation. The speed at which the diffusion of black liquor solids inside the fiber voids and the surrounding liquor takes place is dependent on the concentration difference of the black liquor solids at inside and outside the fibers as well as time allowed for diffusion, temperature and turbulence around the fibers. Larger concentration difference, higher temperature and higher turbulence lead to faster diffusion which results in fast equilibrium.

## **2.2 Modelling and Simulation of Pulp Washing: A Review**

Washing of cellulose fibers in the pulp mill is a combination of dilution/drainage and displacement operations. The theoretical treatment of these operations basically has been based on macroscopic models of the washing equipment. For a more detailed description of the displacement washing, a microscopic model is suggested.

In macroscopic models the process is described in terms of material balances around the washing stages and used to study the parametric influence on the performance of washing system. These models cannot account for various mass transfer mechanism of washing such as sorption, diffusion and dispersion. Studies of washing system by using macroscopic models were described by some earlier researchers such as Tomiak (1973), Norden et al. (1973), Phillips and Nelson (1977), Norden and Viljakainen (1980), Norden et al. (1982), Norden and Viljakainen (1983), Luthi (1983), Nierman (1986), Cullinan (1986), Oxby et al. (1986), Haywood (1995), Kukreja et al (1995, 1996, 1998), Pacheco et al. (2006) and Anttila et al. (2007).

Tomiak (1973) developed a Mathematical theory of pulp washing and reslurrying, which would permit comparing different liquor recovery systems in general and predicting the performance of multi-stage counter current washing from laboratory, pilot plant, or full scale tests for single stage washing system in particular. Norden et al. (1973) described the Mathematical models for the efficiency of recirculation of liquor and washing drum based upon experimental investigations and investigated only the washing-out alkali. The influence of various operating variables and the wash liquor ratio upon the efficiency factor of washing drum was shown graphically. The efficiency

factors of three drums in series were also compared when each drums runs under equivalent operating conditions. Phillips and Nelson (1977) described the various types of equipment using diffusion or displacement washing principles. Combinations of these equipments with other types of washing systems were examined. A rapid, simplified method of estimating salt cake losses from any combination of washing equipment was also presented together with performance figures. Norden and Viljakainen (1980) have described the calculation of washing processes stepwise in series when equilibrium between wash liquor and the pulp is influenced by the adsorption processes. The equilibrium curve is approximated with the help of two or more straight lines when adsorption effects were included. The outlet concentration was calculated with the help of Norden efficiency factor. Norden et al. (1982), Norden and Viljakainen (1983) applied a simple mass transfer model to pulp washing on rotary drums. The model comprises two parameters, the number of mass transfer units of a differential contact semi batch washing stage and wash liquor ratio. The model and superposition method were applied to a drum washer with one, two and three washing zones. The mass transfer correlation based on the measurement on an industrial vacuum washer was presented for both pine and birch sulphate pulp. A numerical example of multi-zone washer calculations was also presented. Luthi (1983) used the equivalent displacement ratio to compare the test results from any pulp washer and to compare washers of different designs, independent of inlet and discharge consistency while Nicrman (1986) used the Norden Efficiency to predict the performance of counter-current pulp washers. Cullinan (1986) stated that, counter current washing of pulp on rotary filters is a mass transfer process amenable to analysis by the classical techniques of non equilibrium staged operations. Such analysis establishes the connections among the overall, stage, local efficiencies and underlying mass transfer rate in the wash zone. Haywood (1995) focused on modelling of horizontal belt washers. The seven stage horizontal belt washer at Impson Tacoma Kraft mill was used for modelling purpose. The data was used to develop the CGEMS models showing stage wise working efficiencies, displacement ratio and overall dilution factor. Kukreja et al (1995, 1996, 1998) described some parameters of rotary vacuum washer performance and their correlations. These parameters were the wash liquor usage (dilution factor, wash liquor ratio), solute removal (wash yield, displacement ratio, and solid reduction ratio) and efficiency parameters (soda loss, Norden's and modified Norden's efficiency parameters, % efficiency). Pacheco et al. (2006) presented a calculation procedure for rotary drum vacuum filters used in brown stock washing. In the model of a rotary vacuum filter, brown stock washing was fitted into a set of basic unit operations. These operations were modeled by combining mass

balance equations with constant pressure filtration equations. This set of equations was solved by using system/engineering analysis methodology. Anttila et al. (2007) illustrated the performance of various washers and washing systems and the effect of washing system on the other parts of the processes. The results also illustrated the importance of minimizing the amount of washing water and applicability of duplex steels in the washing section and introduced the novel method for recovering acids that are bound as esters during washing.

Microscopic models primarily define the mechanism of the washing process. These models are based on filtration theory of flow through porous media and also take care of diffusion, dispersion and adsorption-desorption phenomena occurring due to electrolytes/ macromolecules, water and fiber interactions. Microscopic models were used to study the washing system by various investigators such as Kuo (1960), Brenner (1962), Sherman (1964), Pellett (1966), Neretnieks (1974), Grahs (1975), Perron and Lebeau (1977), Han and Edwards (1988), Cullinan (1991), Lindsay (1994), Al-Jabari et al. (1994), Kukreja (1996), Eriksson and Gren (1996), Kumar (2002), Potucek (1997, 2001a, 2001b, 2003, 2005), Babu and Gupta (2004), Tervola and Rasanen (2005), Arora et al. (2006a, b), and Tervola (2006). Some of the process models by these researchers are presented in Table 2.1.

Kuo (1960) developed a model for the washing of filter cakes, assuming that mass transfer existed between the stagnant film and the bulk fluid. Author presented a model with the assumption that wash liquor followed the plug flow in the cake pores. The flow channel and the filtrate film were taken to be uniform cross section with transport of solute between the wash liquor and the filtrate occurring at a rate proportional to the solute concentration. The model equations were solved analytically using Laplace transform. Brenner (1962) presented an axial dispersion model depending upon axial dispersion coefficient only. In this model neither the concentration of solute adsorbed on the particle surface nor the porosity of the bed were considered and the Danckwart's boundary conditions had been followed. Laplace transform technique was used for the analytical solution of the model.

Table 2.1 Mathematical models for pulp washing used by previous investigators

S. No.	Transport Equation	Adsorption Isotherm	Boundary Conditions at $z=0$ and/or $z=L$ for all $t > 0$	Reference
1.	$D_L \left( \frac{\partial^2 c}{\partial z^2} \right) = u \left( \frac{\partial c}{\partial z} \right) + \left( \frac{\partial c}{\partial t} \right) + \frac{1}{\epsilon_r} \left( \frac{\partial n}{\partial t} \right)$	(i) $n = k_1 c + k_2$ (ii) $\frac{\partial n}{\partial t} = k_1 c - k_2 n$	$c = C_s$	Lapidus and Amundson (1952)
2.	$\frac{\partial n}{\partial t} = k_1 (n - c) - u \frac{\partial c}{\partial z}$	$\frac{\partial n}{\partial t} = k_2 (c - n)$	do	Kuo (1960)
3.	$D_L \left( \frac{\partial^2 c}{\partial z^2} \right) = u \left( \frac{\partial c}{\partial z} \right) + \left( \frac{\partial c}{\partial t} \right)$	-----	$uc - D_L \frac{\partial c}{\partial z} = uC_s$  $\frac{\partial c}{\partial z} = 0$	Brenner (1962)
4.	$D_L \left( \frac{\partial^2 c}{\partial z^2} \right) - u \left( \frac{\partial c}{\partial z} \right) = \left( \frac{\partial c}{\partial t} \right) + \left( \frac{1-\epsilon}{\epsilon} \right) \left( \frac{\partial n}{\partial t} \right)$	$n = kc$	$c(0,t) = f(t) = C_s (k_0 + k_1 t + k_2 t^2 + k_3 t^3 + k_4 t^4) e^{-\lambda t}$	Sherman (1964)
5.	$D_L \left( \frac{\partial^2 c}{\partial z^2} \right) - u \left( \frac{\partial c}{\partial z} \right) = \left( \frac{\partial c}{\partial t} \right) + \left( \frac{1-\epsilon}{\epsilon} \right) \left( \frac{\partial q}{\partial t} \right)$	$\frac{\partial q}{\partial t} = k \frac{\partial c}{\partial z}$	$\frac{\partial q}{\partial t} = 0$	Pellett (1966)
6.	$D_L \left( \frac{\partial^2 c}{\partial z^2} \right) - u \left( \frac{\partial c}{\partial z} \right) = \left( \frac{\partial c}{\partial t} \right) + \left( \frac{1-\epsilon}{\epsilon} \right) \left( \frac{\partial q}{\partial t} \right)$	$\frac{\partial q}{\partial t} = \frac{k_F R}{K} (Kc - q_s)$	$uc - D_L \epsilon \frac{\partial c}{\partial z} = uC_s$  $\frac{\partial c}{\partial z} = 0$  $q(0, z, t) \neq \infty$  $q(R, z, t) = q_s$	Neretnieks (1972, 1974)
7.	$\epsilon_d \frac{\partial c}{\partial t} + \epsilon_s \frac{\partial c_s}{\partial t} + C_F \frac{\partial w}{\partial t} = \epsilon_d D_L \frac{\partial^2 c}{\partial z^2} - \epsilon_d u \frac{\partial c}{\partial z}$ $\epsilon_s(z) \frac{\partial c_s}{\partial t} = k_1 a_1 (c - c_s) - C_F(z) \frac{\partial w}{\partial t}$ $C_F(z) \frac{\partial w}{\partial t} = k_2 a_2 (c_s - c_s^*)$	$w = \frac{Ac^* c_s}{1 + Bc^* c_s}$	$uc - D_L \frac{\partial c}{\partial z} = uC_s$  $\frac{\partial c}{\partial z} = 0$	Grahs (1975)
8.	$\epsilon_d(z) \frac{\partial c}{\partial t} + \epsilon_s(z) \frac{\partial n}{\partial t} + \epsilon_d(z) u(z) \frac{\partial c}{\partial z} = 0$	$\frac{\partial c}{\partial t} = k(c - n)$	$c = C_s$	Perron and Lebeau (1977)
9.	$D_L \left( \frac{\partial^2 c}{\partial z^2} \right) - u \left( \frac{\partial c}{\partial z} \right) = \left( \frac{\partial c}{\partial t} \right) + \left( \frac{1-\epsilon}{\epsilon} \right) \left( \frac{\partial q}{\partial t} \right)$	---	-----	Viljakainen (1985)

10.	$\left(\frac{\partial c}{\partial t}\right) = D_L \left(\frac{\partial^2 c}{\partial z^2}\right) - u \left(\frac{\partial c}{\partial z}\right)$ <p style="text-align: center;">and</p> $\epsilon \frac{\partial q}{\partial t} + (1 - \epsilon) \rho_s \frac{\partial n}{\partial t} + u \frac{\partial q}{\partial z} = 0$	$\frac{\partial n}{\partial t} = k_1 \frac{\epsilon}{\rho_s (1 - \epsilon)} q$ $\left(1 - \frac{n}{n_{\max}}\right) - k_2 n \frac{n}{n_{\max}}$	$q(0, t) = C_0$ and $n(0, t) = N_0$	Al-Jabari et al. [1994]
11.	$D_L \left(\frac{\partial^2 c}{\partial z^2}\right) - u \left(\frac{\partial c}{\partial z}\right) = \left(\frac{\partial c}{\partial t}\right) + \left(\frac{1 - \epsilon}{\epsilon}\right) \left(\frac{\partial n}{\partial t}\right)$	$\frac{\partial n}{\partial t} = k_1 c - k_2 n$ $\frac{\partial n}{\partial t} = k(c - n)$ and $n = kc$ .	$uc - D_L \frac{\partial c}{\partial z} = uC_s$ $\frac{\partial c}{\partial z} = 0$	Kukreja (1996)
12.	$D_L \left(\frac{\partial^2 c}{\partial z^2}\right) = u \left(\frac{\partial c}{\partial z}\right) + \left(\frac{\partial c}{\partial t}\right)$	-----	do	Potucek (1997)
13.	$\frac{\partial^2 C}{\partial Z^2} = Pe \left(\frac{\partial C}{\partial Z} + \frac{\partial C}{\partial T} + \mu \frac{\partial N}{\partial T}\right)$ <p>(Dimensionless form)</p>	do	do	Kumar (2002)
14.	$-D_L \left(\frac{\partial^2 c}{\partial z^2}\right) + u \left(\frac{\partial (vc)}{\partial z}\right) + \left(\frac{\partial c}{\partial t}\right) + \left(\frac{1 - \epsilon}{\epsilon}\right) \left(\frac{\partial q}{\partial t}\right)$	$q_s = \frac{q_m Kc_s}{1 + Kc_s}$	$c_{in} = c - \frac{D_L}{v} \frac{\partial c}{\partial z}$ $\frac{\partial c}{\partial z} = 0$	Babu and Gupta (2004)
15.	$D_L \left(\frac{\partial^2 c}{\partial z^2}\right) - u \left(\frac{\partial c}{\partial z}\right) = \left(\frac{\partial c}{\partial t}\right) + \left(\frac{1 - \epsilon}{\epsilon}\right) C_F \left(\frac{\partial q}{\partial t}\right)$	$q = \frac{Ac}{1 + Bc}$	$uc - D_L \frac{\partial c}{\partial z} = uC_s$ $\frac{\partial c}{\partial z} = 0$	Arora et al. (2006 b)
16.	$D_L \left(\frac{\partial^2 c}{\partial z^2}\right) - u \left(\frac{\partial c}{\partial z}\right) = \left(\frac{\partial c}{\partial t}\right) + \left(\frac{1 - \epsilon}{\epsilon}\right) \left(\frac{\partial n}{\partial t}\right)$	$n = \frac{ABc}{1 + Bc}$	do	Kumar et al. (2010 b)

Sherman (1964) has developed the Mathematical model on similar lines with Brenner (1962), and followed the step input boundary conditions instead of Dankwart's boundary conditions. The model was applied on viscose fibers and glass beads. The bulk fluid concentration and the concentration of solute adsorbed on particle surface were related by linear adsorption isotherm. Pellett (1966) extended the model of Sherman (1964) by accounting for intra-fiber diffusion of a solute linearly adsorbed to the viscose fibers, as well as for fiber to liquid phase mass transfer resistance and studied the longitudinal dispersion of solute, intra particle diffusion of solute and liquid phase mass transfer for the particles of cylindrical and spherical geometry by using a modified step function input. The studies of Sherman (1964) and Pellett (1966) provided insight into the modelling of washing of pulp fiber bed. Neretnieks (1974) presented a Mathematical model for continuous counter-current adsorption. The mechanisms of the instantaneous diffusion in the particles, film resistance and dispersion in the fluid phase were included. The equilibrium between the phases was assumed to be linear. The influence of particle size, bed length and velocities on the adsorption efficiency was discussed. The models equations were solved by Laplace transform method. Grahs (1975) developed a Mathematical model for displacement washing of packed beds of porous materials, especially cellulose fibers. The model took into consideration, dispersion, linear or nonlinear adsorption of substance on the solid material, zones of stagnant liquor, and the variable consistency in the packing material in the bed. The equations were solved numerically by a double orthogonal collocation method. Perron and Lebeau (1977) had taken the model equation without considering the effect of longitudinal dispersion coefficient and presented static models of washers after a theoretical analysis of the different phenomena taking place on a drum of a rotary drum washer, and then dynamic models were reported. A mathematical expression had been formulated for cake length and filtrate flow rate through cake formation zone using Darcy's law by assuming constant pressure drop, negligible hydrostatic pressure and non compressibility of cake. The diffusion of the solute within the fibers towards the washing liquor was described by a differential equation which was solved assuming that the mass transfer rate through the stagnant film is finite. For the solution of the model Laplace transform technique was used. Han and Edwards (1988) presented a new washer model and applied it to optimize filter washing operation and control. The mat formation in the model was described by Ruth's equation and a variable specific resistance. For a given drum speed and vacuum, the mat thickness and vat level were calculated from these filtration consideration. Using this model author concluded that to minimize total dissolved solids (TDS) carryover from brown stock washing for a



fixed shower flow; drum vacuum was the most important operating variable. Cullinan (1991) developed a model of primary mass transfer mechanisms involved in pulp washing, diffusion and displacement with the emphasis on the different behavior of the inorganic and organic components of the liquor. The model matched well with the available data. The significance difference between sodium and lignin removal is quantified. This has important implications in regard to the potential for the production of chlorinated organics in subsequent bleaching operations. Lindsay (1994) has followed the dispersion model in terms of the radial coordinates for dye transport through porous media and assumed the effective dispersion coefficient ( $D_0$ ) to be constant. Al-Jabari et al. (1994) modeled theoretically the process of flow through a packed bed of pulp fibers and deposition of the fibers of fillers passing through the bed. The flow was described by a residence time distribution and assumed to be completely segregated so that the bed can be divided into a number of sections, each characterized by a constant fluid velocity. The model described the deposition process in the constant velocity sections by the system of two partial differential equations (PDEs) describing particle transport and deposition kinetics. The transport equation consisted of convective, unsteady state and rate of deposition terms. The equation describing the kinetics was of a Langmuir type, similar to the one describing gas molecular adsorption. This system of PDEs, along with appropriate boundary and initial conditions, was solved numerically for the two dependent variables (particle concentration in suspension and fiber) and then the exit solute concentration is calculated to give the particle break through curves. The system of PDEs was solved by using Galerkin finite element method, with the predictor-corrector time integration technique of the forward-backward Euler type. Kukreja (1996) have followed the axial dispersion model with linear and finite rate isotherms with Danckwart's boundary conditions and attempt has been made to define possible applicable performance evaluation parameters used by various investigators and compare to each other. The most important parameter is the efficiency of the washing expressed in terms of the solute concentration in the discharged as well as extracted liquor and the filtrate flow rate with or without the filter medium resistance. Laplace Transform was used for the solution of the pulp washing model. Eriksson and Gren (1996) presented a model which combined both micropore (particle phase) and macropore (bulk fluid phase) diffusion models to study the washing behavior of filter cakes. The model was based on the washing operation of lime mud used in pulp and paper industry. For the simulation experimental data of granular particles having spherical geometry has been used. Kumar (2002) derived the Mathematical models for washing zone of a rotary vacuum washer from basic equation of continuity in one dimensional form for flow through

porous media with adsorption and desorption isotherm equations for two species namely  $\text{Na}^+$  and lignin. Parametric effects of various input parameters were studied by plotting the breakthrough curves. Finite difference method was used for the solution of pulp washing models. Potucek (1997, 2001a, 2001b, 2003, 2005) followed an axial dispersion model similar to Brenner (1962). The linear rate adsorption isotherm was used to correlate bulk fluid concentration and the concentration of solute adsorbed on the particle surface. Author studied the behavior of softwood pulp fibers. The data of washing cell consisting of a vertical glass cylinder 110 mm high and 36.4 mm inside diameter and closed at the lower end by a permeable septum was used to validate the model. The interpretation of numerical and experimental values was made using the statistical tools. Babu and Gupta (2004) studied a mathematical model for a fixed bed isothermal adsorption column with porous adsorbent. Simulation was carried out to understand the influence of axial dispersion, external film resistance, and solid diffusion resistance on adsorption using the above model. The mathematical equations were solved simultaneously using finite difference explicit scheme. The effects of flow rate, mass of adsorbent and initial concentration of adsorbate were studied. Rapid occurrence of breakthrough time was observed for higher flow rates of effluent, lower mass of adsorbent and high initial concentration of effluent. Tervola and Rasanen (2005) described the cake washing of freely mobile ions by an advection dispersion equation proposed by Brenner (1962), combined with Donnan equilibrium and an overall ion transfer model between the external liquid phase and the fiber phase of the kraft pulp. The ion exchange rate coefficients between the phases were determined from the earlier published leaching test results for oxygen delignified Scandinavian hardwood kraft pulp. The calculated results for various elements during the acid displacement were compared with the published displacement experiments. Arora et al. (2006a, b) presented an extended mathematical model related to diffusion–dispersion during flow through multi-particle system. The technique of orthogonal collocation on finite elements was applied on the axial and radial domain of the system of governing partial differential equations. The convergence and stability of the solutions was also checked. Effect of different parameters like axial dispersion coefficient, reaction rate kinetics, interstitial velocity, bed porosity, cake thickness, and particle radius on exit solute concentration was presented. Numerical results were found matching with the experimental results significantly. Tervola (2006) developed a Fourier series solution method for solving a multistage countercurrent cake washing problem, so that the solute concentration gradient inside a cake between washing stages was obtained. The cake washing process was described by the advection–dispersion equation presented by Brenner (1962). The

model was solved to explore the multistage countercurrent cake washing in a segregated and a non-segregated wash effluent circulation. The segregated wash effluent circulation gave better solute recovery than the non-segregated wash effluent circulation especially when the wash ratio was taken near to one.

Some researchers concentrated mainly on the control of the pulp washing system but in the process they did dynamic modelling of washing system. Bender et al. (1988) developed an operation on line computer-system for controlling the brown stock washers. Nase and Sjoberg (1989) analyzed the benefits that could be achieved with a multi-variable control system over a conventional control system in a washing plant. The basic idea was to allow the levels of the filtrate tanks to fluctuate within certain limits and in that way act as a buffer in the event of disturbances. Turner et al. (1993) studied the dynamic behavior of a brown stock washing system and minimize the effect on process disturbances on the removal of dissolved solids from the pulp. The operation of brown stock washing plant was simulated using PAPDYN, a dynamic modular simulation package. Turner and Livingstone (1995) developed a method to separate a representative stream of filtrate from washed pulp leaving the last drum washer in the brown stock area. This development allowed automatic feedback control to be implemented in the washing area for the first time at many mills.

Mathematical models of any process are required to be validated. Validation is carried out by comparing the solution of the model with plant data or experimental data generated in the laboratory. Experiments are also carried out for estimation of various parameters of physical model equations. Experiments have been carried out by various investigators for the study of mechanism of pulp washing. Gren and Grahs (1973) presented the results from washing experiments on pine sulphate pulps of different yield. Grahs (1976) found well suited mathematical model proposed in earlier investigation for the displacement washing of cellulose fibers by the analysis of results from washing experiments. Gren and Storm (1985) studied the influence of some fundamental variables of the displacement washing operation on softwood kraft pulp in laboratory experiment. The experimental data obtained in this method can be a basis for the design of efficient washing equipment and can be used in the study of fundamental mechanisms of the displacement washing. Penttila et al. (1986) carried out the experimental work on laboratory scale, and a three-stage drum washing plant was simulated. Wong and Reeve (1990) carried out experiments on nylon and various modified pulp fibers using Potassium Chloride. They studied the unsteady state diffusion

in fiber bed and observed that in fiber suspension, the effective diffusivity decreases linearly with increasing fiber volume fraction, where this fraction represents the total volume of fibers and encumbered water. Author also observed that fiber volume fraction can be estimated by the water retention value or hydrodynamic specific volume and hence the effective diffusivity of a solute in any bed of fibers can be calculated. Potucek and Skotnicova (2002) investigated the mechanism of the displacement washing of unbleached kraft pulp in a laboratory washing cell. Wash liquids with various pH values varying in the range from 2 to 11 were used to displace black liquor from the pulp bed. Using the step function input change method, the washing breakthrough curves obtained experimentally were described by the axially dispersed plug flow model. Potucek and Pulcer (2004) simulated brown stock washing by using a laboratory displacement washing cell. The displacement of black liquor from the kraft pulp bed was described by the dispersion flow model containing one dimensionless parameter, the Peclet number, for alkali lignin and sodium as the tracers. Potucek and Pulcer [2006] investigated the two basic mechanisms of displacement washing of pulp fibers with urea solutions. Experiments were carried in a laboratory washing cell that simulated a single stage of displacement washing. The step-change method was employed in investigation of alkali lignin profile in outlet stream of washing effluents. The addition of urea solution with wash water resulted in decrease in a liquid layer immobilized on the fiber surface. It had a positive effect on the washing efficiency expressed in terms of the void local efficiency.

Besides pulp washing models few other investigators have developed the models for some other systems but quite similar to pulp fibers. Sridhar et al. (1994) and Sridhar (1996a, 1996b, 1999) studied the affinity separation of a packed bed model using non linear adsorption isotherm. Mathematical model was formulated to include the mass transfer coefficients, film resistance coefficients and porosities of bed and particle. The model was defined for glass beads having spherical geometry. The efficiencies were calculated for both the solute recovery and adsorbent utilization. The set of nonlinear equations were solved by moving finite element method and orthogonal collocation. Liao and Shiau (2000) followed the axial dispersion model with linear adsorption isotherm to check the removal of phenol from the solution in the activated carbon and the amberlite resins XAD-4 fixed bed adsorbers. Author solved the set of equations analytically using Laplace transform. Szukiewicz (2000) presented an approximate model for the diffusion reaction processes. The model was developed using radial coordinates to describe reaction in porous spherical particles. Liu and Bhatia (2001) described the adsorption problems with steep

gradients in bidisperse solids and obtained the solution by using a semi discrete Petrov-Galerkin finite element method. Farooq and Karimi (2003) presented a dispersed plug flow model for steady state laminar flow in a tube with first order sink at wall involving two dimensions. The two dimensional model was reduced to a one dimensional model using the iterative techniques and then solved analytically. Alhumaizi (2006) simulated the diffusion-convective-reaction problem by using adaptive collocation method. The method was based on dividing the solution domain into active and inactive zones in such a way that the collocation points remain concentrated in regions of solution variation.

From the detailed analysis of the above models, it is observed that majority of the investigators have followed the axial dispersion model in one or the other form. Kuo (1960) was almost the first to introduce the concept of film resistance in the washing of pulp fibers. After that Pellett (1966) and Neretneiks (1974) have followed the micro and macroscopic study of the washing process by combining the models for particle phase and the bulk fluid phase. Majority of the investigators have followed either the linear or finite rate adsorption isotherm to correlate bulk fluid concentration and the concentration of solute adsorbed on the particle surface to reduce the mathematical complexities. Grahs (1975) and Arora et al. (2006a, b) have followed the Langmuir adsorption isotherm to solve their model for single stage washing. There are various other investigators who have contributed a large to the study of the washing of pulp fibers, e.g., Norden et al. (1973), Gren and Storm (1985), Luthi (1985), Cullinan (1991), Smith and Duffy (1991), Turner et al. (1993). One common feature of the above authors is that all of them have worked on wood pulp fibers either hardwood or softwood. Majority of the investigators have presented the generalized model for fibers and granular particles. Grahs (1975) have given a model especially for pulp fibers by introducing the terms like consistency of fibers, fiber porosity and the amount of solute adsorbed on the fiber surface. However, the radius of swollen fibers, film resistance mass transfer coefficients and volume equilibrium constants were ignored. These parameters have their effect on the washing behavior of pulp fibers as discussed by Sherman (1964), Pellett (1966), Perron and Lebeau (1977), Gren and Storm (1985) and Potucek (1997). As these parameters have their impact in the washing process, these can't be ignored during the Mathematical modelling of the equipment.

### 2.2.1 Mathematical model of pulp washing

The objective of the present study is to extend the mathematical model in an elaborative manner to describe the washing process and then solved by using a straightforward numerical technique. In this investigation an attempt has been made to describe the detailed model, compatible with the practical system. The mechanics involved is the sum of displacement of the liquor by movement of water plug controlled by fluid mechanics, dispersion due to back mixing, diffusion to concentration gradient and adsorption desorption due to relative affinity of various solutes towards the fiber surface. Keeping the above considerations, model is developed for single stage washing by considering simple material balance equation and solved numerically using pdepe solver in MATLAB source code. To improve the washing performance the solution is further extended for multistage washing system. Parametric effects are also studied on the washing efficiency of multi-stage brown stock washer for some important parameters.

### 2.3. Description of Mathematical Model of Pulp Washing

In order to get the relevant description of the main phenomena, displacement washing operation is separated from the other washing operations and schematically described as follows:

The mat of pulp fibers can be assumed to be stationary packed bed of homogeneous symmetrical cylindrical fibers. Instantaneous behavior of any system of this type can only be expressed by an equation involving the variables and their partial derivatives. For setting up a differential equation, consider a thin slice of a filter cake (pulp mat) as shown in Figure 2.1, through which filtrate or wash water flows

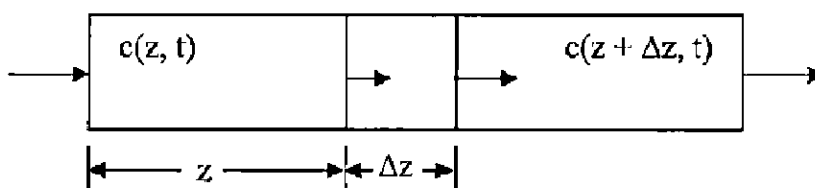


Figure 2.1 A simple shell balance

#### 2.3.1 Model attributed to axial dispersion

Considering axial dispersion only, material balance across the simple shell shown in Figure 2.1, in the z direction can be written as

*Rate of Mass of solute in + Rate of Mass production by chemical reaction*

*= Rate of Mass out + Rate of Mass Accumulation in the liquid*

If  $A'$  is the area of the bed,  $\varepsilon_t$  is the total average porosity (sum of porosities in the displaceable liquid  $\varepsilon_d$  and in the immobile phase  $\varepsilon_s$ ),  $u$  is the velocity of the liquor in the mat,  $c$  is the concentration in the liquid phase, the equation in one dimension can be written as:

$$(uc \varepsilon_t A')_{z,t} - (uc \varepsilon_t A')_{z+\Delta z,t} = \left[ \frac{\partial}{\partial t} (c \varepsilon_t A' \Delta z) \right]_{z,t} \quad (1)$$

where  $z < \bar{z} < z + \Delta z$ .

Taking  $\varepsilon_t$  and  $A'$  as constant and taking the limit as  $\Delta z \rightarrow 0$ , one can obtain the following equation,

$$- \varepsilon_t c \left( \frac{\partial u}{\partial z} \right) = \varepsilon_t u \left( \frac{\partial c}{\partial z} \right) + \varepsilon_t \left( \frac{\partial c}{\partial t} \right) \quad (2)$$

The above equation contains primarily one accumulation term, related to dispersion-diffusion.

Using Fick's second law of diffusion, i.e.

$$- c \left( \frac{\partial u}{\partial z} \right) = (D_L + D_V) \left( \frac{\partial^2 c}{\partial z^2} \right) \quad (3)$$

it reduces to,

$$(D_L + D_V) \left( \frac{\partial^2 c}{\partial z^2} \right) = u \left( \frac{\partial c}{\partial z} \right) + \left( \frac{\partial c}{\partial t} \right) \quad (4)$$

According to Sherman (1964) the longitudinal dispersion coefficient  $D_L$  is a function of flow pattern within the bed (unless very low flow rates are used). The molecular diffusion coefficient  $D_V$  is very small (1000 times less) compared to  $D_L$  and so may be neglected.

$$D_L \left( \frac{\partial^2 c}{\partial z^2} \right) = u \left( \frac{\partial c}{\partial z} \right) + \left( \frac{\partial c}{\partial t} \right) \quad (5)$$

Model equation (5) of pulp washing for axial dispersion is same as obtained by Brenner (1962) for the washing of cellulose fibers. This equation represents the basis for the mathematical models of displacement washing, where  $t$  is the time from the commencement of the displacement,  $z$  is the distance from the point of introduction of the displacing fluid,  $c = c(z, t)$  is the solute

concentration in the liquor,  $D_L$  is the axial dispersion coefficient,  $u$  is the average interstitial velocity of the fluid  $u = \frac{V_w}{A_c \varepsilon_t}$  and  $L$  is length of the bed.

### 2.3.2 Model attributed to axial dispersion as well as particle diffusion

In this model two accumulation terms are considered, one related to dispersion- diffusion and another related to adsorption-desorption. Other terms are velocity gradient and convective flow terms. In this case the material balance across the simple shell given in Figure 2.1, in the  $z$  direction can be written as:

*Rate of Mass of solute in + Rate of Mass production by chemical reaction*  
 = *Rate of Mass out + Rate of Mass Accumulation in the liquid phase + Rate of Mass accumulation in the solid phase due to Adsorption-Desorption.*

The equation in one dimension can be written as:

$$(uc\varepsilon_t A')_{z,t} - (uc\varepsilon_t A')_{z+\Delta z,t} = \left[ \frac{\partial}{\partial t} \{ (c\varepsilon_t A' \Delta z + n(1-\varepsilon_t)A' \Delta z) \} \right]_{z,t} \quad (6)$$

where  $z < \bar{z} < z + \Delta z$ . Taking  $\varepsilon_t$  and  $A'$  as constant and taking the limit as  $\Delta z \rightarrow 0$ , one can obtain the following expression,

$$-\varepsilon_t c \left( \frac{\partial u}{\partial z} \right) = \varepsilon_t u \left( \frac{\partial c}{\partial z} \right) + \varepsilon_t \left( \frac{\partial c}{\partial t} \right) + (1-\varepsilon_t) \left( \frac{\partial n}{\partial t} \right) \quad (7)$$

The above equation contains principally two accumulation terms, one related to dispersion-diffusion and another related to adsorption-desorption. Using Fick's second law of diffusion the following equation is obtained,

$$(D_L + D_v) \left( \frac{\partial^2 c}{\partial z^2} \right) = u \left( \frac{\partial c}{\partial z} \right) + \left( \frac{\partial c}{\partial t} \right) + \frac{(1-\varepsilon_t)}{\varepsilon_t} \left( \frac{\partial n}{\partial t} \right) \quad (8)$$

Again using the assumption of Sherman (1964), that molecular diffusion coefficient  $D_v$  is very small compared to  $D_L$  and so may be neglected. Writing  $(1-\varepsilon_t)/\varepsilon_t$  as  $\mu$  for convenience, the equation (4) may be written as



$$D_L \left( \frac{\partial^2 c}{\partial z^2} \right) = u \left( \frac{\partial c}{\partial z} \right) + \left( \frac{\partial c}{\partial t} \right) + \mu \left( \frac{\partial n}{\partial t} \right) \quad (9)$$

This is a non homogeneous, linear, first degree, second order, parabolic, partial differential equation. Here  $u$ ,  $\epsilon$ , and  $D_L$  are functions of  $z$  while  $c$  and  $n$  are functions of both  $z$  and  $t$ . As the lumen of the fiber is porous and the same is true with the wall of the fiber, the porosity values for these cases are different from the porosity of the interfiber mass. Therefore three porosity values are required to represent the pulp mat system. It is extremely difficult to distinguish precisely between the values of porosity at the lumen and at the wall. Therefore, for practical calculations these are assumed to be the same. Hence, to describe the system, two porosity values are assumed, one for the interfibers  $\epsilon_d$  and another for intrafibers  $\epsilon_s$ , so that  $\epsilon_d + \epsilon_s = \epsilon_t$ , the total porosity for the entire system. The model equation (9) is same as dispersion model for pulp washing given by Sherman (1964), Pellett (1966) and Kukreja (1996).

### 2.3.3 Adsorption-desorption isotherm for various species of black liquor

To inter-relate the intrapore solute concentration and the concentration of solute adsorbed on the fiber surface two types of isotherms are followed namely, linear adsorption isotherm and non linear adsorption isotherm. Vast literature is available for linear adsorption isotherm [Brenner (1962), Lapidus and Amundson (1952), Sherman (1964), Pellett (1966), Neretneiks (1972), Perron and Lebeau (1977), Wong and Reeve (1990), Lindsay (1994), Kukreja et al. (1995), Potucek (1997), Liu and Bhatia (2001), Liao and Shiao (2000)]. This adsorption isotherm is followed because it linearise the differential equation describing the behavior of fluid flow and reduces the mathematical complexities. Paucity is there in the literature regarding non linear Langmuir adsorption isotherm for pulp fibers. Fogelberg and Fugleberg (1963), Hartler and Rydin (1975), Ohlsson and Rydin (1975), Grahs (1975), Gullichsen and Ostman (1976), Eriksson and Gren (1996), Arora et al. (2006a & b) are among the few investigators who have studied Langmuir adsorption isotherm for pulp fibers. The details of the adsorption isotherms which are used in the present investigation are as follows.

Lapidus and Amundson (1952) used the adsorption isotherm given by

$$\frac{\partial n}{\partial t} = k_1 c - k_2 n \quad (10)$$

and assumed that the rate of adsorption is finite and plotted the effect of longitudinal diffusion for an infinite column in which equilibrium is established locally. Initial adsorbate concentration was assumed to be zero.

Sherman [1964] described the adsorption of diacetyl solution by porous viscous fibers with simple isotherm equation i.e.

$$n = kc \text{ or } \frac{\partial n}{\partial t} = k \frac{\partial c}{\partial t} \quad (11)$$

and assumed that the liquid solid concentration inside the fibers and surrounding the fibers to be identical at any time and at any position within the bed, implying that diffusion both within the fiber and between the fiber and the surrounding fluid is sufficiently rapid which does not affect the rate of the overall transport process.

Perron and Lebeau [1977] used the isotherm equation i.e.

$$\frac{\partial n}{\partial t} = k(c - n) \quad (12)$$

the diffusion of the solute within the fibers towards the washing liquor is described by a partial differential equation (12), which is solved assuming that the mass transfer rate through the stagnant film is finite.

Fogelberg and Fugleberg (1963) used Langmuir adsorption isotherm to describe the relationship between the concentration of the solute in the liquor and concentration of the solute on the fibers

i.e. 
$$n = \frac{ABc}{(1 + Bc)} \quad (13)$$

where A and B are Langmuir constants.

Adsorption isotherms given by equations (10), (11) and (12) are linear while the Langmuir isotherm given by (13) is non linear. For the present study the adsorption isotherms given by equations (10), (11), (12) is used for the simulation of single stage washing and equation (13) is used for the simulation of multistage washing also.

### 2.3.4. Initial and boundary conditions

Slightly different initial and boundary conditions have been proposed by various investigators. Initial and boundary conditions used in the present investigation are given below:

Most of the investigators have used initial conditions i.e.

$$c(z, t) = C_0, n(z, t) = N_0 \quad \text{at } t = 0, z \in (0, L) \quad (14)$$

Brenner (1962), Grahs (1975), Kukreja (1996) and Kumar (2002) used following boundary condition at the inlet of the bed is

$$uc - D_L \frac{\partial c}{\partial z} = uC_s, \text{ at } z = 0 \text{ for all } t > 0 \quad (15)$$

Perron and Lebcau (1977) give the boundary condition at the inlet of the bed

$$c = C_s, \text{ at } z = 0 \text{ and } t > 0 \quad (16)$$

At bed exit boundary condition given by (17) is used by many investigators such as Brenner (1962), Grahs (1975), Kukreja (1996) and Kumar (2002) and Arora et al. (2006a, b)

$$\frac{\partial c}{\partial z} = 0, \text{ at } z = L \text{ and } t > 0 \quad (17)$$

In the present investigation two cases arise for two different boundary conditions at inlet of the bed given by (14) and (15) together with bed exit (17). Various models of pulp washing have been developed which are plausible, with consideration of the effect of longitudinal dispersion coefficient and simple adsorption isotherm models both linear as well as non linear. These possible models are summarized in the Table 2.3 in Dimensionless form. Transport equation (9) of pulp washing model is same for all the models except the model 1 in which the transport equation (5) is used. The models are also differed by subjecting to various initial and boundary conditions.

### 2.3.5. Conversion into dimensionless form

Models are converted into dimensionless form by using certain dimensionless parameters like Peclet number (or Bodenstein number), dimensionless time, dimensionless thickness and

dimensionless concentration given in Table 2.2. Since the models are differ with respect to adsorption isotherm so the expression of some variable in dimensionless form is changed accordingly.

**Table 2.2 Dimensionless parameters**

Parameters	Dimensionless form	Model No.	Notations
Peclet number, Pe	$Pe = \frac{uL}{D_L}$	1, 2, 3, 4, 5, 6, 7, 8, 9	$\mu \rightarrow$ Constant in terms of porosity $[(1-\epsilon_t)/\epsilon_t]$
Dimensionless thickness, Z	$Z = \frac{z}{L}$	1, 2, 3, 4, 5, 6, 7, 8, 9	$c \rightarrow$ Concentration of solute in liquor, $kg/m^3$
Dimensionless time, T	$T = \frac{ut}{L}$	1, 2, 3, 4, 5 & 8, 9	$C \rightarrow$ Dimensionless, solute concentration in liquor
	$T = \frac{ut}{(1 + \mu k)L}$	6, 7	$C_0 \rightarrow$ Concentration of solute inside the vat, $kg/m^3$
Dimensionless concentration of solute in liquor, C	$C = \frac{c - C_s}{C_0 - C_s}$	1, 2, 3, 4, 5, 6, 7	$C_s \rightarrow$ Concentration of solute in wash liquor, $kg/m^3$
	$C = \frac{c}{C_0}$	8, 9	$D_L \rightarrow$ Longitudinal dispersion coefficient, $m^2/s$
Dimensionless concentration of solute in fiber, N	$N = \frac{n - C_s}{C_0 - C_s}$	2, 3, 4, 5	$K \rightarrow$ Dimensionless mass transfer coefficient
	$N = KC$	6, 7	$k \rightarrow$ Mass transfer coefficient, $1/s$
	$N = \frac{n}{N_0}$	8, 9	$k_1 \rightarrow$ Mass transfer coefficient, $1/s$
Dimensionless mass transfer coefficient, K	$K = \frac{k_1}{k_2}$	1, 2, 4	$k_2 \rightarrow$ Mass transfer coefficient, $1/s$
	$K = 1$	3, 5	$L \rightarrow$ Length of cake, m
G (Constant)	$G = \frac{k_2 L}{u}$	1, 2, 4	$n \rightarrow$ Concentration of solute on the fiber, $kg/m^3$
	$G = \frac{k L}{u}$	3, 5	$N_0 \rightarrow$ Concentration of solute on the fiber, at the inlet, $kg/m^3$
H (Constant)	$H = \frac{(K - 1)C_s}{C_0 - C_s}$	1, 2, 4	$t \rightarrow$ Time, s
	$H = 0$	3, 5	$u \rightarrow$ Liquor speed in cake pores, $m/s$
$\mu'$ (Constant)	$\mu' = \frac{\mu N_0}{C_0}$	8, 9	$z \rightarrow$ Cake thickness at time t, m

**Table 2.3 Existing mathematical models for washing zone used in present investigation  
(Dimensionless Form)**

S. No.	Transport Equation	Adsorption Isotherm	Boundary Conditions	Remark
1.	$\frac{\partial^2 C}{\partial Z^2} = Pe \left( \frac{\partial C}{\partial Z} + \frac{\partial C}{\partial T} \right)$	-----	$C(0, T) = 1$ , For $T > 0$ & $\frac{\partial C}{\partial Z} = 0$ , at $Z = 1$	Solution technique validation
2.	$\frac{\partial^2 C}{\partial Z^2} = Pe \left( \frac{\partial C}{\partial Z} + \frac{\partial C}{\partial T} + \mu \frac{\partial N}{\partial T} \right)$	$\frac{\partial N}{\partial T} = G(H + KC - N)$	$C(0, T) = 1$ , For $T > 0$ & $\frac{\partial C}{\partial Z} = 0$ , at $Z = 1$	Single stage solution
3.	$\frac{\partial^2 C}{\partial Z^2} = Pe \left( \frac{\partial C}{\partial Z} + \frac{\partial C}{\partial T} + \mu \frac{\partial N}{\partial T} \right)$	$\frac{\partial N}{\partial T} = G(C - N)$	$C(0, T) = 1$ , For $T > 0$ & $\frac{\partial C}{\partial Z} = 0$ , at $Z = 1$	Single stage solution
4.	$\frac{\partial^2 C}{\partial Z^2} = Pe \left( \frac{\partial C}{\partial Z} + \frac{\partial C}{\partial T} + \mu \frac{\partial N}{\partial T} \right)$	$\frac{\partial N}{\partial T} = G(H + KC - N)$	$\frac{\partial C}{\partial Z} = PeC$ , At $Z = 0$ , $T > 0$ & $\frac{\partial C}{\partial Z} = 0$ , at $Z = 1$	Single stage solution
5.	$\frac{\partial^2 C}{\partial Z^2} = Pe \left( \frac{\partial C}{\partial Z} + \frac{\partial C}{\partial T} + \mu \frac{\partial N}{\partial T} \right)$	$\frac{\partial N}{\partial T} = G(C - N)$	$\frac{\partial C}{\partial Z} = PeC$ , At $Z = 0$ , $T > 0$ & $\frac{\partial C}{\partial Z} = 0$ , at $Z = 1$	Single stage solution
6.	$\frac{\partial^2 C}{\partial Z^2} = Pe \left( \frac{\partial C}{\partial Z} + \frac{\partial C}{\partial T} + \mu \frac{\partial N}{\partial T} \right)$	$\frac{\partial N}{\partial T} = K \frac{\partial C}{\partial T}$	$C(0, T) = 1$ , For $T > 0$ & $\frac{\partial C}{\partial Z} = 0$ , at $Z = 1$	Single stage solution
7.	$\frac{\partial^2 C}{\partial Z^2} = Pe \left( \frac{\partial C}{\partial Z} + \frac{\partial C}{\partial T} + \mu \frac{\partial N}{\partial T} \right)$	$\frac{\partial N}{\partial T} = K \frac{\partial C}{\partial T}$	$\frac{\partial C}{\partial Z} = PeC$ , At $Z = 0$ , $T > 0$ & $\frac{\partial C}{\partial Z} = 0$ , at $Z = 1$	Single stage solution
8.	$\frac{\partial^2 C}{\partial Z^2} = Pe \left( \frac{\partial C}{\partial Z} + \frac{\partial C}{\partial T} + \mu' \frac{\partial N}{\partial T} \right)$	$N = \frac{ABC_o C}{(1 + BC_o C)}$	$C(0, T) = 1$ , For $T > 0$ & $\frac{\partial C}{\partial Z} = 0$ , at $Z = 1$	Single stage and Multistage solution with parametric study
9.	$\frac{\partial^2 C}{\partial Z^2} = Pe \left( \frac{\partial C}{\partial Z} + \frac{\partial C}{\partial T} + \mu' \frac{\partial N}{\partial T} \right)$	$N = \frac{ABC_o C}{(1 + BC_o C)}$	$\frac{\partial C}{\partial Z} = PeC$ , At $Z = 0$ , $T > 0$ & $\frac{\partial C}{\partial Z} = 0$ , at $Z = 1$	Single stage and Multistage solution with parametric study

The Peclet number (Pe) is a measure of the relative importance of advection to diffusion. Diffusion here is turbulent diffusion. The higher the Peclet number, the more important is advection. Peclet number is a dimensionless number relevant in the study of transport phenomena in fluid flows, which takes care of local velocities  $u$ , bed thickness  $L$  and longitudinal coefficient  $D_L$  ( $Pe = uL/D_L$ ). For constant bed depth it can show the variational effect of  $u$  and  $D_L$ . All models with respective boundary and initial conditions in dimensionless form are given in Table 2.3.

## 2.4 Solution Technique

The model concerned with the unsteady state operation of brown stock washing leads to a system of partial differential equations. Selection of solution technique depends on kind of partial differential equation like Homogeneous/ non-homogeneous, linear / non-linear or quasi linear, order and degree of equation, nature of the equation like parabolic, elliptic and hyperbolic or a mixed type tricomi form. To answer these questions it is an imperative necessity to go on to the details of the genesis of the differential equation. While the answers to the few questions are straight forward, some are difficult to answer. In this section the model developed is defined to what category it belongs? Thereafter the solution technique is sought for.

The model developed of pulp washing is a non homogeneous, linear, first degree, second order, parabolic, partial differential equation. The mathematical model of pulp washing for axial dispersion only is given by transport equations (5). For axial dispersion as well as particle diffusion the pulp washing model is given by transport equation (9), combined with the corresponding equation of isotherm. For the solution of these washing models various boundary conditions are used as mentioned earlier.

When washing model given by transport equation (9) is combined with any linear as well as nonlinear adsorption isotherms then it becomes extremely intricate in nature and practically appears to be unsolvable for multistage washing system; even by using any sophisticated numerical techniques. As mentioned earlier that the problem for single washer with its simplified version has been solved analytically by Brenner (1962), Kukreja (1996) using Laplace transform and numerically using Orthogonal Collocation by Grahs (1975) and Arora et al. (2006a, b). Arora et al. (2006a, b) first discretized the partial differential equations into differential algebraic equations, which are then solved using ode15s solver separately. Kumar (2002) attempted to solve the washing model using Finite difference method. Solution of such type transient convection-diffusion-reaction problems are also obtained by Liu and Bhatia (2001) by Petrov-Galerkin method and Alhumaizi (2006) by moving collocation method. While Tervola (2006) developed a Fourier series solution method for solving a multistage countercurrent cake washing problem. All these methods are very complex and time consuming. Application of such solution techniques in control systems is not possible due to the more processing time and involvement of high mathematical skills at operator level [Kumar et al. (2010b)].

In the present investigation a different numerical technique for the solution of such types of models is selected, which is easy to use, more efficient in processing time and gives the results with accuracy i.e. pdepe solver in MATLAB source code. Pdepe solver solves initial-boundary value problems for systems of parabolic and elliptic partial differential equations in the one space variable  $x$  and time  $t$ . Pdepe solver first discretized the partial differential equations into ordinary differential algebraic equations. The ordinary differential algebraic equations (ODEs) resulting from the discretization in space are integrated to obtain the approximate solutions for the given values of time.

## 2.5 Validation of the Solution Technique

For the validation of the solution technique (pdepe solver), the solution of displacement washing model 1 (Table 2.3) is obtained by taking  $Pe = 100$  using pdepe solver and compared with the analytical and numerical solutions of Brenner (1962) and Grahs (1975) respectively. Same data is used for simulation. The 3-Dimensional (3-D) behavior of the dimensionless concentration with respect to the dimensionless time and dimensionless cake thickness is shown by the Figure 2.2. The results of all three different solution techniques up to  $T = 1.2$  is presented in the Table 2.4.

[Since the solution for  $Pe = 100$  by Brenner (1962) and Grahs (1975) is available in the literature up to  $T = 1.2$ ]. To see the steady state behavior of the solution some imaginary layers of the cake are considered and for the solution dimensionless time is increased from  $T = 1.0$  to  $T = 2.0$  as shown in Figure 2.2. The comparison of the results at dimensionless distance at  $Z = 1$  for all values of dimensionless time with work of previous researchers is shown in the Figure 2.3.

Comparison shows that pdepe solver gives good accuracy and the magnitude of error is very low. It can be seen that at  $T = 0.5$  the error is 0.04% which is minimum and oscillate up to 9.13% in such a way that at  $T = 0.6$  error is 0.44%, at  $T = 0.7$  error is 2.16%, at  $T = 0.8$  error is 4.39%, at  $T = 0.9$  error is 2.89%, at  $T = 1.0$  error is 3.81%, at  $T = 1.1$  error is 8.53%, at  $T = 1.2$  error is 9.13% [Singh et al. (2008)].

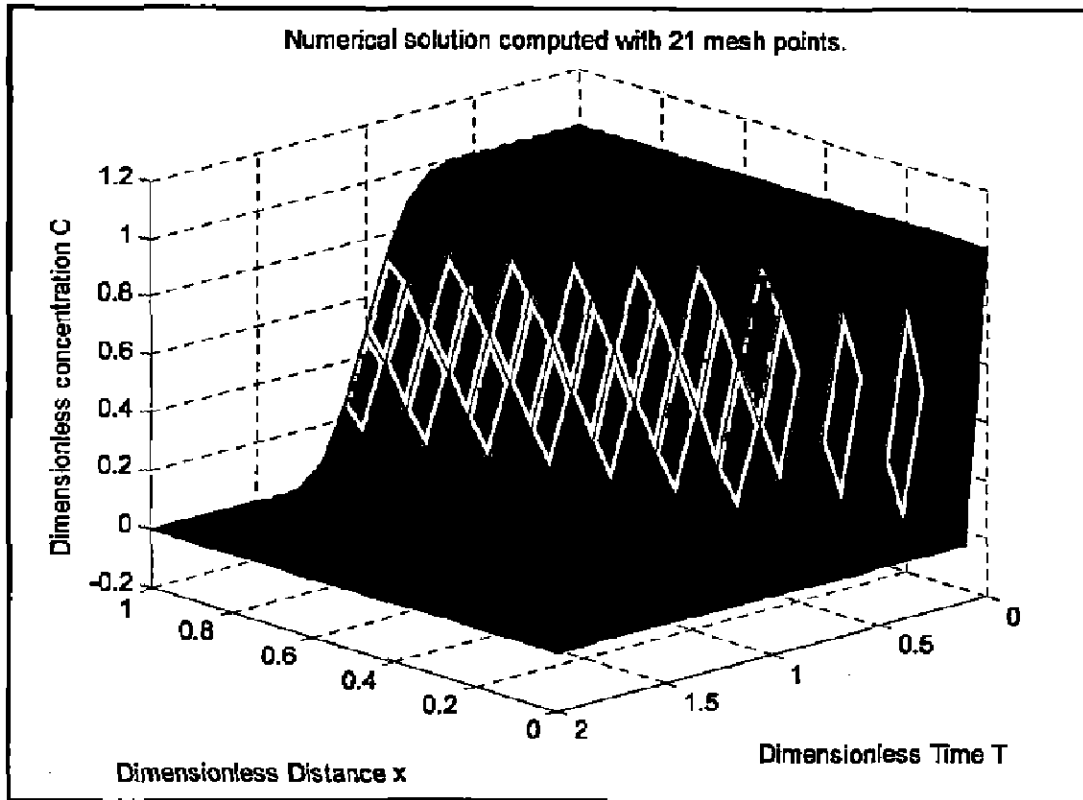


**Figure 2.2 C vs. Z & T profile for model 1**

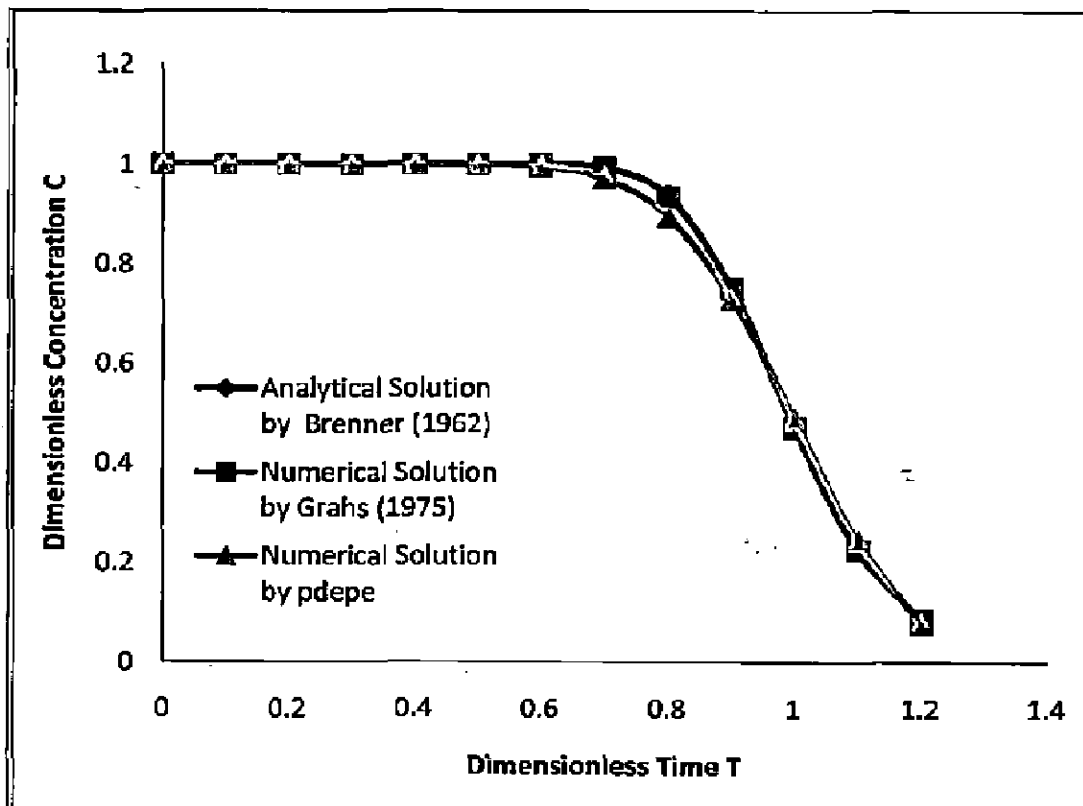


**Figure 2.3 Comparison of the solutions of model 1 for  $Pe = 100$**



**Table 2.4 Comparison of solutions at same  $Pe = 100$  for different solution techniques**

Dimensionless Time T	Analytical Solution by Brenner (1962)	Numerical Solution by Grahs (1975)	Numerical Solution by pdepe
0.0	1.0000	1.0000	1.0000
0.1	1.0000	1.0000	1.0000
0.2	1.0000	1.0000	1.0000
0.3	1.0000	1.0000	1.0000
0.4	1.0000	1.0000	1.0000
0.5	1.0000	0.9993	0.9996
0.6	0.9998	1.0004	0.9954
0.7	0.9935	0.9931	0.9720
0.8	0.9361	0.9361	0.8950
0.9	0.7521	0.7521	0.7303
1.0	0.4721	0.4721	0.4901
1.1	0.2273	0.2269	0.2467
1.2	0.0854	0.0853	0.0776

## 2.6 Solution of the Washing Models for Single Stage

Eight different models (models 2 to 9) are presented in Table 2.3 to describe the single stage washing. For control purpose the transient behavior of the solute concentration in the black liquor is of more interest, rather than solute concentration in fiber. Thus in the present work value of  $\partial N/\partial T$  in terms of  $\partial C/\partial T$ ,  $C$ ,  $C_0$ ,  $N$  and  $N_0$  is obtained by differentiating the isotherm equation, and then substituted in the transport equation and an attempt has been made to solve these equations directly by using 'pdepe' solver in MATLAB source code. Data obtained by Grahs (1974) for the species sodium ( $Na^+$ ) is used for simulation (Table 2.5). For obtaining much accurate solution of the above mentioned washing models, dimensionless bed depth as well as dimensionless time is divided into 21 equal parts and then the influence of these parameters ( $Z$  and  $T$ ) on  $C$  is estimated. To study the steady state behavior of the breakthrough curve some imaginary layer of the cake is considered and dimensionless time is increased from  $T = 1.0$  to  $T = 2.0$ . The behaviors of exit dimensionless solute concentration with respect to dimensionless time as well as dimensionless cake thickness are shown by 3-D graphs, which are shown from the Figure 2.4 to Figure 2.11. Also the solutions at dimensionless distance  $Z = 1.0$  are obtained and so the value of  $C(1.0, T)$  are presented in Table 2.6 for corresponding values of dimensionless time  $T$ .

It is clear from figures that the dimensionless concentration of the solute in the liquor decreases with the increase of the dimensionless time, whereas increases with the increase in the dimensionless distance. As transportation equations of all models are same and that is why the behavior of the dimensionless concentration with respect to the dimensionless time and dimensionless distance of all models from 2 to 9 are similar as depicted by the Figure 2.4 to Figure 2.11 respectively. This is similar trend as obtained by earlier workers such as Brenner (1962), Grahs (1975), Kukreja (1996), Kumar (2002) and Arora et al. (2006a, b).

**Table 2.5: Data for Simulation for sodium species**

Parameters	Values	Unit
L	0.105	m
$D_L$	$10.8 \times 10^{-7}$	$m^2/s$
$\epsilon_t$	0.928	-
u	$7.33 \times 10^{-4}$	m/s
$C_0$	0.570	$Kg/m^3$
$C_s$	0.005	$Kg/m^3$
A	0.01263	$m^3/Kg$
B	3.955	$m^3/Kg$

**Table 2.6 Solutions of the models 2 to 9 for single stage washing**

Dimensionless Time	Model-2	Model-3	Model-4	Model-5	Model-6	Model-7	Model-8	Model-9
0.0	1.0000	1.0000	1.0000	1.0000	1.0000	1.0000	1.0000	1.0000
0.1	0.9999	1.0000	0.9999	1.0000	1.0000	1.0000	1.0000	1.0000
0.2	0.9998	1.0000	0.9998	1.0000	1.0000	1.0000	1.0000	1.0000
0.3	0.9997	1.0000	0.9997	1.0000	1.0000	1.0000	1.0000	1.0000
0.4	0.9996	1.0000	0.9996	1.0000	1.0000	1.0000	1.0000	1.0000
0.5	0.9991	0.9996	0.9991	0.9996	1.0000	1.0000	0.9992	0.9992
0.6	0.9947	0.9953	0.9948	0.9954	0.9998	0.9998	0.9921	0.9922
0.7	0.9713	0.9719	0.9714	0.9720	0.9984	0.9985	0.9566	0.9568
0.8	0.8941	0.8948	0.8943	0.8950	0.9915	0.9916	0.8533	0.8535
0.9	0.7294	0.7300	0.7297	0.7303	0.9680	0.9681	0.6602	0.6605
1.0	0.4894	0.4899	0.4897	0.4901	0.9089	0.9091	0.4154	0.4155

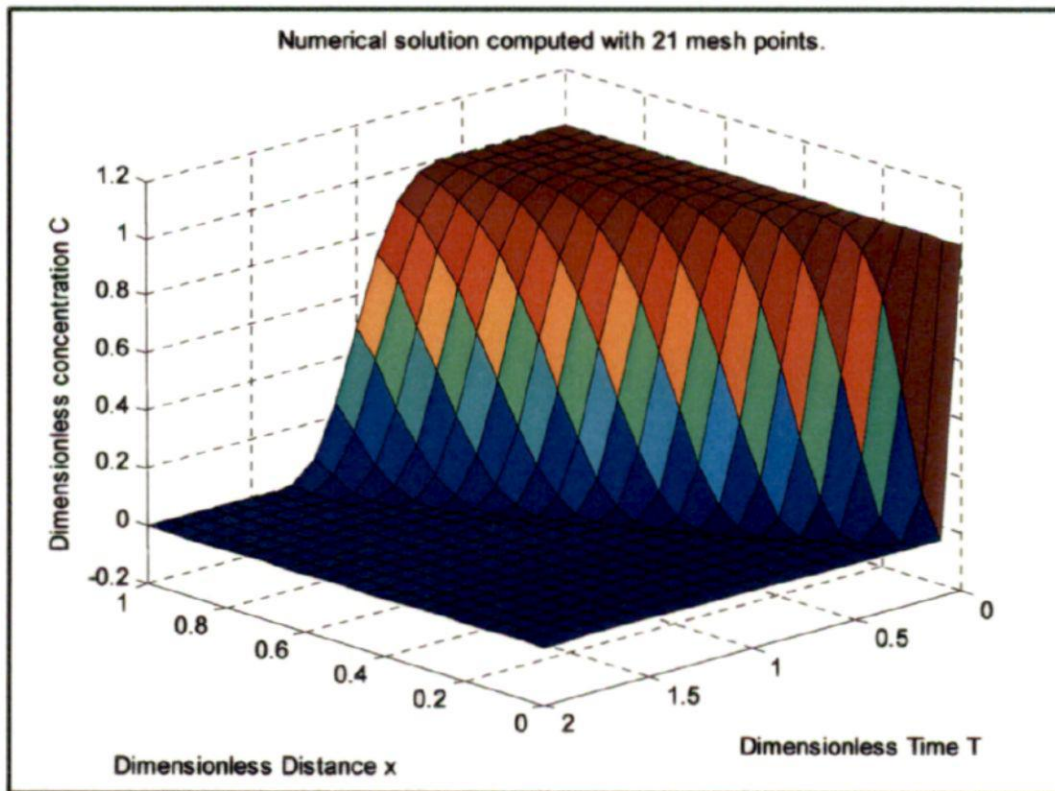


Figure 2.2 C vs. Z & T profile for model 1

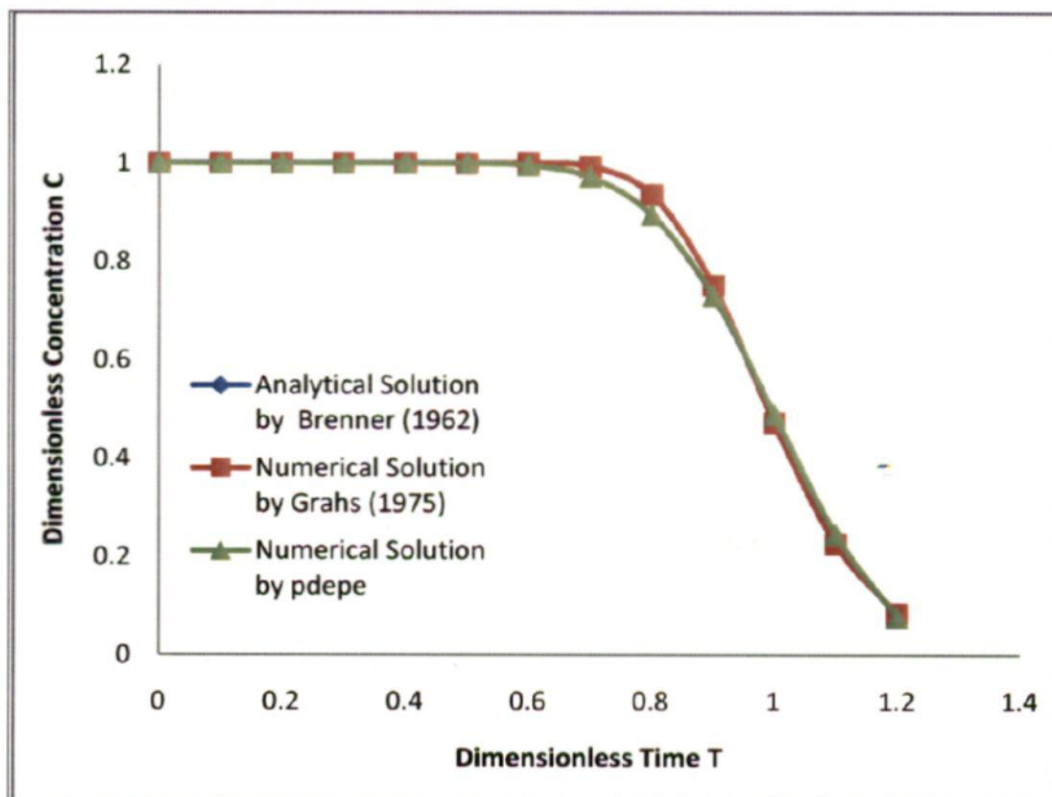


Figure 2.3 Comparison of the solutions of model 1 for  $Pe = 100$

In the present investigation a different numerical technique for the solution of such types of models is selected, which is easy to use, more efficient in processing time and gives the results with accuracy i.e. pdepe solver in MATLAB source code. Pdepe solver solves initial-boundary value problems for systems of parabolic and elliptic partial differential equations in the one space variable  $x$  and time  $t$ . Pdepe solver first discretized the partial differential equations into ordinary differential algebraic equations. The ordinary differential algebraic equations (ODEs) resulting from the discretization in space are integrated to obtain the approximate solutions for the given values of time.

## 2.5 Validation of the Solution Technique

For the validation of the solution technique (pdepe solver), the solution of displacement washing model 1 (Table 2.3) is obtained by taking  $Pe = 100$  using pdepe solver and compared with the analytical and numerical solutions of Brenner (1962) and Grahs (1975) respectively. Same data is used for simulation. The 3-Dimensional (3-D) behavior of the dimensionless concentration with respect to the dimensionless time and dimensionless cake thickness is shown by the Figure 2.2. The results of all three different solution techniques up to  $T = 1.2$  is presented in the Table 2.4.

[Since the solution for  $Pe = 100$  by Brenner (1962) and Grahs (1975) is available in the literature up to  $T = 1.2$ ]. To see the steady state behavior of the solution some imaginary layers of the cake are considered and for the solution dimensionless time is increased from  $T = 1.0$  to  $T = 2.0$  as shown in Figure 2.2. The comparison of the results at dimensionless distance at  $Z = 1$  for all values of dimensionless time with work of previous researchers is shown in the Figure 2.3.

Comparison shows that pdepe solver gives good accuracy and the magnitude of error is very low. It can be seen that at  $T = 0.5$  the error is 0.04% which is minimum and oscillate up to 9.13% in such a way that at  $T = 0.6$  error is 0.44%, at  $T = 0.7$  error is 2.16%, at  $T = 0.8$  error is 4.39%, at  $T = 0.9$  error is 2.89%, at  $T = 1.0$  error is 3.81%, at  $T = 1.1$  error is 8.53%, at  $T = 1.2$  error is 9.13% [Singh et al. (2008)].

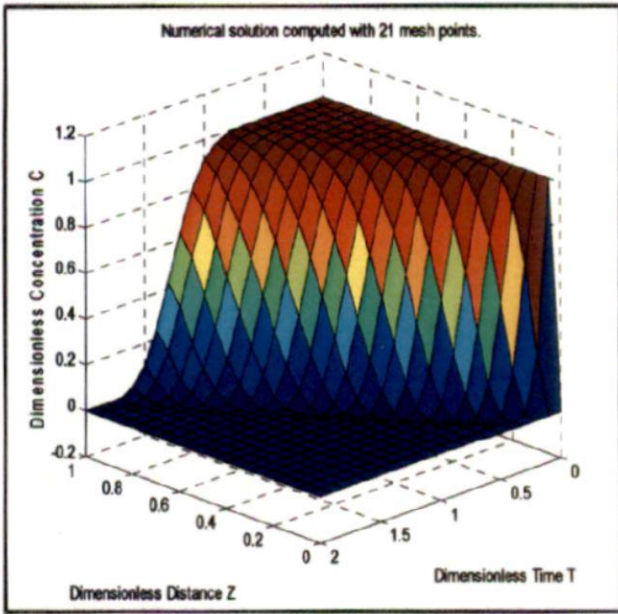


Figure 2.8 C vs. Z & T profile for model-6

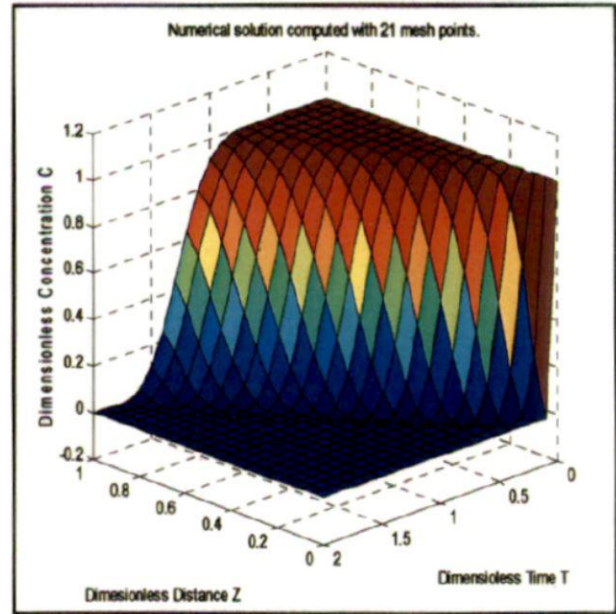


Figure 2.9. C vs. Z & T profile for model-7

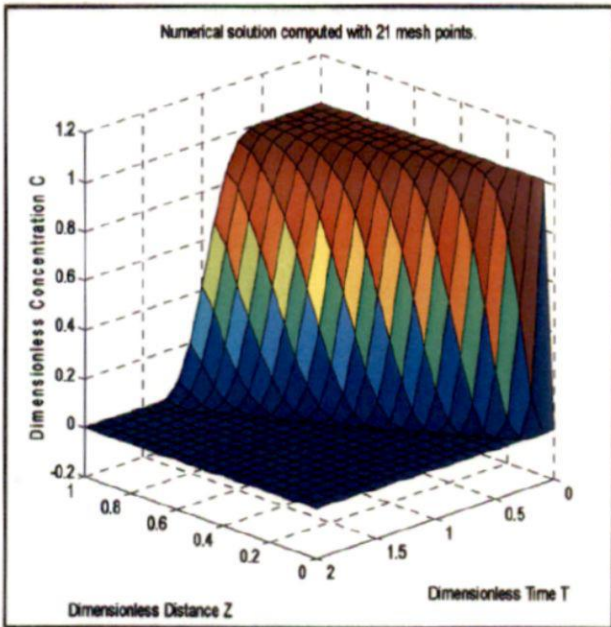


Figure 2.10 C vs. Z & T profile for model-8

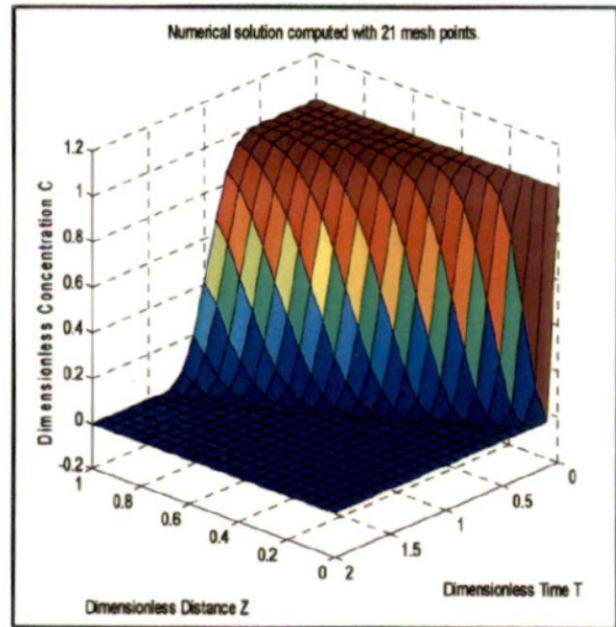


Figure 2.11. C vs. Z & T profile for model-9



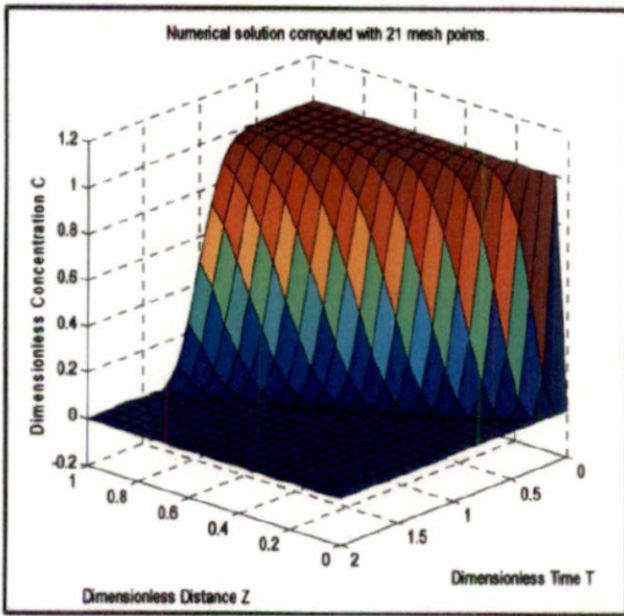


Figure 2.4 C vs. Z & T profile for model-2

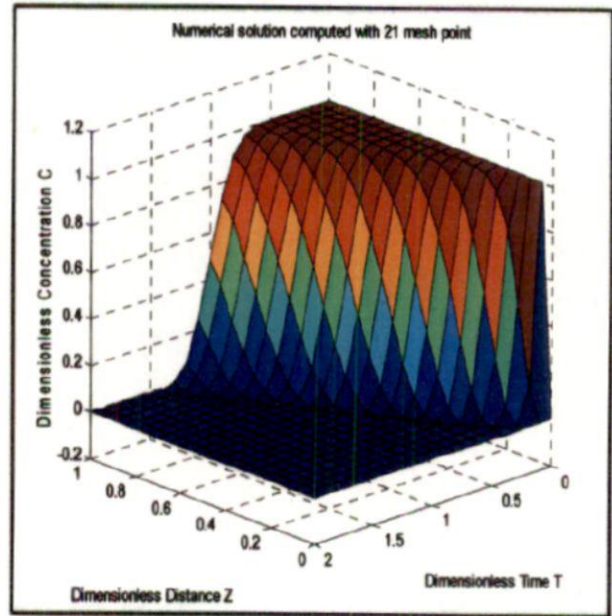


Figure 2.5. C vs. Z & T profile for model-3

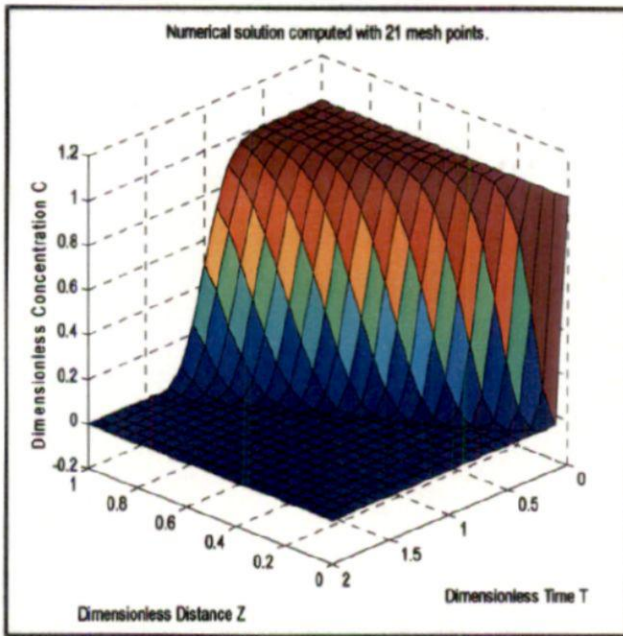


Figure 2.6 C vs. Z & T profile for model-4

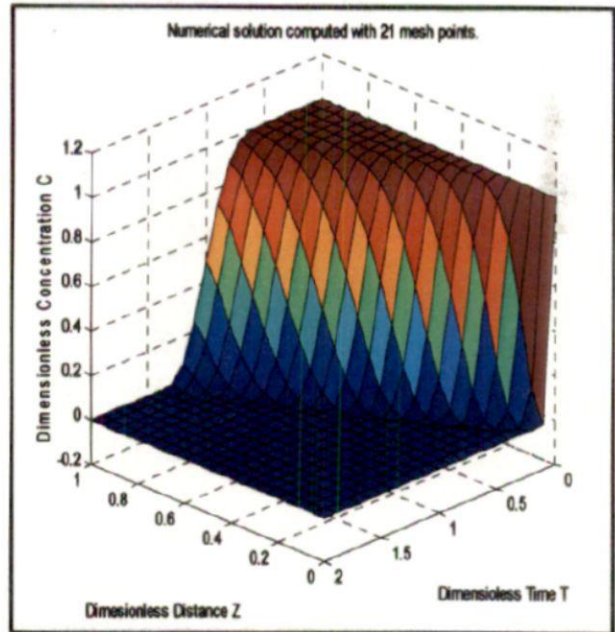


Figure 2.7. C vs. Z & T profile for model-5

## 2.7. Multistage Pulp Washing

To maximize washing effectiveness, while at the same time minimizing the amount of water used, counter flow washing is used. Counter flow is an engineering technique wherein two process streams interact as they move in opposite directions. As applied to pulp washing this means a series of washers is set up with the final wash being performed with clean water. The waste water from the last washer is then used to wash the stock in the second from the last washer. Water from the second to last washer is used to wash stock in a third to last washer and so on for the total number of washers' used. Typically three or four washers are required to adequately clean the black liquor from the digested pulp [Gallagher (1999)].

Mathematical treatment of the multistage countercurrent cake washing process is challenging. As the cake travels without reslurrying and is washed with progressively cleaner wash liquid, it develops a concentration profile or gradient that varies from stage to stage. [Crotagino et al. (1987), Edwards et al. (1976), Tomiak (1979b), Wakeman and Tarleton (1999)]. Thus, different recoveries are obtained at different stages. Tomiak (1979a) developed a method for predicting the performance of a belt filter. The method was based on the material balance equations for an individual stage; a fraction of the original liquid which is left in the cake discharges from a stage and washes liquid addition makes a contribution to the average overall cake concentration in the subsequent stages. The same sort of approach was used for solute material balance equation and a performance parameter for each stage was given; for instance the fraction of recoverable solute removed from the cake in each stage [Haywood (1995), Wakeman and Tarleton (1999)]. Other models are based on the theories developed by Tomiak (1973) in which the cake was represented with a number of perfectly mixing cells in series. In multistage countercurrent cake washing, mixing cells create an array. The wash effluent from the current stage to the previous stage circulates counter currently. The number of the mixing cells in the stage controls the washing efficiency for the stage. Ala-Kaila (1997) and Bilmez et al. (2000) applied a similar approach. Tervola (2006) developed a Fourier series solution for multistage counter current cake washing. The cake washing process was described by the advection-dispersion equation given by Brenner (1962). The solution method was employed to explore the multistage counter current cake washing in segregated and a non-segregated wash effluent circulation.

In the present investigation a typical four stages counter current washing system is considered. A series of four washers are set up for pulp washing with the final wash being performed with clean water. The steady state material balance equations can be easily be obtained for each washer with the help of the Figure 2.12 [Kukreja (1996)].

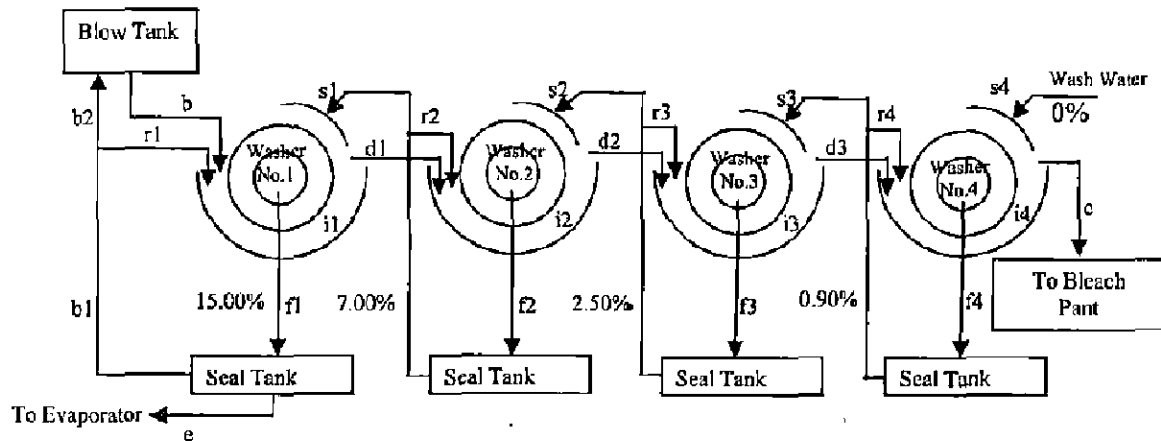


Figure 2.12 Flow diagram of a counter current washing system with four drum washers

## 2.8. Solution of Pulp Washing Models for Multistage

The pulp washing model as obtained in previous section with transport equation (9) and nonlinear Langmuir adsorption isotherm are used. The numerical solution is obtained for two different boundary conditions. Thus the models 8 and 9 (Table 2.3) are considered for the solution of multi-stage washing.

To find the solution of models 8 & 9 for multi-stage the values of various process parameters for washing zone of a washer is used given by Grahs (1974) for sodium ion species and are presented in Table 2.5. Steady state data of nearby paper mill presented in Table 2.7 is used for the solution of washing zone models for all four washers (stages).



**Table 2.7 Process data of four stage brown stock washing system [Kukreja (1996)]**

Input Parameters	Washer 1	Washer 2	Washer 3	Washer 4
$C_{yi}$ (%)	1.25	1.25	1.25	1.25
$C_{yd}$ (%)	12.00	12.00	13.00	14.00
$x_i$ (%)	15.59	7.29	2.62	0.96
$x_s$ (%)	7.00	2.50	0.90	0.50
$x_f$ (%)	15.00	7.00	2.50	0.90
$x_d$ (%)	10.12	3.77	1.58	0.30
$x_r$ (%)	15.00	7.00	2.50	0.90
$L_i$ (kg/Kg)	79.00	79.00	79.00	79.00
$L_s$ (kg/Kg)	10.33	10.33	9.69	9.14
$L_f$ (kg/Kg)	82.00	82.00	82.00	82.00
$L_d$ (kg/Kg)	7.33	7.33	6.69	6.14
$L_r$ (kg/Kg)	72.31	71.67	71.67	72.31

The washing liquor for the washers' 1, 2 & 3 contains the dissolved solids 7.00 %, 2.50 %, 0.9 % and in the last washer, fresh water is used which also contains 0.5% dissolved solids. The incoming pulp from the digester has the consistency 12%. In the vacuum rotary filter the feed consistency is 1.25% and the discharge consistencies are 12%, 13% and 14% (Table 2.7). The feed flow (1.25%) is thickened in the cake forming stage of the filter to the discharge consistency (let assume), so for instance (1/0.0125 - 1/0.120) kg/kg liquid is removed in the first washer. The filtrate coming from cake forming stage and from the displacement washing zone are mixed together. This filtrate is used for the dilution from the previous washer discharge to the feed consistency (1.25%). Peclet number of each washer (displacement zone) is calculated so that the measured dissolved dry solids or sodium values are near to the calculated values.

Peclet number has been included as dimensionless parameters in the solution of the models. For the washer No. 1, the Peclet number  $Pe = 71.26$  (by using  $Pe = u L / D_L$ ) has been used based on the simulation data presented in Table 2.5. Based on the data given in Table 2.7, the dimensionless time for the first and second washers is  $L_s/L_d$  i.e.  $10.33/7.33 = 1.41$ , for the third washer is  $9.69/6.69 = 1.45$  and finally for the last washer is  $9.14/6.14 = 1.49$ . Thus the exit dimensionless solute concentration for washer No. 1 & 2 is taken at  $T = 1.41$  and similarly for third and fourth washers at  $T = 1.45$  &  $T = 1.49$  respectively. The exit dimensionless solute concentrations for all

four washers at aforesaid values of dimensionless time are also presented in Table 2.8, for both the models.

**Table 2.8 Solutions of the models 8 & 9 for four washers (stages)**

T	Model 8				Model 9			
	Washer No. 1	Washer No. 2	Washer No. 3	Washer No. 4	Washer No. 1	Washer No. 2	Washer No. 3	Washer No. 4
0.1	1.0000	1.0000	1.0000	1.0000	1.0000	1.0000	1.0000	1.0000
0.2	1.0000	1.0000	1.0000	1.0000	1.0000	1.0000	1.0000	1.0000
0.3	1.0000	0.9998	0.9997	0.9997	1.0000	0.9998	0.9997	0.9996
0.4	1.0000	0.9964	0.9949	0.9946	1.0000	0.9963	0.9947	0.9944
0.5	0.9991	0.9769	0.9704	0.9695	0.9991	0.9764	0.9696	0.9686
0.6	0.9919	0.9211	0.9067	0.9046	0.9919	0.9297	0.9049	0.9027
0.7	0.9596	0.8195	0.7985	0.7954	0.9594	0.8172	0.7957	0.7925
0.8	0.8708	0.6832	0.6604	0.6568	0.8704	0.6803	0.6569	0.6533
0.9	0.7085	0.5357	0.5153	0.5118	0.7080	0.5327	0.5118	0.5082
1.0	0.4997	0.3990	0.3827	0.3795	0.4993	0.3963	0.3796	0.3762
1.1	0.3039	0.2856	0.2732	0.2702	0.3037	0.2834	0.2706	0.2675
1.2	0.1682	0.1993	0.1892	0.1863	0.1681	0.1976	0.1872	0.1842
1.3	0.0991	0.1377	0.1284	0.1254	0.0990	0.1365	0.1269	0.1239
1.4	----	----	----	0.0831	----	----	----	0.0820
1.41	0.0733	0.0925	----	----	0.0733	0.0918	----	----
1.45	----	----	0.0706	----	----	----	0.0697	----
1.49	----	----	----	0.0570	----	----	----	0.0563

Based on C vs. T data of previous washer, the Peclet number of subsequent washer is obtained by using algorithm given by Kumar (2002). The Peclet number for displacement washing zone of second and subsequent washers are estimated approximately by considering open vessel as used by Han and Edwards (1988), Edwards et al. (1986) and Potucek (1997). The following algorithm given by Kumar (2002) is used for calculating the Peclet number for the subsequent washers.

- Obtain C vs. T data for the first washer by solution of the model

- Find out the mean time  $\tau_i = \frac{\sum T_i C_i \Delta T_i}{\sum C_i \Delta T_i}$

- Find the spread of the distribution, measured by the variance representing the spread of the

$$\text{distribution } \sigma^2 = \frac{\sum T_i^2 C_i \Delta T_i}{\sum C_i \Delta T_i} - \tau_i^2$$

- Fit the dispersion model for the large extent of the dispersion for open vessel

$$\sigma_a^2 = \frac{\sigma^2}{\tau_i^2} = 10 \left( \frac{D_L}{uL} \right) = \frac{10}{Pe}$$

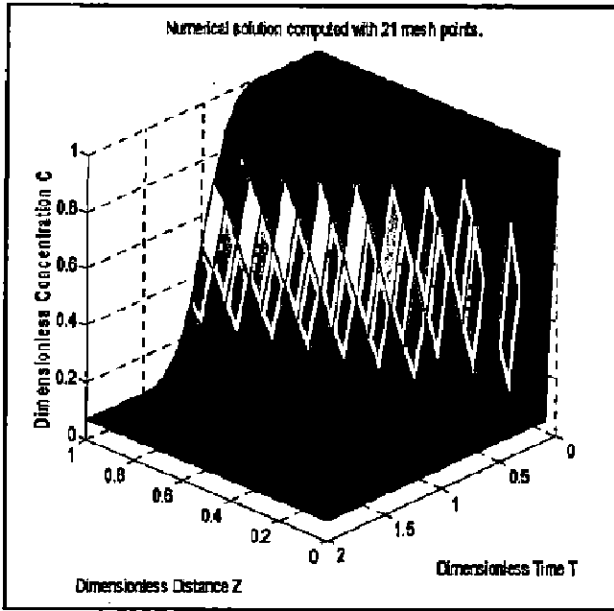
The Peclet number obtained by this algorithm for washers No 2, 3 & 4 for both the models 8 & 9 are presented in Table 2.9.

Exit dimensionless solute concentration for previous stage washer is converted into absolute concentration and is used as initial concentration for the subsequent washer. Dimensionless initial solute concentration on fiber i.e.  $N_0$ , porosity term  $\mu'$  etc are calculated by using initial absolute concentration of previous washer and are also presented in Table 2.9 for all four washers.

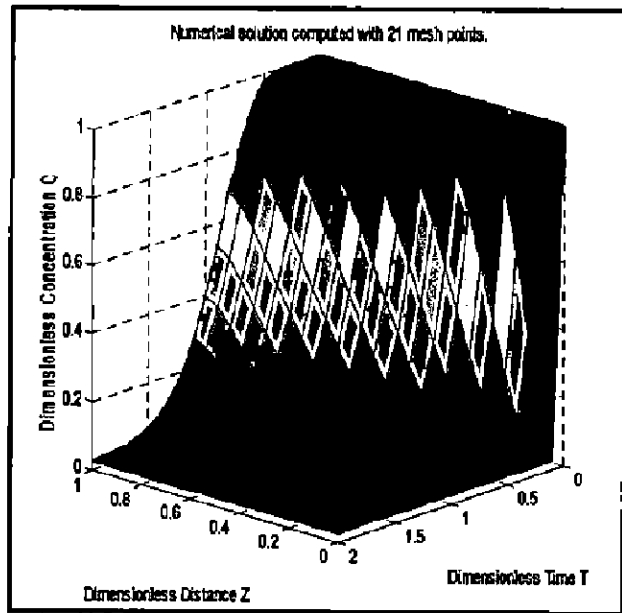
**Table 2.9 Peclet Number (Pe),  $N_0$  and  $\mu'$  for all four washers**

Washer No.	Model-8			Model-9		
	Pe	$N_0$ (Kg/m <sup>3</sup> )	$\mu'$	Pe	$N_0$ (Kg/m <sup>3</sup> )	$\mu'$
1.	71.26	0.009	$1.23 \times 10^{-3}$	71.26	0.009	$1.23 \times 10^{-3}$
2.	21.94	0.002	$3.93 \times 10^{-3}$	21.93	0.002	$3.93 \times 10^{-3}$
3.	19.90	0.0002	$5.60 \times 10^{-3}$	19.90	0.0002	$5.60 \times 10^{-3}$
4.	19.70	0.00001	$3.88 \times 10^{-3}$	19.67	0.00001	$3.88 \times 10^{-3}$

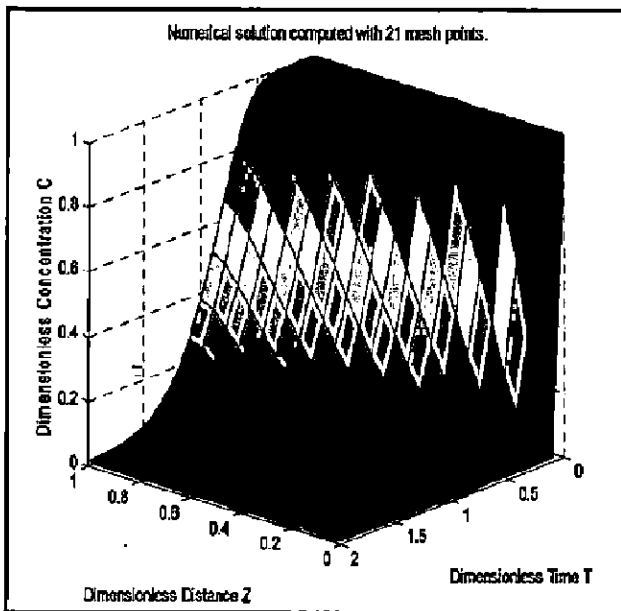
Dimensionless bed depth as well as dimensionless time is divided into 21 equal parts and then the influence of Z & T on C is estimated. The behavior of exit dimensionless solute concentration with respect to dimensionless time as well as dimensionless cake thickness are depicted using input curve at Z = 0 to break through curves at Z = 1, by 3-D graphs which are shown from the Figure 2.13(a) to Figure 2.13(d) for model 8 and Figure 2.14(a) to Figure 2.14(d) for model 9 for all four washers respectively. The washing results for both the models are slightly different at three to four decimal places, so it may concluded that the boundary conditions do not influence much on the washing results.



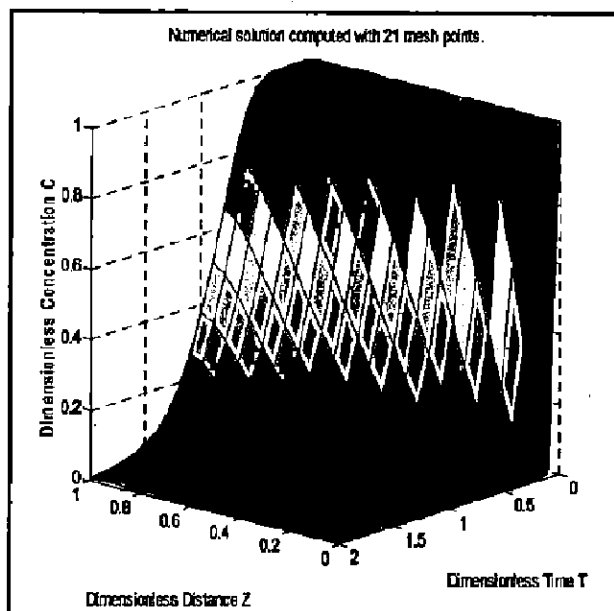
(a) C vs. Z & T profile for washer No. 1



(b) C vs. Z & T profile for washer No. 2

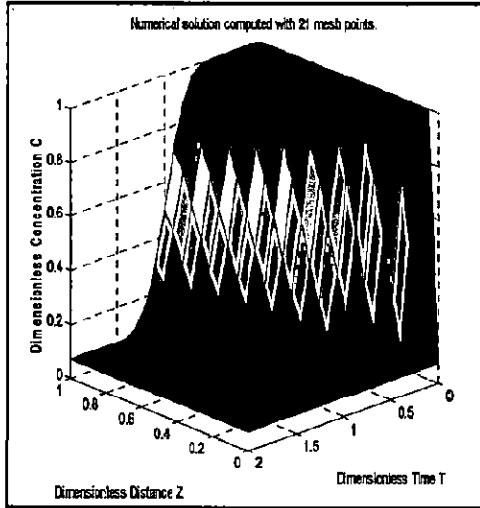


(c) C vs. Z & T profile for washer No. 3

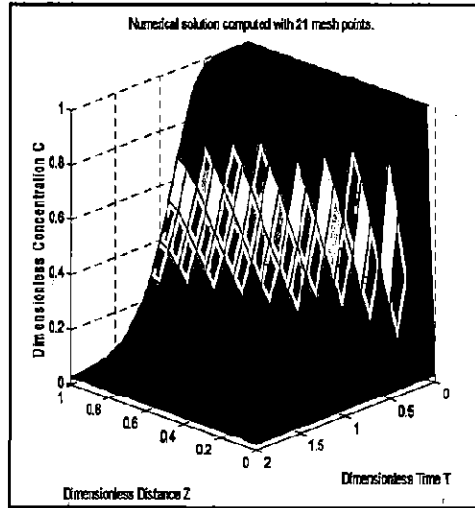


(d) C vs. Z & T profile for washer No. 4

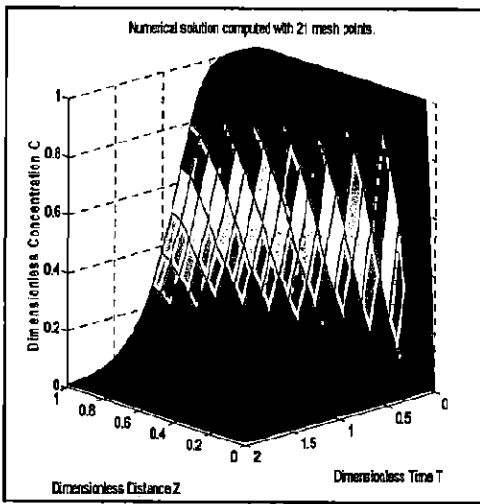
Figure 2.13 Solution of different stages (washers) for model-8



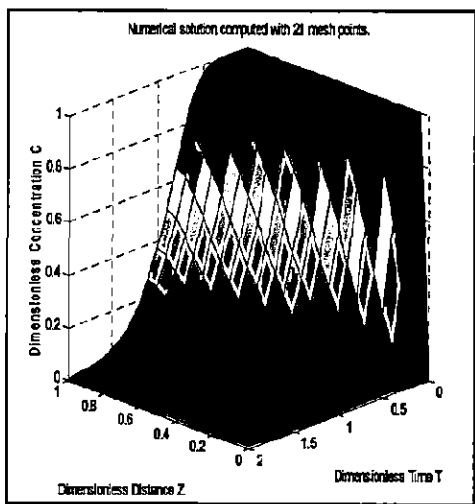
(a) C vs. Z & T profile for washer No. 1



(b) C vs. Z & T profile for washer No. 2



(c) C vs. Z & T profile for washer No. 3



(d) C vs. Z & T profile for washer No. 4

Figure 2.14 Solution of different stages (washers) for model-9

## 2.9 Analysis of Parametric Effects on Efficiency of Multistage Brown Stock Washers

The effects of various parameters on performance of single stage brown stock washer in paper industry are studied for different species of black liquor by some earlier researchers like Grahs (1974), Kukreja (1996), Kumar (2002), Arora et al. (2006a, b) and Kumar et al. (2009a, b). Grahs (1974) studied the effects of dimensionless time, wash ratio, longitudinal dispersion coefficient, mass transfer coefficient and cake porosity for sodium and lignin ion species of black liquor. Kukreja (1996) discussed the various parametric effects with a view to analyze the performance of brown stock washer and interrelationship between various parameters like fractional submergence, rpm, filtrate flow rate, cake thickness, inlet vat consistency and fiber production rate. Kumar (2002) studied the parametric effect by modifying the range of the parameters used by Grahs (1974), using two different kinds of linear adsorption isotherms in the model for both sodium and lignin species. Arora et al. (2006a) studied the parametric effect of various parameters like Peclet number, interstitial velocity, cake thickness, bed porosity, reaction rate constants and distribution ratio on exit solute concentration. One common feature of the above work is that all have studied the parametric effect for single stage washing to reduce the mathematical complexities. The parametric study for the multistage washing system is very typical task. Recently the author studied the effect of various parameters on the exit solute concentration by varying the range of parameters at mid cake thickness as well as bed exit by using three linear adsorption isotherms for both sodium and lignin species using pdepe solver in MATLAB source code for the solution of models for single stage washing [Kumar et al. (2009a, b)]. In the present study the parametric effects are studied for four stage washing system. Non linear Langmuir isotherm is used to correlate the interfiber and intrafiber concentration. Thus for the effects of various parameters like, Peclet number, kappa number and porosity on efficiency of multi-stage brown stock washers are obtained by solving the models 8 & 9 (Table 2.3) for four stage washing system with different values of the above parameters. The range of basic input parameters is used as given by Kumar (2002). In order to achieve the above goal one needs some data for the fiber, fiber bed, kraft black liquor concentration such as, cake thickness, pulp pad consistencies, velocities through bed and Langmuir constants. In the absence of any reliable industrial data, the data given by Grahs (1974) (Table 2.5) has been used for the basis of simulation.

The parametric effects of Peclet number, kappa number and porosity are shown by the C vs. T graphical representations for constant bed depth at  $Z = 1.0$  and the effects of dimensionless cake thickness and dimensionless time are shown by C vs. Z & T profiles (3-D graphs) for the various values of parameters for sodium ion species.

### **2.9.1. Effects of pecelet number on exit solute concentration**

The range of Peclet number from 20 to 110 is found to be valid for pulp washing as suggested by earlier investigators including Grahs (1974) and further modified by Kumar (2002). The effect of Peclet number is studied for the same range. To see the steady state behavior of the curves some idle layer of the cake is considered and behaviour of the solution curve is also checked by increasing the dimensionless time from  $T = 1.0$  to  $T = 2.0$ . The variation in the Peclet number is applied in the first washers and the influence on C vs. T profiles is studied for all four washers. The Peclet number for the second and subsequent washer is calculated as discuss previously in section 2.8. The effects of Peclet number on the exit solute concentration for all four washers are shown from Figure 2.15 to Figure 2.22 for both the models 8 & 9. In the first washer, the stream of the curves start from  $C = 1.0$ , descending differently but however converge at  $T = 1.1$  and again diverge from each other in topsy-turvy manner, this fact is found to be in agreement with Kumar (2002). For Peelet number below 20 (say 10 to 19) more deviation in the profile is observed. Hence the higher Peclet number shows the minimum deviation in the shape of breakthrough curves as shown in the C-T profiles (Figure 2.15 and Figure 2.16) of washer 1 for both models 8 & 9. The deviation for  $Pe = 20$  is maximum for  $T = 0.5$  to  $T = 1.0$ , which continually decreases for higher Peclet numbers. The Peclet number has significant influence on dynamic behavior of solute concentration for washer 1 which decreases continuously for washer 2 to 4 for both the models as shown from Figure 2.17 to Figure 2.22. This is due to the range of variation in Peclet number for first washer is from 20 to 120, which reduces in second washer from 19.69 to 22.49, for third washer from 19.65 to 19.96 and for the fourth washer is from 19.664 to 19.672 for model 8 (range for model 9 are slightly different).

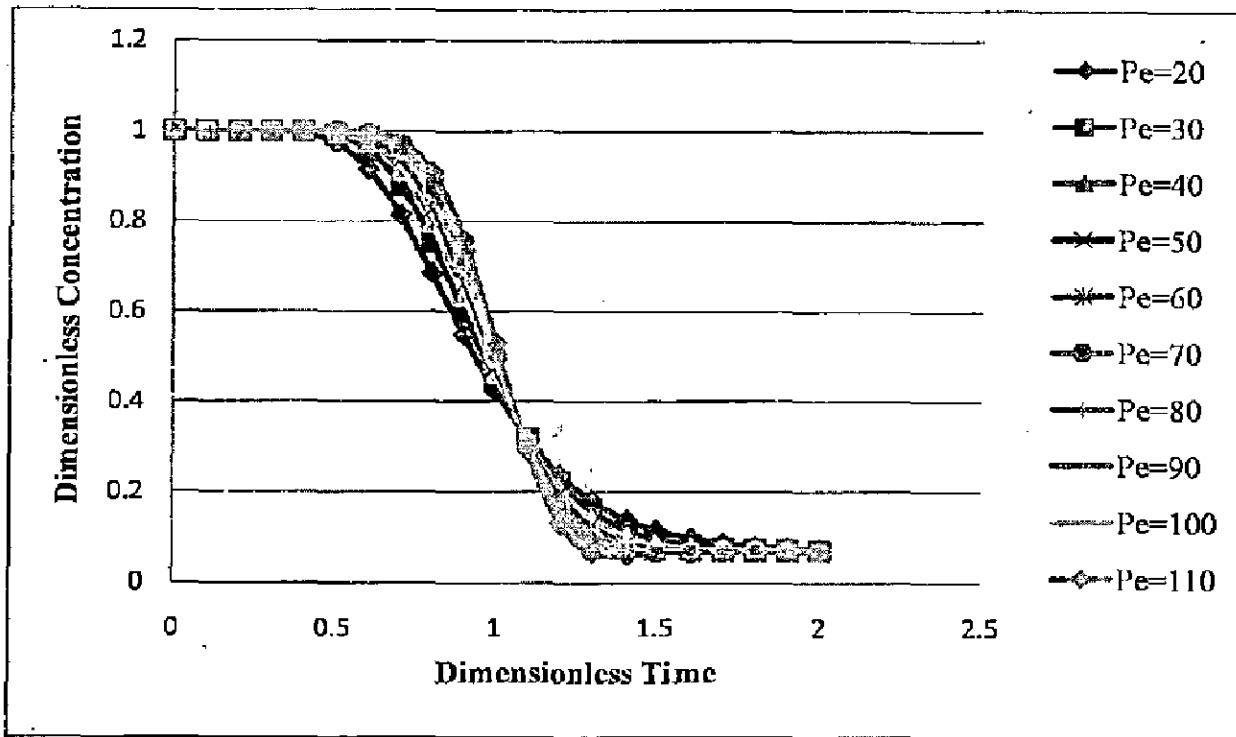


Figure 2.15 C vs. T profile for various values of Pe at bed exit of washer-1 for model-8

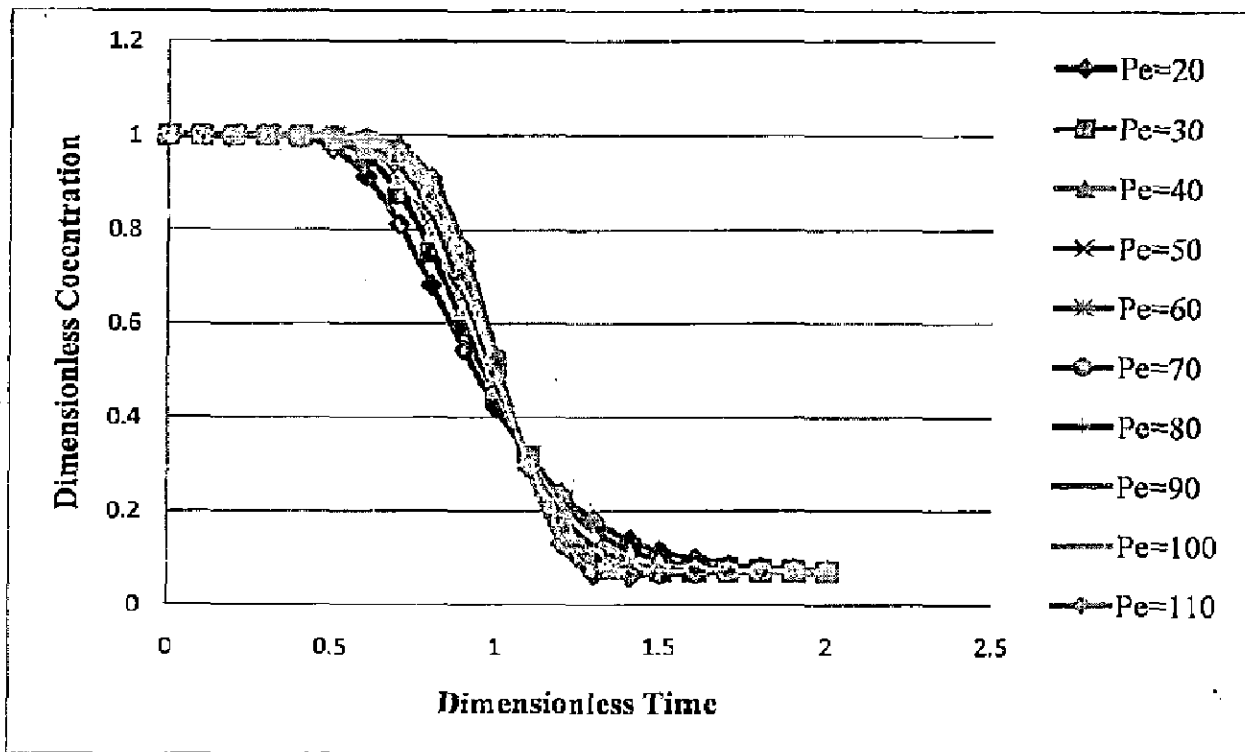


Figure 2.16 C vs. T profile for various values of Pe at bed exit of washer-1 for model-9



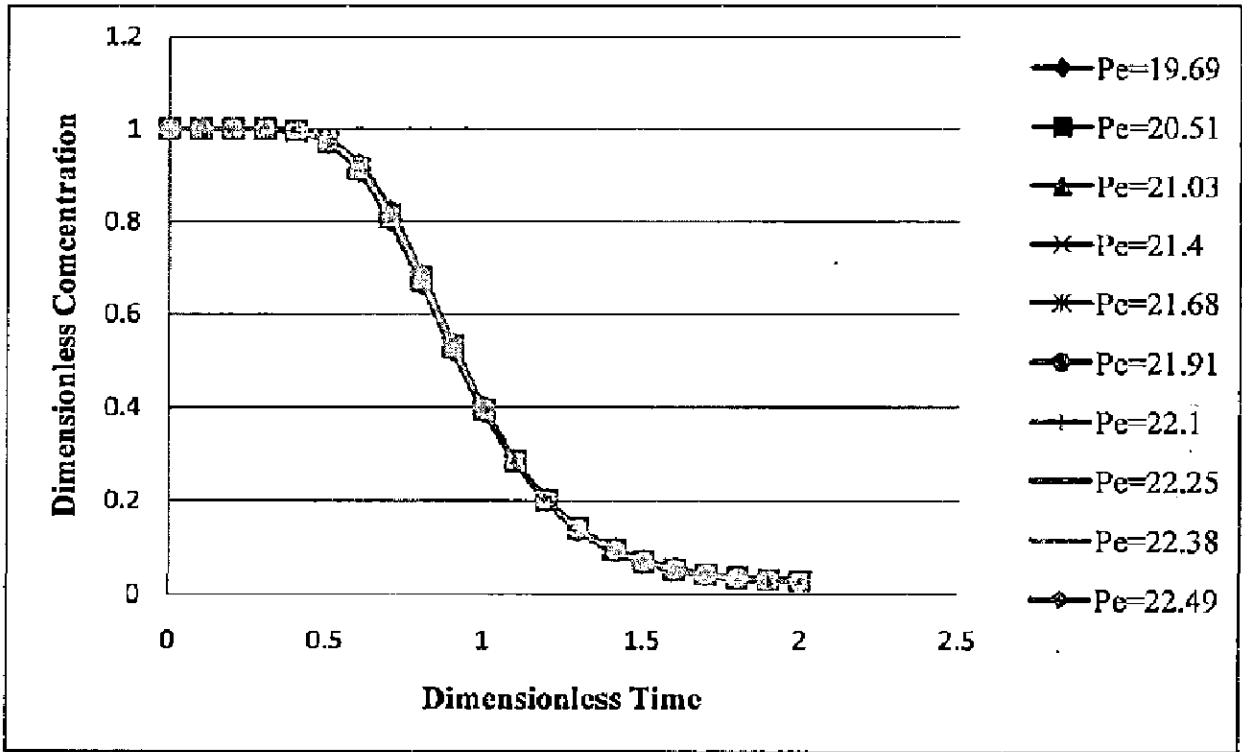


Figure 2.17 C vs. T profile for various values of Pe at bed exit of washer-2 for model-8

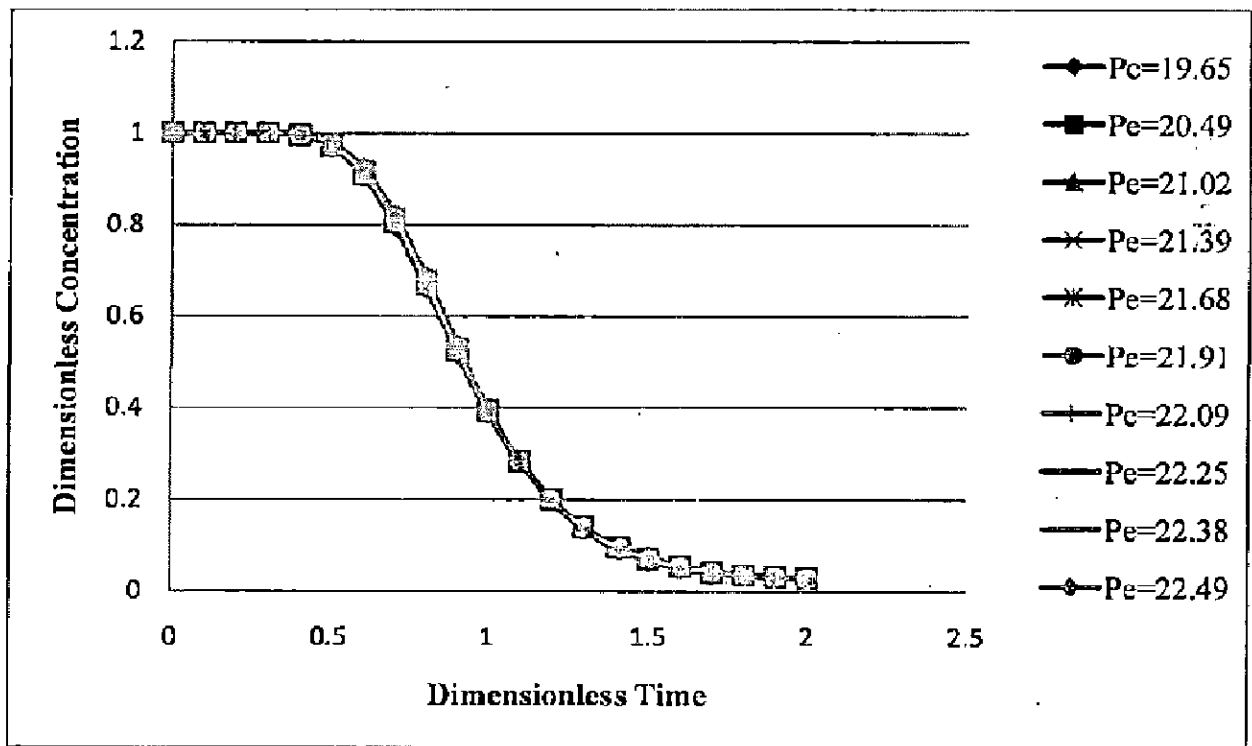


Figure 2.18 C vs. T profile for various values of Pe at bed exit of washer-2 for model-9

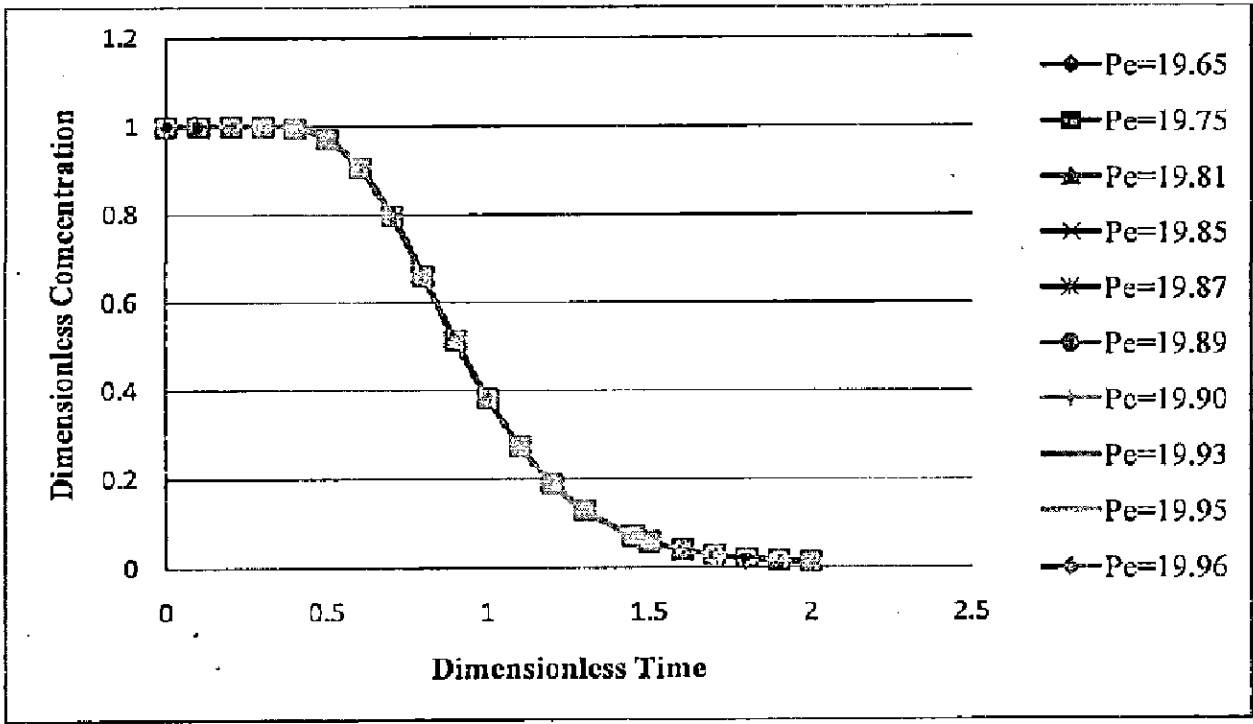


Figure 2.19 C vs. T profile for various values of Pe at bed exit of washer-3 for model-8

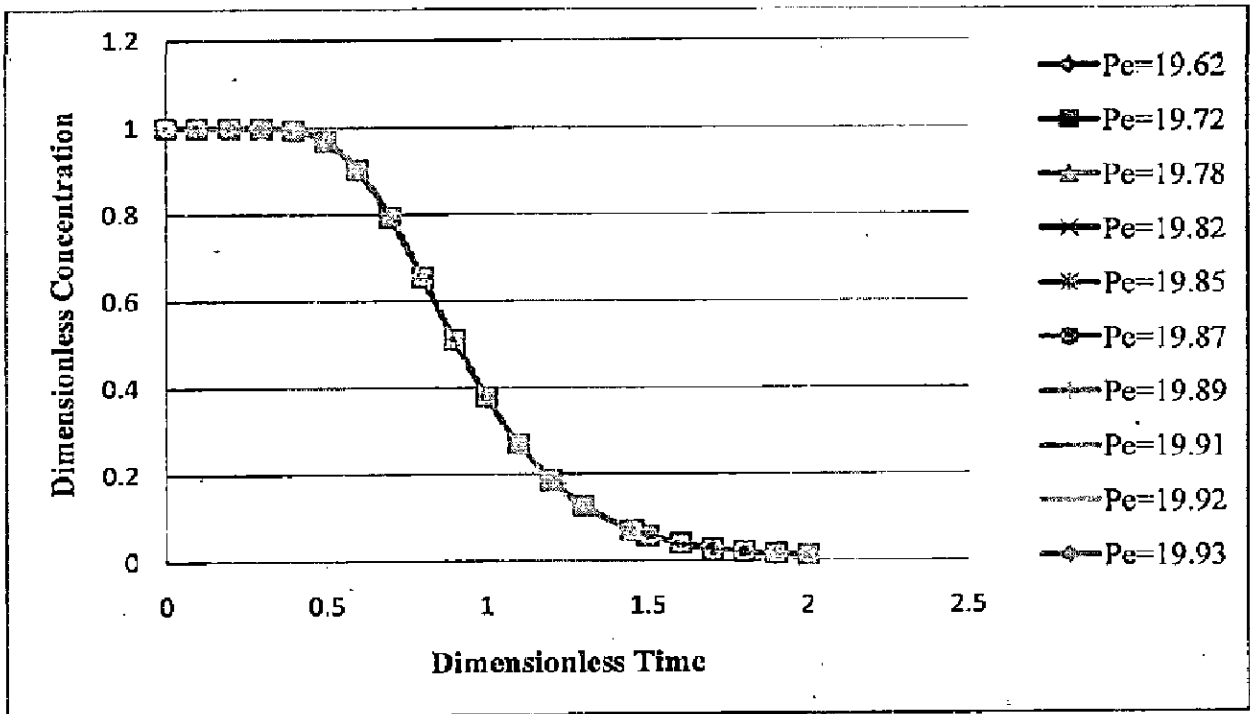


Figure 2.20 C vs. T profile for various values of Pe at bed exit of washer-3 for model-9

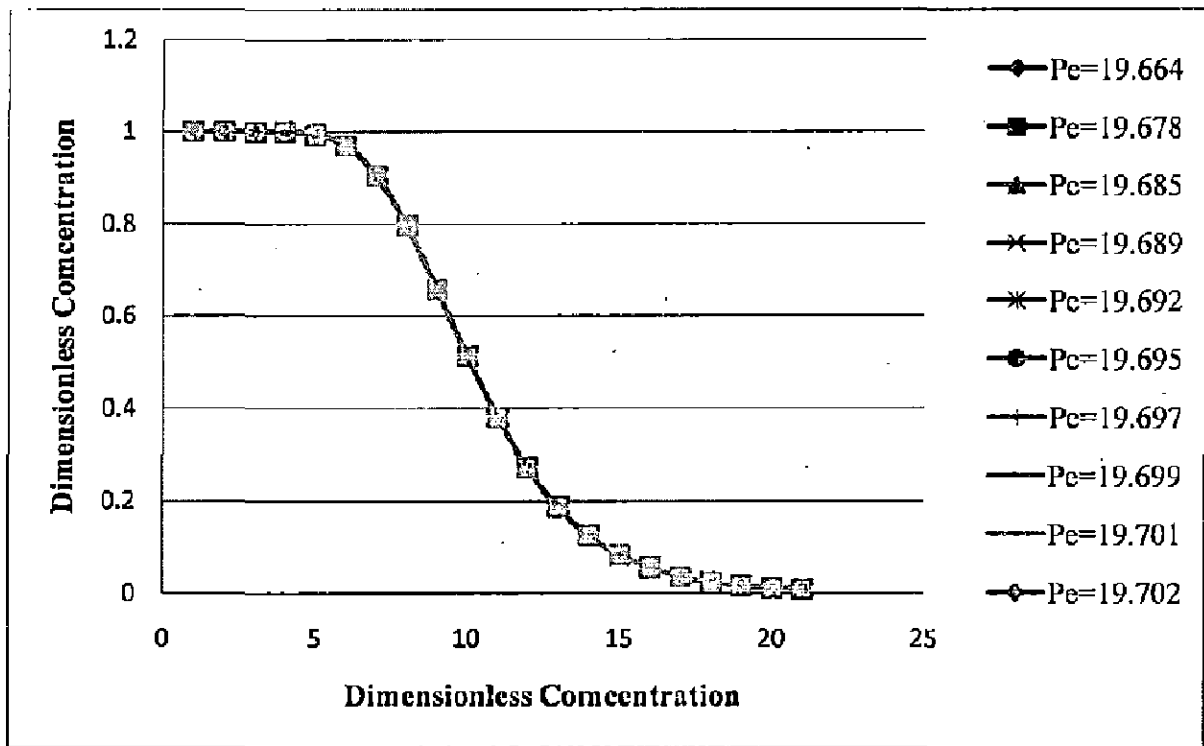


Figure 2.21 C vs. T profile for various values of Pe at bed exit of washer-4 for model-8

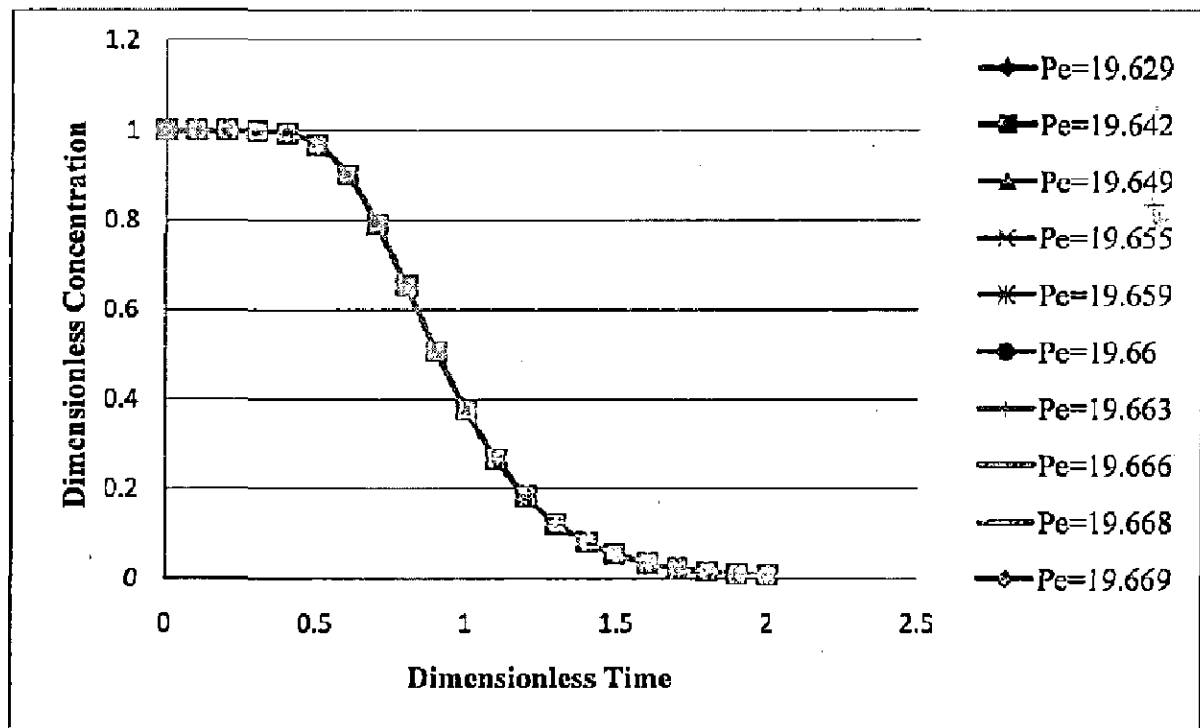


Figure 2.22 C vs. T profile for various values of Pe at bed exit of washer-4 for model-9

### 2.9.2. Effects of kappa number on exit solute concentration

The Kappa number is an indication of the residual lignin content or bleachability of wood pulp. Although, it should be noted that there is no general relationship between the Kappa number and the lignin content, and it depends on type of raw material and delignification process. Neither pulp washing model equation nor Langmuir adsorption isotherm contain any term related to kappa number. However it was observed by the previous researcher that Langmuir constants depend on the kappa number. Grahs (1974) reported a linear relationship, if  $c/n$  is plotted against  $c$ , if the isotherm is of Langmuir type. It is, then easy to determine the Langmuir constants A and B from the intercept and slope of the straight line. For the purpose four sample of pine sulphate pulp of different kappa number is used. Thus for the parametric study of kappa number the data obtained by Grahs (1974) (Table 2.10) is used in which Langmuir constants A and B is obtained for four different pine sulphate pulps (pulp of different kappa numbers).

The solutions of the both washing models is obtained for all different values of the kappa number and C vs. T profile arc shown by the Figure 2.23 to Figure 2.30. Varying the kappa number from 22.4 to 72.6 in the first washer, a very small deviation observed in the C-T profiles for all washers which is negligible in the engineering practice. If some imaginary layer of the cake is considered and solution is obtained by increasing the dimensionless time from  $T = 1.0$  to  $T = 2.0$ , the breakthrough curve reaches the steady state for all washers. It is also clear by the C vs. T profile that the curve for the first washer is steady state at  $T = 1.5$  while for other washer at  $T = 2.0$  for both the models 8 & 9.

Table 2.10 Peclet Number for all four washers

S. No.	Kappa Number	A	B
1.	22.4	0.01324	6.586
2.	43.4	0.01401	5.232
3.	49.7	0.01263	3.955
4.	72.6	0.01195	2.798

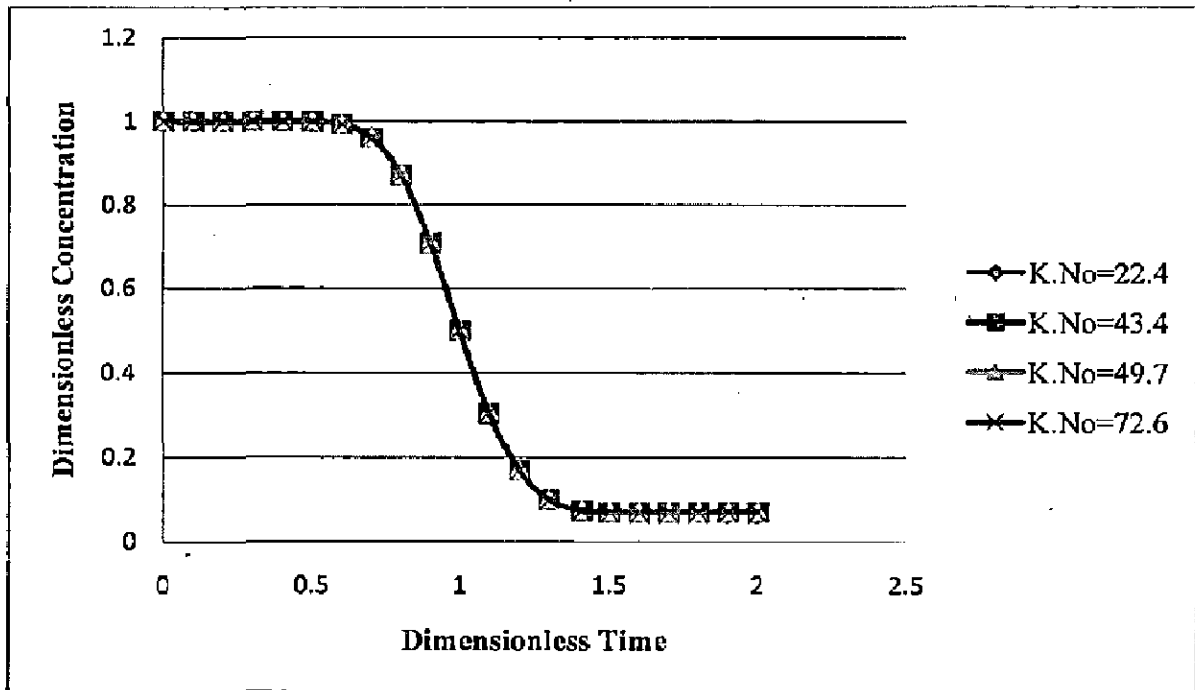


Figure 2.23 C vs. T profile for various values of K. No. at bed exit of washer-1 for model-8

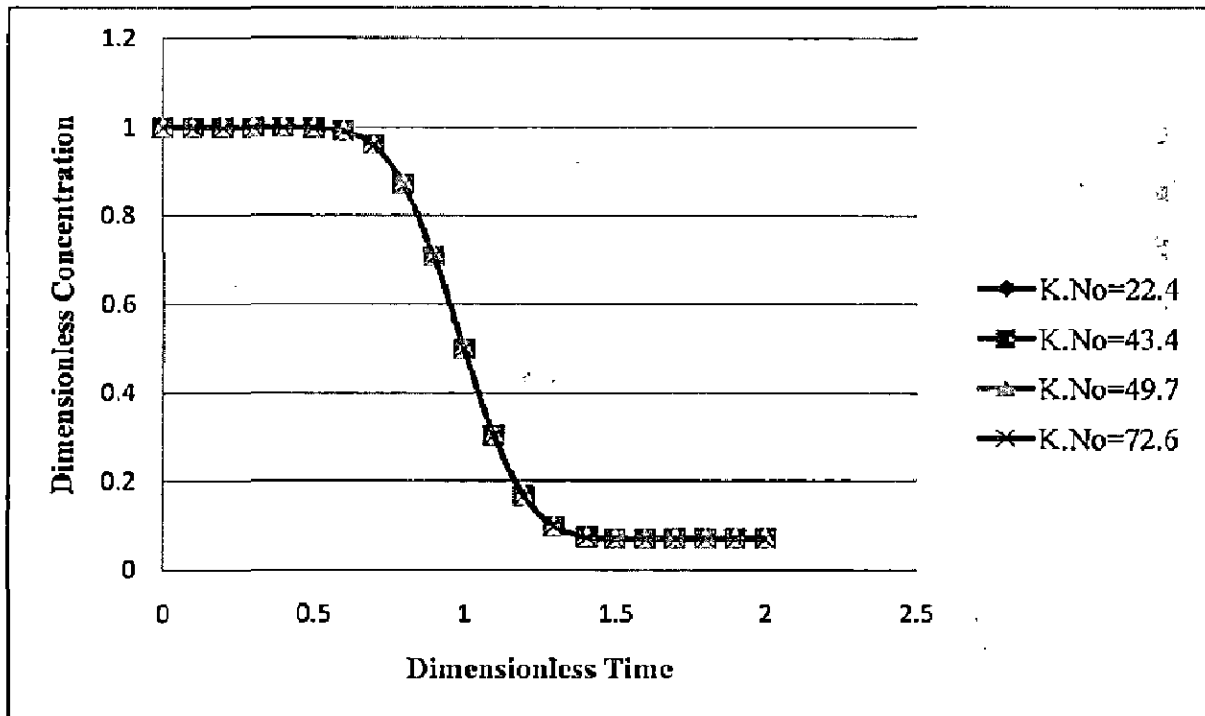
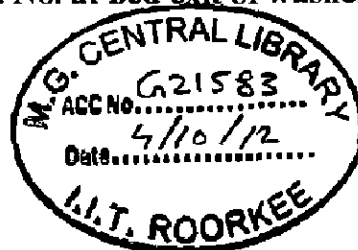


Figure 2.24 C vs. T profile for various values of K. No. at bed exit of washer-1 for model-9



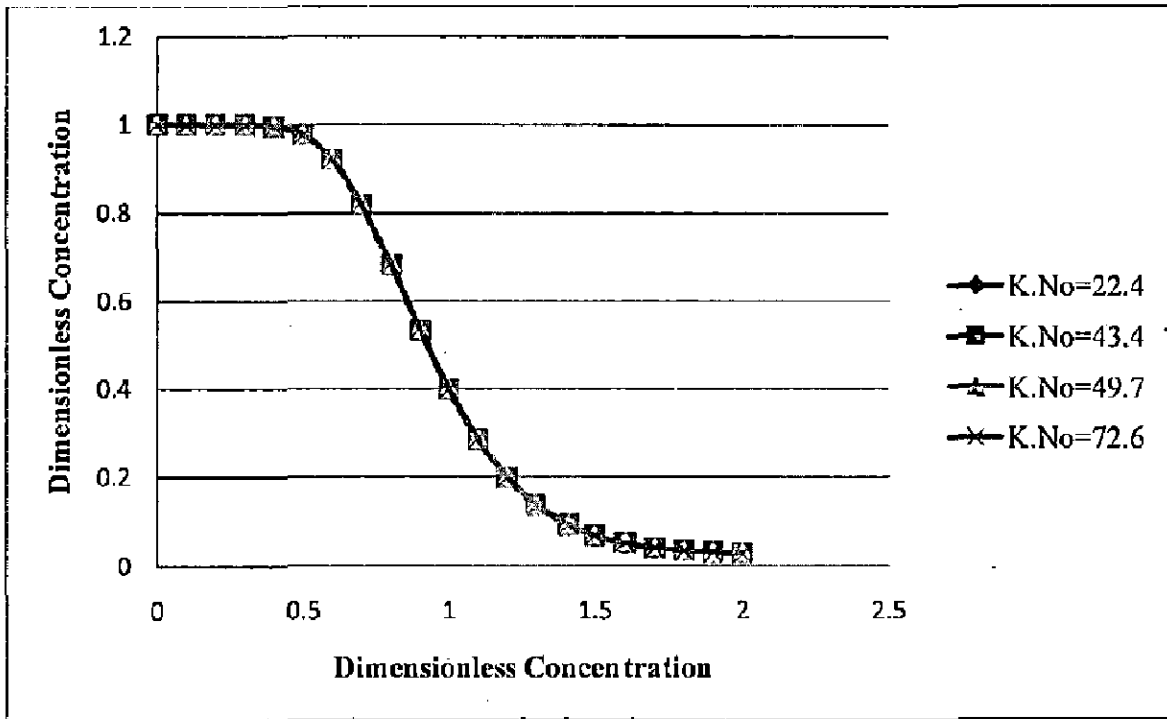


Figure 2.25 C vs. T profile for various values of K. No. at bed exit of washer-2 for model-8

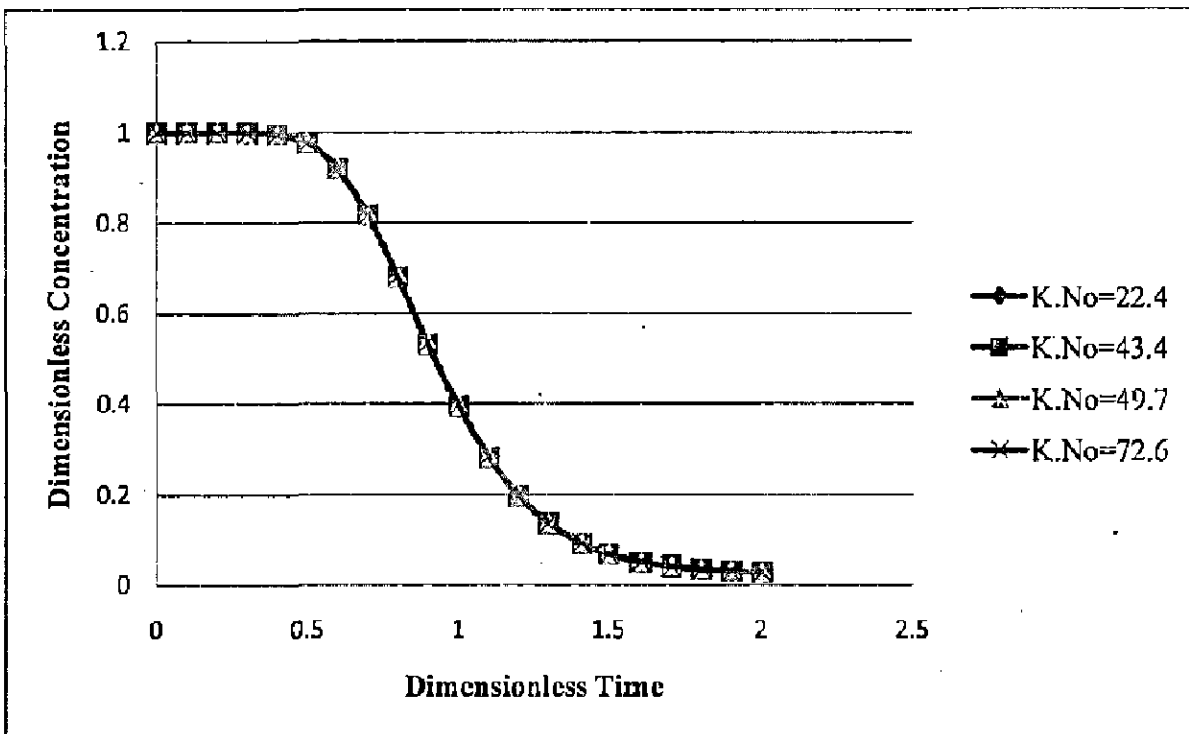


Figure 2.26 C vs. T profile for various values of K. No. at bed exit of washer-2 for model-9

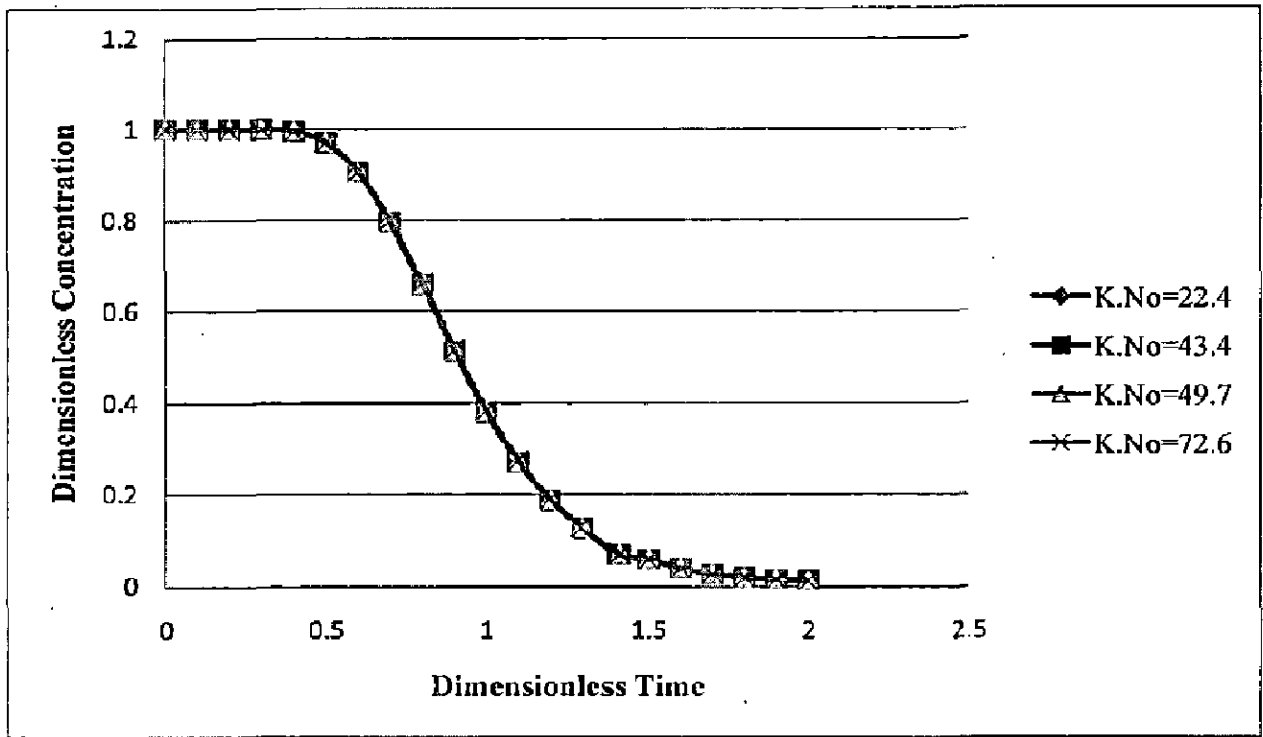


Figure 2.27 C vs. T profile for various values of K. No. at bed exit of washer-3 for model-8

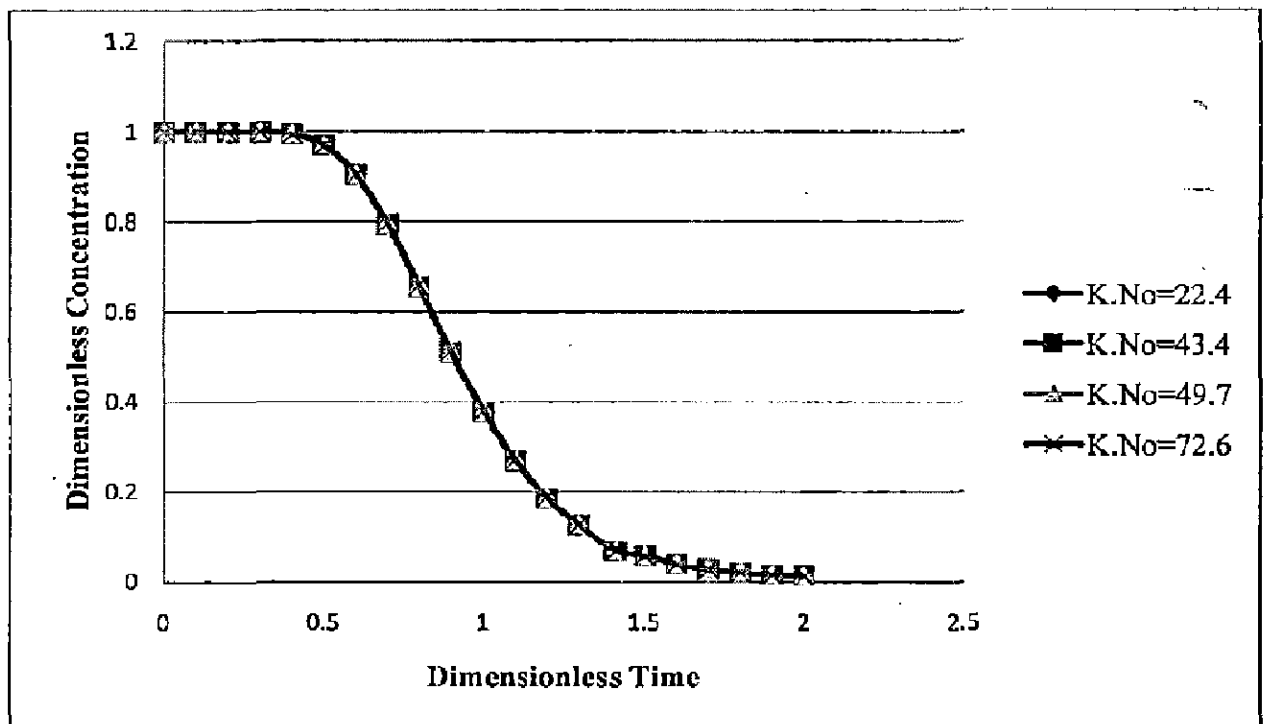


Figure 2.28 C vs. T profile for various values of K. No. at bed exit of washer-3 for model-9

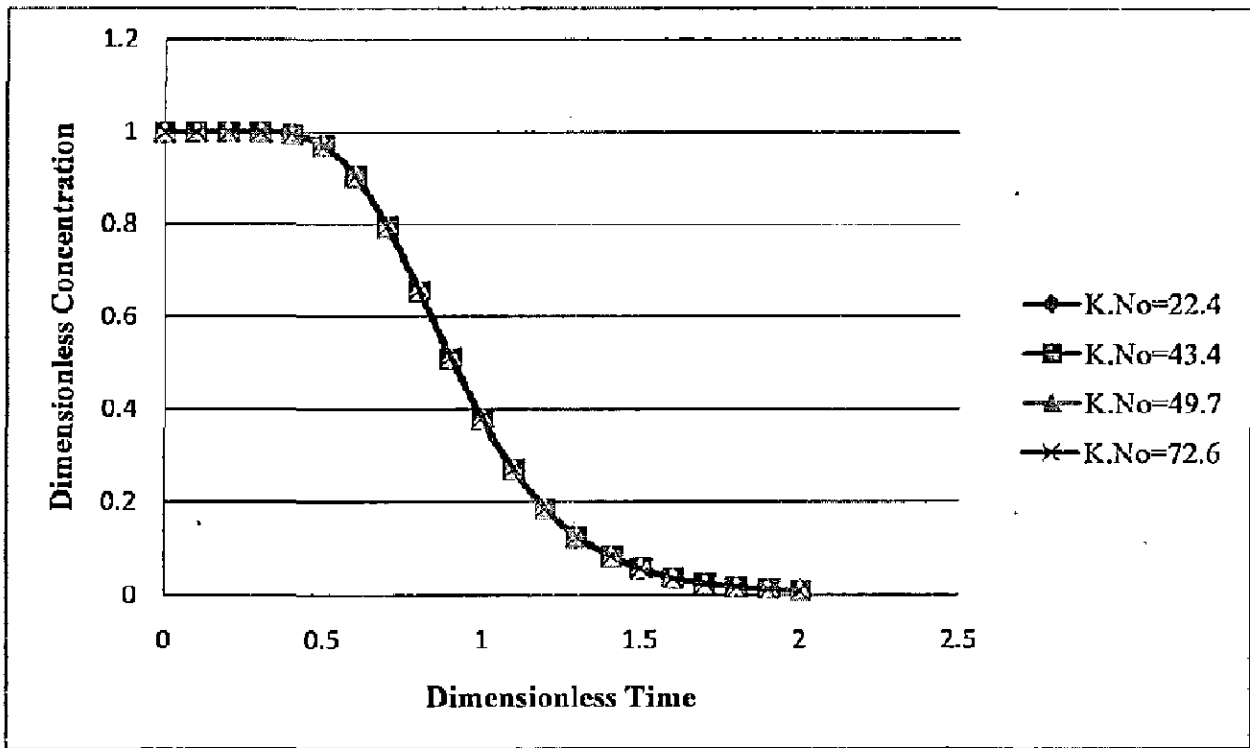


Figure 2.29 C vs. T profile for various values of K. No. at bed exit of washer-4 for model-8

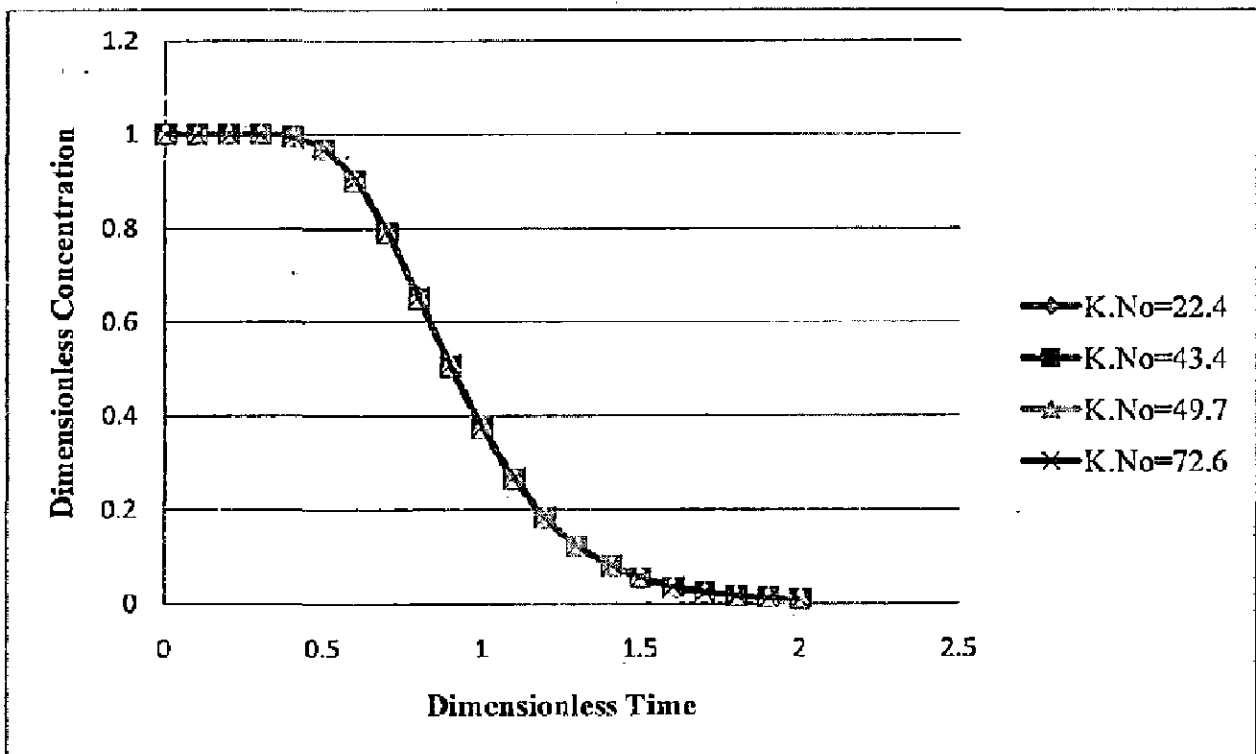


Figure 2.30 C vs. T profile for various values of K. No. at bed exit of washer-4 for model-9



### 2.9.3. Effects of porosity on exit solute concentration

Porosity is defined as the ratio of the volume available for flow to the total volume. Porosity of the mat is an important factor as the hydrodynamics of the filtration is highly influenced by the porous path through which the fluid will move. In the present case, porosity is based on the average consistency of the mat during the cake formation zone. The air effect on the porosity has been neglected. Porosity of the pulp suspension varies from 0.1 to 0.99, but is always less than 1. Longer range is considered to cover not only the entire range of suspension hebetated by the stock in the paper making process in practice, but also to cover the porosity value of the flowing zone (0.7 to 0.85), stagnant zone (0.1 to 0.2) and total mean porosity values above 0.90. So for the study of the effect of porosity on exit solute concentration, the value of the porosity is taken from 0.1 to 0.95 as used by Kumar (2002).

The variation in the porosity is also applied on first washer and then the influence in C vs. T profile is observed for all washers for both the models 8 & 9. The C vs T profiles for different porosity at the bed exit i.e at  $Z = 1.0$ , are shown from the Figure 2.31 to Figure 2.38 for both the models for sodium ion species of black liquor. The deviation in the breakthrough curve start after  $T = 0.5$ . For the porosity values below 0.40 (say 0.10 to 0.30) significant deviations in the profile is observed, and while the higher porosity values show the practically no deviation in the shape of breakthrough curves. From the figures, it is also clear that maximum deviation is observed at  $\epsilon = 0.10$  for all four washers. It is also observed that deviation increases from first washer to last washer. To study the steady state behavior of the curve some imaginary layer of the cake is considered and effect is also checked by increasing the dimensionless time from  $T = 1.0$  to  $T = 2.0$ . From the figures it is also clear that the washer 1 achieves steady state before  $T = 1.5$  while all other washers achieve steady state after  $T=1.5$ .

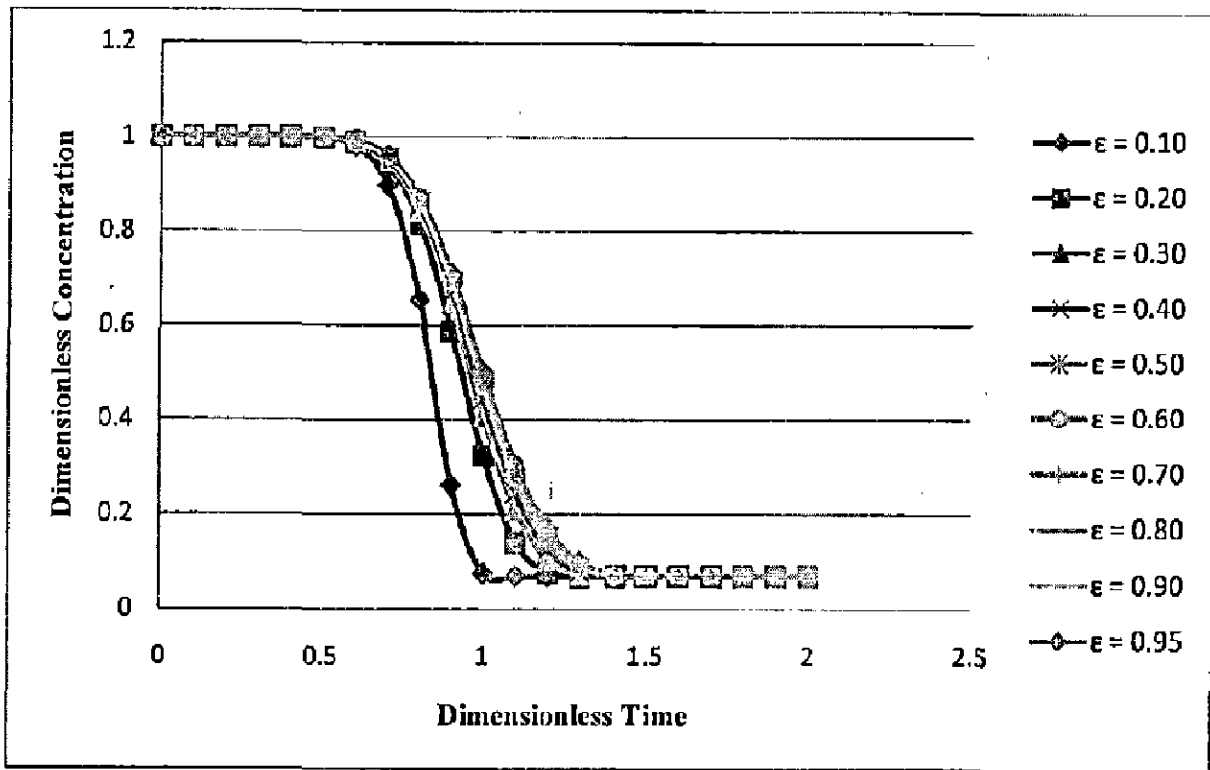


Figure-2.31 C vs. T profile for various values of porosity at bed exit of washer-1 for model-8

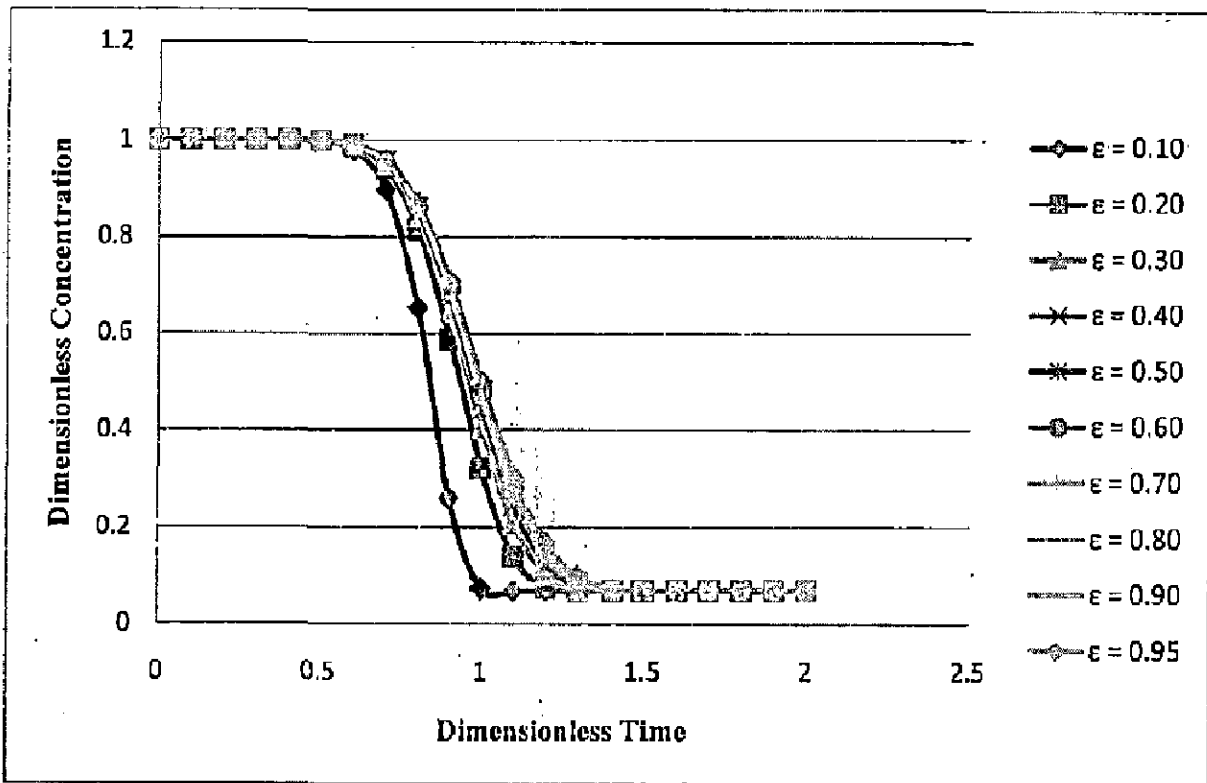


Figure 2.32 C vs. T profile for various values of porosity at bed exit of washer-1 for model-9

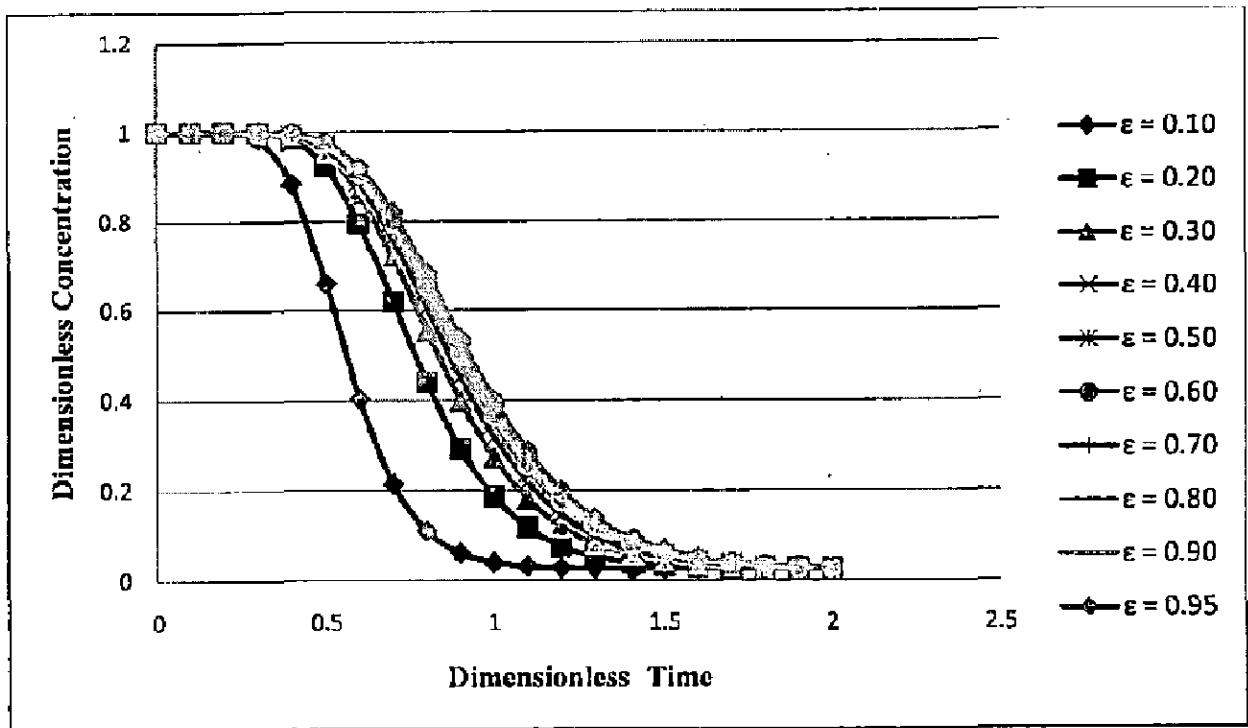


Figure 2.33 C vs. T profile for various values of porosity at bed exit of washer-2 for model-8

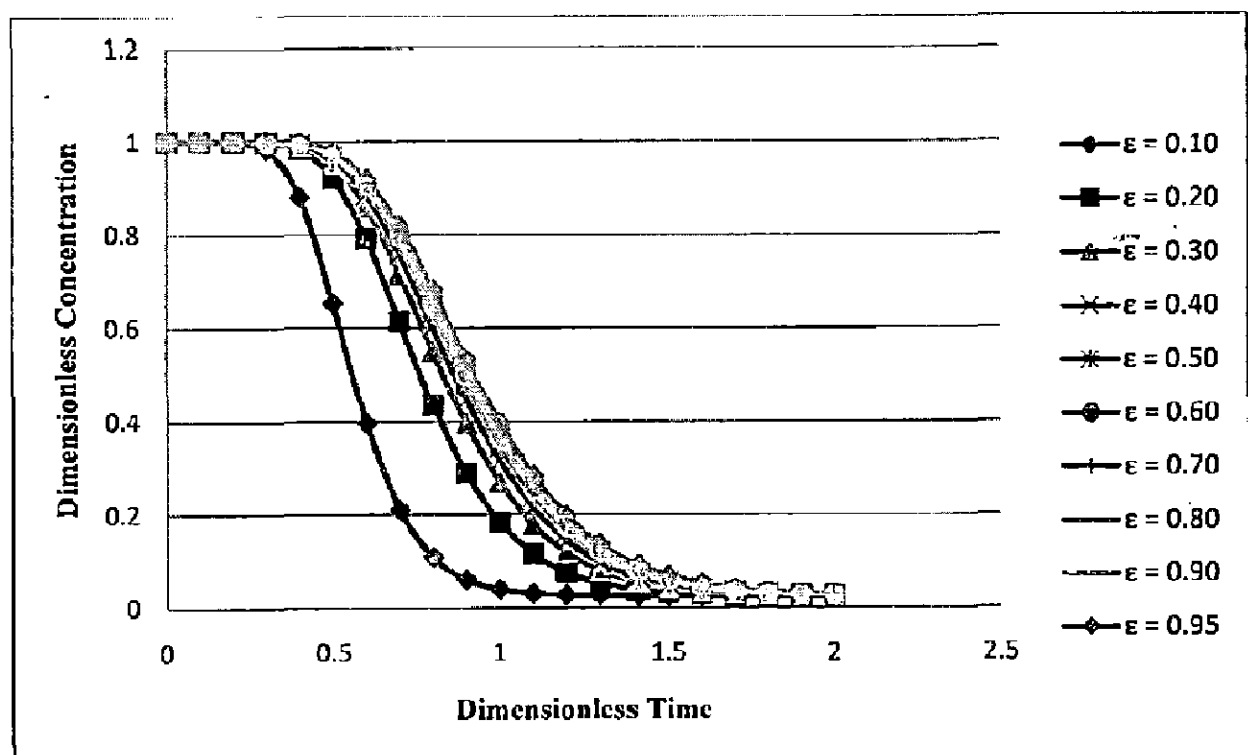


Figure 2.34 C vs. T profile for various values of porosity at bed exit of washer-2 for model-9

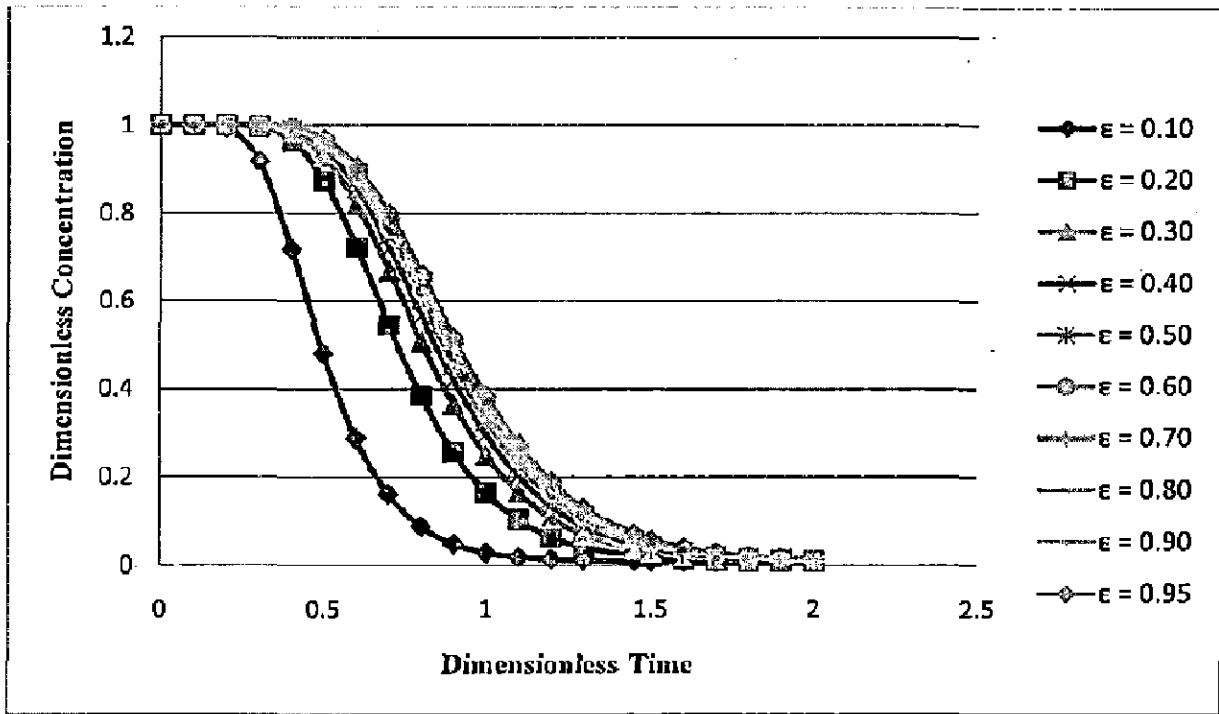


Figure 2.35 C vs. T profile for various values of porosity at bed-exit of washer-3 for model-8

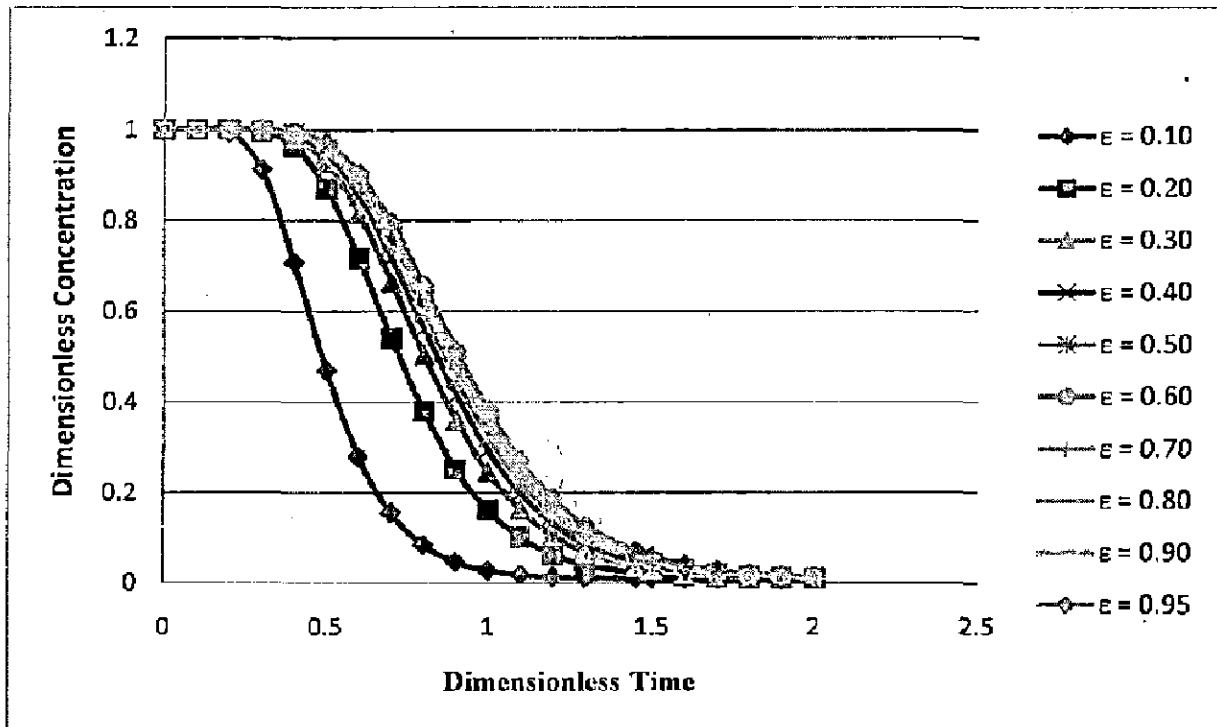


Figure 2.36 C vs. T profile for various values of porosity at bed exit of washer-3 for model-9

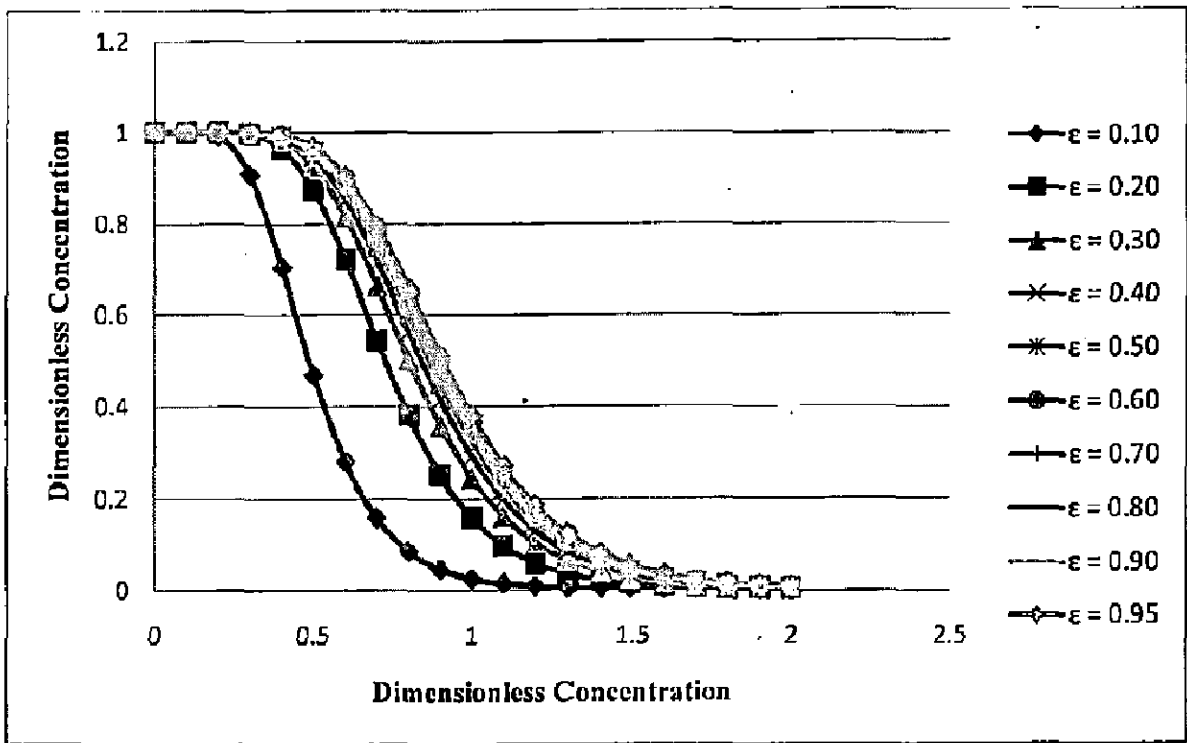


Figure 2.37 C vs. T profile for various values of porosity at bed exit of washer-4 for model-8

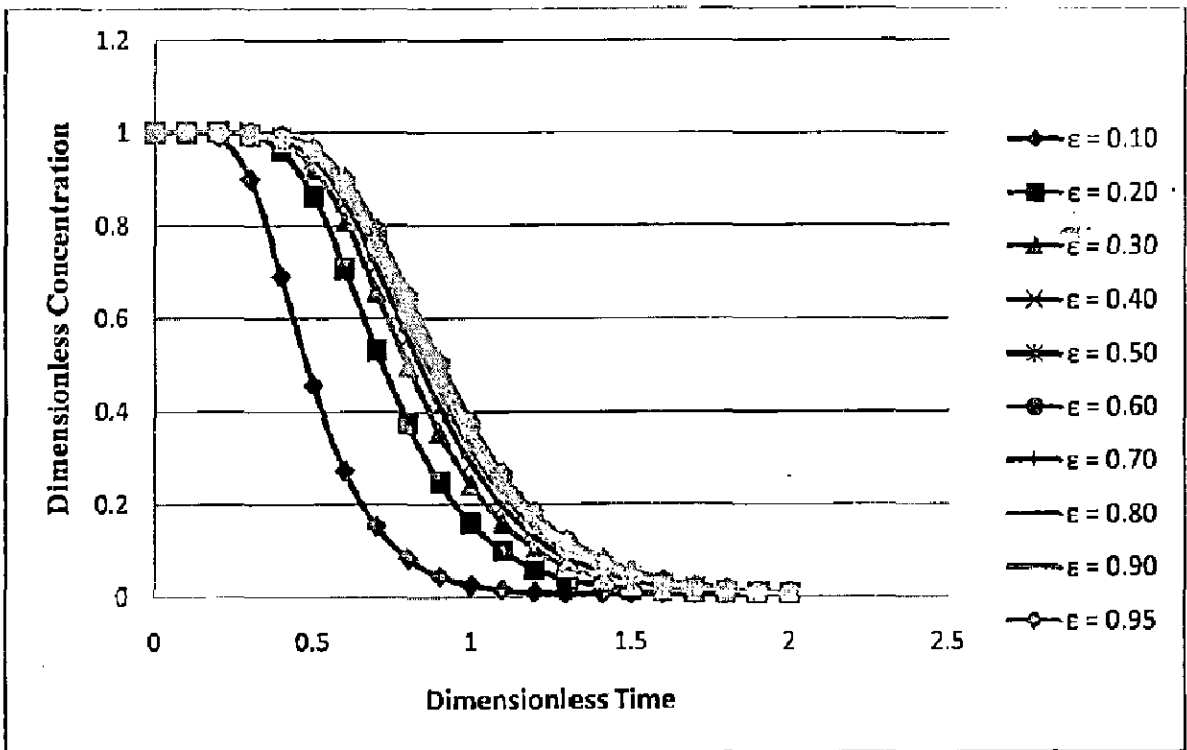


Figure 2.38 C vs. T profile for various values of porosity at bed exit of washer-4 for model-9

## 2.10. Conclusion

In the present investigation pulp washing models based on diffusion model of longitudinal mixing in beds of finite length with varying initial and boundary conditions applicable to displacement washing with axial dispersion and particle diffusion are proposed. Firstly, the solution of washing model based on axial dispersion only was obtained. The model with varying initial and boundary conditions is proposed to be solving through pdepe solver in MATLAB source code. The present solution technique is validated with the solutions of Brenner (1962) with analytical method and Grahs (1975) based on numerical technique (Orthogonal Collocation) for same Peclet number ( $Pe=100$ ). The results are in good agreement with the analytical solution by Brenner (1962) and numerical solution by Grahs (1975) with negligible error and shows better accuracy than Kumar (2002).

In further investigation mathematical models described for washing zone applicable to displacement washing with axial dispersion and particle diffusion of a rotary vacuum washer in Paper Industry has been studied. Linear as well as non-linear (Langmuir isotherm) adsorption isotherms are used to describe the relationship between the concentration of the solute in the liquor and concentration of the solute on the fibers. The numerical solutions of the pulp washing model are obtained for the various adsorption isotherms by using different boundary conditions with the help of "pdepe" solver in MATLAB source code. For obtaining much accurate solution of the above mentioned washing models, dimensionless bed depth as well as dimensionless time is divided into 21 equal parts and then the influence of these parameters ( $Z$  and  $T$ ) on  $C$  is estimated. The behaviors of exit solute concentration with respect to time as well as variable cake thickness are shown by 3-D graphs. It is clear from figures that the dimensionless concentration of the solute in the liquor decreases with the increase of the dimensionless time, whereas increases with the increase in the dimensionless distance, which is same as obtained by earlier workers. Thus it is observed that with change in the cake thickness and time, significant changes occur in the concentration profiles. Numerical results thus obtained are compared with earlier workers analytically and numerically. The comparison shows that results are in good agreement with both analytically as well as numerically and also show the suitability of the isotherm coupling with the washing model [Kumar et al. (2010a)].

For the investigation of multistage counter current washing system based on mathematical models derived for displacement washing with axial dispersion and particle diffusion are proposed. Langmuir adsorption isotherm is used to describe the relationship between the concentration of the solute in the liquor and concentration of the solute on the fibers. The numerical solution are obtained for four stages in counter current manner by using “pdepe” solver in MATLAB source code and taking  $Pe = 71.26$  for first washer based on the simulation data. Peclet numbers for second and subsequent washers are obtained by using the algorithm given by Kumar (2002). For each stage of a series of four washers, the variations in the dimensionless solute concentration with respect to dimensionless time as well as dimensionless cake thickness are shown by 3-D graphs [Kumar et al. (2010b)]. Parametric effect of the various parameters is also studied for varying range of parameters for each washer individually of the four stage washing system.

The following conclusions may be drawn from the present study

1. Boundary conditions do not influence significantly on the washing results.
2. Pdepe solver can be used successfully for the solution of multistage pulp washing model.
3. The pdepe solver used in the present investigation is simple, elegant and convenient for solving two point boundary value problems with varying range of parameters and show a comparable performance with QUICK method in terms of CPU time and average numerical errors.
4. The algorithms in this solver are easy to set up, and so the method represents an advantage and good alternative to the available techniques for such type of problems.

### 3.1 Introduction

Indian pulp and paper mills using hardwood and bamboo as a major raw material are predominantly based on a kraft pulping process. Kraft pulping process (also called soda- sulphate process) use recycled white liquor (a mixture of primarily NaOH, Na<sub>2</sub>S, Na<sub>2</sub>CO<sub>3</sub> and many other minor constituents) from soda recovery process. A block diagram of the entire process of pulp mill, including the chemical recovery process is presented in Figure 3.1. This process flow diagram shows relationships among major operations and processes involved for paper making.

The chemical pulping processes involve cooking of wood (e.g. hardwood-cucalyptus, softwood-pine) or non-wood (bamboo, bagasse, rice straw, wheat straw, kenaf, jute stick, mesta etc.) with cooking chemicals at different concentrations and a definite liquor to raw material ratio called bath ratio in a pressure vessel called "Digester" by means of direct or indirect steam. The temperature (140<sup>o</sup>C–175<sup>o</sup>C) and pressure (5-9 bar) are maintained for a present time schedule (cooking time 90 min-150 min). The time at temperature is also another process parameter besides chemical dose, bath ratio and pressure which control the pulping process. Instead of a batch process, continuous digester can also be an option. The cooking process softens and dissolves cementic material, lignin holding the fibers in wood/non-wood and results in their ready separation when the pulp is discharged or blown from the digester by lowering pressure. The fibers remain intact and subjected to various operations like coarse screening, washing, fine screening, cleaning, bleaching, stock preparation-refining/ beating, wet end operations, pressing, drying, calendaring, reeling, winding and final finishing for producing paper. Brown stock washing (BSW) system is the main key equipment to separate pulp fibers from the black liquor associated with the pulp after blown down from the digester. The waste liquor obtained after washing the pulp with fresh water is as earlier mentioned a black liquor, which contains a large amount of inorganic (sodium and calcium based) and organic chemicals (poly-dispersed lignin and carbohydrate based) in varying proportions. Typical constituents of bamboo based black liquor are shown in Table 3.1.



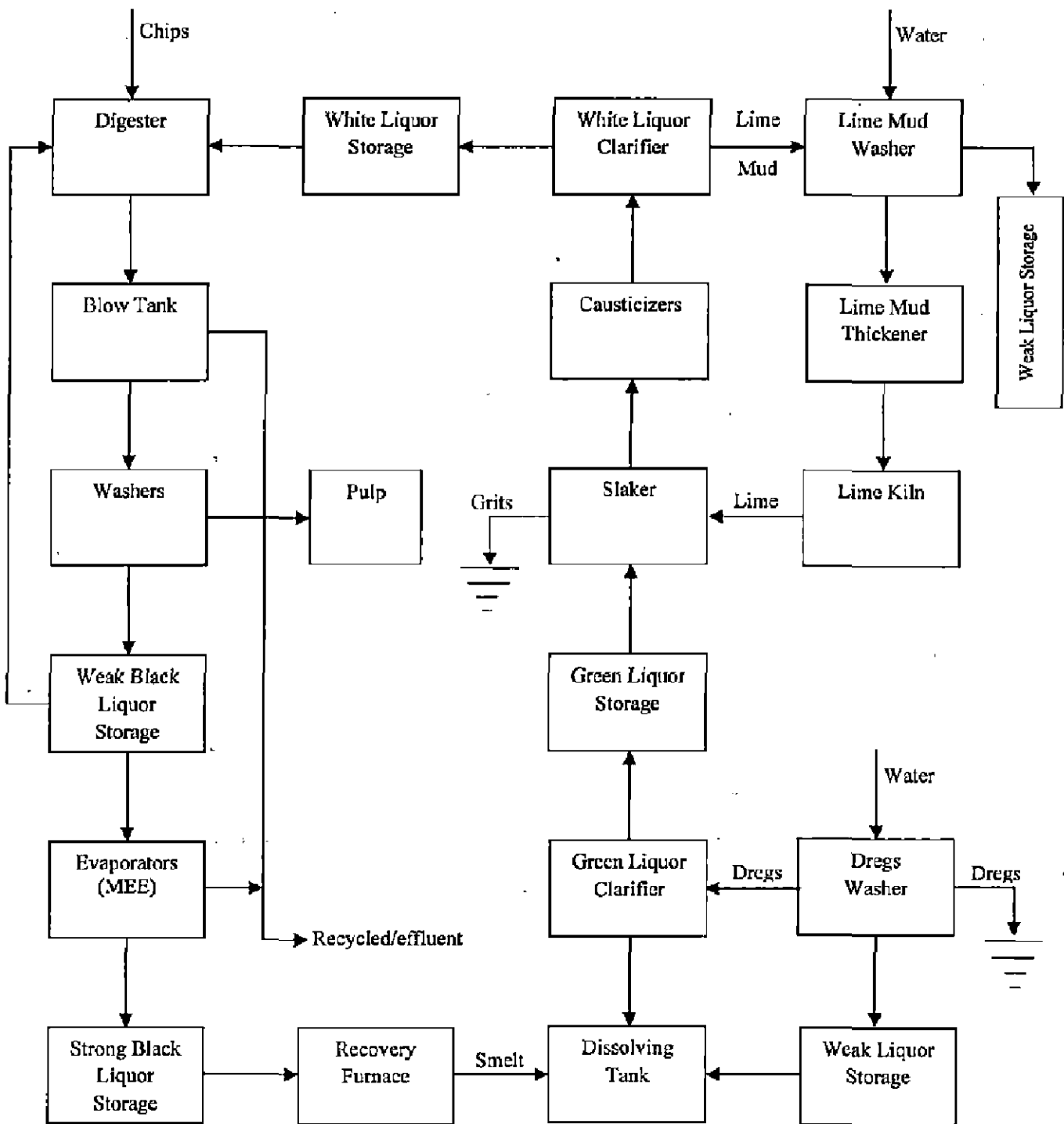


**Figure 3.1 Block diagram of a pulp mill**

**Table 3.1 Weak kraft black liquor constituents**

S. No.	Organic Compounds	Inorganic Compounds
1.	Ligneous Materials (Polyaromatic in character)	Sodium Hydroxide
2.	Saccharinic Acids (Degraded Carbohydrates)	Sodium Sulphide
3.	Low Molecular weight organic acids	Sodium Carbonate
4.	Resin and Fatty Acid Soaps	Sodium Sulphate
5.	Sugars	Sodium Thiosulphate
6.		Sodium Polysulphides
7.		Elemental Sulphur
8.		Sodium Sulphite

The spent liquor is therefore most important as it contains many valuable chemicals which can be regenerated economically in a process called chemical recovery process. The recovery of chemicals in turn gives large amount of thermal energy in form of process steam. Co-generation of electrical power can also be a byproduct if pressure in the boiler is raised to a higher level. Therefore the entire economy of the pulp and paper industry depends largely on the performance of its chemical recovery section. In fact the lignin and other organic components in black liquor generate heat when incinerated in a recovery furnace which in turn generates steam and electricity, as indicated above. The recovery operation is largely influenced by the organic and its solid contents of black liquor, its handling, and processing methodology. Generally, the operation involves concentration in an evaporator, combustion in a furnace at a concentration of 64-65% solid contents, and causticizing of sodium carbonate to sodium hydroxide by slaked lime in a series of equipments (green liquor clarifier, lime slacker causticizers, recausticizers, mud washers, mud filters etc.) and final calcinations of lime sludge for lime recovery. Concentration in evaporation operation generally performed in a long tube vertical (LTV) or Falling film evaporator. Evaporation is done economically in multiple effect evaporator (MEE) consists of 4 to 7 stages. Generally 10-17 % of the dissolved black liquor solids are processed in a multiple effect evaporator system (MEE) to form concentrated black liquor of approximately 50% solids. During the evaporation process the various physico-chemical properties are changed because of increase in concentration and change in temperature and pressure.

The energy economy of a MEE system is also influenced by the design of liquor flow sequence. As a matter of fact, MEE may be arranged in a variety of ways. Forward feed, backward feed, mixed feed and parallel feed are four general designs of liquor flow sequences. Parallel flow has its own limitation for black liquor concentration. Due to very high viscosity of concentrated liquor and its non-newtonian characteristics, it becomes difficult to process black liquor in a forward feed sequence. However, this is employed in Sugar Industry. Many North American black liquor evaporation plants generally employ a 5-6-4-3-2-1 or 6-5-4-3-2-1 liquor flow sequences. Literature is also available [Bhargava et al. (2008a, b)] which indicates that backward feed usually results in the best overall economy (balancing both capacity and steam economy, defined as vapor generated per mass of externally supplied steam). Therefore backward feed is the most commonly employed sequence. To save some amount of electrical energy the mixed feed sequence are also prevalent in many of the pulp and paper mills. However, it is not clearly known that in which body the weak black liquor as a feed should be introduced to get the best economy or least steam consumption. Although, it is a fact that with the change of the sequence the economy and energy efficiency will also be changed. Therefore, there is an imperative necessity to pay attention to these aspects.

Long tube vertical (LTV) evaporator is widely used natural circulation evaporator. It has long tube bundle fitted with a shell. The shell is projected into a larger diameter chamber or vapor head at the top. The feed enters the tube bundle at the bottom, flow through the tubes once, while undergoing vigorous boiling, and discharges into the vapor head and impinges on a deflector plate above the free top end of the tube bundle. This removes most of the entertained liquid droplets from the vapor. The concentrated liquor leaves the vapor chamber through a pipe and is withdrawn. The principle advantage of the LTV evaporators are: high heat transfer coefficient, low cost, low liquid hold up and less floor space requirement. The disadvantages are: high headroom requirement, unsuitable for viscous and scale-forming materials.

In the falling film evaporator liquid flows down in the inner walls of the tubes in a vertical tube bundle. The tubes are heated by condensing steam or any other hot liquid on the shell side. As the feed liquor flows down the tube wall, water vaporizes and the liquid concentration gradually increases. Thick liquor is withdrawn from the bottom and the vapor goes to a separator where the

entrained liquid droplets are separated. Heat transfer rate in falling film evaporator is quite high and the contact time of the liquid with the hot wall remains low. For these reasons, device is suitable for heat-sensitive materials. Use of falling film technology has been found in a wide variety of engineering application, although its application in pulp and paper industry is recent practice [Alhusseini et al. (1998)].

The evaporation process consumes maximum energy in paper manufacturing operation. It is reported that in cellulosic fiber and filament industries in India, the consumption of steam in evaporation process comes about  $1.75 \times 10^6$  tons per year [Pollard et al. (1992)]. Rao and Kumar (1985), Kumana (1990) pointed out that the Multi-effect evaporator system alone consumes around 24-30% of the total steam consumed of a large paper mill. Therefore, it calls for a thorough investigation into its analysis and various energy reduction schemes. In order to achieve this, it would be desirable to develop mathematical model that can be used to predict the performance of the evaporation process.

### **3.2 Modelling and Simulation of Multi-effect Evaporation: A Review**

Various researchers developed the mathematical model of the MEE system of various process industries based on steady state conditions. Lambert et al. (1987) developed a system of non-linear equations governing the general MEE system (applicable for various industries) and presented a calculation procedure for reducing this system to a linear form and solved iteratively by the Gauss elimination technique. Boiling point rise (BPR) and nonlinear enthalpy relationships in terms of temperature and solid concentration were included in the model. The results of linear and nonlinear techniques were compared. Koko and Joye (1987) compared the linear and non-linear method and demonstrated that, linear method is faster, much more stable, and have more desirable convergence characteristics than widely used nonlinear method. Patel and Babu (1996) developed the computer program for the design and calculation procedure of single and multiple effect evaporators for general evaporation plant.

El-Dessouky et al. (1998), El-Dessouky et al. (2000), Al-Ansari et al. (2001), and Khademi et al. (2009) discussed the modelling and simulation for MEE system for the desalination process. El-

Dessouky et al. (1998) developed mathematical model of the multiple effect evaporation (MEE) desalination process to determine the effects of the important design and operating variables on the parameters controlling the cost of producing fresh water. The model assumed the practical case of constant heat transfer areas for both the evaporators and feed preheaters in all effects. In addition, the model considered the impact of the vapor leak in the venting system, the variation in thermodynamic losses from one effect to another, the dependence of the physical properties of water on salinity and temperature, and the influence of non condensable gases on the heat transfer coefficients in the evaporators and the feed preheaters. The modified fixed-point iterative procedure was used to solve the large number of highly nonlinear equations describing the MEE desalting system. The algorithm is consisted of 10 calculation blocks and 6 logical blocks. The algorithm was implemented using L-A-S computer aided language. El-Dessouky et al. (2000) presented a performance analysis for the parallel feed multiple effect evaporation system. Analysis was performed as a function of the heating steam temperature, salinity of the intake seawater, and number of effects. The mathematical models of the parallel and parallel/cross flow MEE systems included basic material and energy balance equations as well as correlations for estimating the heat transfer coefficients, the thermodynamic losses, pressure drops, and physical properties. The iterative procedure based on Newton's method with an iteration error of  $10^{-4}$  was used for the solution of the models. Results were presented as a function of parameters controlling the unit product cost, which included the specific heat transfer area, the thermal performance ratio, the conversion ratio, and the specific flow rate of the cooling water. Al-Ansari et al. (2001) modeled the single effect evaporation desalination process with adsorption heat pump. The mathematical model for the single effect adsorption vapor compression desalination system included balance equations for the evaporator, feed pre-heaters, adsorption bed, and desorption bed with certain assumptions. The analysis gave variations in the thermal performance ratio, the specific heat transfer area, and the specific flow rate of cooling water. Khademi et al. (2009) presented the steady-state simulation and optimization of a six-effect evaporator in desalination process with provision of its relevant software package. In this investigation, the modelling equations of each of the existing building blocks were written in a steady-state condition. These equations were used for simulation and process optimization of the entire vaporizing unit while exercising the simplifying assumptions. The effect of different parameters on consumed steam produced distilled water and

performance parameter (GOR) was presented. The feed mass flow rate, condenser pressure and operating time were optimized for this system.

Various investigators Cadet et al. (1999), Ugrin and Urbicain (1999), Bakker et al. (2006), Kaya and Sarac (2007) and Karimi et al. (2007) studied and developed steady state model of the evaporation plant related to food/juice industries. Cadet et al. (1999) developed a model based on energy and mass balance of the evaporator system. The model included semi-empirical equilibrium functions and was implemented in a sugar plant. Ugrin and Urbicain (1999) presented an algorithm for the design and simulation of multi-effect evaporators, with forward and backward feed. The mass and enthalpy balances and the heat transfer rate equations posed around each effect were linearized as suggested by Lambert et al. (1987), and a new iterative scheme was proposed to ensure convergence and stability while considering boiling-point rise. Bakker et al. (2006) demonstrated that the control of the concentrated total solids exiting from a multi-pass, multi effect falling film evaporator can be enhanced by the use of cascade architecture. In addition to measuring the primary process variable (the final concentrate total solids), a surrogate process variable (the total solids after the first pass) was measured and used in the cascade strategy. Kaya and Sarac (2007) developed a mathematical model for multiple-effect evaporators. These evaporators had cocurrent, countercurrent and parallel flow operation options. Each operation was investigated with and without pre-heaters. The effect of pre-heating on evaporation process was investigated from the point of energy economy. Karimi et al. (2007) used inferential cascade control. The control of three-effect falling-film evaporator in Isfahan milk powder factory was discussed. It was shown that by using linear Kalman filter and process measurements, total solid concentration of first effect product can be significantly estimated. The estimated state was used in inferential cascade control as secondary measurement. The results of inferential cascade control algorithm were compared with those of conventional feedback control algorithm.

Researchers such as Ray and Singh (2000), Algehed and Berntsson (2003), Ray et al. (2004), Ray and Sharma (2004), Fang and Zhiming (2004), Bhargava et al. (2008a, b), and Khanam and Mohanty (2010) studied the modelling and simulation of the evaporation plant of a Paper Industry. Ray and Singh (2000) attempted to design a sextuple effect black liquor evaporator system for

paper industry and developed a system of 12 nonlinear simultaneous equations based on steady state mass and energy balances, heat transfer rate, equilibrium relationships and physico-chemical/physico-thermal properties of liquor. Algehed and Berntsson (2003) suggested a novel design for evaporation plant and reported that using this design, live steam demand for evaporation can be reduced with approximately 70% compared to a conventionally designed evaporation plant. Ray et al. (2004) compared the performance of split feed sequences, with and without condensate flash and product flash. As usual the models are based on steady state mass balance, enthalpy balance and heat transfer rate equations interlinked with overall heat transfer coefficient, obtained from the model given by Gudmundson (1972), and suitable correlations of physico-thermal properties of black liquor including BPR values as a function of temperature and concentration. A programme was developed in FORTRAN-77 language. The numerical techniques used was Newton Raphson method with Jacobian matrix and method of Gauss elimination with partial pivoting supplemented with LU decomposition with the aid of Hilbert norms. The gains in SE, reduction in SC and area requirement were quantitatively estimated. The algorithm developed is general in nature and can be used for any other sequences practiced in Indian mills with the required modification. Ray and Sharma (2004) extended the above algorithm for mixed feed with condensate and product flash for additional advantages of energy gains and higher steam economy in mixed feed sequence. Fang and Zhiming (2004) presented a mathematical model based on a turbulent two-phase flow with multiple components to investigate the transport processes of black liquor in a falling film evaporator. Akanksha et al. (2007) studied the problem of gas absorption into a falling film reactor in the case of an instantaneous reaction. A diffusion-convection-reaction model was developed taking momentum, mass and heat transfer effects into account. The performance of the model was examined for sulphonation of tridecylbenzene. The resultant equations were solved using a finite difference backward implicit scheme. Bhargava et al. (2008 a & b) developed a nonlinear model for a sextuple effect flat falling film evaporator (SEFEFE) system employed for concentrating weak black liquor in an Indian Kraft Paper Mill. The model incorporated different operating strategies such as condensate-, feed- and product-flashing, and steam- and feed-splitting. The developed model was used to analyze six different feed flow sequences including backward as well as mixed flow sequences. For these feed flow sequences the effects of variations of input parameters vapor temperature and feed flow rate on output parameters

such as steam consumption and steam economy were studied to find the optimal feed flow sequence. Khanam and Mohanty (2010) proposed different energy reduction schemes (ERSs) to reduce the consumption of steam for a multiple effect evaporator (MEE) system. These ERSs were condensate-, feed- and product-flashing and vapor bleeding. Further a new scheme was proposed where condensate of vapor chest of an effect was used to preheat the liquor, entering into that effect using a counter current heat exchanger.

Scanty literature is available on statistical modelling of such type of heat and mass transfer process. Prasad et al. (2002) investigated the influence of data uncertainty on the performances of concentric counter flow heat exchanger using a method based on two point distribution (TPD). For the studies, the available deterministic solution [Prasad (1987)] and TPD analysis [Karmeshu and Lara-Rasano (1987)] were utilized. Expressions were presented for the expected values, variance and standard deviations due to uncertainties in fluid inlet temperatures and heat transfer coefficients separately as well as due to their combined effect.

Although the methods of design and steady state operation of single and multi-effect evaporators of various process industry including paper industry, are well documented in the literature. The dynamic behavior of two or three effect MEE systems in process industries like sugar, food, desalination and paper is studied only by few researchers. In the beginning, interest in developing Mathematical models for multiple effect evaporators was focused on the possibility of incorporating open loop simulations for conventional control purposes. However, in the 1970's, most studies have emphasized the development of state space models to incorporate the use of multivariable controllers and state estimations. First, the steady-state condition, and then the dynamic behavior of the equipment were analyzed [Newell and Lee (1989)].

In the beginning there was also a combination of empirical models and theoretical derivations. Johnson (1960) presented several empirical models with the aim of obtaining an adequate representation of the plant and its control system for a falling film evaporator. On the other hand, Andersen et al. (1961) described an evaporator through five ordinary differential equations; after a reduction and linearization, the mathematical model was utilized to simulate control with an analog computer. Kropholler and Spikins (1965) described an empirical input-output model of a one-



effect evaporator and analyzed the PID controller tuning. Andre and Ritter (1968) adequately described the open loop dynamic response of a laboratory scale double effect evaporator by a simple mathematical model based on the unsteady state material and energy balances associated with the various elements of the system. Excellent agreement was achieved between the experimentally determined response of the evaporator to large disturbances in steam rate and feed rate and the predicted response based on the digital computer solution of the non linear model. Bolmstedt and Jernquist (1976, 1977) developed a computer program to simulate the steady state condition of a multiple effect evaporator and presented a dynamic simulator through blocks that can be utilized to simulate more complex plants. Bolmstedt (1977) developed a computer program for simulation of the dynamic behavior of general multiple effect evaporation plants. The computer program, called DYNEFF, consisted of a number of dynamic blocks comprising the necessary differential and algebraic equations for evaporator vessels, flash tanks, heat exchangers, etc., DYNEFF was used in combination with a previously presented computer program, called INDUNS, for calculation of all the necessary initial values. INDUNS perform a design or evaluation calculation of the desired multiple effect evaporation plant, and transfers the steady-state data as well as the flow sheet data to DYNEFF. El-Nashar and Qamhiyeh (1990) developed a simulation model for predicting the transient behavior of Multi-effect stack-type (MES) distillation plants. Transient heat balance equations were written for each plant component in terms of the unknown temperatures of each effect. The equations were solved simultaneously to yield the time-dependent effect of temperature as well as performance ratio and distillate production. Model was validated with actual plant operation data obtained from the MES evaporator at Abu Dhabi solar desalination plant. The results of the simulation program were further compared with data taken during start-up, and agreement was found to be reasonable. Tonelli et al. (1990) presented a computer package for the simulation of MEE for the concentration of liquid foods and studied the dynamic response. It was based on a non-linear mathematical model and an illustrative case study for a triple effect evaporator for apple juice concentrate was presented. The response of disturbances in steam pressure and feed flow rate obtained by the solutions of the mathematical model was in excellent agreement with the experimentally determined response. Hanbury (1995) presented a steady-state solution to the performance equations of a Multi-effect distillation (MED) plant. The simulation was based on a linear decrease in boiling heat transfer coefficient, unequal

inter effect temperature differences, and equal effect thermal loads from the second effect down. The developed model was successfully used in describing the dynamic behavior of MED systems. Aly and Marwan (1997) developed a dynamic model for the MEE process to study the transient behavior of the system. This model allowed the study of system start-up, shutdown, load changes and troubleshooting in which the plant performance changed significantly. Each effect in the process was represented by a number of variables which are related by the energy and material balance equations for the feed, product and brine flow. These equations were solved simultaneously to predict the dynamic behavior of system. The effect of feed flow, feed temperature, live steam flow changes on plant performance parameters such as temperature, brine salinity, product flow rate and brine level was investigated to test the validity of the model. Cadet et al. (1999) proposed a model to be inserted in a control strategy which included as many real physical properties as possible. The final aim was to widen the validation domain of the nonlinear control. The dynamic accuracy of the nonlinear model was of great importance in the control performances. Winchester and Marsh (1999) developed and analyzed a model of a falling film evaporator with mechanical vapor recompression for the purpose of examining the coupling and functional controllability of the three core control loops for effect temperature, product dry mass fraction and product flow rate. Miranda and Simpson (2005) described a phenomenological, stationary and dynamic model of a multiple effect evaporator for simulation and control purposes. The model included empirical knowledge about thermo physical properties that must be characterized into a thermodynamic equilibrium. The developed model consisted of differential and algebraic equations those were validated using a parameter sensitivity method using industrial plant data. The simulation results showed a qualitatively acceptable behavior. Svandova et al. (2006) did the steady-state analysis and dynamic simulation of a methyl tertiary-butyl ether (MTBE) reactive distillation. The basic kinetic model of MTBE production was applied for simulation of the process in a CSTR with total condenser. The steady-state behavior of the system was studied in terms of the input parameters, i.e. feed flow rate of methanol, feed flow rate of hydrocarbons, reflux ratio and heating rate and ratio of hydrocarbons in the feed. The dynamic behavior of the system during the start-up of the CSTR with total condenser was studied. Gonzalez-Bustamante et al. (2007) developed the models based on the strict fulfillment of conservation laws-mass, linear momentum, angular momentum and energy and implemented in the

MATLAB/SIMULINK environment (and its toolboxes and blocksets). Thus, a real integrated design platform is provided covering process and control techniques. The model developed has been applied to the analysis of transients in a natural gas line which supplies a boiler at a steam-electric power plant.

No work presented on the dynamic response of MEE system in paper industry except Stefanov and Hoo (2003, 2004). Stefanov and Hoo (2003) developed a distributor parameter model (System of partial differential equations) of black liquor falling film evaporator, based on first principles knowledge about the fluid dynamics and heat transfer processes for a falling film lamella type evaporator. Primarily, the model describes falling film evaporation on one lamella. The model was solved using orthogonal collocation on finite elements in the presence of scaling and disturbances in the mass feed rate, feed dry solids content, and wall temperature. Stefanov and Hoo (2004) extended a single plate model to develop a fundamental distributed parameter model of a multiple-effect falling-film evaporator plant that consisted of one super concentrator and four falling film evaporators and solved numerically. The model describes the important phenomena of evaporation, heating, and condensation for different hydrodynamic regimes as well as the pressure dynamics of the multi-effect evaporator plant. Experimental investigations were performed to determine the model dimensions. Stefanov and Hoo (2004) studied the dynamic responses for backward feed sequence. The effect of boiling point rise was neglected and LSODE (Livermore solver for ordinary differential equations, implicit system) solver, included in ODEPACK given by Hindmarsh (1982) was used for simulation. The execution time was approximately 14 h on a 1.2 GHz Athlon node, which was equivalent to 1 h of real time for the dynamic simulation of plate type falling film MEE system. This technique is complex and more time consuming.

By the analysis of the above models, it is observed that majority of the investigators have followed the material, energy balance equations for developing the model of MEE system and obtained the steady state simulation by using different kind of techniques. Some of them also studied the dynamic behavior of the MEE system by taking the disturbances in the input parameters for various industries. Normally the main difference among these mathematical models is the heuristic

knowledge which is incorporated in their development and as well as the technique which is used for simulation.

In the present investigation an attempt has been made for study of dynamic responses for tubular type falling film MEE system. The lumped parameter model (System of ordinary differential equations) of sextuple effect falling film evaporator system of a paper industry is developed by using unsteady state energy and material balance equations and Physico-thermal properties of black liquor including the effect of boiling point rise for backward as well as mixed and split-feed sequences. The transient behavior of the system is studied by disturbing the input parameters like feed flow rate, feed concentration, feed temperature and steam temperature. For the steady state and dynamic simulation 'fsolve' and 'ode45' solver in MATLAB source code are used respectively.

### **3.3 Physico-Thermal/Chemical Properties of Black Liquor and Water**

To formulate material and energy balance equation in each body of multiple effect evaporator system, expressions of physical properties of black liquor are needed. These physico-chemical properties are the explicit function of concentration of both the organic and inorganic constituents of black liquor and temperature as well. These properties change with the variation of the temperature and pressure from first to last effect and also from bottom to the top of each effect of multiple effect evaporator system. The important physico-chemical/ physico-thermal properties of black liquor are: Density ( $\rho$ ), specific heat ( $C_p$ ), Boiling Point Rise (BPR), Latent heat of vaporization etc. The relationships for some of the important properties are discussed below and the expressions used in the present study are presented in Table 3.2.

#### **3.3.1 Density of black liquor ( $\rho$ )**

Density of black liquor varies with, solid concentration, temperature and ratio of organic to inorganic constituents and type of raw material. High temperature and low inorganic matter decrease the density values. However, the effect of temperature on density of black liquor is usually neglected when compared to the effect of changes in solid content.

Regestad (1951) presented following useful expression relating the density of black liquor to solid contents.

$$\rho = 1007 + 6.0 X - 0.495 T \quad (3.1)$$

where X = total solids (%), and T = temperature in °K

Veeramani and Koorse (1975) calculated experimentally the density or specific gravity of black liquors obtained from pulping of fibrous raw materials such as bamboo, bagasse, salai, eucalyptus and mixed hardwoods at 70°C, using commercial samples and the results were presented in graphs with concentration as a parameter.

Another empirical equation given by Gullichsen and Fogelholm (2000) for estimation of density is as follows

$$\rho_{25} = 997 + 649 X \quad (3.2)$$

$\rho_{25}$  is liquor density at 25°C in kg/m<sup>3</sup>.

For estimation of density at any temperature the following correlation was given by Gullichsen and Fogelholm (2000)

$$\rho_T / \rho_{25} = 1.008 - 0.237 (T / 1000) - 1.94(T/1000)^2 \quad (3.3)$$

Ray and Singh (2000) & Ray and Sharma (2004) reported the following expression for the density of black liquor

$$\rho = 1007 - 0.495 T + 0.6 X \quad (3.4)$$

where T is black liquor temperature, °C, X is solid concentration and 'ρ' is density of black liquor in kg/m<sup>3</sup>

### 3.3.2 Specific heat of black liquor ( $C_p$ )

Organic and inorganic constituents of black liquor tend to decrease specific heat. Specific heat of black liquor,  $C_p$ , is a function of solid content and temperature. Specific heat of black liquor decreases with increase in solid content as well as increase in temperature.

Gullichsen and Fogelholm (2000) used the following relationship to estimate specific heat of black liquor

$$C_p = 4.216(1-X) + \{1.675 + (3.31T)/1000\} X + (4.87 - 20T/1000) (1-X) X^3 \quad (3.5)$$

Ray and Singh (2000) & Ray and Sharma (2004) reported the following empirical equation for specific heat of wood based black liquor as a function of the above parameters.

$$C_p = 4190 [1.0 - 3.234\{X/(1.8T + 32)\}] \quad (3.6)$$

where  $C_p$  is black liquor specific heat in  $\text{kJ/kg}^\circ\text{C}$

X the dry solids concentration, T is the temperature of the black liquor,  $^\circ\text{C}$ .

### 3.3.3 Specific heat of water ( $C_{pw}$ )

Based on the data reported by Perry et al. (1963) the correlation of specific heat of water with temperature is expressed as follows.

This is valid for temperature ranging from 273  $^\circ\text{K}$  to 383  $^\circ\text{K}$ .

$$C_{pw} = 4211.2 - 2.1036(T) + 0.0035706 (T^2) - 0.0016983(T^3) + 0.35052 \times 10^{-6}(T^4) \quad (3.7)$$

where  $C_{pw}$  is in  $\text{kJ/kg}^\circ\text{C}$ .

### 3.3.4 Boiling point rise (BPR)

To calculate the effective temperature difference in each stage of multiple effect evaporators, boiling point rise (BPR) plays an important role. The boiling point rise is the difference between the boiling temperature of black liquor and that of pure water at the same pressure. Boiling point

rise is smaller at lower concentration and increase with increase in solid content. In fact, it is a strong function of solids content of black liquor while it is a very weak function of pressure and hence temperature. An increase of 1<sup>0</sup> C in saturation temperature due to increase in saturation pressure results in about 0.6 % rise in boiling point rise.

Hultin (1968) reported the boiling point rise as a function of solid content (TS) as follows:

$$\text{BPR} = K [(TS) / \{100 - (TS)\}] \quad (3.8)$$

where K is a constant,

Another relation to estimate boiling point rise of the black liquor is given by Gullichsen and Fogelholm (2000)

$$\text{BPR} = \{6.173 X - 7.48 X^{1.5} + 32.747 X^2\} * \{1 + 0.6(T1 - 3.7316) / 100\} \quad (3.9)$$

Ray and Singh (2000) and Ray and Sharma (2004) reported the following empirical equation for BPR of the black liquor is

$$\text{BPR} = 41.4 (X - 1)^2$$

X = Solid concentration,

T1 = Temperature of black liquor at specified pressure, in <sup>0</sup>C

### 3.3.5 Latent heat of vaporization of water ( $\lambda$ )

Latent heat is the heat released or absorbed by a chemical substance or a thermodynamic system during a change of phase that occurs without a change in temperature. For striking enthalpy balance around different effects of evaporator, the temperature dependence of latent heat of vaporization, saturation pressure of water, enthalpy of saturated water, and enthalpy of saturated steam are required.

Perry et al. (1984) is suggested the following relation for the latent heat of vaporization

$$\lambda = 2519.5 - 2.653 (T) \quad (3.10)$$

where T is in °C and λ in kJ/kg

Ray (1995) proposed the following equation for latent heat of vaporization

$$\lambda = 60347.4 - 169.558 (T) + 0.858193 (T^2) - 0.00211784 (T^3) + 0.00000176 (T^4) \quad (3.11)$$

where T is in °K and λ in kJ/kg mole

### 3.3.6 Enthalpy of saturated water (hl)

Enthalpy of saturated water given by Perry et al. (1984) is

$$hl = \alpha T + \beta \quad (3.12)$$

where α = 4.1832 and β = 0.127011 and T is in °K, and enthalpy in kJ/kg

### 3.3.7 Enthalpy of saturated steam/ vapor (hv)

The enthalpy of saturated steam proposed by Perry et al. (1984) is as follows

$$hv = \gamma T + \delta \quad (3.13)$$

where γ = 1.75228 and δ = 2503.35 and T is in °K and enthalpy in kJ/kg



**Table 3.2 Physico-thermal properties of black liquor, saturated steam and condensate**

S. No.	Properties	Equations	Function Parameters	Reference
1.	Boiling Point Rise	$BPR = \{6.173 X - 7.48 X^{1.5} + 32.747 X^2\} * \{1 + 0.6(Tv - 3.7316)/100\}$	X = Solid Concentration	Gullichsen and Fogelholm (2000)
2.	Black Liquor Density, Kg/m <sup>3</sup>	$\rho = (997 + 649 X) \{1.008 - 0.237 (Tl/1000) - 1.94(Tl/1000)^2\}$	Tv = Steam Temperature, °C	
3.	Specific Heat Capacity, kJ/kg.°C,	$Cp = 4.216(1-X) + \{1.675 + (3.31Tl)/1000\} * X + (4.87 - 20Tl/1000) (1-X) X^3$	Tl = Black Liquor Temp. in °C,	
4.	Enthalpy of saturated water	$hl = \alpha T + \beta,$ Where $\alpha = 4.1832$ and $\beta = 0.127011,$	T = Temperature of water, °K	Perry et al. (1984)
5.	Enthalpy of saturated steam	$hv = \gamma T + \delta,$ Where $\gamma = 1.75228$ and $\delta = 2503.35,$	T = Temperature of steam, °K	
6.	Latent Heat of Vaporization, kJ/kg	$\lambda = 2519.5 - 2.653 T$	T = Temperature of steam, °C	

### 3.4 Modelling and Simulation of MEE System

#### 3.4.1 System description

The Multiple Effect Evaporators (MEE) system selected for present investigation is a sextuple effect falling film evaporator (SEFFE) system that is being operated in a nearby Indian Kraft Paper Mill for concentrating weak black liquor. The schematic diagram of a backward feed SEFFE system is shown in Figure 3.2.

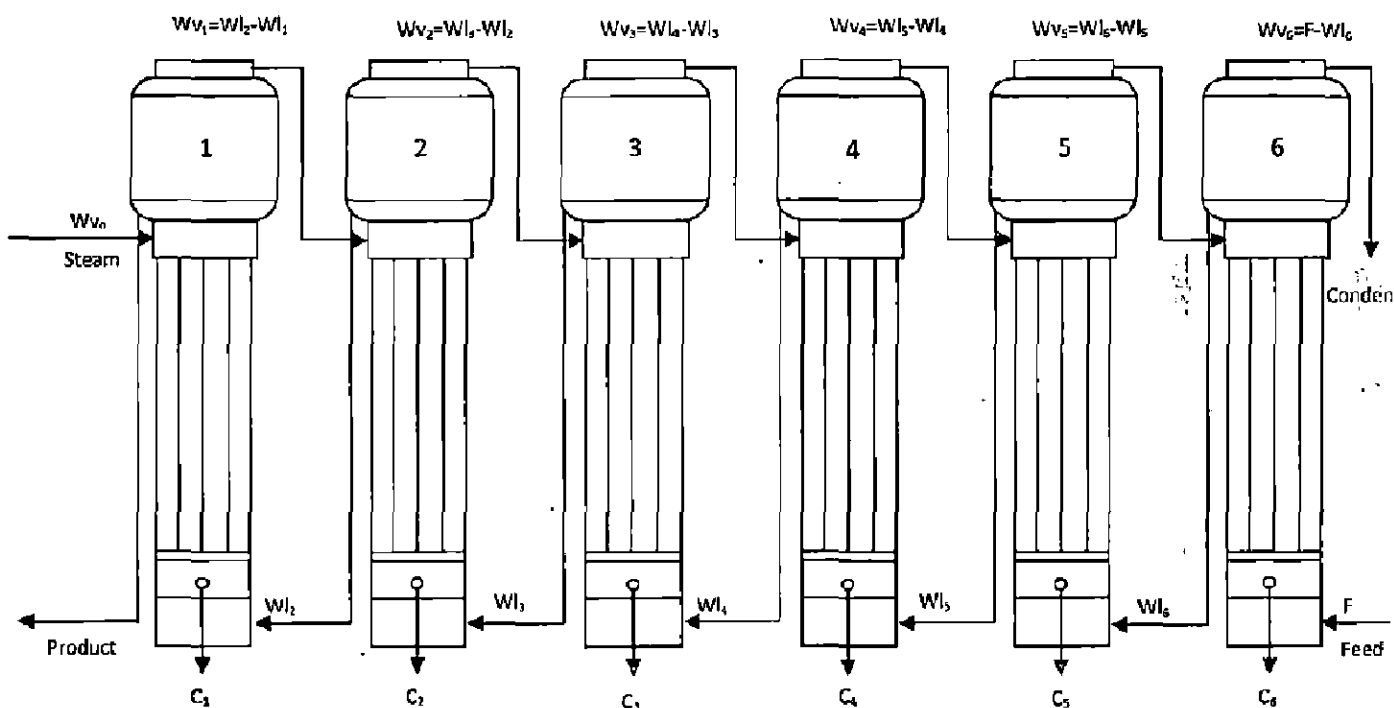


Figure 3.2 Schematic diagram of multiple effect evaporator

Each effect accommodates three streams, namely tube-side heating stream, vapor produced through the evaporation process, as well as the liquor flow from one effect to another. Each stream is defined by a number of independent variables like flow rate, temperature and solid contents. The streams are also defined by some dependent variables such as pressure and enthalpy. A typical representation of the model variables for  $i^{\text{th}}$  effect is shown in the Figure 3.3. These conventions are followed throughout the work.

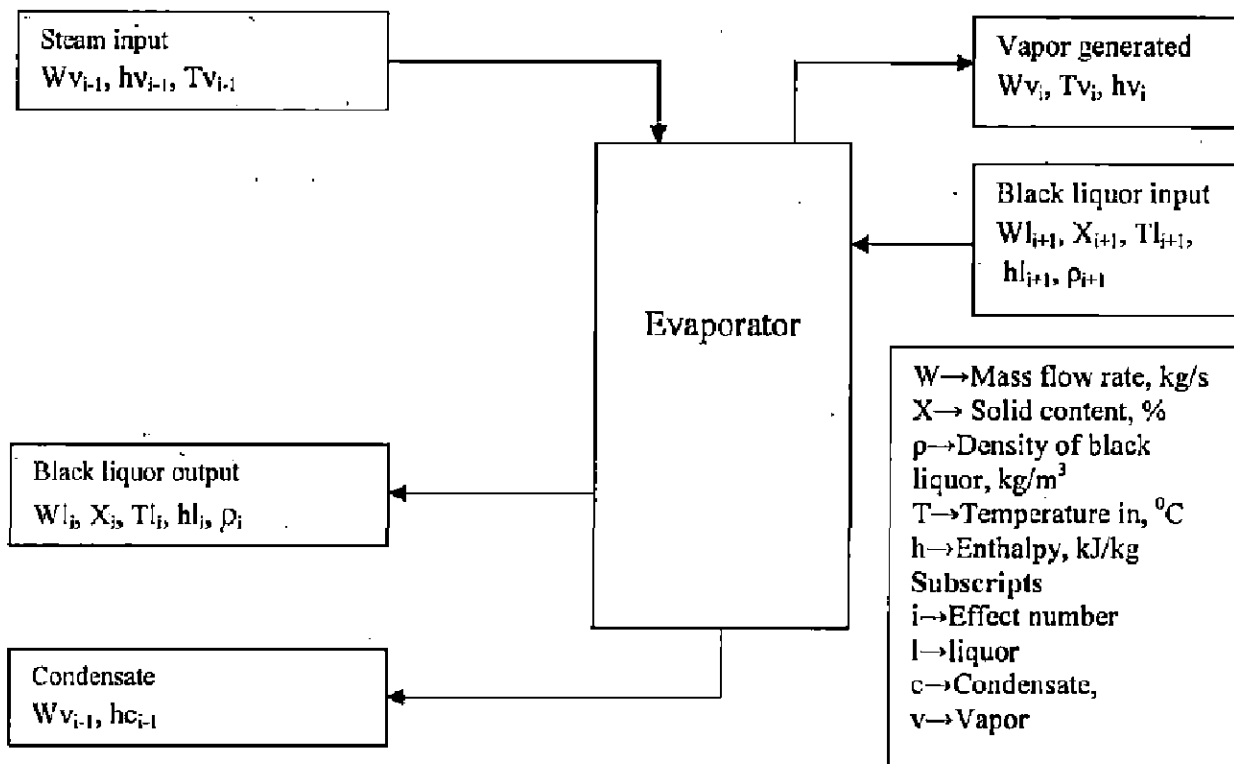


Figure 3.3 Block diagram with variables used for the  $i^{\text{th}}$  effect

### 3.5. Development of Mathematical Model

In the present investigation the lumped parameter type (system of ordinary differential equations) mathematical model of sextuple effect (tubular falling film with liquor flow inside the tube) falling film evaporator system of a paper industry is developed based on the work proposed by Aly and Marwan (1997) by using unsteady state energy and material balance equations and physico/chemical properties of black liquor for backward feed sequence. The material and energy flow for  $i^{\text{th}}$  effect is shown in the Figure 3.3. Model equations are developed for  $i^{\text{th}}$  effect by using material and energy balance equations. The equations stating the physico/chemical properties of the black liquor are presented in Table 3.2. The following assumptions are made for the development of the model.

- Vapor generated by the process of concentration of black liquor is saturated.
- Energy and mass accumulation in the vapor lump is very small as compared to the enthalpy of the steam and can be neglected.

Model is extended by considering boiling point rise (BPR) with increasing concentration of solution. After the development of the model for backward feed, the model also developed for mixed as well as split feed sequences.

### 3.5.1. Mathematical modelling for sextuple effect evaporators using backward feed sequence

The flow diagram of liquor, steam and condensate for the backward feed is shown in the Figure 3.4. In the backward feed sequence, feed is introduced to the last effect and partly concentrated liquor flows to the fifth, fourth, third, second and then to the first effect from which the concentrated liquor is withdrawn. Saturated steam is fed to the shell of the first effect, and vapor generated therein flows to the shell of second effect and acts as the heating medium there. The vapor generated in the second effect supplies heat for boiling the liquor in the third effect. In this manner steam generated in each effect is supplied to the next effect. The steam generated in the last effect is condensed by the condenser.

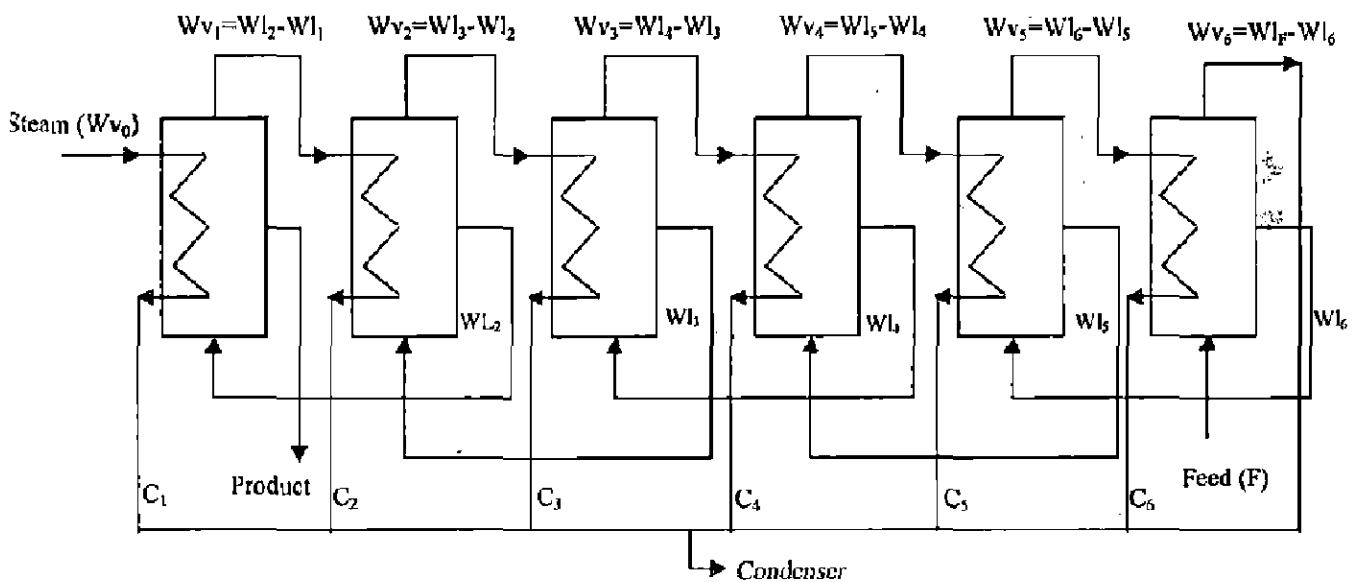


Figure 3.4 Flow diagram of Sextuple backward feed evaporator ( $\rightarrow 6 \rightarrow 5 \rightarrow 4 \rightarrow 3 \rightarrow 2 \rightarrow 1$ )

Material balance for liquor in the  $i^{\text{th}}$  effect:

$$\frac{d}{dt} Ml_i(t) = Wl_{i+1} - Wl_i - Wv_i \quad (3.14)$$

Where  $Ml$  is mass in Kg

Energy balance for liquor in the  $i^{\text{th}}$  effect:

$$\frac{d}{dt}(Ml_i(t) * hl_i) = Wl_{i+1}hl_{i+1} - Wl_ihl_i - Wv_ihv_i + Wv_{i-1}hv_{i-1} - Wv_{i-1}hc_{i-1} \quad (3.15)$$

$$\text{and } Wv_{i-1} = \frac{Q}{hv_{i-1} - hc_{i-1}}$$

$Q$  is the rate of heat transfer and also  $Q = U_i A_i (Tv_{i+1} - Tv_i - BPR_i)$

Where  $U$  is the overall heat transfer coefficient (OHTC),  $\text{kJ/sec.m}^{20}\text{C}$

$A$  is the shell area,  $\text{m}^2$

Material balance for solids in  $i^{\text{th}}$  effect:

$$\frac{d}{dt}(Ml_i(t) * X_i(t)) = Wl_{i+1}X_{i+1} - Wl_iX_i \quad (3.16)$$

The vapor and liquor in  $i^{\text{th}}$  effect are in equilibrium and the relation for the liquor and vapor temperature defined in terms of boiling point rise (BPR) is as follows:

$$Tl_i = Tv_i + BPR_i \quad (3.17)$$

where boiling point rise (BPR) is a function of temperature and solid concentration

Differentiating equation (3.17) with respect to time we get

$$\frac{d}{dt}Tl_i(t) = \left( \frac{d}{dt}Tv_i(t) \right) \left\{ 1 + \left( \frac{\partial}{\partial Tv} BPR_i \right) \right\} + \left( \frac{\partial}{\partial X} BPR_i \right) \left( \frac{\partial}{\partial t} X_i(t) \right) \quad (3.18)$$

Now  $Ml_i$  can be written as:

$$Ml_i = AL_i \rho_i \quad (3.19)$$

where  $\rho_i$  is the density of the liquor for  $i^{\text{th}}$  effect, which is the function of temperature and solid concentration,  $A$  is the shell area of the evaporator and  $L_i$  is the liquor level for  $i^{\text{th}}$  effect.

Differentiating equation (3.19) with respect to time

$$\frac{d}{dt}Ml_i(t) = AL_i(t) \left( \frac{d}{dt} \rho_i \right) + A \rho_i \left( \frac{d}{dt} L_i(t) \right) \quad (3.20)$$

Since  $\rho_i$  is a function of temperature  $Tl$  and concentration  $X$ , this equation reduces into equation

(3.21) by substituting of  $\frac{d}{dt}Tl_i(t)$  from equation (3.18) and rearranging the terms.

$$\begin{aligned} \frac{d}{dt}Ml_i(t) &= A\rho_i\left(\frac{d}{dt}L_i(t)\right) + AL_i(t)\left(\frac{d}{dTl}\rho_i\right)\left\{1 + \frac{\partial}{\partial Tv}BPR_i\right\}\left(\frac{d}{dt}Tv_i(t)\right) \\ &+ AL_i(t)\left\{\left(\frac{\partial}{\partial t}\rho_i\right)\left(\frac{\partial}{\partial X}BPR_i\right) + \left(\frac{\partial}{\partial X}\rho_i\right)\right\}\left(\frac{d}{dt}X_i(t)\right) \end{aligned} \quad (3.21)$$

Comparing the resultant differential equation (3.21) with equation (3.14) we get

$$C1 = C2\left(\frac{d}{dt}L_i(t)\right) + C3\left(\frac{d}{dt}Tv_i(t)\right) + C4\left(\frac{d}{dt}X_i(t)\right) \quad (3.22)$$

where

$$C1 = Wl_{i+1} - Wl_i - Wv_i$$

$$C2 = A\rho_i$$

$$C3 = AL_i(t)\left(\frac{\partial}{\partial Tl}\rho_i\right)\left\{1 + \left(\frac{\partial}{\partial Tv}BPR_i\right)\right\}$$

$$C4 = AL_i(t)\left\{\left(\frac{\partial}{\partial Tl}\rho_i\right)\left(\frac{\partial}{\partial X}BPR_i\right) + \left(\frac{\partial}{\partial X}\rho_i\right)\right\}$$

Enthalpy is a function of temperature. Differentiating  $Ml_i(t)*hl_i(t)$  with respect to time and

substituting  $\frac{d}{dt}Tl_i(t)$  from equation (3.18) and  $\frac{d}{dt}Ml_i(t)$  from the equation (3.21)

$$\begin{aligned} \left(\frac{d}{dt}Ml_i(t)\right)hl_i + Ml_i(t)\left(\frac{d}{dt}hl_i\right) &= A\rho_i hl_i\left(\frac{d}{dt}L_i(t)\right) + AL_i(t)\left(1 + \frac{\partial}{\partial Tv}BPR_i\right) \\ &\left\{\rho_i\left(\frac{\partial}{\partial Tl}hl_i\right) + \left(\frac{\partial}{\partial Tl}\rho_i\right)hl_i\right\}\left(\frac{d}{dt}Tv_i(t)\right) + AL_i(t)\left(\frac{d}{dt}X_i(t)\right) \\ &\left\{\rho_i\left(\frac{\partial}{\partial Tl}hl_i\right)\left(\frac{\partial}{\partial X}BPR_i\right) + \rho_i\left(\frac{\partial}{\partial X}hl_i\right) + hl_i\left(\frac{\partial}{\partial Tl}\rho_i\right)\left(\frac{\partial}{\partial X}BPR_i\right) + \left(\frac{\partial}{\partial X}\rho_i\right)hl_i\right\} \end{aligned} \quad (3.23)$$

Comparing the resultant differential equation (3.23) with equation (3.15) we get

$$C5 = C6\left(\frac{d}{dt}L_i(t)\right) + C7\left(\frac{d}{dt}Tv_i(t)\right) + C8\left(\frac{d}{dt}X_i(t)\right) \quad (3.24)$$

where

$$C5 = Wl_{i+1}hl_{i+1} - Wl_ihl_i - Wv_ihv_i + Wv_{i+1}hv_{i+1} - Wv_{i-1}hc_{i-1}$$

$$C6 = A\rho_i hl_i$$

$$C7 = AL_i(t) \left( 1 + \frac{\partial}{\partial Tv} BPR_i \right) \left\{ \rho_i \left( \frac{\partial}{\partial Tl} hl_i \right) + hl_i \left( \frac{\partial}{\partial Tl} \rho_i \right) \right\}$$

$$C8 = AL_i(t) \rho_i \left\{ \left( \frac{\partial}{\partial Tl} hl_i \right) \left( \frac{\partial}{\partial X} BPE_i \right) + \left( \frac{\partial}{\partial X} hl_i \right) \right\} + AL_i(t) hl_i \left\{ \left( \frac{\partial}{\partial Tl} \rho_i \right) \left( \frac{\partial}{\partial X} BPR_i \right) + \left( \frac{\partial}{\partial X} \rho_i \right) \right\}$$

Finally differentiating  $Ml_i(t) * X_i(t)$  with respect to time and substituting the value of  $\frac{d}{dt} Ml_i(t)$  from equation (3.21) and rearranging the equation and representing it in the form of coefficients .

$$C9 = C10 \left( \frac{d}{dt} L_i(t) \right) + C11 \left( \frac{d}{dt} Tv_i(t) \right) + C12 \left( \frac{d}{dt} X_i(t) \right) \quad (3.25)$$

where

$$C9 = Wl_{i+1} X_{i+1} - Wl_i X_i$$

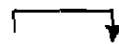
$$C10 = \Lambda \rho_i X_i$$

$$C11 = AL_i X_i \left( \frac{\partial}{\partial Tl} \rho_i \right) \left\{ 1 + \left( \frac{\partial}{\partial Tv} BPR_i \right) \right\}$$

$$C12 = AL_i \left[ \rho_i + X_i \left\{ \left( \frac{\partial}{\partial Tl} \rho_i \right) \left( \frac{\partial}{\partial X} BPR_i \right) + \left( \frac{\partial}{\partial X} \rho_i \right) \right\} \right]$$

Thus the equations (3.22), (3.24) and (3.25) form a set of differential equations representing the liquor flow inside the evaporator and the solid content of the liquor for the  $i^{th}$  effect. These final equations, represents the dynamics of multi-effect evaporators, derived from basic energy and mass balance equations and using various terms related to physical properties of black liquor, water and steam like density and specific heat of the liquor, boiling point rise (BPR), enthalpy of water and saturated steam. Further equations are applied to all the six effects for  $i = 1, 2, 3, 4, 5$  and 6.

### 3.5.2. Mathematical modelling for sextuple effect evaporators using mixed feed sequence



The flow diagram for mixed feed ( $6 \leftarrow 5 \rightarrow 4 \rightarrow 3 \rightarrow 2 \rightarrow 1$ ) is shown in Figure 3.5. In this case the feed is given to 5<sup>th</sup> effect and the thick liquor from 5<sup>th</sup> goes into 6<sup>th</sup> and from 6<sup>th</sup> into 4<sup>th</sup> up to the first effect. To obtain the model equations for the mixed feed few changes are required in the feeding

variables of the model developed for backward feed. The material balance as well as energy balance is changed for the 4<sup>th</sup>, 5<sup>th</sup> and 6<sup>th</sup> in terms of feeding variables.

Material and energy balance for liquor in the  $i^{\text{th}}$  effect for  $i = 1, 2$  and  $3$  can be represented by equations (3.22), (3.24) and (3.25).

Since in the mixed feed sequence the feed is given to fifth effect and then thick liquor move from 5<sup>th</sup> to 6<sup>th</sup> and from 6<sup>th</sup> to 4<sup>th</sup> effect thus the material balance equations for  $i = 4, 5$  and  $6$  are given by

$$\text{For } i = 4 \quad \frac{d}{dt} Ml_4(t) = Wl_6 - Wl_4 - Wv_4 \quad (3.26a)$$

$$\text{For } i = 5 \quad \frac{d}{dt} Ml_5(t) = F - Wl_5 - Wv_5 \quad (3.26b)$$

$$\text{For } i = 6 \quad \frac{d}{dt} Ml_6(t) = Wl_5 - Wl_6 - Wv_6 \quad (3.26c)$$

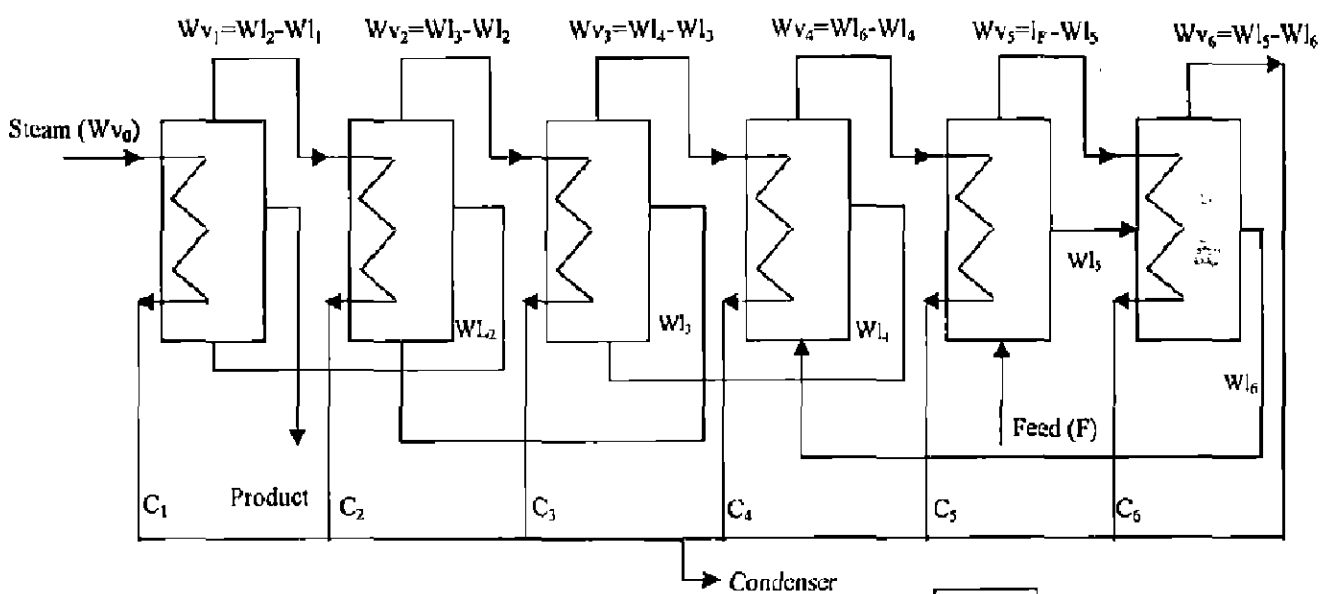


**Figure 3.5** Flow diagram of Sextuple mixed feed evaporator (6←5 4→3→2→1)

Similar changes are applied to obtain, energy and solid balance for  $i = 4, 5$  and  $6$ . Finally, for mixed feed, the changed expressions of the coefficients  $C_1, C_5$  and  $C_6$  are obtained for  $i = 4, 5$  and  $6$  as follows

$$\text{For } i = 4 \quad C1 = Wl_6 - Wl_4 - Wv_4,$$



$$C5 = Wl_6hl_6 - Wl_4hl_4 - Wv_4hv_4 + Wv_3hv_3 - Wv_3hc_3,$$

$$C9 = Wl_6X_6 - Wl_4X_4$$

For  $i = 5$   $C1 = F - Wl_5 - Wv_5,$

$$C5 = Fhl_F - Wl_5hl_5 - Wv_5hv_5 + Wv_4hv_4 - Wv_4hc_4,$$

$$C9 = FX_F - Wl_5X_5$$

For  $i = 6$   $C1 = Wl_5 - Wl_6 - Wv_6,$

$$C5 = Wl_5hl_5 - Wl_6hl_6 - Wv_6hv_6 + Wv_5hv_5 - Wv_5hc_5,$$

$$C9 = Wl_5X_5 - Wl_6X_6$$

The remaining coefficients from C2, C3, C4, C6, C7, C8, C10, C11 and C12 are same as backward feed sequence for  $i = 1$  to 6.

### 3.5.3. Mathematical modelling for sextuple effect evaporators using split feed sequence

The flow diagram for split feed is shown in the Figure 3.6. In this case of split feed the feed is equally given to 5<sup>th</sup> and 6<sup>th</sup> effects and the thick liquor from both 5<sup>th</sup> and 6<sup>th</sup> effect moves into 4<sup>th</sup> effect and from 4<sup>th</sup> to 3<sup>rd</sup> effect and so on up to the first effect. To obtain the model equations for the split feed few changes are required in the feeding variables in the model developed for backward feed. For the split feed the material, energy and solid balance equations are changed for the 4<sup>th</sup>, 5<sup>th</sup> and 6<sup>th</sup> effect in terms of feeding variables.

Material and energy balance for liquor in the  $i^{\text{th}}$  effect for  $i = 1, 2$  and  $3$  can be represented by equations (3.22), (3.24) and (3.25). Since in the split feed sequence the feed is divided equally to fifth and sixth effect and then thick liquor move from 5<sup>th</sup> and 6<sup>th</sup> together into 4<sup>th</sup> and from 4<sup>th</sup> to 3<sup>rd</sup> up to the first effect, thus the material balance equations for  $i = 4, 5$  and  $6$  are given by

$$\text{For } i = 4 \quad \frac{d}{dt} Ml_4(t) = Wl_5 + Wl_6 - Wl_4 - Wv_4 \quad (3.27a)$$

$$\text{For } i = 5 \quad \frac{d}{dt} Ml_5(t) = \frac{F}{2} - Wl_5 - Wv_5 \quad (3.27b)$$

For  $i = 6$

$$\frac{d}{dt} Ml_6(t) = \frac{F}{2} - Wl_6 - Wv_6 \quad (3.27c)$$

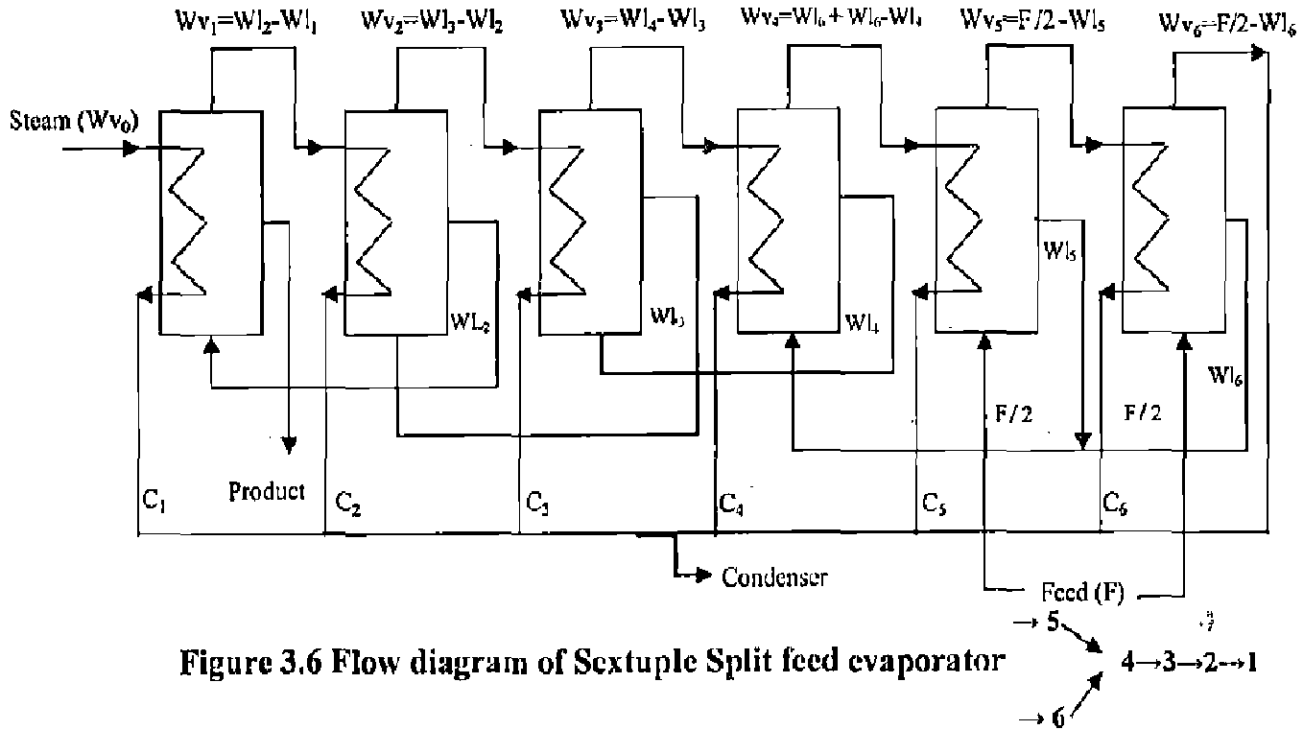


Figure 3.6 Flow diagram of Sextuple Split feed evaporator

Similar changes are applied to obtain, energy and solid balance for  $i = 4, 5$  and  $6$ . Finally, for split feed, the changed expressions of the coefficients  $C_1, C_5$  and  $C_9$  are obtained for  $i = 4, 5$  and  $6$  as follows

$$\text{For } i = 4 \quad C1 = Wl_5 + Wl_6 - Wl_4 - Wv_4,$$

$$C5 = Wl_5hl_5 + Wl_6hl_6 - Wl_4hl_4 - Wv_4hv_4 + Wv_3hv_3 - Wv_3hc_3,$$

$$C9 = Wl_5X_5 + Wl_6X_6 - Wl_4X_4$$

$$\text{For } i = 5 \quad C1 = \frac{F}{2} - Wl_5 - Wv_5,$$

$$C5 = \frac{F}{2}hl_F - Wl_5hl_5 - Wv_5hv_5 + Wv_4hv_4 - Wv_4hc_4,$$

$$C9 = \frac{F}{2}X_F - Wl_5X_5$$

$$\text{For } i = 6 \quad C1 = \frac{F}{2} - Wl_6 - Wv_6,$$

$$C5 = \frac{F}{2} h l_F - W l_6 h l_6 - W v_6 h v_6 + W v_5 h v_5 - W v_5 h c_s$$

$$C9 = \frac{F}{2} X_F - W l_6 X_6$$

The remaining coefficients from C2, C3, C4, C6, C7, C8, C10, C11 and C12 are same as backward feed sequence for  $i = 1$  to 6.

### 3.6. Simulation Studies

To study the dynamic response of any chemical process initial values of the process variables are needed. For this purpose, steady state solution of that system is obtained first. Data for simulation purpose is taken from literature. The range of operating parameters are taken according to Gupta (2001) as shown in Table 3.3 and duly modified according to mill conditions. For the calculation of the rate of heat transfer an overall heat transfer coefficient (OHTC) is required. For falling film evaporator, the range of overall heat transfer coefficient (OHTC) is given by various researchers. Typical values of overall heat transfer coefficients between 500-2500 k Cal/h m<sup>2</sup> °C is suggested by Dutta (2005) for the general evaporators, Algehed and Berntsson (2003) suggested the values of OHTC nearly 1300 W/m<sup>2</sup> °C for black liquor evaporation. Gullichsen and Fogelholm (2000) gave the range of OHTC between 500-2000 W/m<sup>2</sup> °C for all six effects of a sextuple evaporator system to raising the concentration of black liquor from 10% to 50%. After discussion with few Indian paper mills, values of OHTC are taken in the range of 1000-1200 k Cal/hm<sup>2</sup> °C for the present study and the values for each effect are presented in Table 3.3

**Table 3.3 Range of operational parameters [Gupta (2001)]**

S. No.	Operational Parameter	Parameter's Range	Values
1.	Liquor feed flow rate, kg/sec	18.00-25.00	23.98
2.	Liquor feed Temperature, °C	70.00-90.00	80.00
3.	Liquor feed concentration	0.10-0.52	0.10
4.	Steam Temperature, °C	135-140	139
5.	Last body saturation, °C	48-52	49
6.	Liquor product concentration	0.48-0.52	0.50
7.	Heat transfer Coefficients (k Cal/hm <sup>2</sup> °C)	1000-1200	1000 (i), 1050 (ii), 1100 (iii), 1150 (iv), 1175 (v), 1200 (vi)

### 3.6.1 Solution technique

A number of engineering problems can be formulated into differential equations. The analytical methods of solving differential equations are applicable only to a limited class of equations. Quite often differential equations appearing in physical problems do not belong to any of these familiar types and one is obliged to resort to numerical methods. These methods are of even greater importance when we realize that computing machines are now readily available which reduce numerical work considerably.

The multiple effect evaporator arrangements are quite cumbersome to perform calculations for. To ease the workload a developed computer based methods to perform the calculations is used. Thus for the solution of models in steady state conditions, 'fsolve' solver in MATLAB is used, which is an equation solver used to solve nonlinear equations by the least squares method. For the solution of unsteady state model 'ode45' solver in MATLAB is used, which solves initial value problems for ordinary differential equations (ODEs). Ode45 is based on an explicit Runge-Kutta (4, 5) formula, the Dormand-Prince pair. It is a one-step solver - in computing  $y(t_n)$ , it needs only the solution at the immediately preceding time point,  $y(t_{n-1})$ .

### 3.6.2 Steady state simulation

Steady state model of the MEE system for backward feed is obtained by equating the accumulation terms in the equations (3.22), (3.24) and (3.25) to zero i.e.  $C_1 = 0$ ,  $C_5 = 0$  and  $C_9 = 0$ . After substituting the expressions of enthalpies, boiling point elevation and liquor density etc. and heat transfer rate, 12 nonlinear equations in 12 unknowns are obtained similar to the previous work carried out by Gupta (2001). Similarly the systems of 12 nonlinear equations with 12 unknowns are obtained for mixed and split feed also by using the modified values of  $C_1$ ,  $C_5$  and  $C_9$  as discussed in sections 3.4.3.2 and 3.4.3.3. For obtaining the steady state solution of the sextuple effect evaporator system there is a need to solve the system of nonlinear simultaneous equations.

The steady state solution is presented in Table 3.4, Table 3.5 and Table 3.6 for backward, mixed and split feed sequences respectively. The input values are shown in bold face in the respective Table. The required steam, heat transfer area and Steam economy (SE) is calculated and also

presented in aforesaid Tables. SE is the ratio of total water evaporated in MEE system with fresh steam consumption.

**Table 3.4 Steady state solution of sextuple effect evaporator for backward feed**

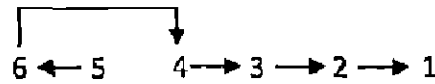
( $\rightarrow 6 \rightarrow 5 \rightarrow 4 \rightarrow 3 \rightarrow 2 \rightarrow 1$ )

Items	Effects					
	I	II	III	IV	V	VI
Input Liquor Concentration (kg/kg)	0.2849	0.2033	0.1608	0.1352	0.1184	0.1
Output Liquor Concentration (kg/kg)	0.5	0.2849	0.2033	0.1608	0.1352	0.1184
Input Liquor Flow (kg/Sec)	8.417	11.7976	14.9092	17.7402	20.2613	23.98
Output Liquor Flow (kg/Sec)	4.796	8.417	11.7976	14.9092	17.7402	20.2613
Input Liquor Temperature (°C)	99.1216	83.0459	70.555	60.0491	50.125	80
Output Liquor Temperature (°C)	125.0388	99.1216	83.0459	70.555	60.0491	50.125
Input Steam Temperature (°C)	139	110.8637	94.065	80.2413	68.6686	58.6385
Output Steam Temperature (°C)	110.8637	94.065	80.2413	68.6686	58.6385	49
Input Steam Flow (kg/Sec)	3.9076	3.621	3.3806	3.1116	2.831	2.5211
Output Steam Flow (kg/Sec)	3.621	3.3806	3.1116	2.831	2.5211	3.7187
Boiling Point Rise (°C)	14.1751	5.0566	2.8046	1.8864	1.4106	1.125
Specific Heat (kJ/kg.°C)	3.3005	3.6333	3.7769	3.8569	3.9072	3.9406
Heat Transfer Area (m <sup>2</sup> )	600.5748					
Stream Consumption (kg/Sec)	3.9076					
Total Evaporation (kg/Sec)	19.184					
Steam Economy	4.9094					

### 3.6.3 Model validation

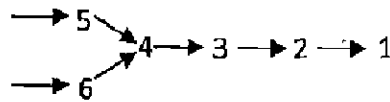
For the validation of model solution is compared with solutions provided by earlier workers. Researchers have used different input data for obtaining the solution. Input data used in the present work is same as used by Gupta (2001). The steady state results obtained are in good agreement with the results presented by Gupta (2001) for backward feed. Data given by earlier researchers such as [Ray and Singh (2000), Ray and Sharma (2004) and Ray et al. (2004)] is also used for the steady state solution of the model for backward, mixed and split feed sequence. The results obtained show the good agreement with the results of above researchers.

**Table 3.5 Steady state solution of sextuple effect evaporator for mixed feed**



Items	Effects					
	I	II	III	IV	V	VI
Input Liquor Concentration (kg/kg)	0.2883	0.2067	0.1639	0.1401	<b>0.1</b>	0.1157
Output Liquor Concentration (kg/kg)	<b>0.5</b>	0.2883	0.2067	0.1639	0.1157	0.1401
Input Liquor Flow (kg/Sec)	8.3173	11.6031	14.627	17.1105	<b>23.98</b>	20.73
Output Liquor Flow (kg/Sec)	4.796	<b>8.3173</b>	11.6031	14.627	20.73	17.1105
Input Liquor Temperature (°C)	99.4662	83.4384	71.0077	50.419	<b>80</b>	61.3928
Output Liquor Temperature (°C)	125.2157	99.4662	83.4384	71.0077	61.3928	50.419
Input Steam Temperature (°C)	<b>139</b>	111.0319	94.3051	80.5579	69.0649	60.2439
Output Steam Temperature (°C)	111.0319	94.3051	80.5579	69.0649	60.2439	<b>49</b>
Input Steam Flow (kg/Sec)	3.8028	3.5213	3.2858	3.0239	2.4835	3.25
Output Steam Flow (kg/Sec)	3.5213	3.2858	3.0239	2.4835	3.25	3.6195
Boiling Point Rise (°C)	14.1838	5.1611	2.8805	1.9428	1.1489	1.419
Specific Heat (kJ/kg.°C)	3.3006	3.6275	3.7704	3.8507	3.9506	3.8924
Heat Transfer Area (m <sup>2</sup> )	591.9614					
Stream Consumption (kg/Sec)	3.8028					
Total Evaporation (kg/Sec)	19.184					
Steam Economy	5.0447					

**Table 3.6 Steady state solution of sextuple effect evaporator for split feed**



Items	Effects					
	I	II	III	IV	V	VI
Input Liquor Concentration (kg/kg)	0.2864	0.2045	0.1617	0.1377	0.1	0.1
Output Liquor Concentration (kg/kg)	0.5	0.2864	0.2045	0.1617	0.1330	0.1427
Input Liquor Flow (kg/sec)	8.3726	11.7261	14.8293	17.4203	11.99	11.99
Output Liquor Flow (kg/sec)	4.796	8.3726	11.7261	14.8293	9.0157	8.4046
Input Liquor Temperature (°C)	101.4446	86.2425	74.4873	59.2380	80	80
Output Liquor Temperature (°C)	126.3474	101.4446	86.2425	74.4873	65.2961	53.18
Input Steam Temperature (°C)	139	112.1079	96.2997	83.3752	72.5542	61.3498
Output Steam Temperature (°C)	112.1079	96.2997	83.3752	72.5542	61.3498	49
Input Steam Flow (kg/sec)	3.8492	3.5766	3.3535	3.1032	2.591	2.9743
Output Steam Flow (kg/sec)	3.5766	3.3535	3.1032	2.591	2.9743	3.5854
Boiling Point Rise (°C)	14.2395	5.1449	2.8673	1.9331	3.9463	4.18
Specific Heat (kJ/kg.°C)	3.301	3.632	3.7761	3.857	3.6469	3.6044
Heat Transfer Area (m <sup>2</sup> )	652.775					
Stream Consumption (kg/sec)	3.8492					
Total Evaporation (kg/sec)	19.184					
Steam Economy	4.9839					

### 3.7 Model Application

Study of the effect of various input parameters on performance of various feeding sequences is also studied by varying the range of input parameters. Optimal feed sequence is obtained by comparing the steam economy of all three feed sequences.

The dynamic responses due to disturbances by step input in various input parameters are also studied. Responses in the face of disturbances are shown by graphical representation with respect to time. The responses are studied by the step input of  $\pm 10\%$  in the various input parameters.

### 3.8 Parametric Effect on the Performance of Various Feeding Sequences

The results obtained from the solution of the models are plotted in graphs and parametric influences are interpreted. Effect of various input parameters on output parameters of MEE system can be measured by different characteristic like steam consumption (SC), steam economy (SE), and area requirement (A). In the present work to study the performance the MEE system, the effect of various input parameters on steam economy (SE) is described and shown from Figure 3.7 to Figure 3.12. Finally the optimal feed sequence is obtained.

#### 3.8.1 Effect of feed temperature on steam economy

Figure 3.7 shows the effect of feed temperature on steam economy (SE) for backward, mixed and split feed respectively. With the rise of feed temperature from 70 to 90°C, the SE increases linearly for all the feed sequences. This is due to the fact that the increase in the feed temperature leads to an increase in the feed enthalpy. From the Figure 3.7 it is clear that the mixed feed sequence is optimal for the entire range of feed temperature considered for the present study.

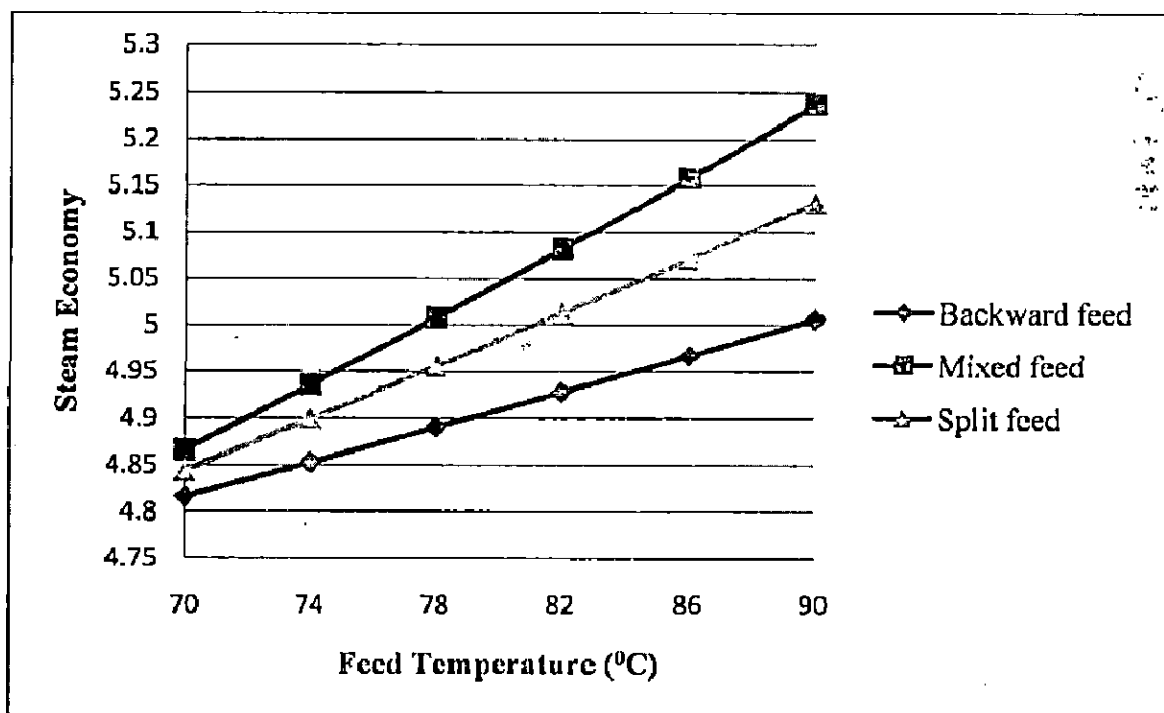


Figure 3.7 Effect of feed temperature on steam economy



### 3.8.2 Effect of steam temperature on steam economy

Figure 3.8 shows the effect of steam temperature on SE for backward, mixed and split feed respectively. With the rise of steam temperature from 130 to 140°C, the SE decreases for all the feed sequences. This is due to the decrease in latent heat of the steam with increase in steam temperature. From the Figure 3.8 it is clear that the mixed feed is the optimal sequence.

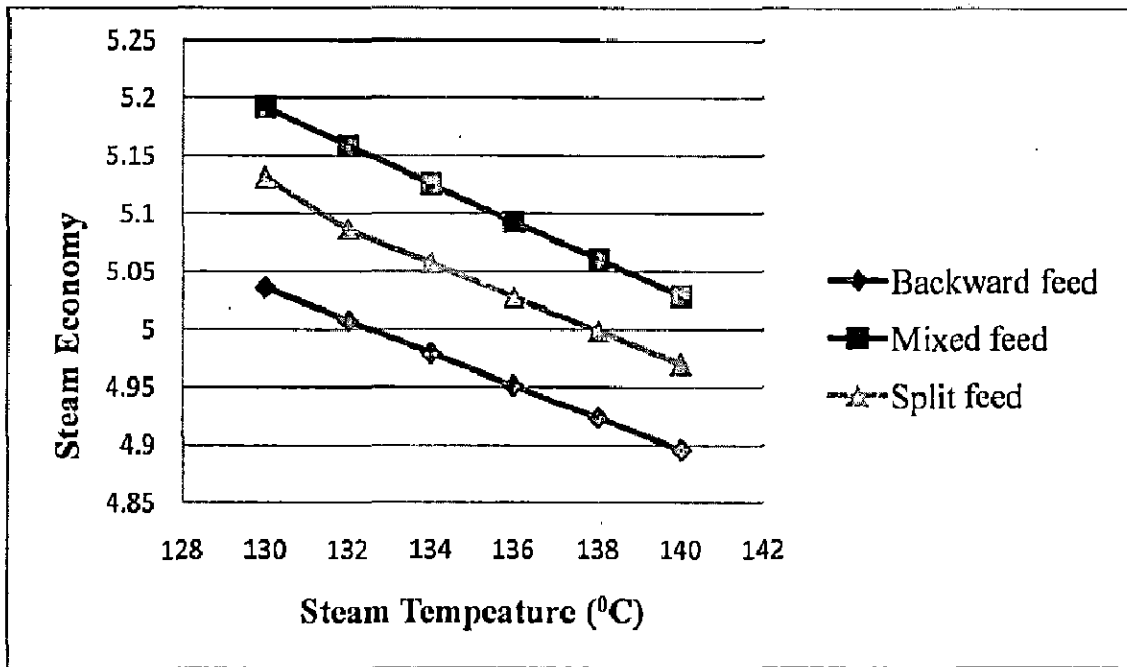


Figure 3.8 Effect of steam temperature on steam economy

### 3.8.3 Effect of feed flow rate on steam economy

Figure 3.9 shows the effect of feed flow rate on steam economy (SE) for all three sequences. With varying the feed flow rate from 18 to 25 kg/s, there is no noticeable change in the SE for all the sequences. It is clear from the Figure 3.9 that the mixed feed is optimal sequence.

### 3.8.4 Effect of feed concentration on steam economy

Figure 3.10 shows that the effect of varying feed concentration from 0.10 to 0.18 on steam economy (SE) for all three sequences. With the rise of feed concentration the SE decreases with increase in feed concentration for all the feed sequences. Mixed feed remains optimal for the entire range of feed concentration. The similar trend is reported by earlier workers [Gupta (2001), Ray and Singh (2000)].

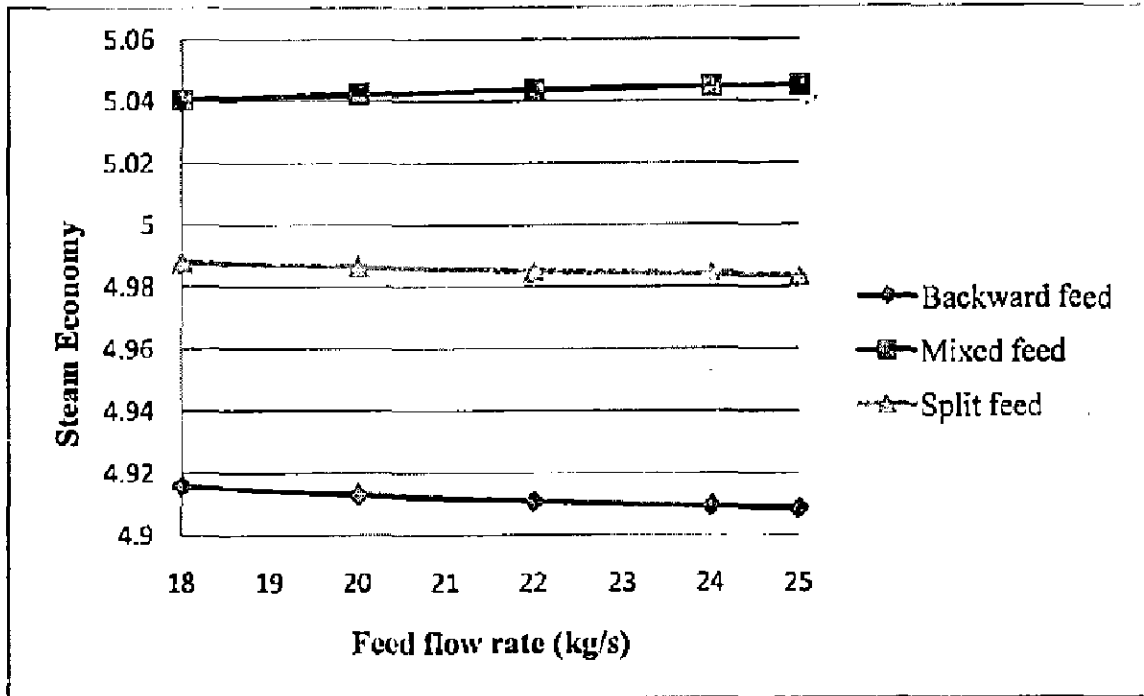


Figure 3.9 Effect of feed flow rate on steam economy

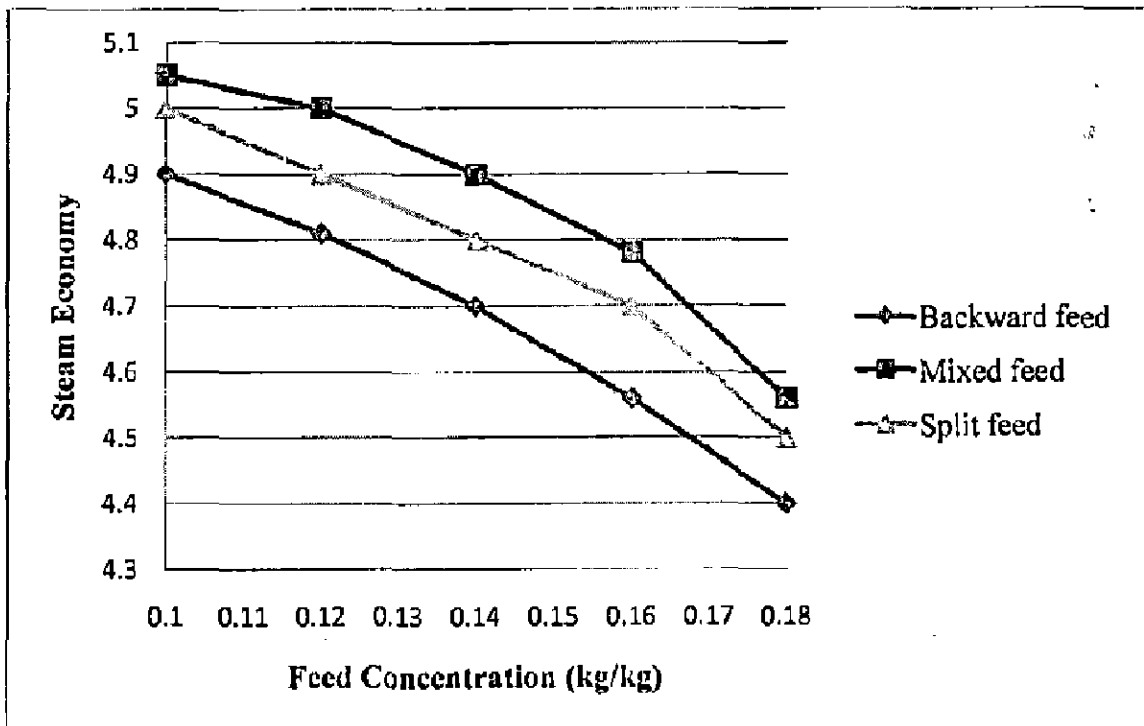


Figure 3.10 Effect of feed concentration on steam economy

### 3.8.5 Effect of product concentration on steam economy

Figure 3.11 shows the effect of varying product target (i.e. output of the first effect) concentration on steam economy (SE) for all three sequences. Figure 3.11 shows that the SE increases with increase in target product concentration for all the feed sequences. The mixed feed sequence is found optimal for the entire range of feed flow rate. This is due to larger amount of water evaporated. But at the same time increase in target concentration may pose other problem like flow of liquor which is not considered in the present study.

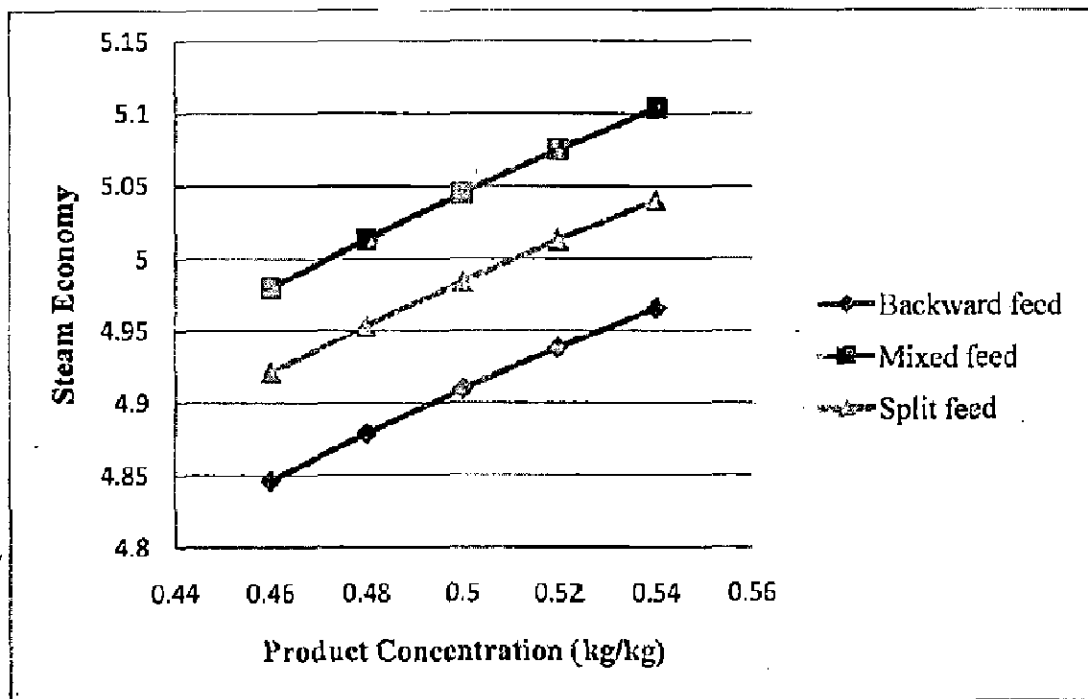
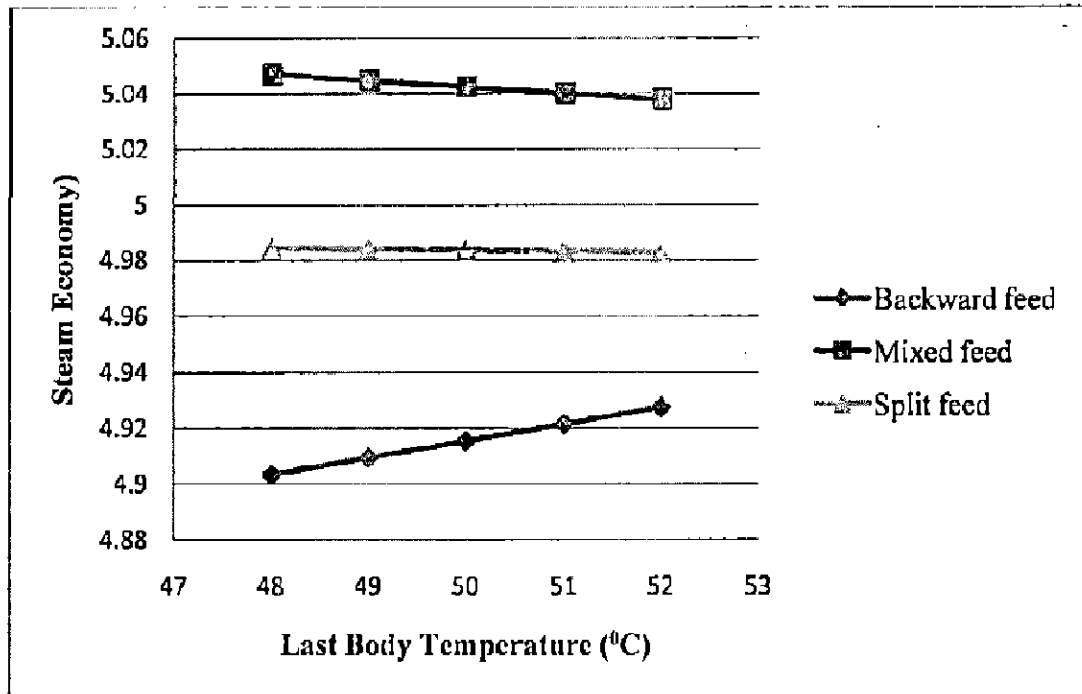


Figure 3.11 Effect of product concentration on steam economy

### 3.8.6 Effect of last body temperature on steam economy

Figure 3.12 shows the effect of varying last body (i.e. output of the first effect) temperature on steam economy (SE) for all three sequences. It is clear from the Figure 3.12 that last body temperature does not have much effect on SE. For all the sequences slight but insignificant change is observed in SE when changing the last body temperature. This may be due to the fact that overall effect of last body temperature on the  $\Delta t$  of each effect is very small.



**Figure 3.12 Effect of last body temperature on steam economy**

### 3.9 Dynamic Simulation

For the dynamic simulation first order nonlinear differential equations (3.22), (3.24) and (3.25) are solved simultaneously for all the six effects representing backward feed and modified form of these equations for mixed and split feed. The initial conditions for the system variables at time = 0 are the values obtained from steady-state solution of the system. The simultaneous solution of such types of nonlinear ordinary differential equations is extremely intricate in nature, even by using sophisticated numerical techniques.

### 3.10 Dynamic Response of MEE System for Various Feed Sequences

The dynamic response on system variables of MEE is studied by creating four types of disturbances namely (i) in feed flow rate, (ii) in feed concentration, (iii) in live steam temperature and (iv) in feed temperature as step input function. System variables selected were (i) Temperature of each effect and (ii) Output concentration of each effect. The disturbance is taken as a step input of  $\pm 10\%$ . Responses to the disturbance for the last (6<sup>th</sup>) and first (1<sup>st</sup>) effects are presented from the Figure 3.13 to Figure 3.20 for backward feed, Figure 3.21 to Figure 3.28 for mixed feed and Figure 3.29 to Figure 3.36 for split feed. These graphs are plotted with respect to time to show how the

variables approach to the new steady state conditions. For the estimation of time for achieving new steady state conditions, times constant ( $\tau$ ) is also calculated and shown in each plot and also presented in Table 3.7, Table 3.8 and Table 3.9 for backward, mixed and split feed respectively.

### 3.10.1 Time constant ( $\tau$ )

In physics and engineering, the time constant, usually denoted by the Greek letter  $\tau$  (tau), is the rise time characterizing the response to a time-varying input of a first-order, linear time-invariant (LTI) system. Physically, the constant represents the time it takes the system's step response to reach  $1 - 1/e \approx 63.2\%$  of its final (asymptotic) value. In the time domain, the usual choice to explore the time response is through the step response to a step input, or the impulse response to a Dirac delta function input. Time constants are a feature of the lumped system analysis (lumped capacity analysis method) for thermal systems, used when objects cool or warm uniformly under the influence of convective cooling or warming.

### 3.10.2 Dynamic response of sextuple effect evaporator for the backward feed

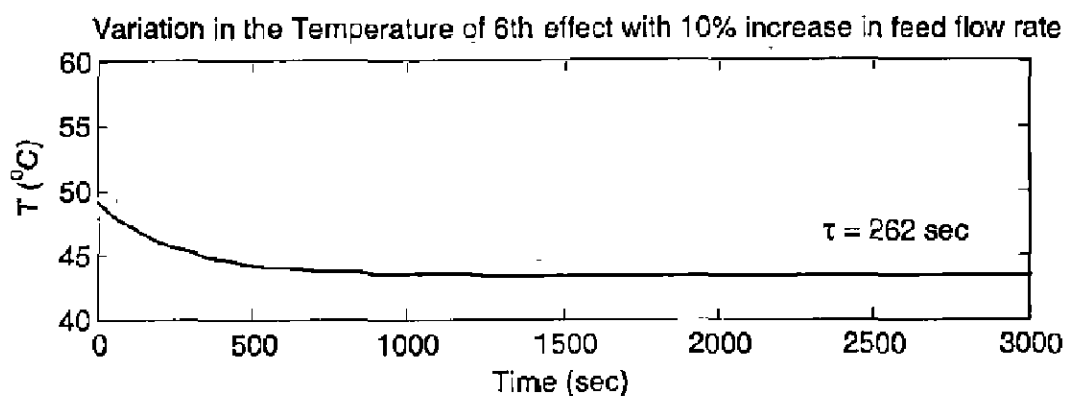
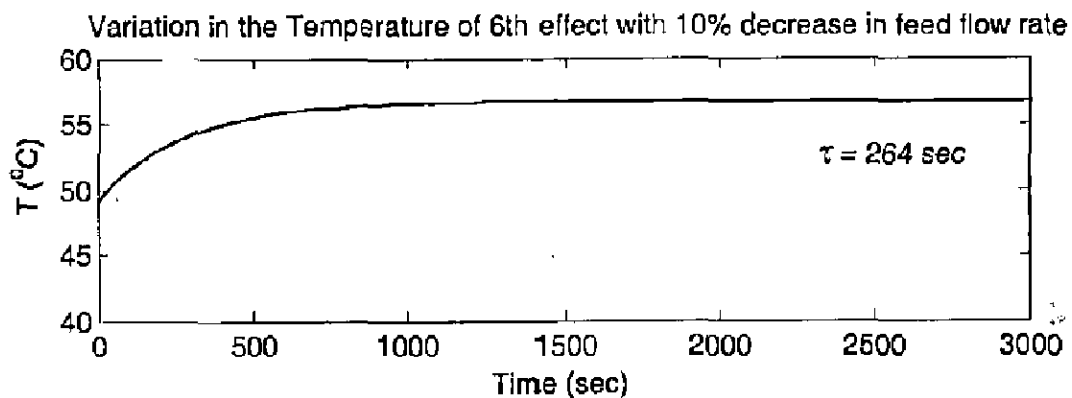
The MEE system is in backward feed ( $\rightarrow 6 \rightarrow 5 \rightarrow 4 \rightarrow 3 \rightarrow 2 \rightarrow 1$ ); hence the input liquor enters the evaporator system from the 6<sup>th</sup> effect and then thick liquor from 6<sup>th</sup> effect to 5<sup>th</sup> and from 5<sup>th</sup> to 4<sup>th</sup> and up to the first effect. Dynamic responses due  $\pm 10\%$  step input in last (connected with condenser i.e. 6<sup>th</sup>) and first effect (connected with live steam i.e. 1<sup>st</sup>) in each case of backward feed are given as follows.

**Table 3.7 Time constant for dynamic response due to 10% step input change in various input variables for backward feed sequence**

Input Variables		Time Constant ( $\tau$ ) in Second			
		6 <sup>th</sup> (Last Effect)		1 <sup>st</sup> (First Effect)	
		Temperature	Concentration	Temperature	Concentration
Feed Flow Rate	-10%	264	2880	330	20760
	+10%	262	2640	324	17340
Feed Concentration	-10%	266	3390	312	19440
	+10%	266	3408	312	19860
Steam Temperature	-10%	265	4380	337	20100
	+10%	264	4440	332	19800
Feed liquor Temperature	-10%	258	3240	336	19890
	+10%	264	3300	329	19960

### 3.10.2.1 Effect of varying feed flow rate

For the variation in the feed parameters the disturbance is applied in the last effect. The effect of  $\pm 10\%$  step input in feed flow rate on the temperature and concentration of last ( $6^{\text{th}}$ ) and first ( $1^{\text{st}}$ ) effects are shown in the Figure 3.13 to Figure 3.14 respectively. The temperature and concentration of both the effects show an increase or decrease with decrease or increase in the feed flow rate. It is obvious as fresh steam supply rate is constant and water to be evaporates and decreases per unit time. The plots (behaviors) show the similar nature as shown by Stefanov and Hoo (2004). Time constant shown in Table 3.7 indicates that response time for temperature change is much less than that of concentration change. Also the steady state in  $6^{\text{th}}$  effect is achieved at a faster rate than the  $1^{\text{st}}$  effect. This is obvious as in backward feed sequence; feed enters first in the  $6^{\text{th}}$  effect so the disturbance dampened out in the  $6^{\text{th}}$  effect at faster rate.



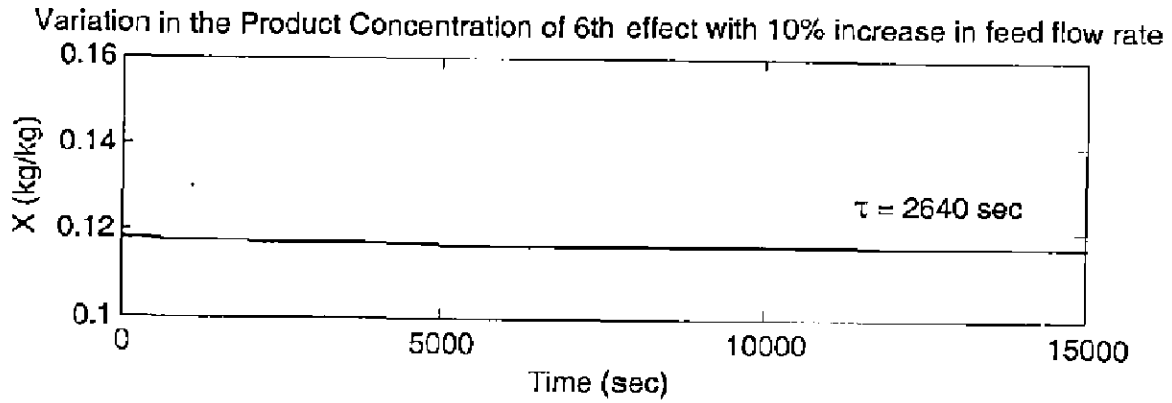
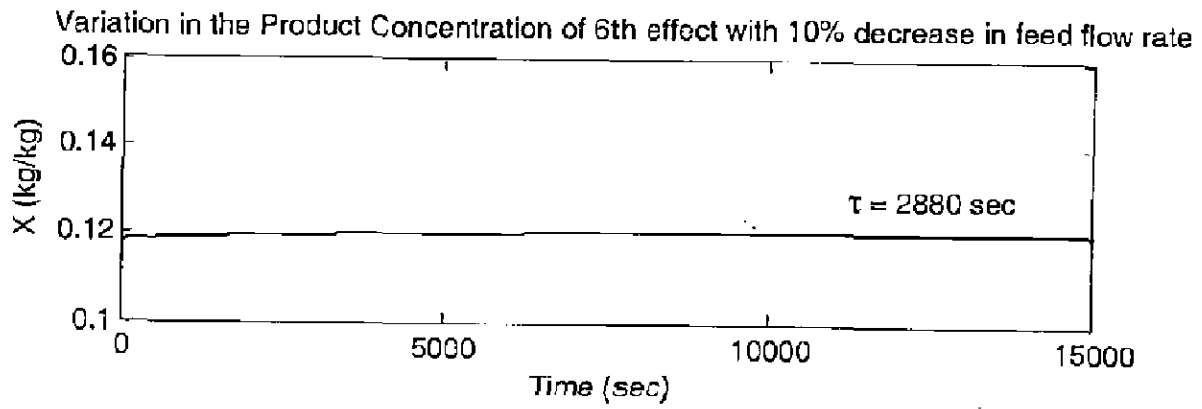
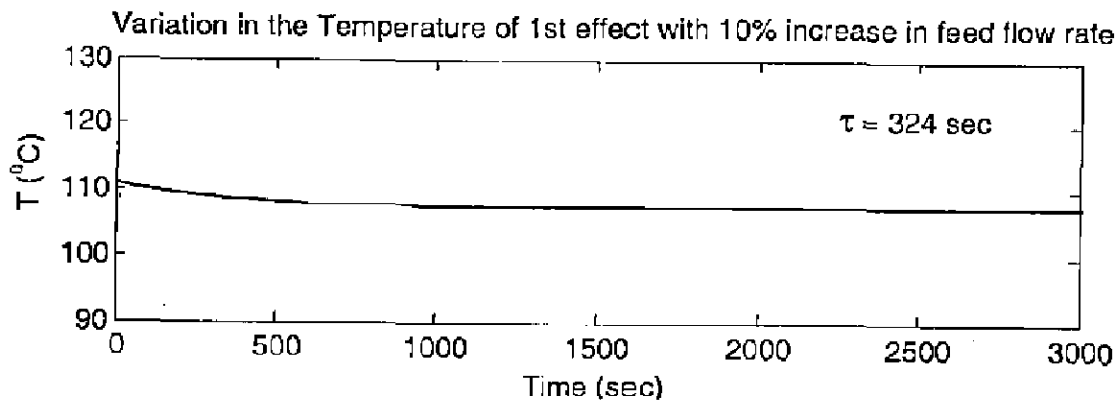
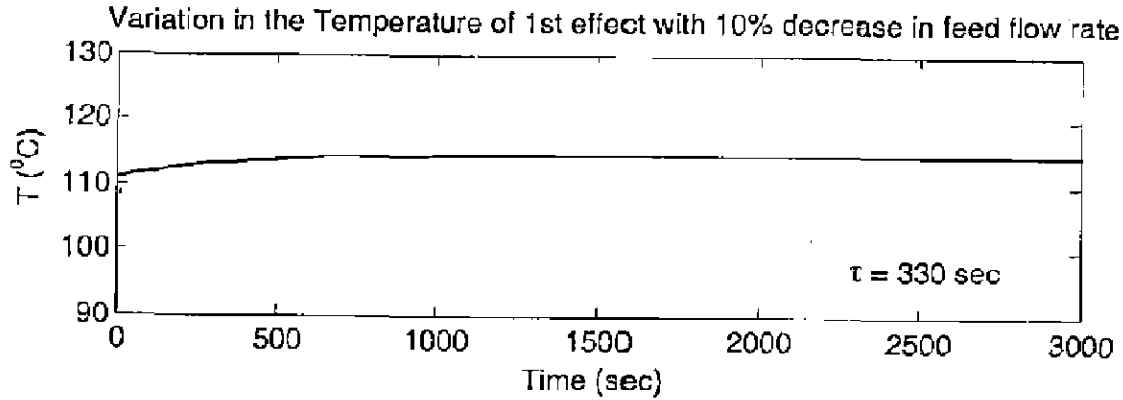


Figure 3.13 Response of 6<sup>th</sup> effect by disturbing  $\pm 10\%$  in the feed flow rate



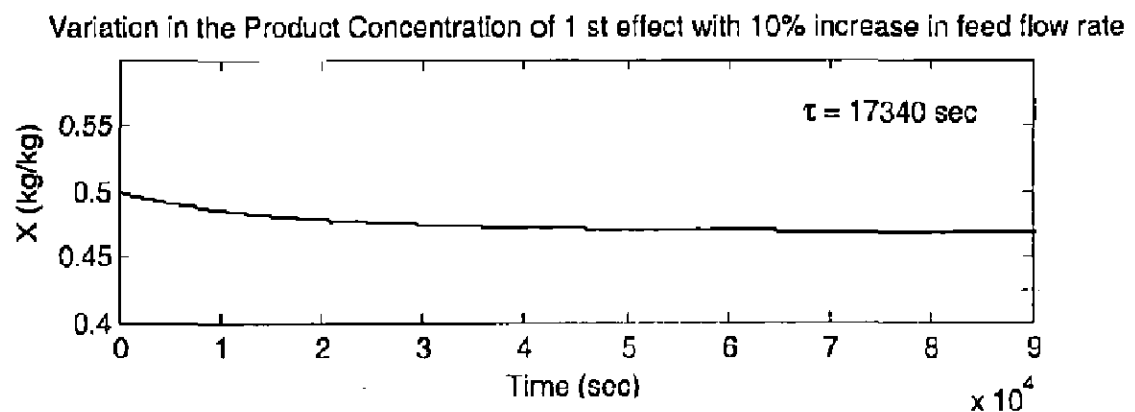
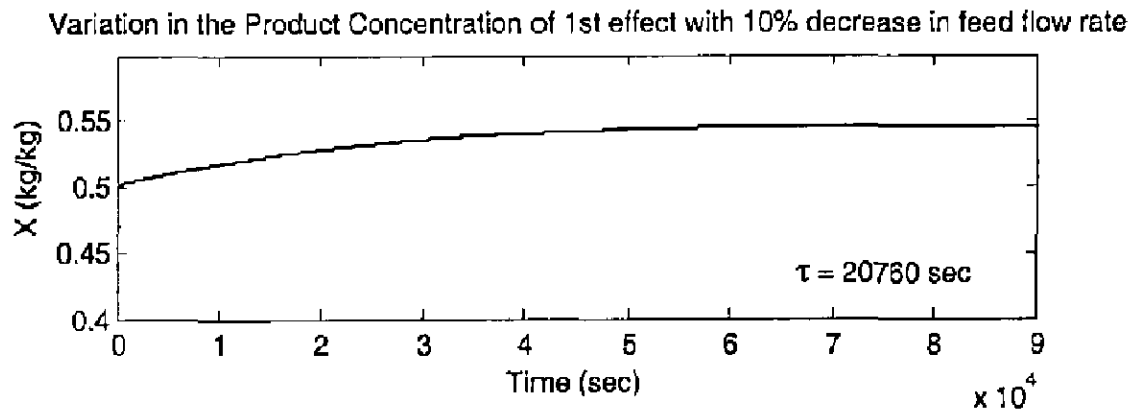


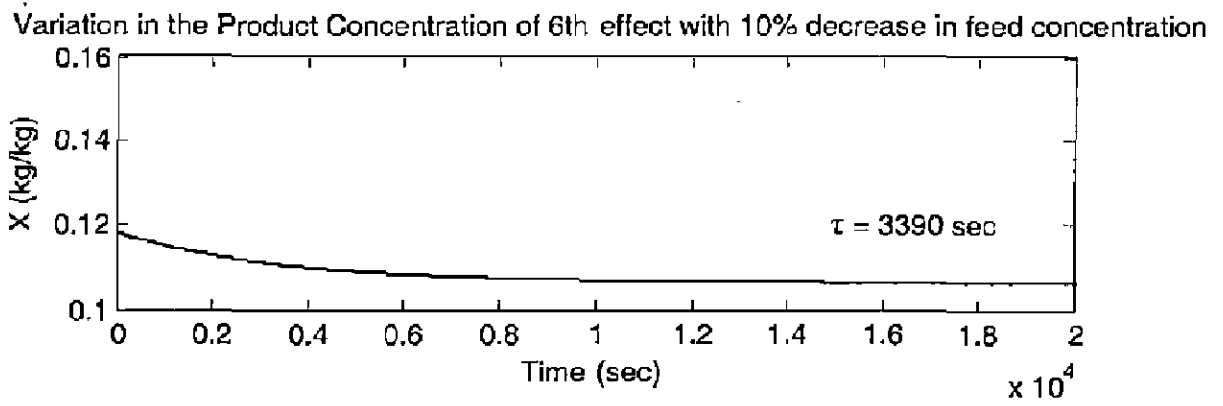
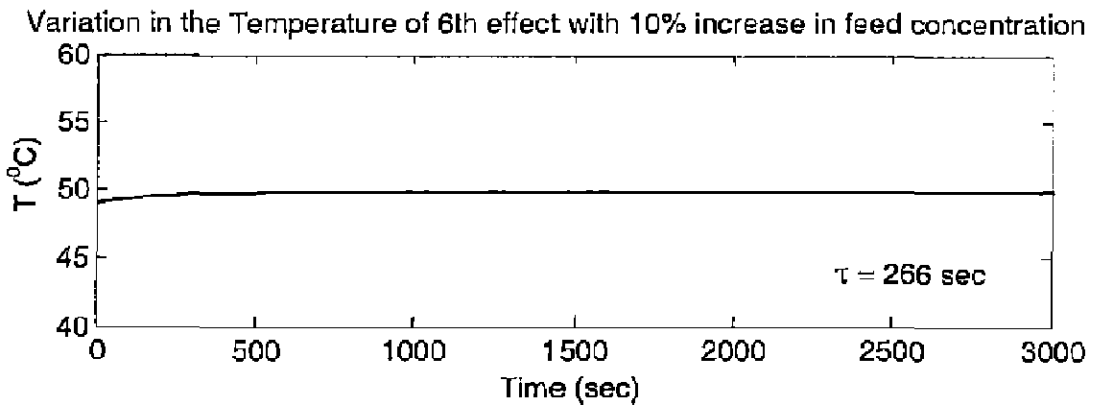
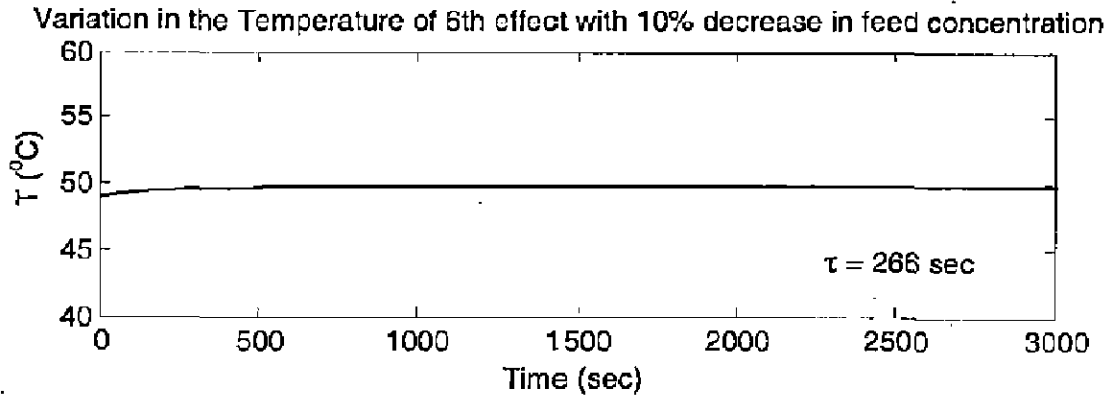
Figure 3.14 Response of 1<sup>st</sup> effect by disturbing  $\pm 10\%$  in the feed flow rate

### 3.10.2.2 Effect of varying feed concentration

For the variation in the feed concentration the disturbance is applied in the last effect. The effect of  $\pm 10\%$  step input in feed concentration on the temperature and concentration of last and first effect are shown in the Figure 3.15 to Figure 3.16 respectively. The dynamic behavior of effect's temperature with respect to disturbances in feed concentration shows slight but insignificant change in temperature. However the change, it observed is unidirectional i.e. the temperature increases irrespective of increase or decrease in feed concentration. The changes in product concentration of both the effect show increase or decrease according as the feed concentration is increase or decrease. This may be due to the fact that  $\Delta T$  across the evaporator system remains constant and vapor-liquid equilibrium of each effect remains almost unchanged for the optimum performance. The nature of the plot is in agreement with the finding of Stefanov and Hoo (2004). Time constant shown in the Table 3.7 indicates that response time for temperature change is much



less than that of concentration change. Since the feed is backward thus the steady state in 6<sup>th</sup> effect is achieved at a faster rate than the 1<sup>st</sup> effect



Variation in the Product Concentration of 6th effect with 10% increase in feed concentration

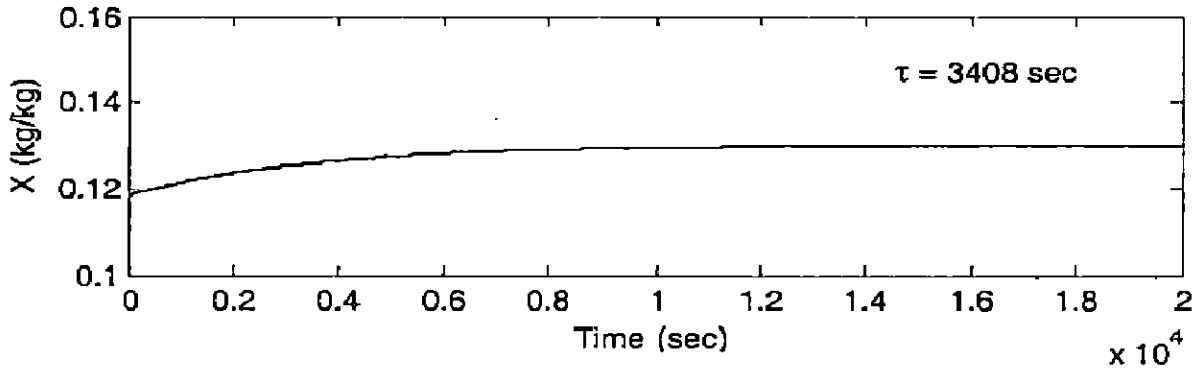
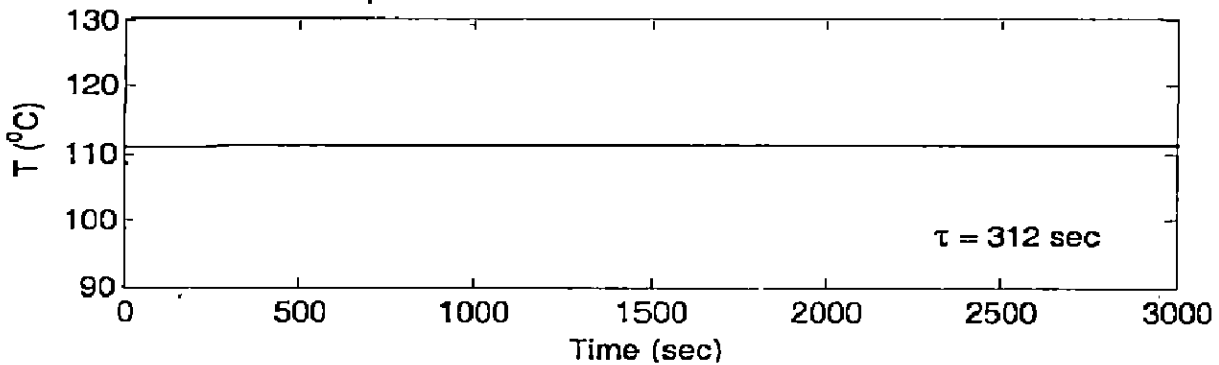
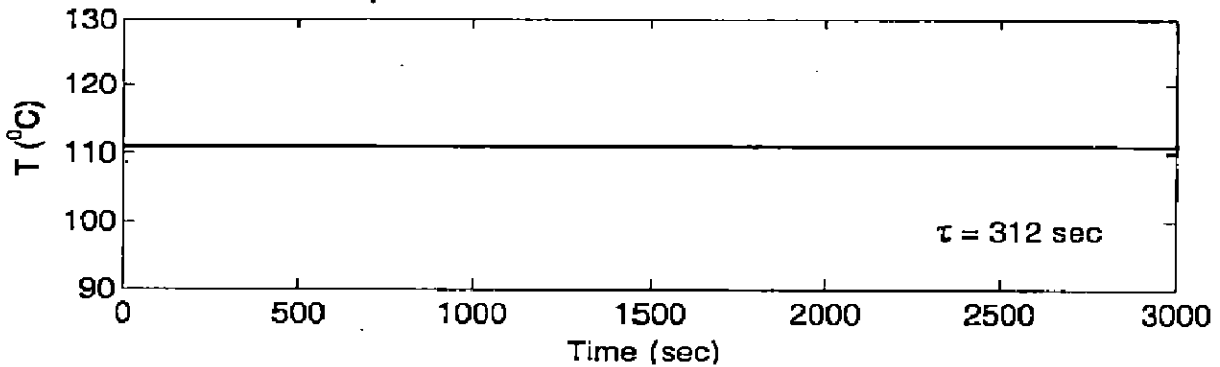


Figure 3.15 Response of 6<sup>th</sup> effect by disturbing  $\pm 10\%$  in the feed concentration

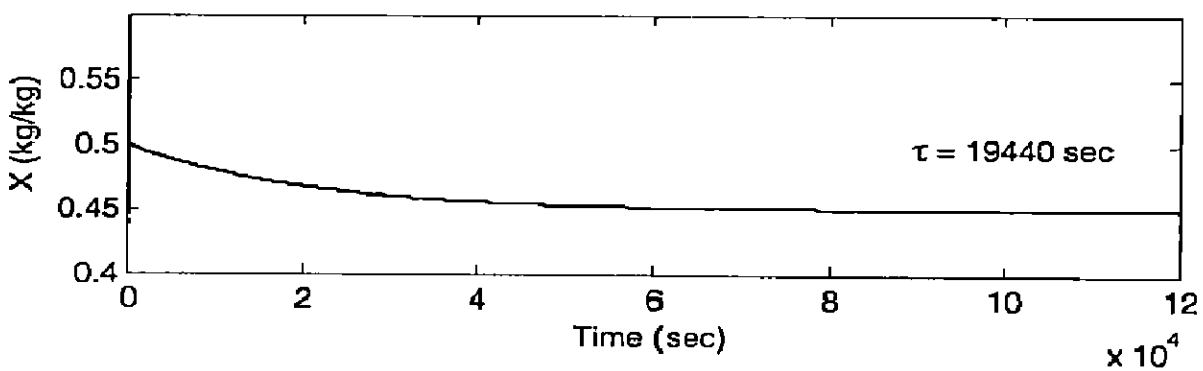
Variation in the Temperature of 1st effect with 10% decrease in feed concentration



Variation in the Temperature of 1st effect with 10% increase in feed concentration



Variation in the Product Concentration of 1st effect with 10% decrease in feed concentration



Variation in the Product Concentration of 1<sup>st</sup> effect with 10% increase in feed concentration

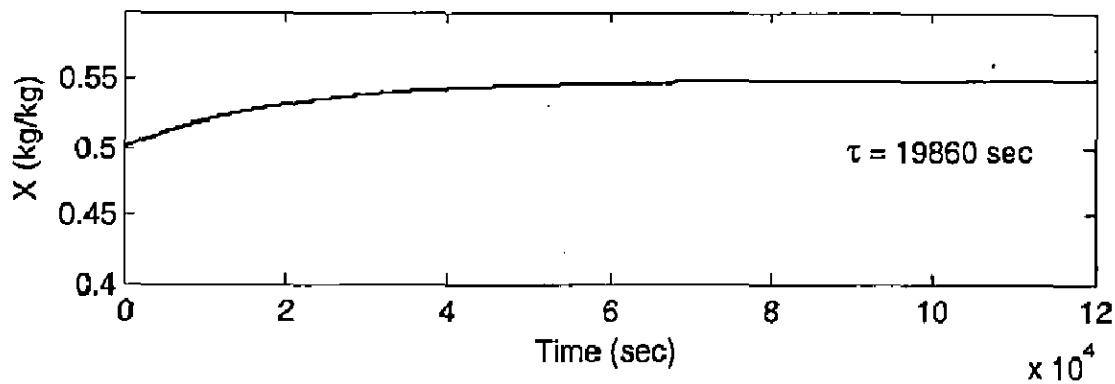


Figure 3.16 Response of 1<sup>st</sup> effect by disturbing  $\pm 10\%$  in the feed concentration

### 3.10.2.3 Effect of varying steam temperature

In backward feed MEE system live steam enters in the first effect. Thus for the variation in the steam temperature, the disturbance is applied in the first effect. The effect of  $\pm 10\%$  step input in steam temperature on the temperature and concentration of last and first effects are shown in the Figure 3.17 to Figure 3.18 respectively. The 10% change in steam temperature results in increase or decrease in the temperature of both the effects before obtaining the steady state for 10% increase or decrease respectively. 10% disturbance in steam temperature does not result in any noticeable change in the product concentration of both the effects. However after scale down Y-axis value it was observed that product concentration increase and then decrease or decrease and then increase for 10% increase or decrease in the steam temperature respectively. The plots show the similar nature as shown by Stefanov and Hoo (2004).

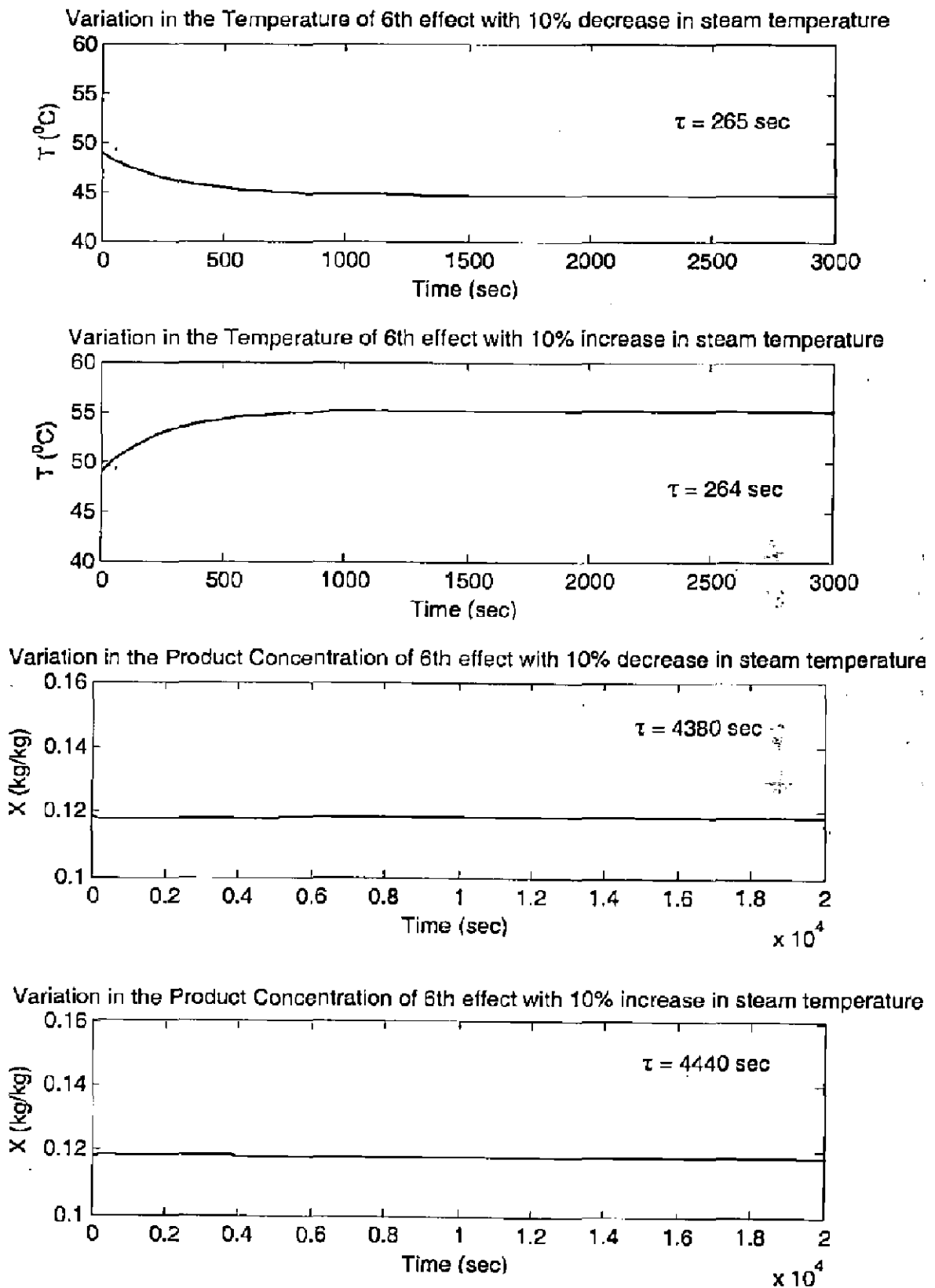


Figure 3.17 Response of 6<sup>th</sup> effect by disturbing  $\pm 10\%$  in the steam temperature

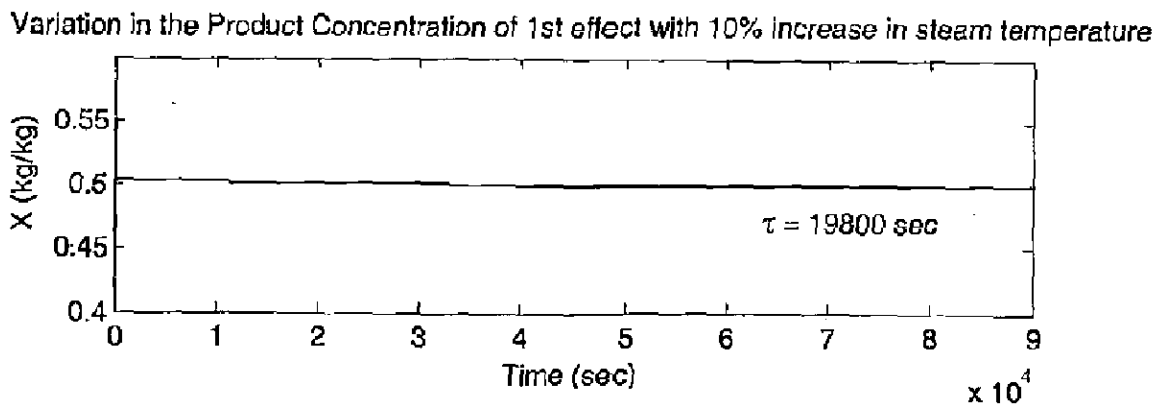
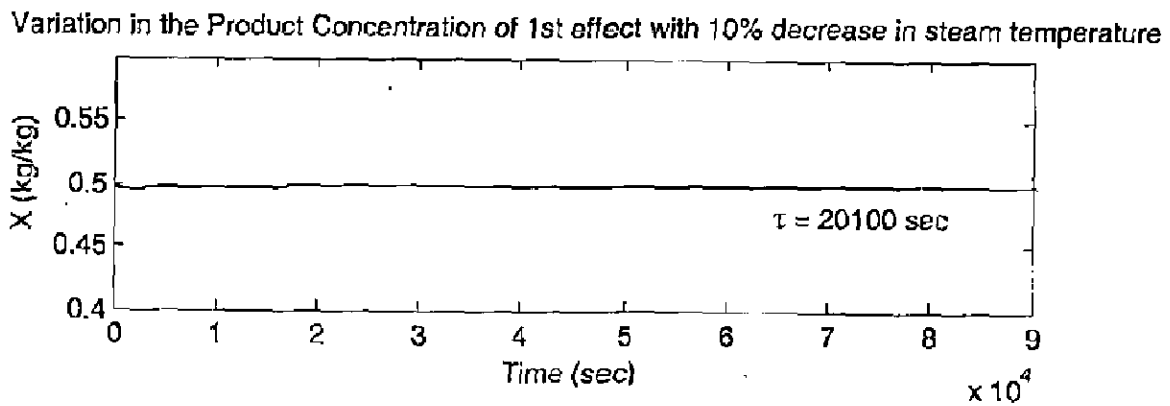
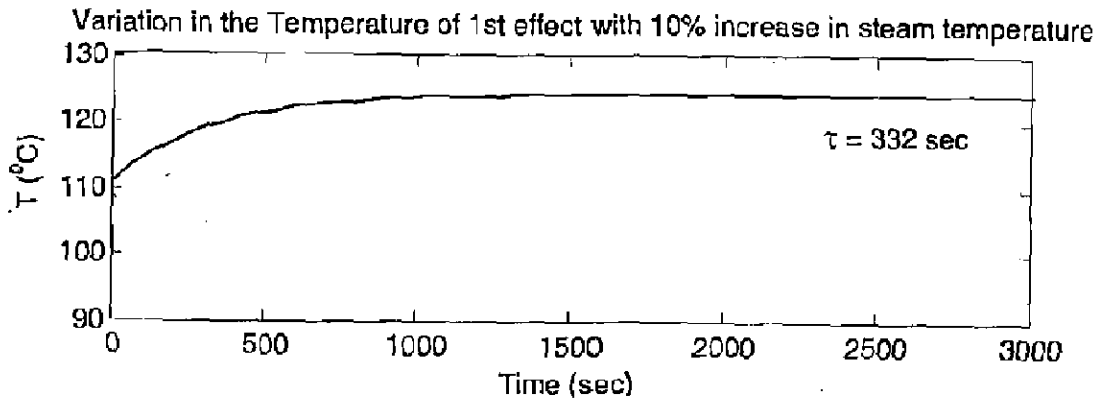
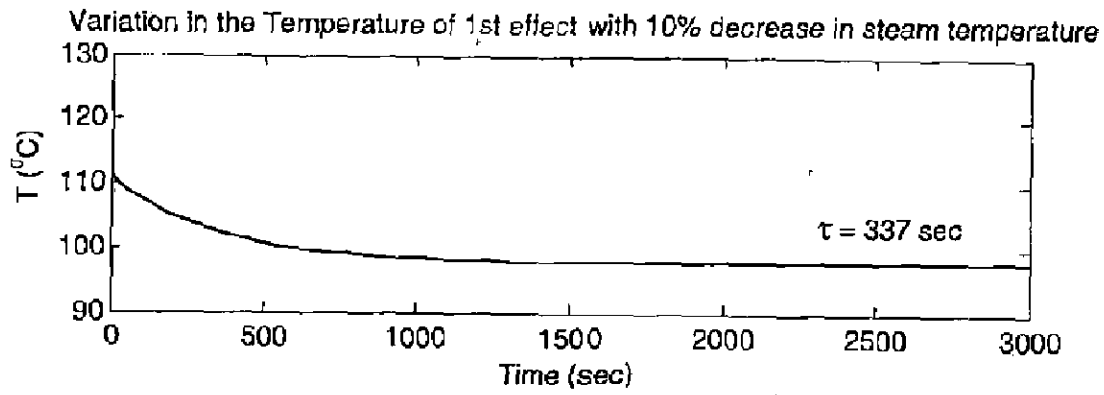
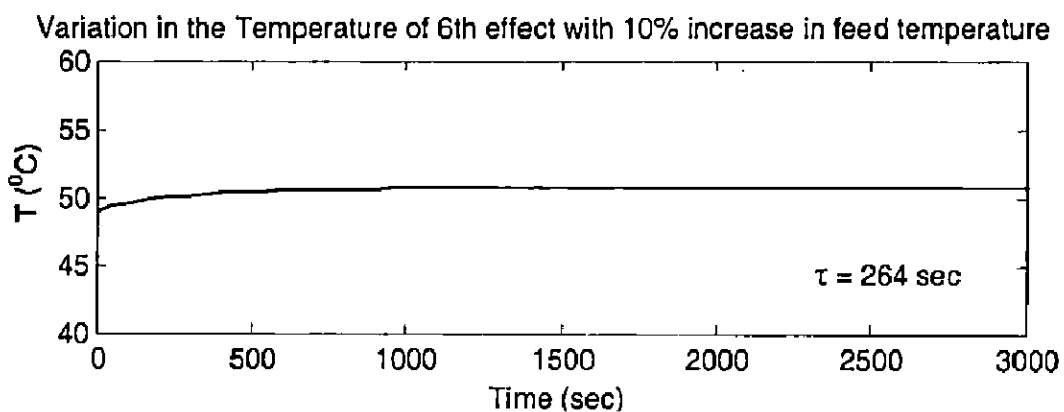
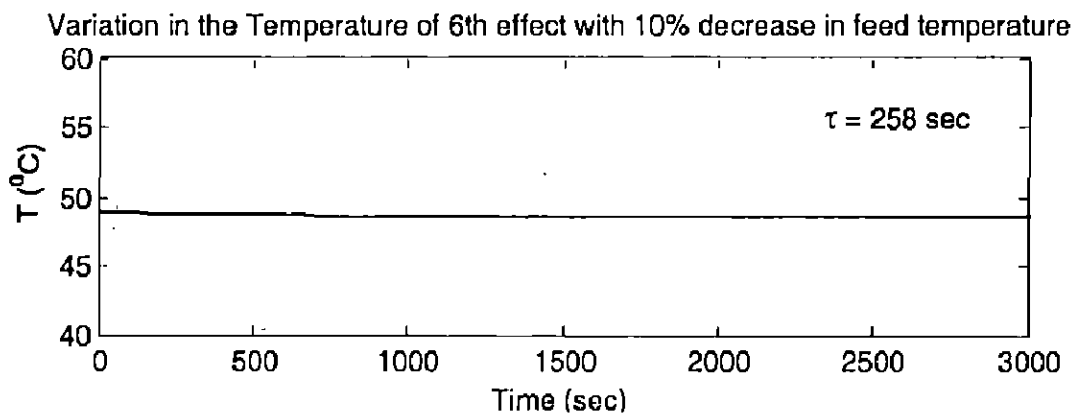


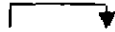
Figure 3.18 Response of 1<sup>st</sup> effect by disturbing  $\pm 10\%$  in the steam temperature

### 3.10.2.4 Effect of varying feed temperature

Since feed liquor enters in the last effect, thus for the dynamic response of the feed temperature the disturbance is applied in the last effect. The effect of  $\pm 10\%$  step change in feed temperature on the temperature and concentration of last and first effect are shown by the Figure 3.19 to Figure 3.20 respectively. It is evident from the figures that 10% disturbance in feed temperature does not bring noticeable change in the temperature and product concentration each effect. However after scale down Y-axis, it is observed that temperature of the both the effect increases and decreases to obtain the steady state with an increase and decrease in feed temperature and the product concentration of each effect first decreases and then increases to obtain the steady state with a very small fluctuations about the steady state up to four to five decimal places in the value of concentrations of both the effect and conversely for 10% increase in feed temperature. The results of Stefanov and Hoo (2004) are similar in nature.



### 3.10.3 Dynamic response of sextuple effect evaporator for the mixed feed



In the mixed feed MEE system such as (6←5 4→3→2→1); the input liquor enters the evaporator system from the 5<sup>th</sup> effect and then thick liquor from 5<sup>th</sup> effect to 6<sup>th</sup> and from 6<sup>th</sup> to 4<sup>th</sup> and up to the first effect. In this section dynamic responses due to ±10% step input in last and first effect in each case of mixed feed are given as follows.

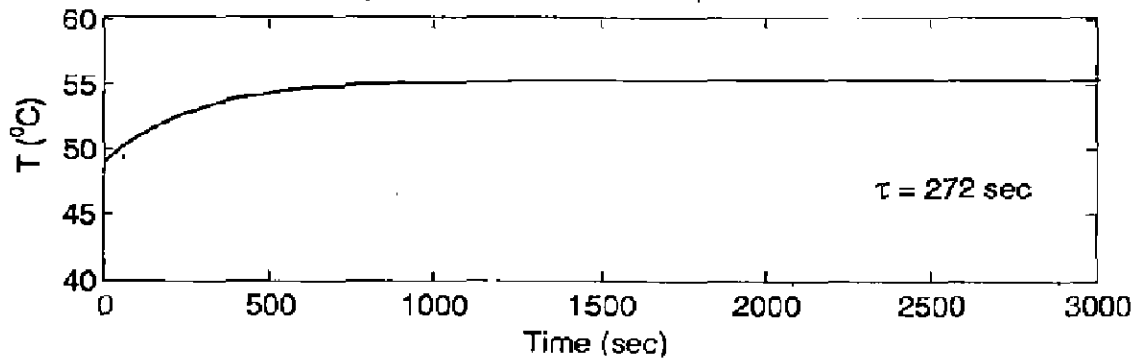
**Table 3.8 Time constant for dynamic response due to 10% step input change in various input variables for mixed feed sequence**

Input Variables		Time Constant ( $\tau$ ) in Second			
		6 <sup>th</sup> (Last Effect)		1 <sup>st</sup> (First Effect)	
		Temperature	Concentration	Temperature	Concentration
Feed Flow Rate	-10%	272	3696	328	20412
	+10%	265	3354	323	16656
Feed Concentration	-10%	258	4068	312	19200
	+10%	258	4080	312	19500
Steam Temperature	-10%	270	3460	335	24300
	+10%	270	3720	330	21320
Feed liquor Temperature	-10%	258	3340	320	20090
	+10%	261	3400	327	20060

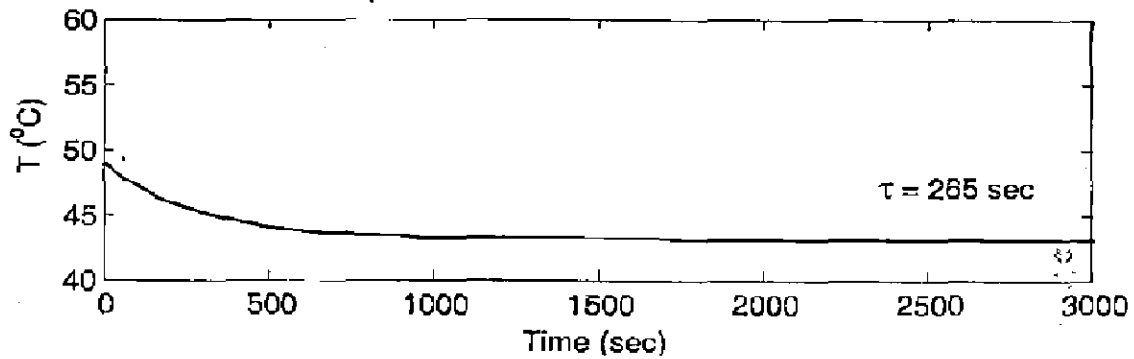
#### 3.10.3.1 Effect of varying feed flow rate

In the present case of mixed feed input thick liquor enters the evaporator system from the 5<sup>th</sup> effect. Thus for the variation in the feed flow rate the disturbance is applied in the 5<sup>th</sup> effect. The effect of ±10% step input in feed flow rate on the temperature and concentration of last effect (connected with condenser i.e. 6<sup>th</sup>) and first effect (connected with live steam i.e. 1<sup>st</sup>) are shown by the Figure 3.21 & Figure 3.22 respectively. The temperature and concentration of both the effects show an increase or decrease with decrease or increase in the feed flow rate. It is obvious as fresh steam supply rate is constant and water to be evaporates and decreases per unit time. The plots are of similar nature as shown in the backward feed sequence. Time constant shown in Table 3.8 indicates that response time for temperature change is much less than that of concentration change. Also the steady state in 6<sup>th</sup> effect is achieved at a faster rate than the 1<sup>st</sup> effect, which is similar as in backward feed.

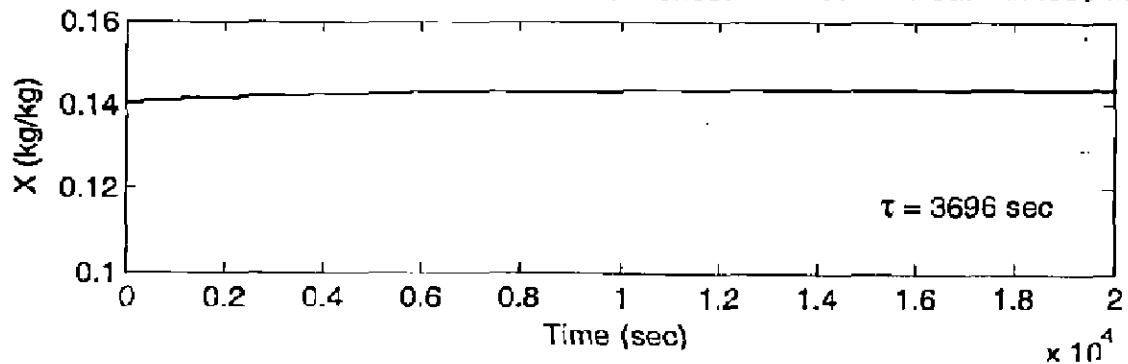
Variation in the Temperature of 6th effect with 10% decrease in feed flow rate



Variation in the Temperature of 6th effect with 10% increase in feed flow rate



Variation in the Product Concentration of 6th effect with 10% decrease in feed flow rate



Variation in the Product Concentration of 6th effect with 10% increase in feed flow rate

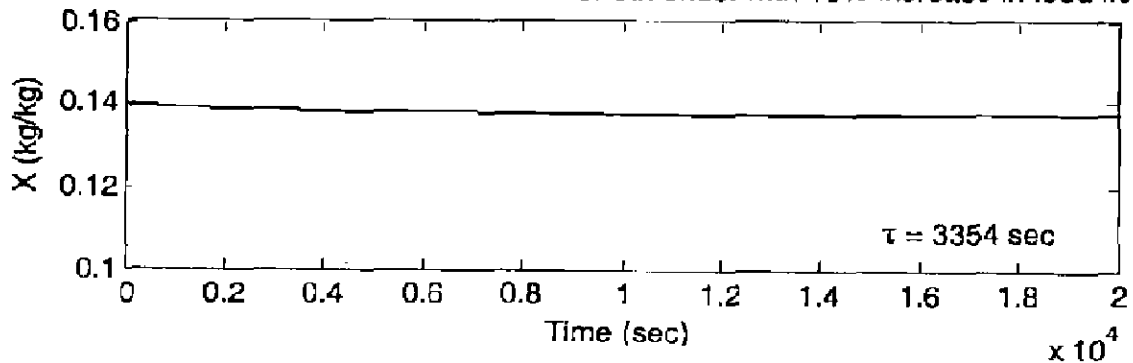


Figure 3.21 Response of 6<sup>th</sup> effect by disturbing  $\pm 10\%$  in the feed flow rate



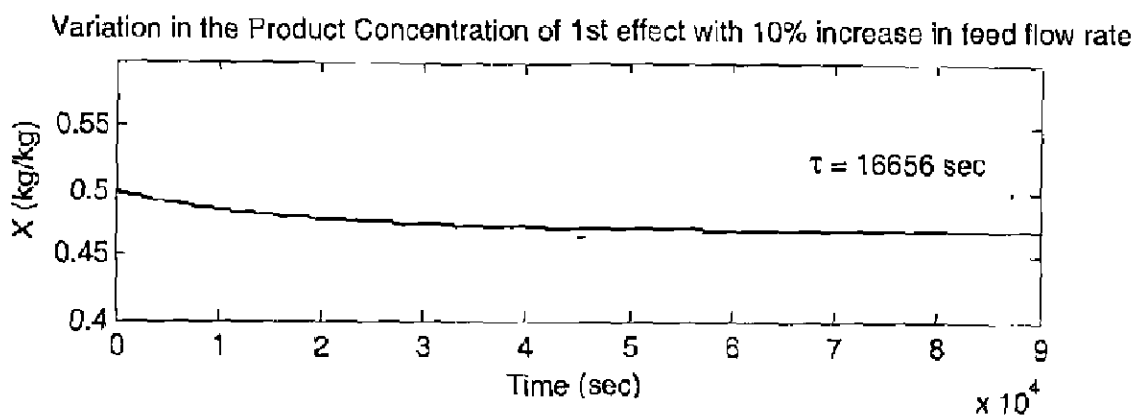
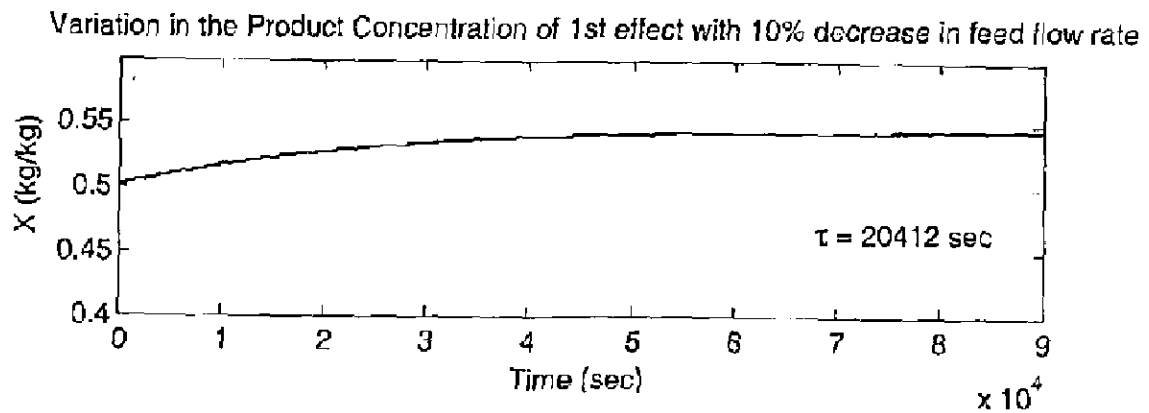
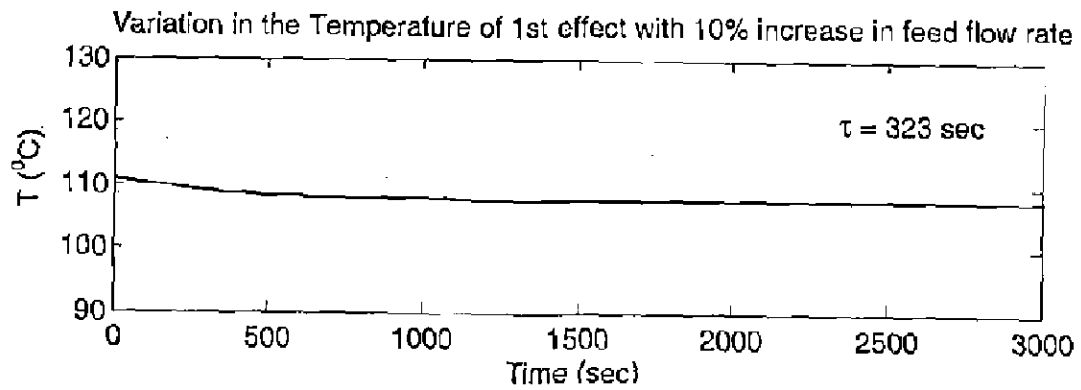
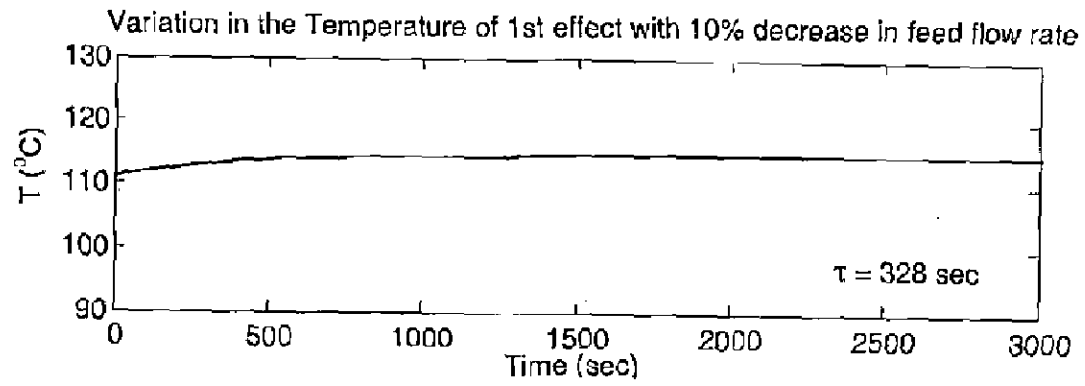
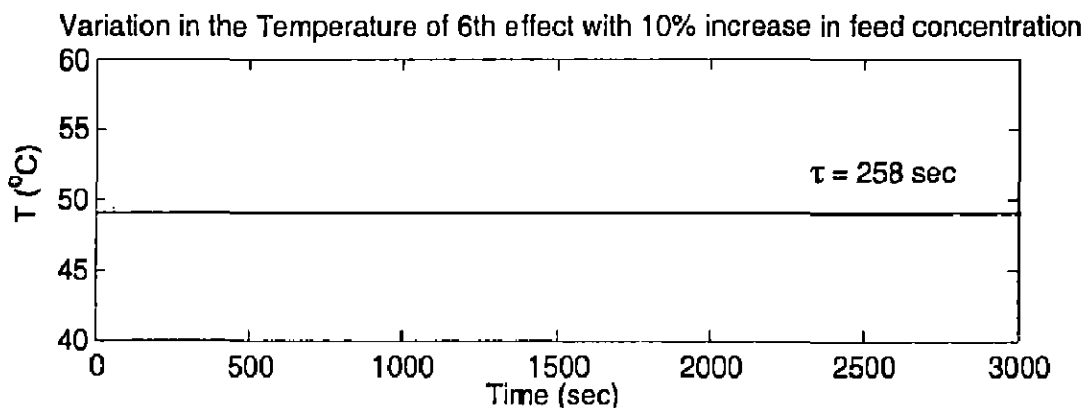
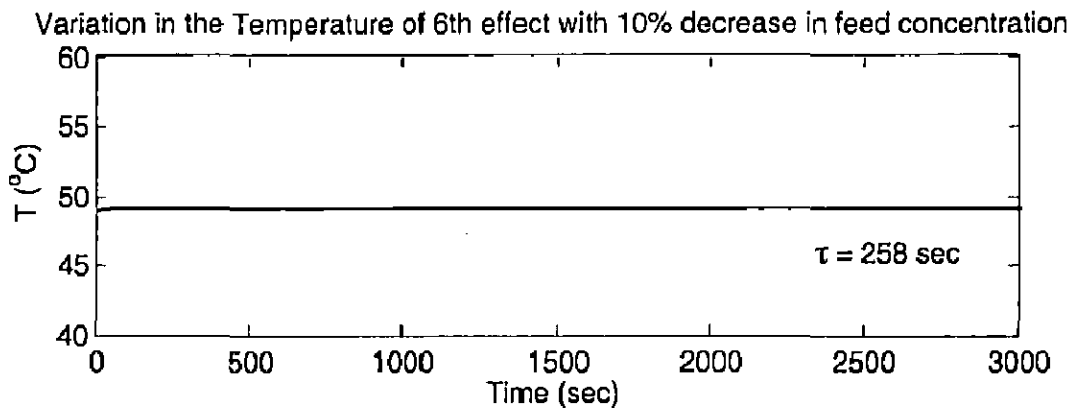


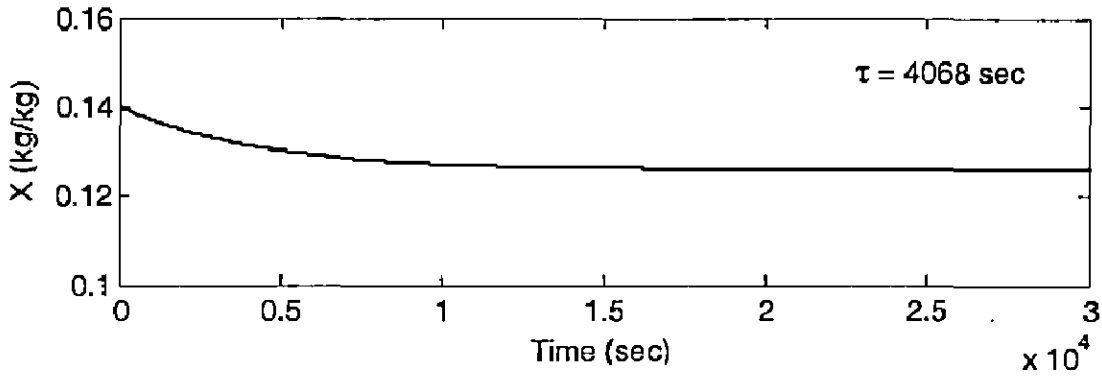
Figure 3.22 Response of 1<sup>st</sup> effect by disturbing  $\pm 10\%$  in the feed flow rate

### 3.10.3.2 Effect of varying feed concentration

For the dynamic response of the feed concentration the disturbance is applied in the 5<sup>th</sup> effect. The effect of  $\pm 10\%$  step input in feed concentration on the temperature and concentration of last (6<sup>th</sup>) and first effect (1<sup>st</sup>) are shown from Figure 3.23 to Figure 3.24 respectively. The dynamic behavior of effect's temperature with respect to disturbances in feed concentration shows slight but insignificant change in temperature. However the change, it observed is unidirectional i.e. the temperature increases irrespective of increase or decrease in feed concentration. The changes in product concentration of both the effect show increase or decrease according as the feed concentration is increase or decrease. This may be due to the fact that  $\Delta T$  across the evaporator system remains constant and vapor-liquid equilibrium of each effect remains almost unchanged for the optimum performance. Time constant are presented in the Table 3.8 indicates that response time for temperature change is much less than that of concentration change.



Variation in the Product Concentration of 6th effect with 10% decrease in feed concentration



Variation in the Product Concentration of 6th effect with 10% increase in feed concentration

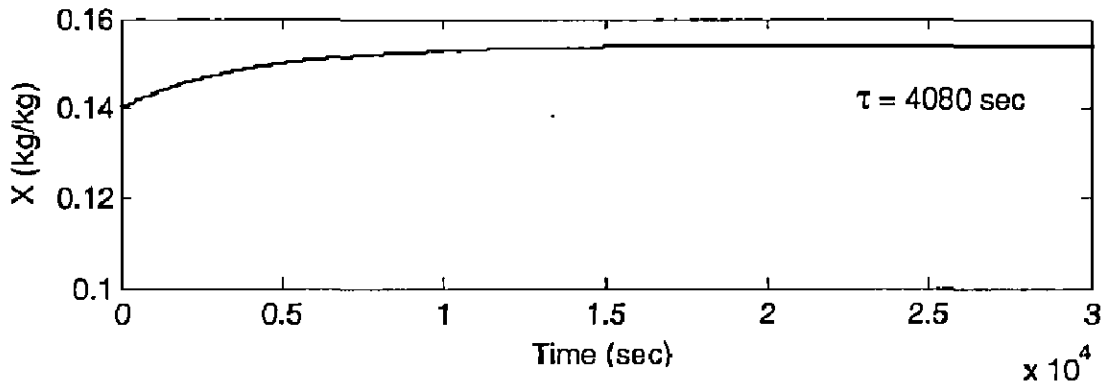
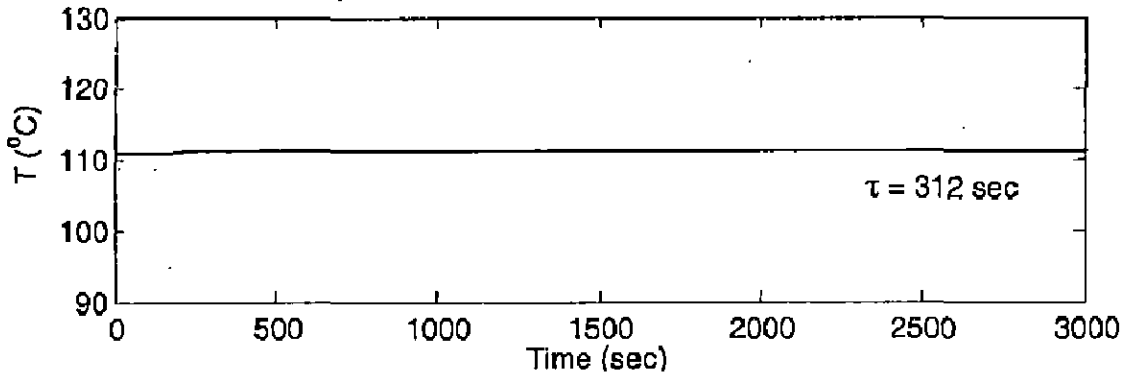
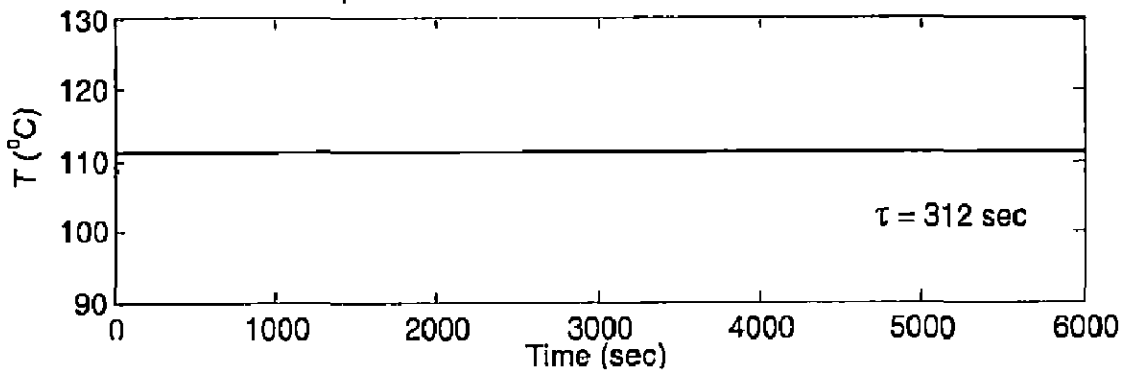


Figure 3.23 Response of 6<sup>th</sup> effect by disturbing  $\pm 10\%$  in the feed concentration

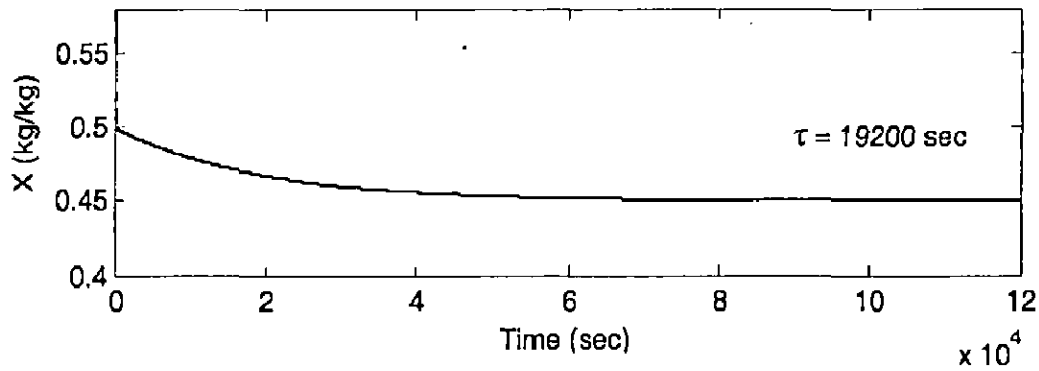
Variation in the Temperature of 1st effect with 10% decrease in feed concentration



Variation in the Temperature of 1st effect with 10% increase in feed concentration



Variation in the Product Concentration of 1st effect with 10% decrease in feed concentration



Variation in the Product Concentration of 1st effect with 10% increase in feed concentration

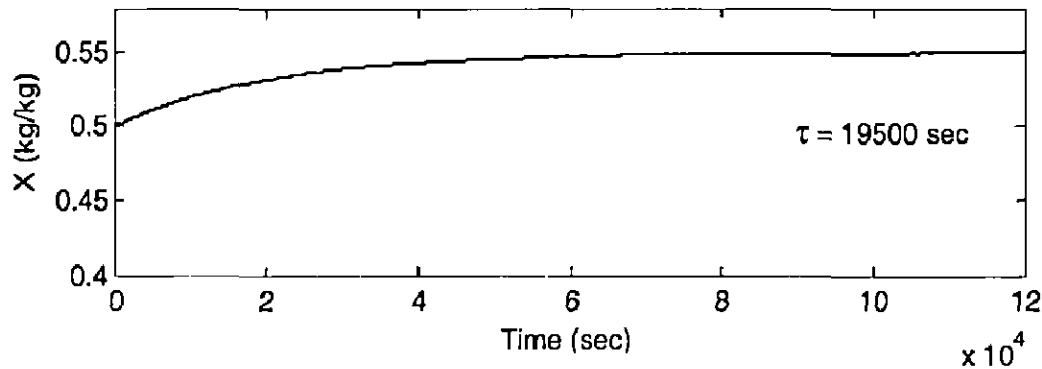


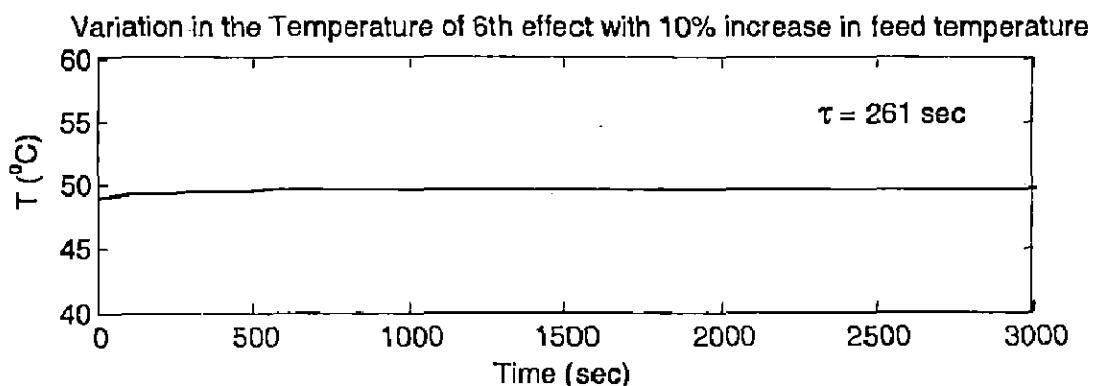
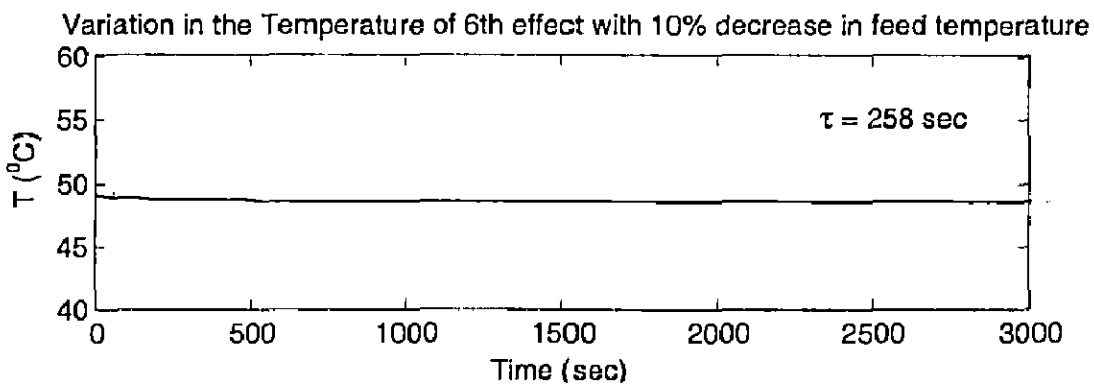
Figure 3.24 Response of 1<sup>st</sup> effect by disturbing  $\pm 10\%$  in the feed concentration

### 3.10.3.3 Effect of varying steam temperature

In MEE system with mixed feed, live steam enters in the first effect. Thus for the variation in the steam temperature the disturbance is applied in the first effect. The effect of  $\pm 10\%$  step input in steam temperature on the temperature and concentration of last and first effect are shown from Figure 3.25 to Figure 3.26 respectively. The 10% change in steam temperature results in increase or decrease in the temperature of both the effects before obtaining the steady state for 10% increase or decrease respectively. 10% disturbance in steam temperature does not result in any noticeable change in the product concentration of both the effects. However after scale down Y-axis value it was observed that product concentration increase and then decrease or decrease and then increase for 10% increase or decrease in the steam temperature respectively.

### 3.10.3.4 Effect of varying feed temperature

Since feed liquor enters in the 5<sup>th</sup> effect for the mixed feed, thus the dynamic response of the feed temperature the disturbance is applied in the 5<sup>th</sup> effect. The effect of  $\pm 10\%$  step change in feed temperature on the temperature and concentration of last and first effect are shown by the Figure 3.27 to Figure 3.28 respectively. It is evident from the figures that 10% disturbance in feed temperature does not bring noticeable change in the temperature and product concentration each effect. However after scale down Y-axis, it is observed that temperature of the both the effect increases and decreases to obtain the steady state with an increase and decrease in feed temperature and the product concentration of each effect first decreases and then increases to obtain the steady state with a very small fluctuations about the steady state up to four to five decimal places in the value of concentrations of both the effect and conversely for 10% increase in feed temperature. The natures of the plots are similar as for backward feed.



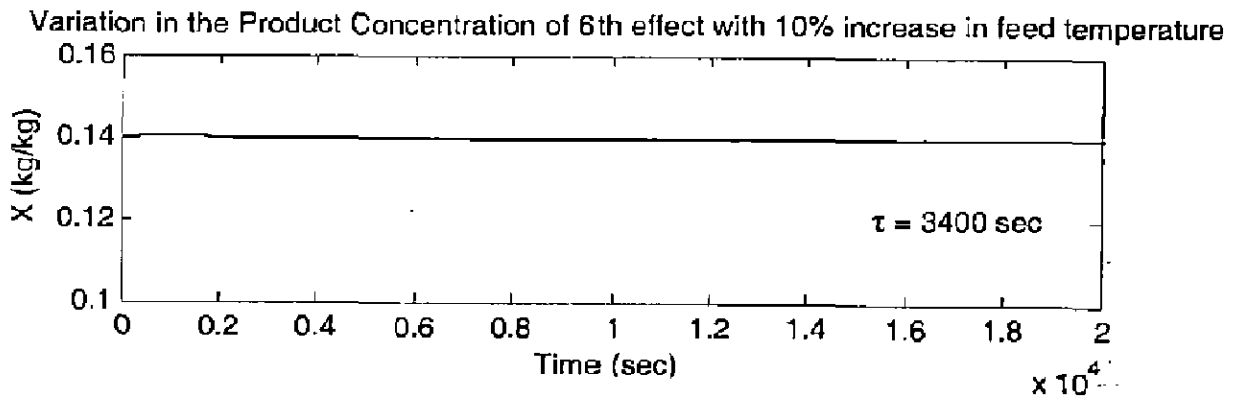
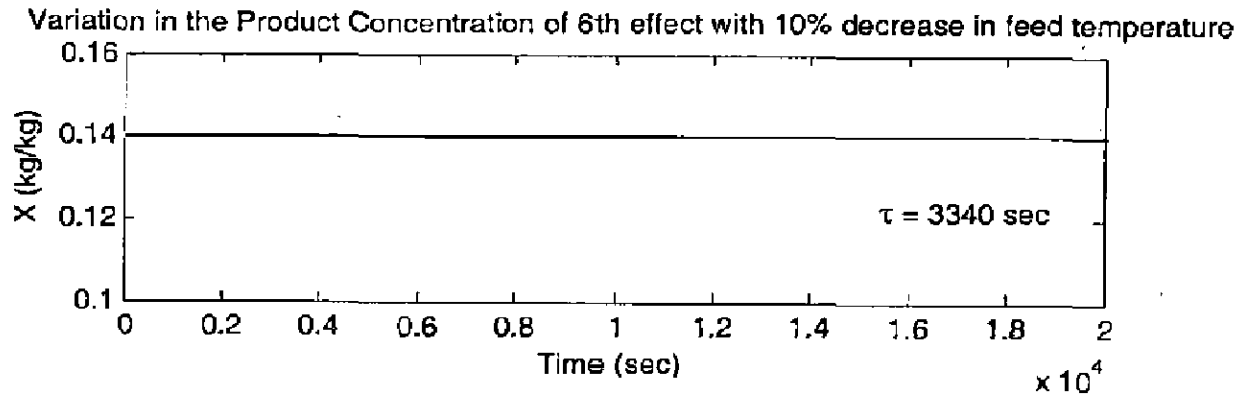
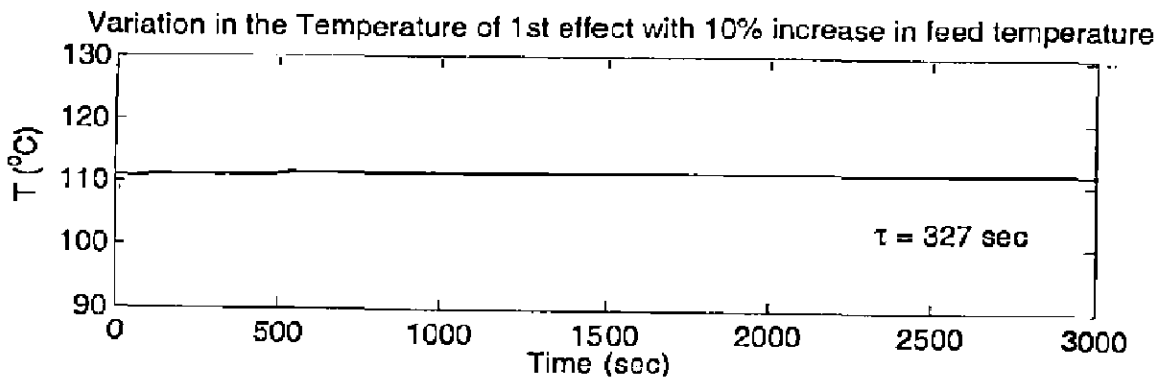
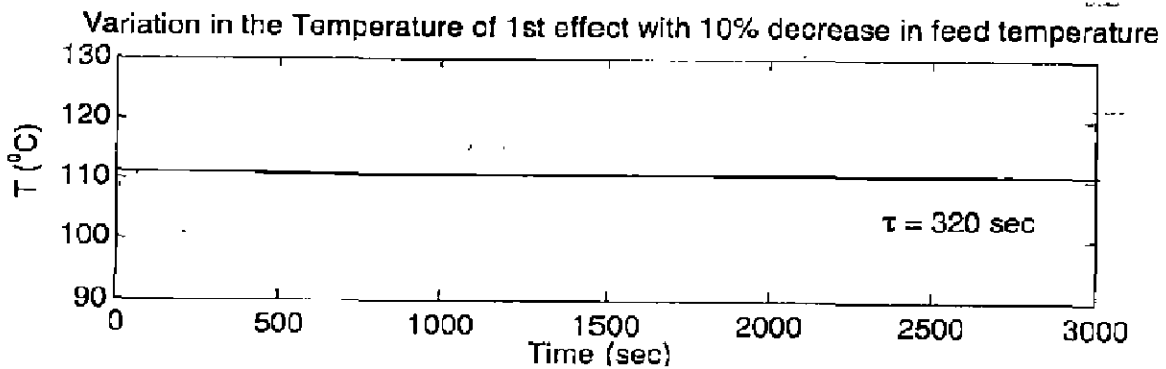
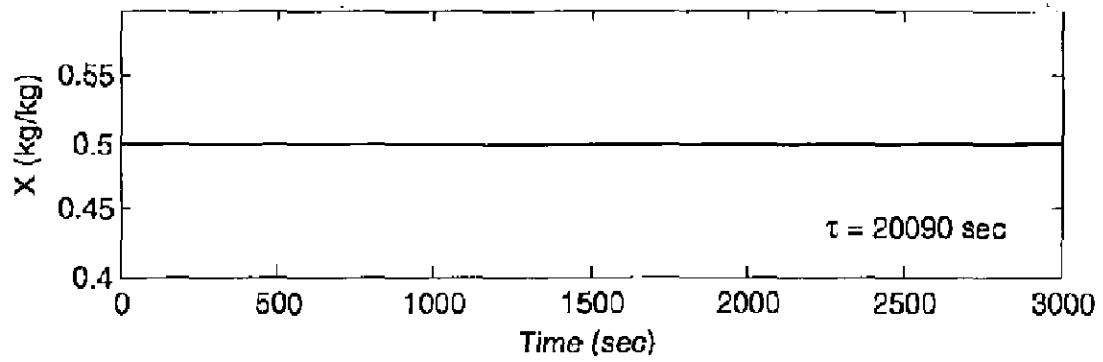


**Figure 3.27 Response of 6<sup>th</sup> effect by disturbing  $\pm 10\%$  in the feed temperature**



Variation in the Product Concentration of 1st effect with 10% decrease in feed temperature



Variation in the Product Concentration of 1st effect with 10% increase in feed temperature

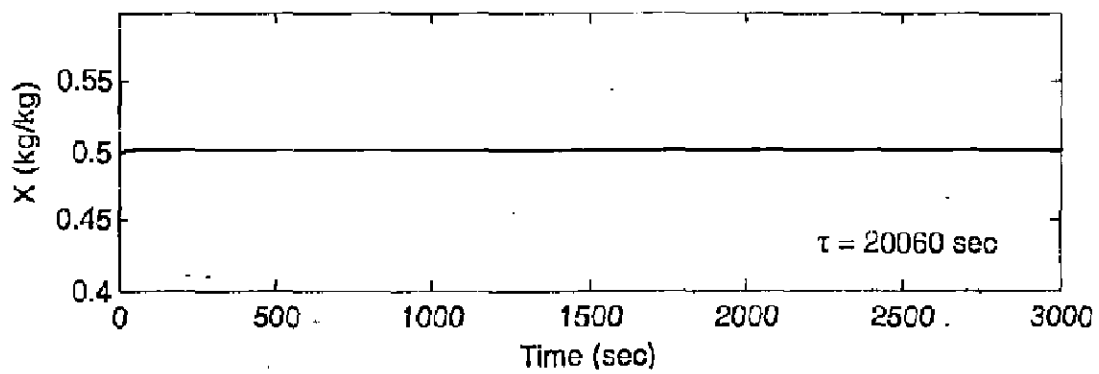


Figure 3.28 Response of 1st effect by disturbing  $\pm 10\%$  in the feed temperature

### 3.10.4 Dynamic response of sextuple effect evaporator for the split feed

The dynamic responses due to disturbances in various input parameters are studied by using split feed in which the total feed is divided equally into 5<sup>th</sup> and 6<sup>th</sup> effect. Hence the input liquor enters the evaporator system from the 5<sup>th</sup> and 6<sup>th</sup> effects and then thick liquor from 5<sup>th</sup> and 6<sup>th</sup> jointly move into to 4<sup>th</sup> and from 4<sup>th</sup> into 3<sup>rd</sup> and up to the first effect. Dynamic responses due to  $\pm 10\%$  step input in last and first effect for each case for split feed are given as follows. Time constants are calculated for each plot and are indicated in plots.

**Table 3.9** Time constant for dynamic response due to 10% step input change in various input variables for split feed sequence

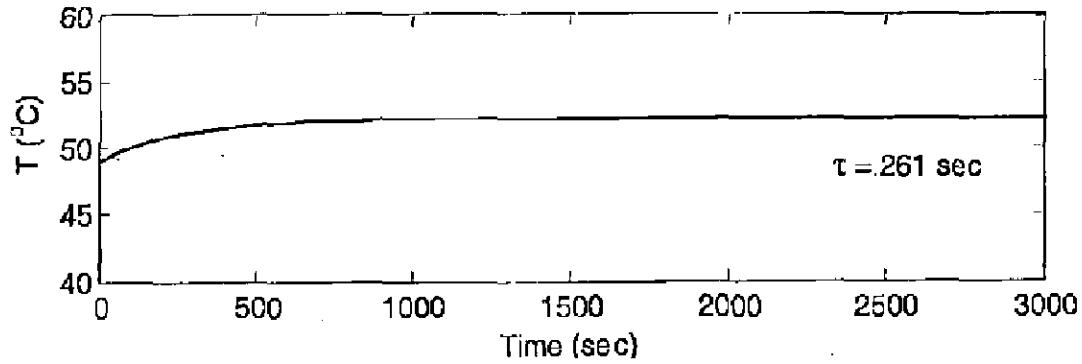
Input Variables		Time Constant ( $\tau$ ) in Second			
		6 <sup>th</sup> (Last Effect)		1 <sup>st</sup> (First Effect)	
		Temperature	Concentration	Temperature	Concentration
Feed Flow Rate	-10%	261	9480	337	21480
	+10%	258	8100	323	16680
Feed Concentration	-10%	264	6390	312	22440
	+10%	264	6408	312	20860
Steam Temperature	-10%	264	4380	336	21107
	+10%	258	4440	330	19662
Feed liquor Temperature	-10%	258	3240	312	23890
	+10%	252	3300	336	22935

#### 3.10.4.1 Effect of varying feed flow rate

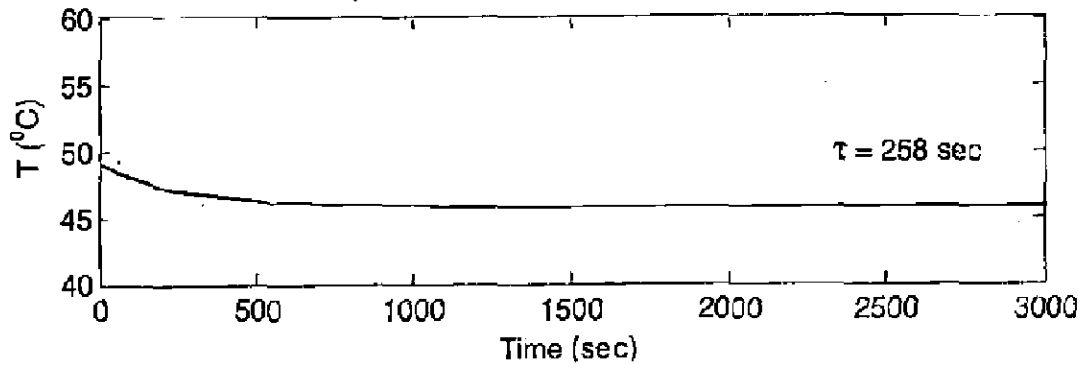
For the dynamic response of the feed parameters the disturbance is applied in the feed of 5<sup>th</sup> and 6<sup>th</sup> effects simultaneously. The effect of  $\pm 10\%$  step change in feed flow rate on the temperature and concentration on last (connected with condenser i.e. 6<sup>th</sup>) and first effect (connected with lie steam i.e. 1<sup>st</sup>) are shown from Figure 3.29 to Figure 3.30 respectively. The temperature and concentration of both the effects show an increase or decrease with decrease or increase in the feed flow rate. It is obvious as fresh steam supply rate is constant and water to be evaporates and decreases per unit time.



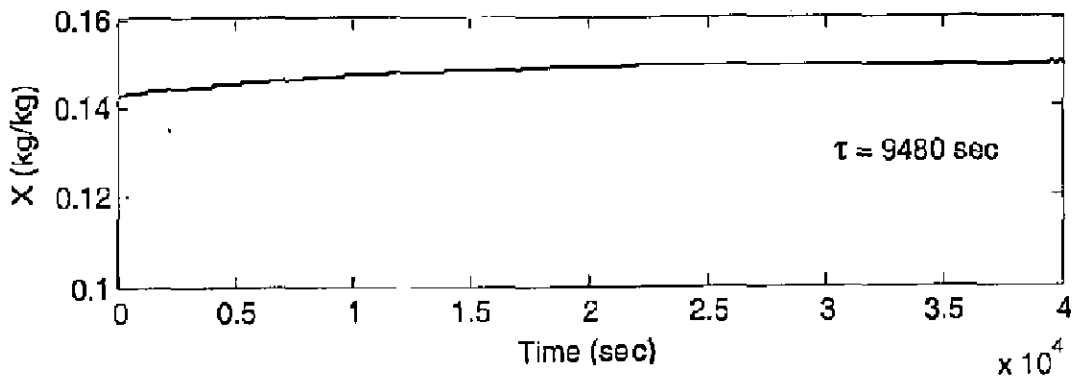
Variation in the Temperature of 6th effect with 10% decrease in feed flow rate



Variation in the Temperature of 6th effect with 10% increase in feed flow rate



Variation in the Product Concentration of 6th effect with 10% decrease in feed flow rate



Variation in the Product Concentration of 6th effect with 10% increase in feed flow rate

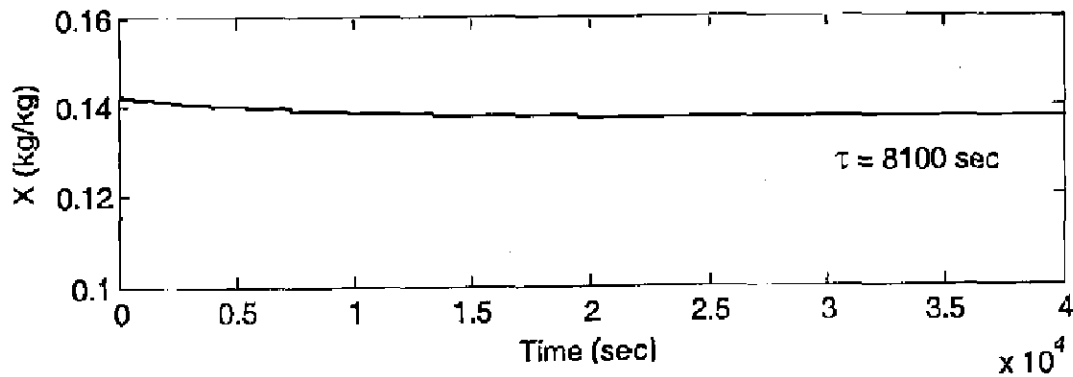


Figure 3.29 Response of 6<sup>th</sup> effect by disturbing  $\pm 10\%$  in the feed flow rate

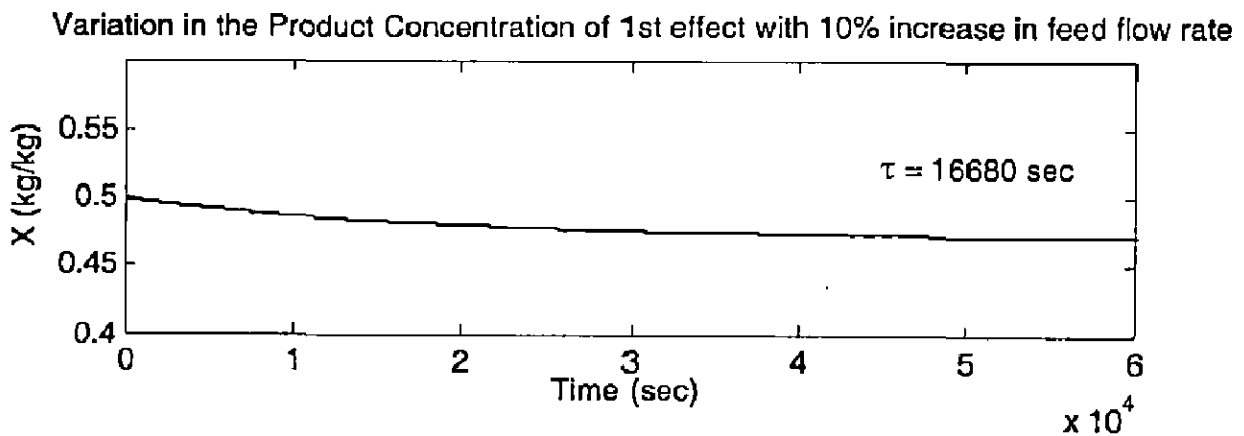
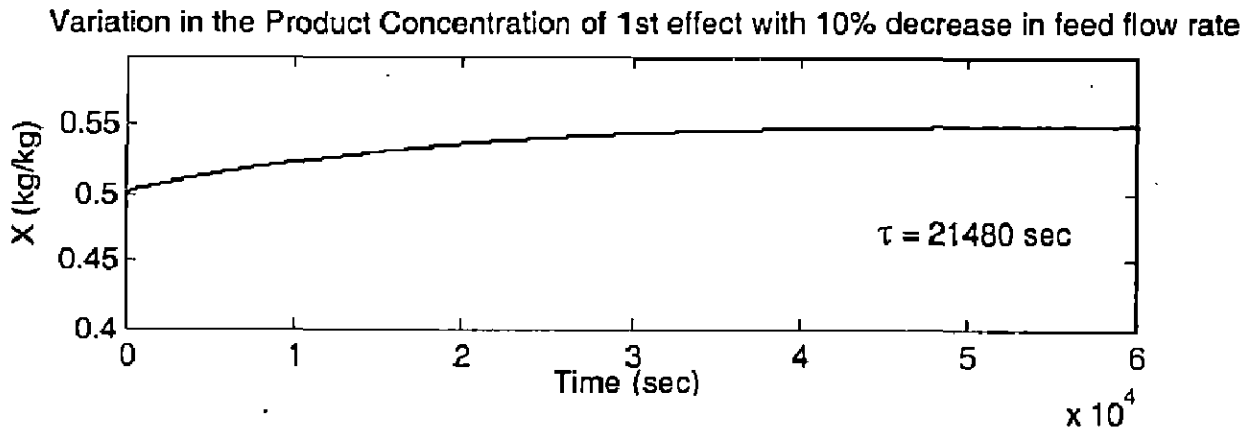
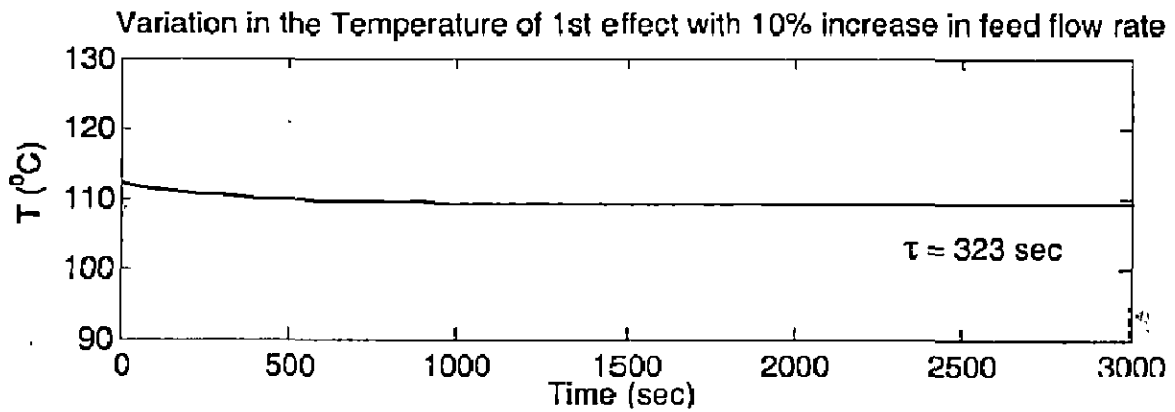
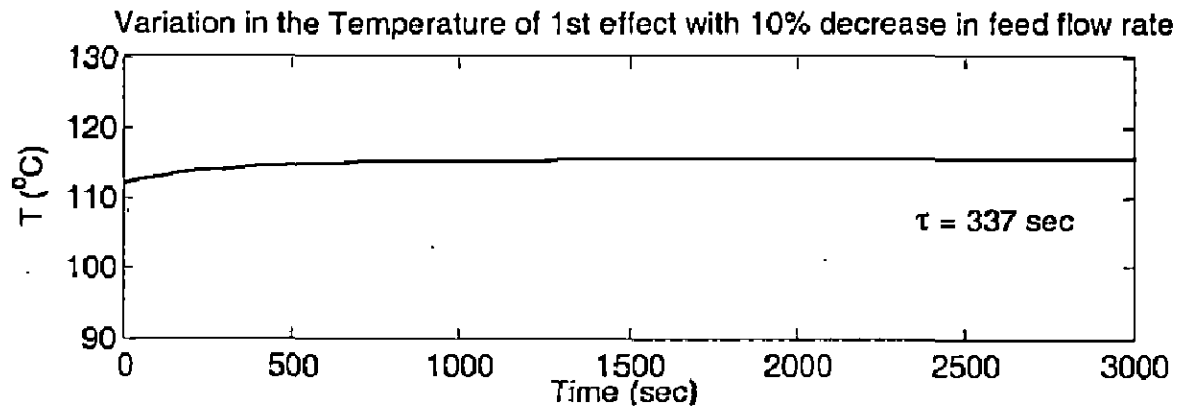
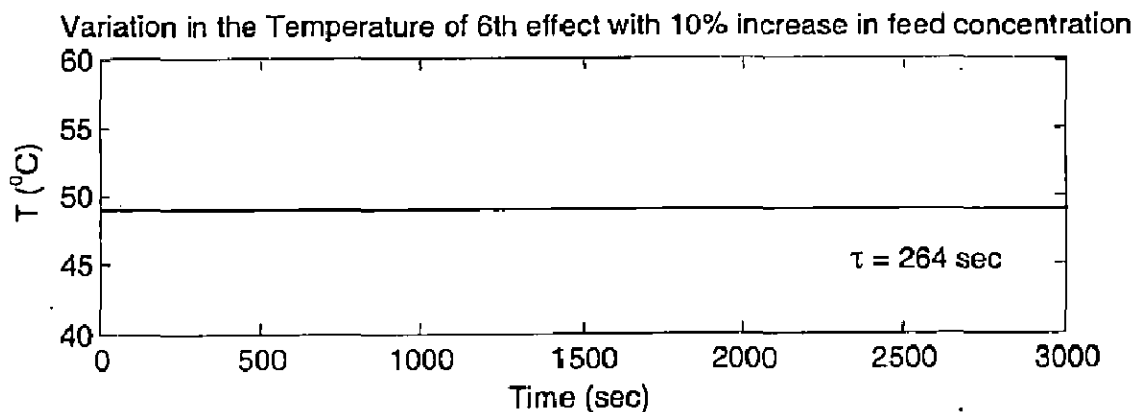
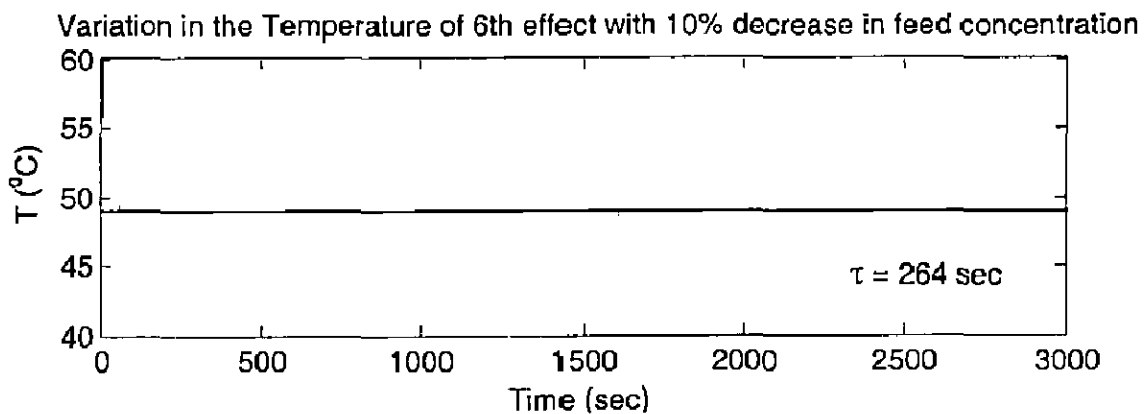


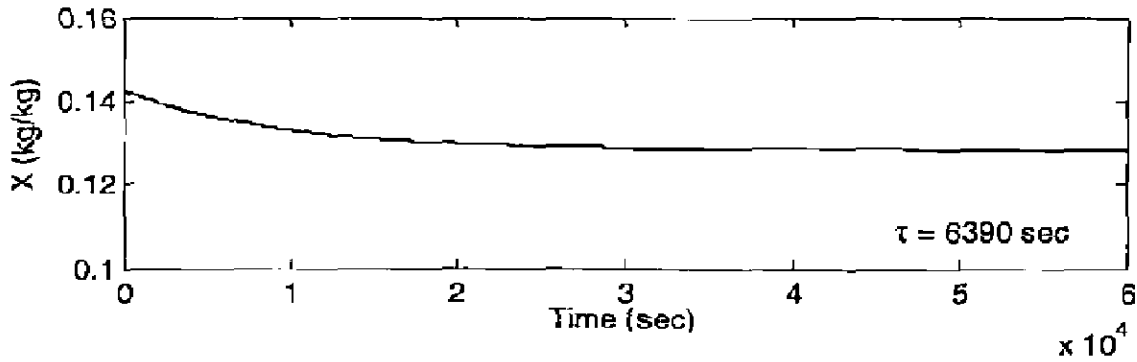
Figure 3.30 Response of 1<sup>st</sup> effect by disturbing  $\pm 10\%$  in the feed flow rate

### 3.10.4.2 Effect of varying feed concentration

For the dynamic response of the feed concentration the disturbance is applied in the feed of 5<sup>th</sup> as well as in the 6<sup>th</sup> effect. The effect of  $\pm 10\%$  step input in feed concentration on the temperature and concentration of last and first effect are shown from Figure 3.31 to Figure 3.32 respectively. The dynamic behavior of effect's temperature with respect to disturbances in feed concentration shows slight but insignificant change in temperature. However the change, it observed is unidirectional i.e. the temperature increases irrespective of increase or decrease in feed concentration. The changes in product concentration of both the effect show increase or decrease according as the feed concentration is increase or decrease. This may be due to the fact that  $\Delta T$  across the evaporator system remains constant and vapor-liquid equilibrium of each effect remains almost unchanged for the optimum performance.



Variation in the Product Concentration of 6th effect with 10% decrease in feed concentration



Variation in the Product Concentration of 6th effect with 10% increase in feed concentration

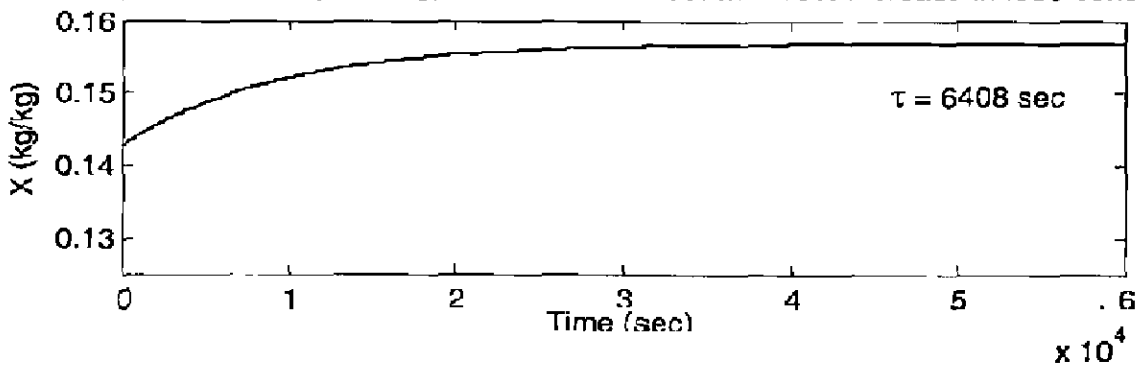
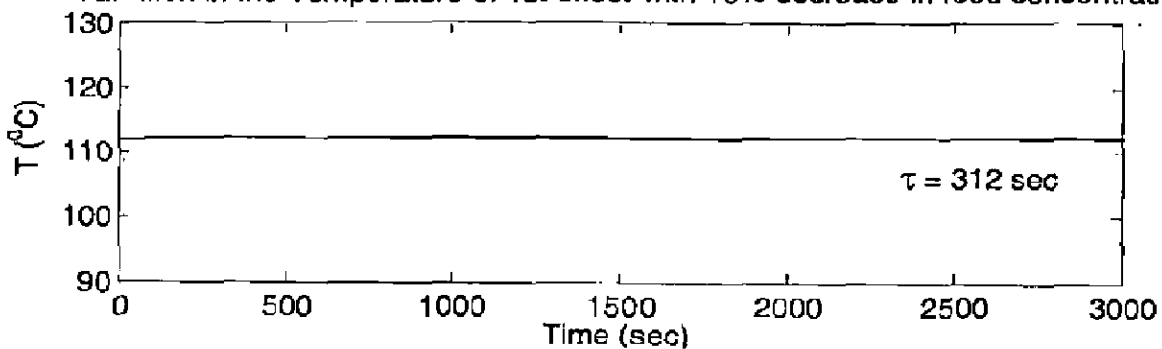
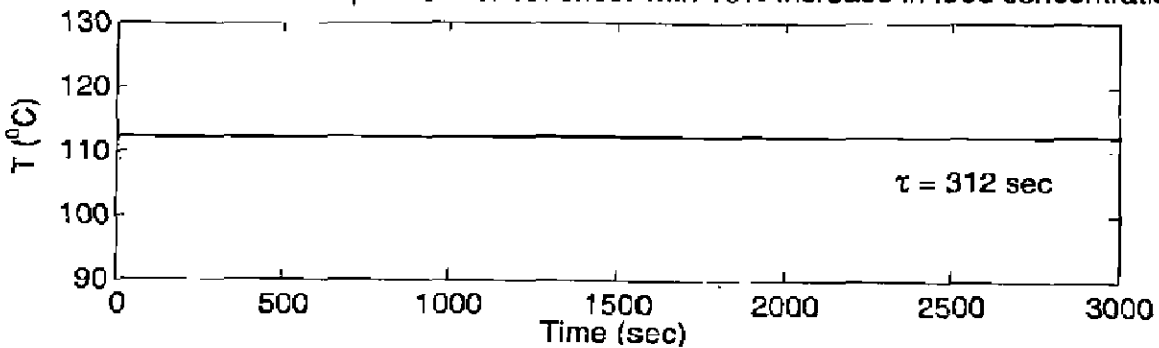


Figure 3.31 Response of 6<sup>th</sup> effect by disturbing  $\pm 10\%$  in the feed concentration

Variation in the Temperature of 1st effect with 10% decrease in feed concentration



Variation in the Temperature of 1st effect with 10% increase in feed concentration



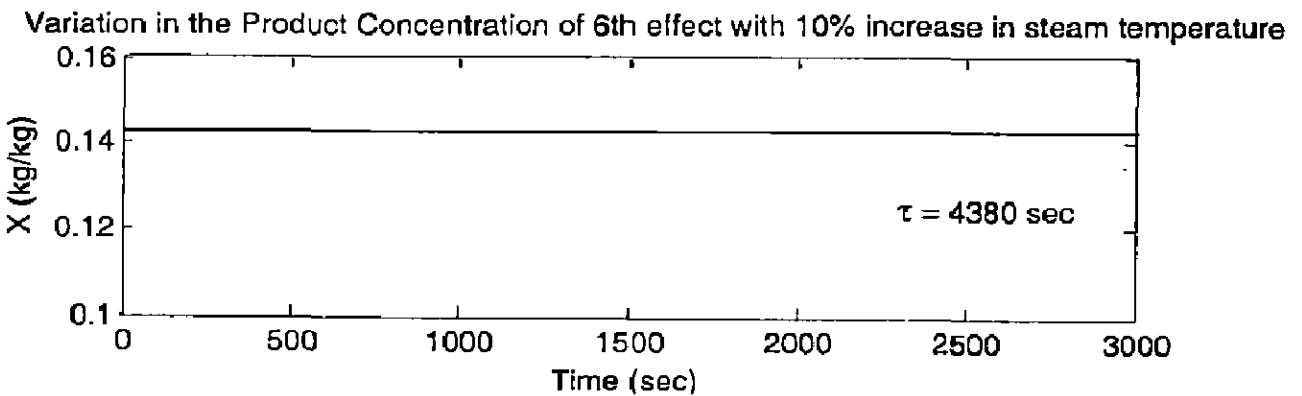
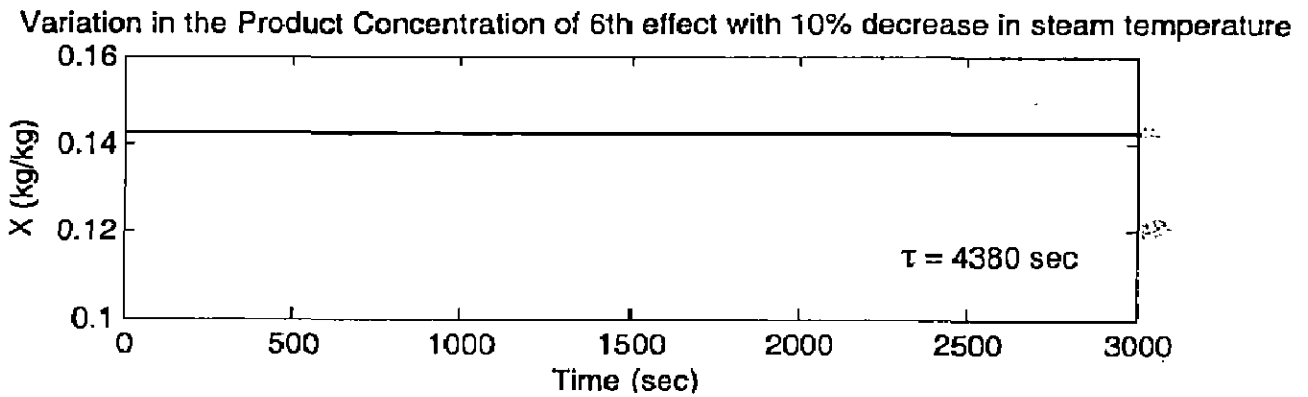
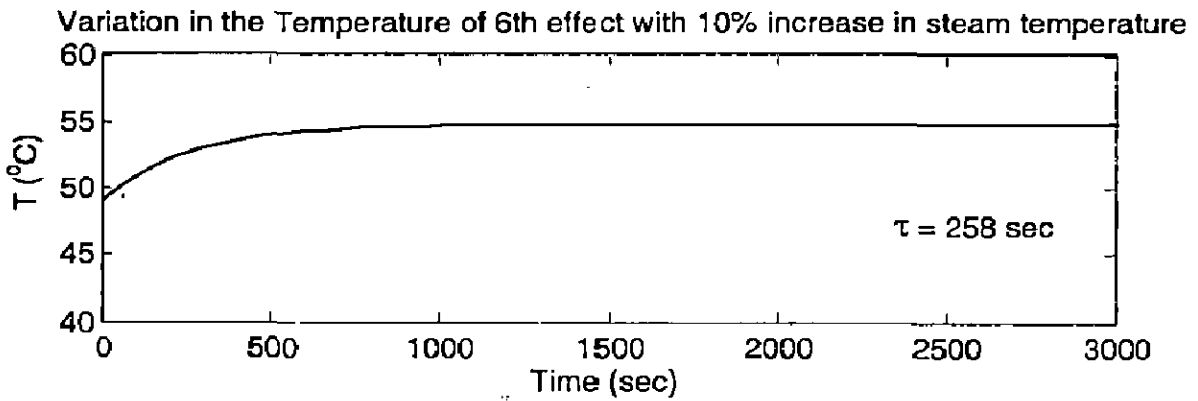
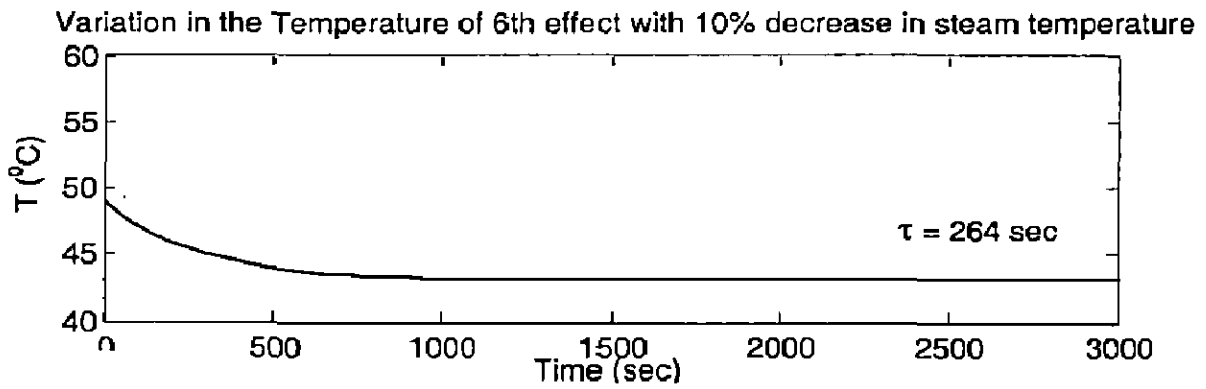
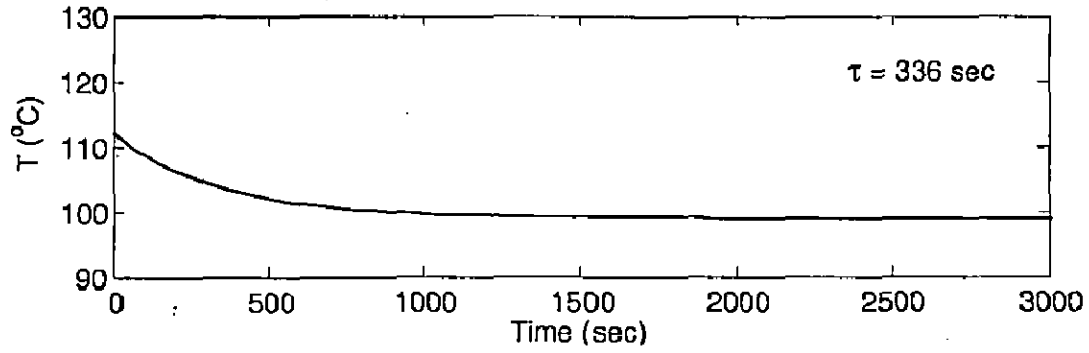
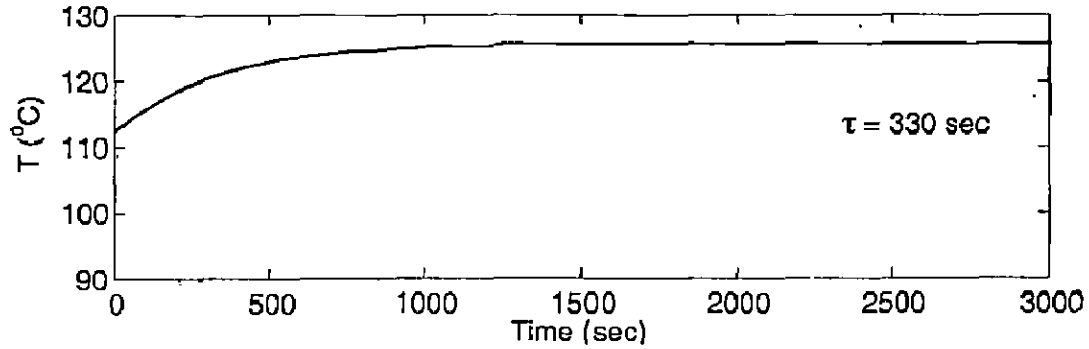


Figure 3.33 Response of 6<sup>th</sup> effect by disturbing  $\pm 10\%$  in the steam temperature

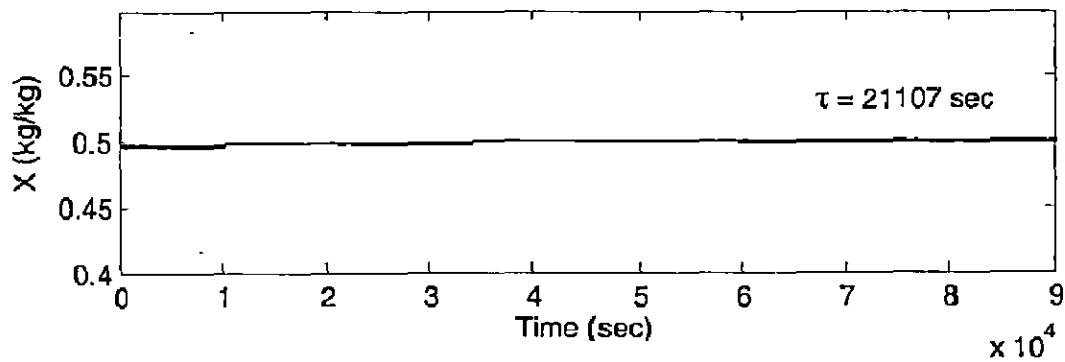
Variation in the Temperature of 1st effect with 10% decrease in steam temperature



Variation in the Temperature of 1st effect with 10% increase in steam temperature



Variation in the Product Concentration of 1st effect with 10% decrease in steam temperature



Variation in the Product Concentration of 1st effect with 10% increase in steam temperature

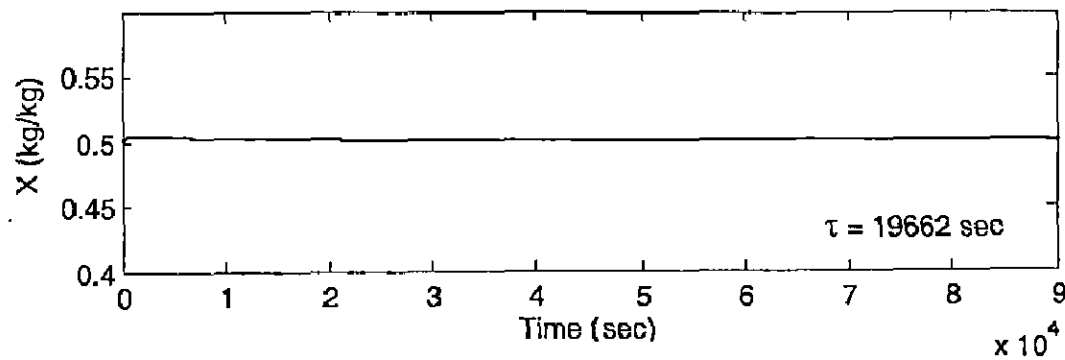
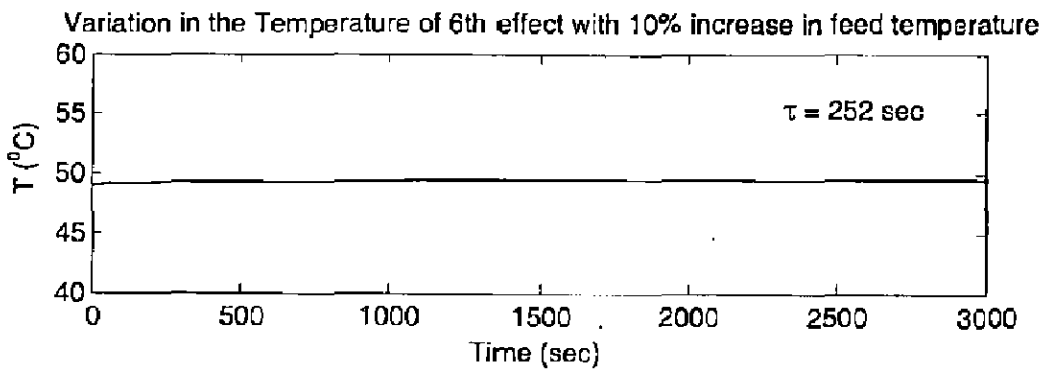
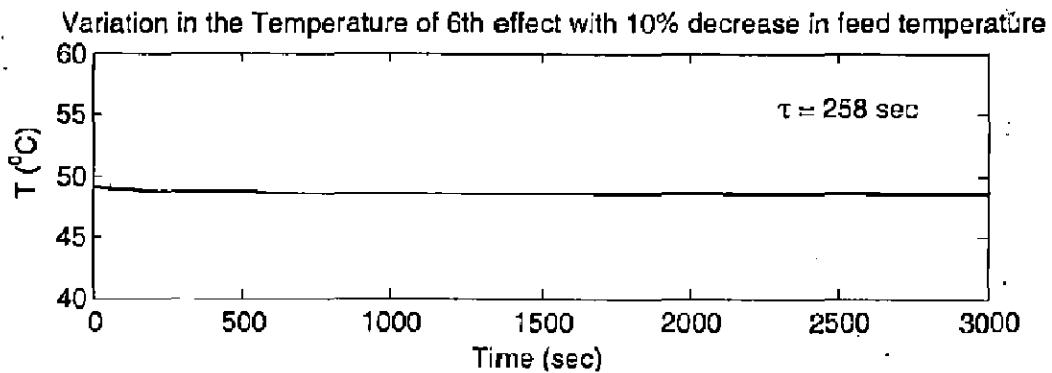


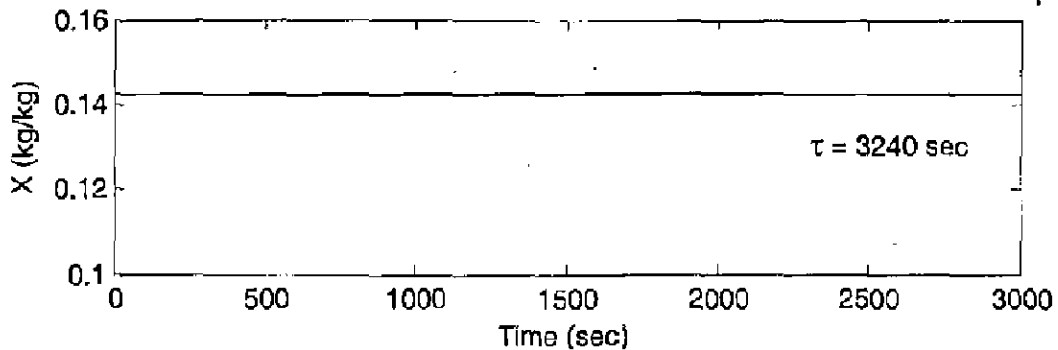
Figure 3.34 Response of 1<sup>st</sup> effect by disturbing  $\pm 10\%$  in the steam temperature

### 3.10.4.4 Effect of varying feed temperature

For the dynamic response of the feed temperature the disturbance is applied in the 5<sup>th</sup> and 6<sup>th</sup> effects simultaneously. The effect of  $\pm 10\%$  variation in feed temperature on the temperature and concentration of both the effect are shown from Figure 3.35 to Figure 3.36 respectively. It is evident from the figures that 10% disturbance in feed temperature does not bring noticeable change in the temperature and product concentration each effect. However after scale down Y-axis, it is observed that temperature of the both the effect increases and decreases to obtain the steady state with an increase and decrease in feed temperature and the product concentration of each effect first decreases and then increases to obtain the steady state with a very small fluctuations about the steady state up to four to five decimal places in the value of concentrations of both the effect and conversely for 10% increase in feed temperature.



Variation in the Product Concentration of 6th effect with 10% decrease in feed temperature



Variation in the Product Concentration of 6th effect with 10% increase in feed temperature

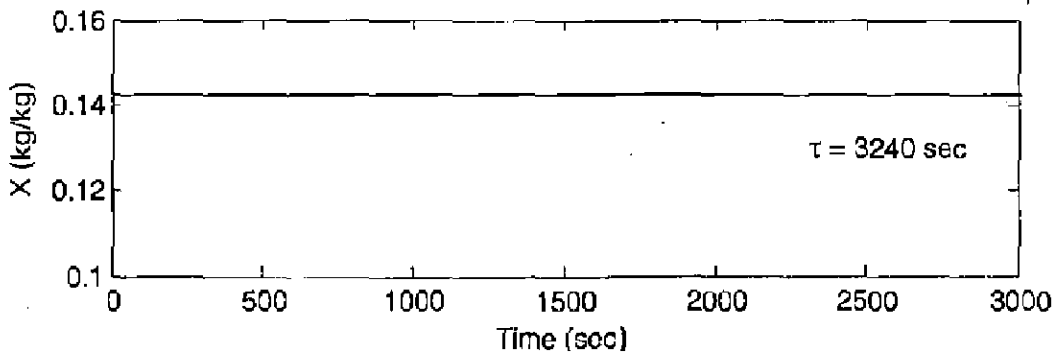
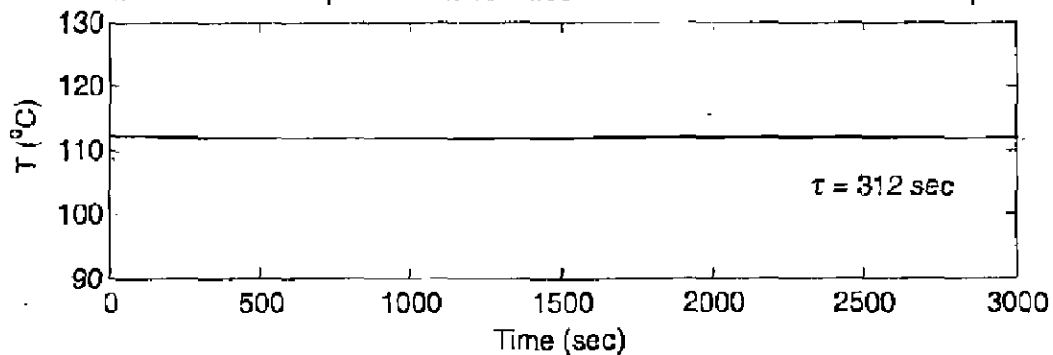
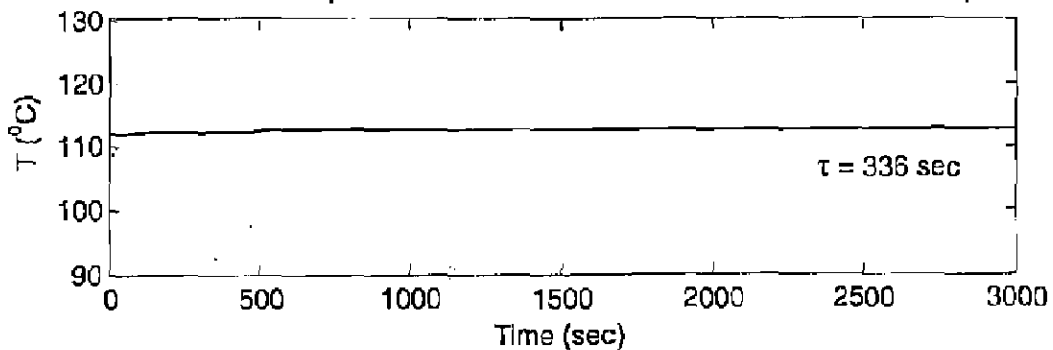


Figure 3.35 Response of 6<sup>th</sup> effect by disturbing  $\pm 10\%$  in the feed temperature

Variation in the Temperature of 1st effect with 10% decrease in feed temperature

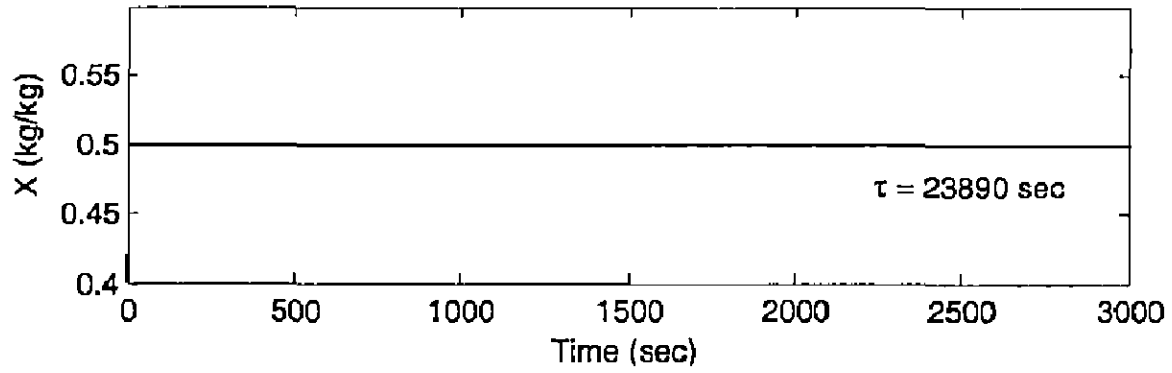


Variation in the Temperature of 1st effect with 10% increase in feed temperature





Variation in the Product Concentration of 1st effect with 10% decrease in feed temperature



Variation in the Product Concentration of 1st effect with 10% increase in feed temperature

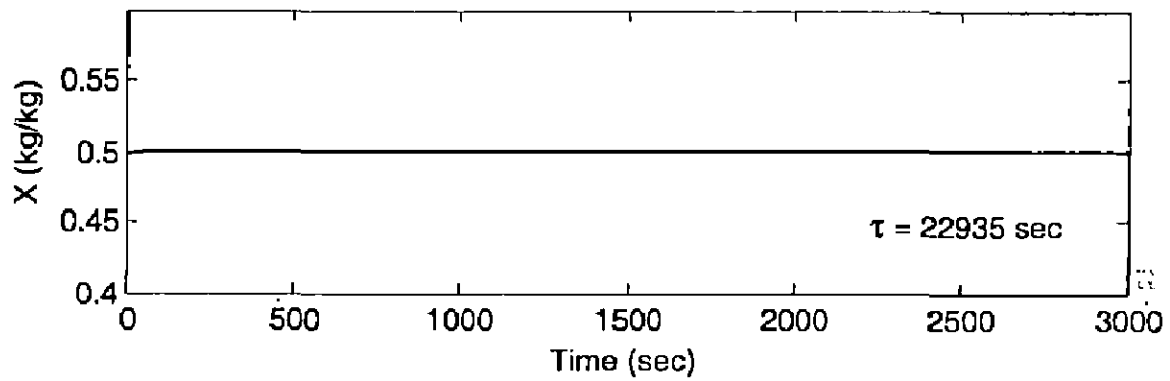


Figure 3.36 Response of 1<sup>st</sup> effect by disturbing  $\pm 10\%$  in the feed temperature

### 3.11 Conclusion

Dynamic modeling is an effective tool in determination of process variables in transient conditions. For designing an effective and efficient control system, it is always desirable to have thorough knowledge of the system behavior in different conditions as well as detailed knowledge of variation in the process variables under transient condition. There is always a desire in the process industry for easier to use and more affordable advanced control technologies and products. There are many complex control problems being handled by traditional control methods that are no longer effective. Due to the regulatory control problems that continue to plague day to day operations in process plants, the results are loss of productivity, quality, and competitiveness. So we need an effective controller, suiting to our system. Dynamic model helps us in better understanding of the process and behavior of its variables, thereby helps in determining a better control system. Thus in the present investigation an unsteady-state lumped parameter models were developed for sextuple effect falling film evaporator for backward, mixed and split feed sequences for concentrating the black liquor by using material, energy balance equations and parametric correlations. For the steady state and dynamic simulation the 'fsolve' and 'ode45' solvers in MATLAB source code is used. The model is validated for the steady state solution using literature data.

The parametric influences of various input parameters on output parameter steam economy (SE) for backward, mixed and split feed sequences is studied by obtaining the steady state solution by varying the range of input parameters feed temperature, steam temperature, feed flow rate, feed concentration, product concentration and last body temperature for a fixed set of other parameters. With the increase of feed temperature steam economy SE increases while decreases with the increase in steam temperature. With the increase of feed flow rate SE remains constant while decreases with the increase of feed concentration. With the increase of product concentration SE increases and with the increase in last body temperature SE increases slightly. Based on the parametric study on steam economy it may be concluded that the mixed feed is always optimal for varying range of all parameters.

In the present investigation an attempt has been made also for dynamic simulation for tubular type falling film MEE system by using 'ode45' solver in MATLAB source code. For the purpose the dynamic model is developed by using mass and energy balance equations. Because no dynamic data are available for further validation, further comparisons cannot be made at this time. However, the steady-state validation together with the fact that the observed responses follow the same nature of the dynamic responses as given by Stefanov and Hoo (2004) for the fundamental distributed parameter model for the MEE system.

The dynamic behavior of each effect's temperature and product concentration was studied by disturbing the liquor flow rate, feed concentration, steam and feed temperatures by  $\pm 10\%$  step input for backward mixed and split feed sequences. Since in all three feed sequences, last effect (6<sup>th</sup>) is connected with condenser and the first effect (1<sup>st</sup>) is connected with live steam. So the effect of  $\pm 10\%$  step input of aforesaid parameters on the temperature and concentration of last (6<sup>th</sup>) and first (1<sup>st</sup>) effects is studied.

The effect of  $\pm 10\%$  step input in feed flow rate on the temperature and concentration of last (6<sup>th</sup>) and first (1<sup>st</sup>) effects show an increase or decrease with decrease or increase in the feed flow rate for all three feed sequences. The effect of  $\pm 10\%$  step input in feed concentration on the temperature last (6<sup>th</sup>) and first (1<sup>st</sup>) effects show a increase or decrease irrespective of increase or decrease while concentration of both effects show increase or decrease according as the feed concentration is increase or decrease for all three feeding sequences. The 10% increase in steam temperature show increase in the temperature of both last and first effects before obtaining the steady state and decrease for 10% decrease for all three feeding sequences. When the steam temperature is increases by 10% the solid concentration of both the effect first increase and then show a exponential decay to obtain the steady state and conversely for 10% decrease for all three feeding sequences. The effect of  $\pm 10\%$  step input in feed temperature on the temperature of last and first effect show an increase and decrease to obtain the steady state with an increase and decrease in feed temperature for all three feeding sequences. When the feed temperature decreases by 10%, the product concentration of last and first effect first decreases and then increases to obtain the steady state with a very small fluctuations about the steady state in four to fifth decimal

places in the value of concentrations of both the effect and conversely for 10% increase in feed temperature for all three feeding sequences.

The transient study shows that the steady state is reached more quickly for temperature in comparison of the solid concentration and all of the responses converge in a smooth fashion for all the feed sequences. When  $\pm 10\%$  step input is applied on feed concentration, it was shown that the slight changes in temperature occur that are unidirectional i.e. the temperature increases in respective of increase or decrease.

#### 4.1. Introduction

Bleaching is a chemical process applied to cellulosic materials to increase their brightness. Brightness is the reflectance of visible light from cellulosic cloth and paper i.e. pulp fibers formed into sheets. Bleaching processes are applied to cellulosic textiles, woven articles made from cotton and linen and cellulosic pulp, in the form of aqueous suspensions of individual fibers separated from cellulosic raw material such as wood and non-woody materials like cotton stalks, straw, reed, jute, sugarcane (bagasse) and bamboo. Bleaching increases the capacity of the paper for accepting printed or written images and so increase its usefulness. Bleaching is also effective in removing unwanted particles that contaminate pulp fibers [Dence and Reeve (1996)].

The whiteness of pulp is measured by its ability to reflect monochromatic light in comparison to a known standard (usually magnesium oxide). The instrument most commonly used for the purpose is the Zeiss Elrepho reflectance meter which provides a diffuse light source. Fully bleached sulfite pulps can give brightness as high as 94, and unbleached kraft pulp as low as 15 Elrepho units. Unbleached pulps exhibit a wide range of brightness values. The sulfite process produces relatively bright chemical pulps, up to 65 Elrepho units, whereas those produced by the kraft, soda and semi chemical processes can be quite dark. Mechanical pulp brightness is mainly a function of the species and condition of the wood pulped. Generally, only those species providing brightness values over 55 Elrepho units are utilized for mechanical pulping [Smook (2001)].

Cellulose and hemicelluloses are inherently white and do not contribute to pulp color. It is generally agreed that "chromophoric groups" on the lignin are principally responsible for color. Oxidative mechanisms are believed to convert part of the lignin's phenolic groups to quinone-like substances that are known to absorb light. Heavy metal ions (e.g., iron and copper) are also known to form colored complexes with the phenolic groups. Extractive materials also can contribute to the color of mechanical pulps made from resinous woods.

Two approaches are used in the chemical bleaching of pulps. One approach is to utilize chemicals that selectively destroy some of the chromophoric groups, but do not materially attack lignin. The other approach is to almost totally remove residual lignin. The selective approach (often referred to as “brightening” to distinguish it from true bleaching) is used for high yield pulps with significant lignin content. This methodology is limited in many cases for achieving brightness values in the range of 70 Elrepho units, but under favorable circumstances, values above so can also be obtained. Although the brightness gains can be substantial, no known method of selective brightening produces a permanent brightening effect. Exposure to light and atmospheric oxygen causes the lignin to rapidly discolor, as can be readily observed with old newspapers.

To produce high-quality, stable paper pulps (as well as dissolving grades), bleaching methods that delignify the pulp must be used. Thus modern bleaching is achieved through a continuous sequence of process stages utilizing different chemicals and conditions in each stage, usually with washing between stages. The early stages of bleaching are usually considered as a continuation of the delignification process started in cooking. The later stages (brightening) employ oxidizing agents to scavenge and destroy the residual color. The entire bleaching process must be carried out in such a way that strength characteristics and other papermaking properties are preserved.

#### **4.1.1 Bleaching sequences**

Bleaching is carried out in a continuous sequence of distinct stages. In the first stage, (C, C/D or D<sub>100</sub>) chlorine and/or chlorine dioxide are used to delignify the pulp. The delignification stage is followed by an extraction stage (E, E<sub>o</sub> or E<sub>op</sub>) where the alkali soluble lignin is removed with caustic, oxygen and/or hydrogen peroxide. In the following stages (D<sub>1</sub>, E<sub>2</sub> and D<sub>2</sub>), pulp brightness is increased by eliminating the chromophoric groups in the lignin.

Multi-stage application of bleaching chemicals provides much greater benefits. Interstage washing, which removes dissolved impurities, is partially responsible for improvement in the extent and efficiency of bleaching, and in addition multistage sequences take advantage of the different action of each chemical and provide synergy in bleaching or delignification. A classic example of synergy between stages is the partial sequence CE, chlorination followed by extraction with sodium hydroxide. Chlorination oxidizes and fragments the lignin but, because it is carried out

under acidic conditions, only part of the degraded lignin dissolves. The following extraction stage is extremely effective in removing the lignin degraded in the preceding chlorination stage. The commonly applied bleaching sequences are shown in Table 4.1.

**Table 4.1 Commonly applied chemical treatments and their shorthand designations**

S. No.	Bleaching Sequence	Conditions
1.	Chlorination (C)	• Reaction with elemental chlorine in acidic medium
2.	Alkaline Extraction (E)	• Dissolution of reaction products with NaOH
3.	Chlorine Dioxide (D)	• Reaction with ClO <sub>2</sub> in acidic medium
4.	Oxygen (O)	• Reaction with molecular oxygen at high pressure in alkaline medium
5.	Hypochlorite (H)	• Reaction with hypochlorite in alkaline medium
6.	Peroxide (P)	• Reaction with peroxide in alkaline medium
7.	Ozone (Z)	• Reaction with ozone in acidic medium

Lower brightness levels can be achieved with fewer stages. A level of 65 Elrepho units can be easily reached with CEH or OH sequence. Intermediate levels of brightness can be achieved with CED, DED, OCED, CEHH, CEHD, or CEHP. Stages between four to six stages are commonly used to achieve “full-bleach” brightness level of 89-91. Numerous CEHDED and CEDED full-bleach systems are in operation dating from 1960's and 1970's. Increasing environmental awareness forcing paper industry in all over the world to switch towards elemental chlorine free bleaching. Chlorine in the first and subsequent stage was substituted by chlorine dioxide which by virtue of 2.63 times oxidizing power than elemental chlorine reduced results into less chemical consumption and pollution. Recently Indian pulp industry has also start shifting to elemental chlorine free (ECF) bleaching. The pulp mills that were using Cl<sub>2</sub> will need process improvements. Engineers and operators in theses mills will have to go through a learning process to operate ECF bleach plants. Process modelling can facilitate this transition process by evaluating process alternatives and operating conditions using simulation instead of costly mill trials.

#### **4.2 Modelling and Simulation of Bleaching Plant: A Review**

A number of simulation studies have been carried out in order to optimize and control the bleach plant in respect minimization of cost as well as the amount of effluents coming-out from the bleach

plant. Freedman (1974) achieved the bleach plant optimization in two stages. First, nonlinear models were formed to represent the bleach reactions in various bleaching stages. Second, the models were used as constraint equations for input to a linear program. The control set points based on the models were optimized. Myers et al. (1989) used GEMS for the optimum design and for the determination of operating conditions of an oxygen delignification system in order to minimize the delignification costs and to reduce the total organic chlorine emissions from the bleach plant. Brooks et al. (1994) used simulation to evaluate the conversion of conventional bleach plant for total chlorine free (TCF) bleaching based on hydrogen peroxide delignified softwood. Parsad et al. (1996) and Jameel et al. (1996) made an economic analysis through simulation of a kraft-oxygen mill with modifications in the pre-bleaching and bleaching systems to incorporate TCF, ECF and closure issues. Gupta (2001) modified the work of Freedman (1974) according Indian paper mill conditions. Gupta (2001) also presented the equation to evaluate pollution loads in terms of COD in a bleach plant effluent.

$$COD = 2.4 * \Delta \text{ Kappa Number} + 0.61 (\text{carry over solids}) \quad (4.1)$$

Where  $\Delta$  kappa number =  $K - K_0$ ,  $K_0$ , being floor kappa number.  $K_0$  depends on the type of fibers (HW, SW etc.), pulping condition, control measures, lignin content and type of lignin. Exact value of this parameter is generally not known and to be calculated through experiments.

Dumont et al. (2006) stated that modern bleach plant can be operated with help of sensor-based control systems, and their economic performance depended heavily on set points chosen by the operators. For this purpose a novel set point generation tool was proposed to minimize the chemical consumption for a multi stage bleach plant.

Dogan and Guruz (2004) proposed a bleach plant model in which each stage is composed of three unit operations as mixer, retention tower and washer and presented a process units and variables of a bleach plant as shown in the Figure 4.1. In a bleaching stage, mixers are used to mix the fiber suspensions with bleaching chemicals, steam or recycle streams. Authors presented the mass balance equations in the mixer for the liquor, fibres, chromophores, chemicals and dissolved solids based on the assumption of perfect mixing and quasi-steady-state. The retention tower was described as the sequence of CSTR-PFR-CSTR reactor in series as proposed by Wang (1993).



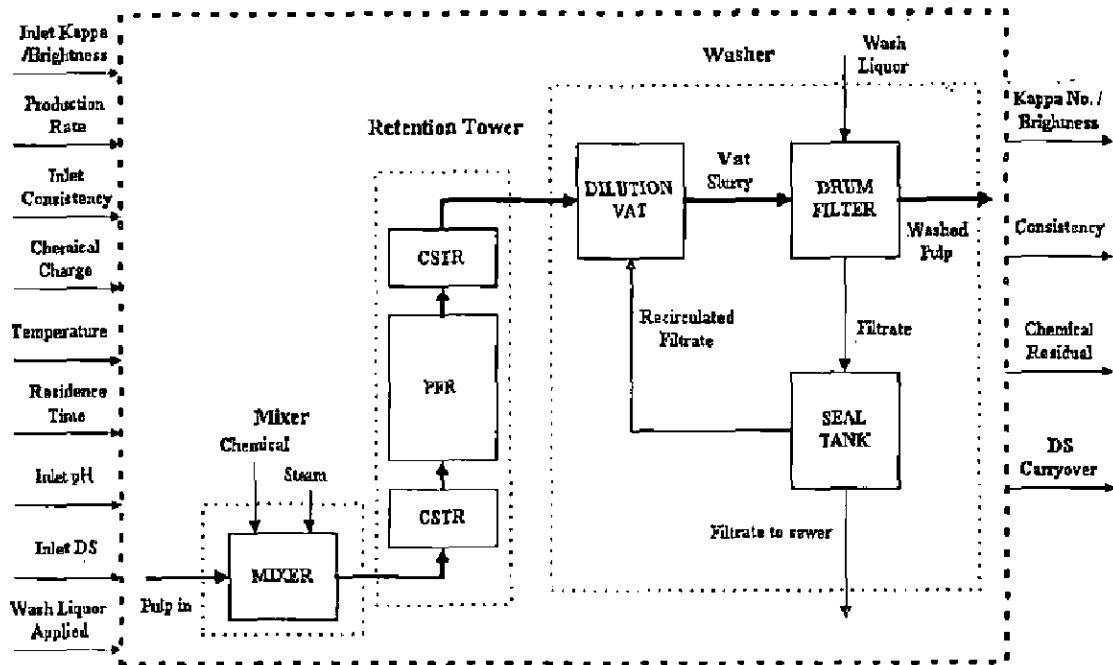


Figure 4.1 Process units and variables of the bleach plant

The modelling of the drum washer was done by dividing it into three parts; as the dilution vat, drum filter and seal tank. In the dilution vat the liquor from the seal tank is mixed with the main pulp stream in order to dilute the pulp to the desired consistency. Therefore, it was modeled as a steady-state mixer. The drum filter is used to remove the dissolved solids and unreacted chemicals from the pulp with wash water. Dogan and Guruz (2004) used Norden efficiency approach [Norden (1966), Norden and Pekkanen (1987)] in order to model the drum filter. In the model, the Norden efficiency factor was taken as 3 for all the washers. In the seal tank the part of the liquor coming from the drum filter is recycled back into the dilution vat and the rest of it is sent to the sewer. Thus, the seal tank was modeled as a splitter.

#### 4.2.1 Bleaching reaction kinetics: A review

Research in the area of bleaching reaction kinetics has not caught up with the rapid changes in the past few years. Although many papers have been published on reaction kinetics of chlorine delignification and chlorine dioxide substitution [Ackert et al. (1975), Germgard and Lindberg (1982), Germgard (1983), Germgard and Karlsson (1985), Germgard et al. (1987), Mackinnon et al. (1993), Saltin and Edwards (1993), Ni et al. (1995)], only a few papers in the literature are devoted to 100% chlorine dioxide delignification kinetics. Initial attempts to describe kinetics of

bleaching stages could not produce the kinetic expression but made some important observations. Chapnerkar (1961) showed that most of the reaction had taken place before his first data point at five minutes. Karter (1968) later used a flow reactor to study the first several minutes of the reaction, and concluded that the reaction was complete after one minute. His data indicated that the reaction was much more rapid than Chapnerkar (1961). For the first time Ackert (1973) presented chlorination kinetics model comprising by two parallel reactions, identified as fast substitution and slow oxidation and assumed that only "active lignin", i.e. total lignin minus the "floor-level" lignin, participated in the reactions. In his experiments, Ackert applied a large excess of chlorine, so that the decrease in chlorine concentration during reaction could be neglected. Furthermore, The scientific community is still divided on how to explain the existence of "floor level" lignin. Two hypotheses were proposed. The first one assumed that the reaction rate was limited by the formation of the so-called "immobilized chlorolignin" layer [Pugliese and McDonough (1989)]. The second assumed the formation of "blocking groups" during chlorination [Berry and Fleming (1987)]. The work proposed by Ni et al. (1990, 1995) supported the second hypothesis and proposed a series of reactions that lead to the formation of these "blocking groups" namely tri-chlorolignin.

Ackert et al., (1975) presented experimental data and kinetic models which described the chlorination of kraft pulp both in a dilute suspension and in a fibrous mat. Singh et al. (1975) studied the kinetics of each stage of a bleaching sequence, CEHD, and also provided the information on bleaching effect of the chemical and its rate of disappearance with time elapsed. In general terms each stage was similar in that a rapid bleaching reaction took place immediately following the mixing of pulp and chemical. The rapid bleaching reaction phase at chlorination, caustic extraction, hypo-chlorite oxidation and chlorine dioxide reaction produced about 80%, 65%, 60% and 70% of the total bleaching effect of the stage, respectively. Following this was a slower bleaching reaction period at each stage which was studied in more detail. The author also explained the order of kinetics in various stages such as the initial rapid reaction of chlorine followed a first order kinetics in chlorine concentration whereas slow reaction was found to follow a second order kinetics in chlorine concentration. Axegard (1979) conducted the experiments, designed to achieve a kinetic model for the first extraction stage. The majority of the experiments were carried out at low pulp consistency in order to provide for good mixing and possibilities of an

accurate determination of the alkalinity. Russell and Freiberg (1989) stated that the increasing in recycle ratio in a chlorination stage in a pulp bleach plant could strongly affect the corrosivity of process streams and change kinetics of chemical reactions occurring in those streams.

Ni et al. (1995) developed the Chlorination kinetics based on a delignification mechanism of kraft pulp chlorination proposed by Ni et al. (1990), which closely linked demethylation and delignification during chlorination and also defined tri-chloro-guaiacyl units in chlorinated softwood kraft lignin as the ‘blocking groups’. Theory of blocking groups was first proposed by Berry and Fleming (1987) to explain the existence of the so-called “floor-level” lignin remain in highly chlorinated pulp. Heterogeneous reaction kinetic model proposed by Pugliese and McDonough (1989) suggested that chlorination was limited by diffusion of chlorine due to progressive pore closure as chlorination continues. Homogeneous reaction kinetics of chlorination of softwood kraft pulp has been presented by a number of authors. Mackinnon (1993) showed that Ackert’s model resulted in unrealistic predictions of the chlorine concentration and lignin content for practical conditions when most of the applied chlorine is consumed. A weakness of model was that the kinetic equations were selected based on their ability to represent the data rather than on fundamental understanding of the chlorination mechanism.

Wang (1993) examined different models in order to represent the retention tower and concluded that in the modelling of retention tower the most important parameter is the bleaching reaction kinetics. Author suggested the percentage of the residence time taken by plug flow was found to vary from 79 to 85% for C tower and 82–90% for E and D towers. Therefore, in the modelling of the retention tower, the ratio of the residence time of the plug flow to overall residence time is taken as 0.8 for C tower and 0.9 for the other towers. Tessier and Savoie (1997) presented a kinetic model for 100% chlorine dioxide delignification based on experimental data. The model consisted of two ordinary differential equations representing the slow and fast reactions of lignin with chlorine dioxide. In addition the linear relationship between the chlorine dioxide consumption and the kappa number decrease. The relationship was found to be independent of the unbleached pulp kappa number. Chandranupap and Nguyen (2000) stated that the pH had a pronounced effect on both kinetics and bleaching efficiency of chlorine dioxide delignification. Chlorine dioxide delignified a *Eucalyptus globulus* kraft pulp at a faster rate and more effectively, at pH 4 than at

pH 2 or pH 10. The findings were consistent with previous suggestions that the kinetics and stoichiometry of chlorine dioxide delignification depend on the degree of conversion of chlorine dioxide into inactive chlorate and chlorite. Barroca et al. (2001) studied the chlorine dioxide delignification of different unbleached kraft pulps from *Eucalyptus globulus*, having kappa numbers of 12 to 18, in the temperature range of 285 °K to 358 °K. The effect of the unbleached pulp kappa number on the initial fast phase of delignification was investigated with respect to the depletion factors for kappa number and chlorine dioxide concentration. Furthermore, the behavior of the floor lignin content of the pulp, or the floor kappa number, was analyzed within this range. The results showed that all pulps exhibit a similar pattern, with respect to temperature, in depletion factors for kappa number and chlorine dioxide concentration. Barroca and Castro (2003) studied to investigate the kinetics of first chlorine dioxide bleaching stage of a *Eucalyptus globulus* kraft pulp. The bleaching reaction was described by an initial short but very fast step, followed by a slower step. The proposed model for the D<sub>1</sub> stage was based on both the light absorption coefficient and the chlorine dioxide concentration. A set of two depletion factors for the chlorine dioxide concentration and for the light absorption coefficient was described as a function of temperature for the fast and short steps of the reaction. The longer and slower periods were described by a homogeneous model. A nonlinear relationship between the chlorine dioxide consumption and the decrease in the light absorption coefficient was established, which was dependent on the extent of delignification but independent of temperature. Moreover, a linear relationship between the upper brightness limit and the temperature was observed. The fit of the experimental results obtained for different temperatures, initial chlorine dioxide concentrations and initial light absorption coefficients was very good, revealing the ability of the model to predict typical mill operating conditions.

Gu and Edwards (2003) presented a unified kinetic model for chlorine dioxide and elemental chlorine bleaching. The purpose of this model was to represent mill bleaching stages for process improvements and operations. The model provided much more information than traditional bleaching kinetic models. However, this model was not for understanding basic bleaching mechanisms. To identify model parameters and validate the model various laboratory bleaching data was used.

Yoon et al. (2004) used principal component analysis to classify various bleaching response variables, including end pH, kappa number, viscosity, and optical properties such as brightness, into different categories. Statistical methods, including factorial design, multiple regression, and response surface methodology were then used successfully to screen the importance of bleaching factors and their interactions. Further models were established to control, predicate, and optimize the bleaching responses. In most cases, the results of empirical modelling coincided well with those from conventional research methods, but the empirical methodology was more economic or less laborious.

Jain et al. (2007) focused on evaluation and comparison of the different modelling approaches of the ECF bleaching process. The important parameters and tendencies were determined from the existing models and experimental data. Identification of these key governing parameters led to propose new comprehensive empirical models, which were simpler, more accurate, applicable to broader range of process conditions and easily adjustable (if required) with different kinds of wood species. Mathematical models were developed for the first chlorine dioxide ( $D_0$ ) and extraction ( $E_0$ ) stage. The chlorine dioxide consumption with respect to kappa number decrease was found to be dependent on temperature, initial kappa number and initial chlorine dioxide charge. The initial ratio of slow and fast kappa numbers in extraction stage was found to be dependent on kappa factor in  $D_0$  stage.

Jain et al. (2009) presented new and improved semi-empirical mathematical models for all the chlorine dioxide stages and extraction stages (including oxygen and/or peroxide reinforced) in full elemental chlorine free (ECF) bleaching sequence. The models predicted variations of kappa number pH brightness, and bleaching chemical consumption at each step of multistage ECF bleaching sequences. The aims of this study were to improve the kinetic and stoichiometric equations involved in the chlorine dioxide stages [ $D_0$ ,  $D_1$ ,  $D_2$ ] for their predictability for different kinds of softwood and hardwood pulps and to model the extraction stages with or without oxygen and/or hydrogen peroxide reinforcement [E, (EO), (EOP), (EP)]. The predicted results fitted very closely to a wide range of laboratory and literature data, the predictability was extended to a greater variety of pulps (softwoods and hardwood pulps, kraft and other alkaline pulps).

From the detailed analysis of the above models, it was observed that through most of the investigators developed the kinetic models by using different methodology but the bleaching reactions were described similarly i.e. an initial short but very fast step followed by a slower step. However these models can not be termed standard models as the value of the parametric constants used to describe these models i.e. activation energy and frequency factor were reported different by different authors. These constants are dependent on the type of raw material and process conditions.

For the first chlorine dioxide stage most of investigators used kinetic model structure similar to the one proposed by Tessier and Savoie (1997) for the fast and slow reactions as well as the presence of unreactive lignin or floor lignin.

The rate of the fast lignin removal is given by

$$r_f = -\frac{dK_f}{dt} = k_f [\text{ClO}_2] K_f \quad (4.2)$$

while the rate of slow lignin removal is given by

$$r_s = -\frac{dK_s}{dt} = k_s [\text{ClO}_2] K_s \quad (4.3)$$

where  $r_f$  and  $r_s$  are the rate of reaction for fast and slow delignification reactions (kappa-number/s);  $K_f$  and  $K_s$  are the kappa number associated to fast and slow lignin (ml 0.1 mol/L  $\text{KMnO}_4$ /g fiber) and  $[\text{ClO}_2]$  is the concentration of chlorine dioxide (mol/L) and  $k_f$  &  $k_s$  are the reaction rate constants.

The reaction rate constants,  $k_f$  &  $k_s$  are assumed to follow the Arrhenius law

$$k_f = k_{f0} \exp(-E_{a_f}/RT) \quad (4.4)$$

$$k_s = k_{s0} \exp(-E_{a_s}/RT) \quad (4.5)$$

For the first extraction stage most of investigators used kinetic model structure similar to the one proposed by Axegard (1979) for the fast and slow reactions. The kinetic structure presented by Axegard (1979) is as follows.

$$r_f = -\frac{dK_{Ef}}{dt} = k_{Ef} [\text{OH}]^{0.2} K_{Ef} \quad (4.6)$$

$$r_s = -\frac{dK_{Es}}{dt} = k_{Es} [\text{OH}]^{0.85} K_{Es} \quad (4.7)$$

The reaction rate constants,  $k_{Ef}$  and  $k_{Es}$  are given by

$$k_{Ef} = k_{Ef0} \exp(-E_{a_f}/RT) * f \quad (4.8)$$

$$k_{Es} = k_{Es0} \exp(-E_{a_s}/RT) * f \quad (4.9)$$

The expression in extraction stage for the ratio of the content of initial fast reacting lignin to the content of initial slow reacting lignin is given by Axegard (1979) is

$$\frac{k_{Ef0}}{k_{Es0}} = A [\text{OH}]^{0.25} \exp(-28000/RT) * f \quad (4.10)$$

Initial ratio of slow and fast kappa number suggested by Jain et al. (2009)

$$\frac{k_{Ef0}}{k_{Es0}} = 27200(-13.604 * f^2 + 7.8719 * f - 0.1266) * [\text{OH}]^{0.25} \exp(-2800/RT) * f \quad (4.11)$$

where  $E_{a_f}$  and  $E_{a_s}$  are the activation energy for fast and slow delignification reaction (kJ/mol) and  $T$  is the temperature ( $^{\circ}\text{K}$ ) and  $R$  is the ideal gas constant (8.314 kJ/mol.K).  $k_{f0}$  ( $k_{Ef0}$ ) and  $k_{s0}$  ( $k_{Es0}$ ) are frequency factor of the fast and slow delignification reaction (L/mol.s) and  $f$  is the kappa factor. The values of the activation energy, frequency factor and the values of floor lignin for  $D_0$  stage and expression of the ratio of floor lignin for E stage reported in the literature are presented in the Table 4.2. However it can be seen that kinetic parameters i.e. activation energy and frequency factor vary with the raw material.

In a modern pulp mill that produces elementally chlorine-free (ECF) pulp, the  $D_0$  stage plays a critical role in determining the end results such as final brightness and pulp strength. It is very important to have accurate and robust models that can be used in controlling and optimizing the process. As more and more pulp mills in India are switching to 100% chlorine dioxide in the first bleaching stage to respond to environmental regulations, there is a need for a kinetic model for chlorine dioxide bleaching of indigenous raw material so that it can be used for process optimization or model based control strategies.

**Table 4.2 Activation energies, frequency factors and floor lignin for 100% chlorine dioxide and extraction stages**

First chlorine dioxide stage							
Fast Delignification Reaction				Slow Delignification Reaction			
S.No.	$E_{a_f}$ (kJ/mol)	$k_{f0}$ (L/mol.min)	Floor Lignin	$E_{a_s}$ (kJ/mol)	$K_{s0}$ (L/mol.min)	References	Floor Lignin
1.	42.9	$2.23 \times 10^8$	$K_{f1}=0.3K_0$	18.7 (softwood)	24.0	Tessier and Savoie (1997)	$K_{f1}=0.4K_0$
2.	68	$2.6 \times 10^{14}$	$K_{f1}=0.3K_0$	2 (softwood)	22.47	Jain et al. (2009)	$K_{f1}=0.5K_0$
			$K_{f1}=0.36K_0$	1.2 (hardwood)			$K_{f1}=0.44K_0$
First extraction stage							
3.	39	$1.96 \times 10^6$	Expression given in equation 4.10	2	0.0103	Axegard (1979)	Expression given in equation 4.11
4.	39	$6.85 \times 10^6$		2	0.0165	Jain et al. (2009)	

In the present study, a steady-state model of a three stage bleach plant (DED) has been developed based on the work presented by Dogan and Guruz (2004) to optimize the chemical consumption. Further in the present investigation the possible applicability of the earlier kinetic models in reproducing the experimental findings was tested. An attempt has been made to investigate the suitability of the kinetic model's parameters taken by earlier researchers for indigenous raw materials namely (i) mixed hardwood and (ii) bagasse pulp for first chlorine dioxide delignification



stage and for extraction stage. For the purpose kinetic model reported in literature are solved first and fitted with the results of laboratory experiment. The experiments of chlorine dioxide stage with the first extraction stage were performed on laboratory scale.

### **4.3 Mathematical Modelling of the Bleach Plant**

The flow sheet of DED bleaching plant is shown in Figure 4.2. Each stage is composed of three unit operations as mixer, retention tower and washer as show in Figure 4.1. Considering that the concentration of reactants is very high in the beginning and fairly low in the end than it is assumed that all retention towers are acting as single PFR. During further course of study all three retention towers are considered as PFR. Proposed mathematical models for mixer, PFR, dilution vat, drum filter and seal tank are presented in Table 4.3.

Model equations related to mixer are simple mass balance equations and are easy to solve. Study of the pulp washing operation is done in the previous chapter of the present work. So the main focus of the present study is on the modelling of retention tower (PFR). The most important parameter in the modelling of PFR is the bleaching reaction kinetics. In the present investigation kinetic model structure for the chlorine dioxide stage given by Tessier and Savoie (1997) [equations (4.2) to (4.5)] and for extraction stage given by Axegard (1979) is used.

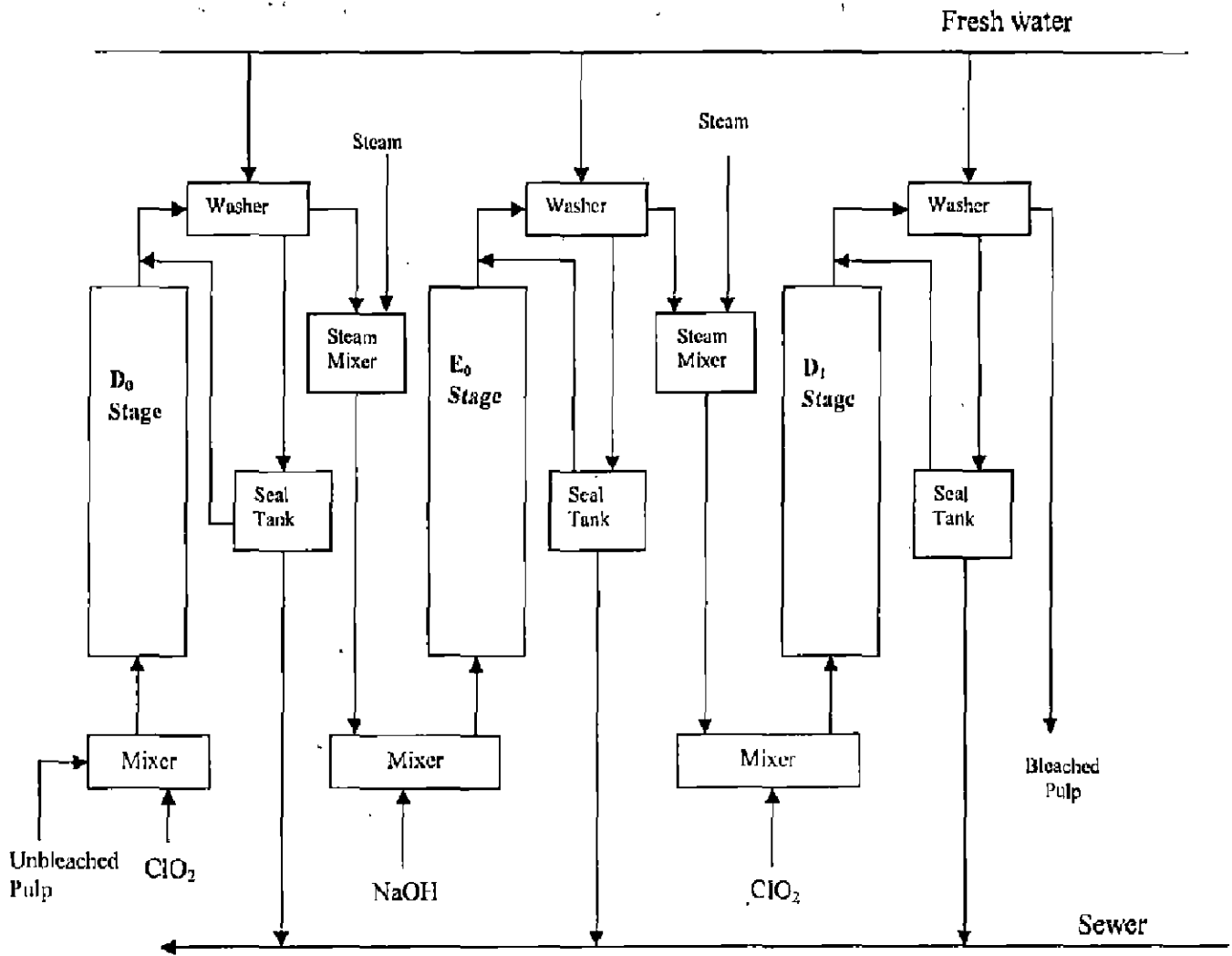


Figure 4.2 Process flow diagram of a DED bleach plant

**Table 4.3 Mathematical models of a bleach plant [Dogan and Guruz (2004)]**

	Liquors	Fibers	Kappa number	Residual Chemical/ Dissolved Solids
<b>Mixer</b>	$F_o = F_i + W_i$	$F_o \frac{C_{yo}}{1 - C_{yo}} = F_i \frac{C_{yi}}{1 - C_{yi}}$	$K_o = K_i$	$F_o L_{jo} = F_i L_{ji} + W_i M_{ji}$
<b>PFR</b>	$F_o = F_i$	$C_{yo} = C_{yi}$	$\frac{dK}{dt} = -r$	$\frac{dL_i}{dt} = -\frac{C_{yo}}{1 - C_{yo}} \psi_i r$
<b>Dilution Vat</b>	$F_v = F_i + W_r$			$L_{DS,v} = \frac{F_i L_{DS,i} + W_r M_{DS,r}}{F_v}$
<b>Drum Filter</b>		$F_t \frac{C_{yt}}{1 - C_{yt}} = F_i \frac{C_{yi}}{1 - C_{yi}}$	$L_{DS,t} = \begin{cases} M_{DS,2} + \frac{RW - 1}{RW E_n / F_v - 1} (L_{DS,v} - M_{DS,2}) \text{ when } RW \neq 1 \\ M_{DS,2} + \frac{1}{E_n} (L_{DS,v} - M_{DS,2}) \text{ when } RW = 1 \text{ where } RW = \frac{V_2}{L_1} \end{cases}$	
	$W_d = W_2 + F_v - F_t$		$M_{DS,d} = \frac{W_2 M_{DS,2} + F_v L_{DS,v} - F_t L_{DS,t}}{W_d}$	
<b>Seal Tank</b>	$W_d = W_1 + W_r$		$M_{DS,d} = M_{DS,t}$	

#### 4.4. Experimental Study

##### 4.4.1 Materials

Unbleached mix hardwood kraft pulp and bagasse pulp were procured from two different pulp and paper mills in India. The pulps were hand washed with plenty of water, screened, air dried, and stored in polythene bags for further bleaching experiments in the laboratory. All the chemicals used were of analytical grade. pH of the pulp suspension was adjusted with 1M NaOH and 1M H<sub>2</sub>SO<sub>4</sub> solutions. Sodium chlorite (NaClO<sub>2</sub>) solution was used for *in situ* generation of chlorine dioxide (D<sub>0</sub> stage) bleaching and NaOH for alkaline extraction (E stage) of the pulp after chlorine dioxide stage.

#### 4.4.2 Experimental procedure

The pulp was subjected to D<sub>0</sub>E bleaching in the laboratory, where D<sub>0</sub> and E stages refer to chlorine dioxide and alkaline extraction with NaOH. Kappa numbers of the unbleached and bleached pulps was determined according to the standard Tappi Test Procedure T- 236 as given in Table 4.5. The unbleached pulp was soaked in water, disintegrated in laboratory disintegrator, and used for bleaching studies for each experiment. Bleaching sequence (D<sub>0</sub>ED<sub>1</sub>) was optimized to obtain the 85% ISO brightness by varying the kappa factor from 0.25-0.35. 85% ISO target brightness is achieved at kappa factor = 0.35, hence further experiment were conducted at 0.35 kappa factor. The chlorine demand was calculated on the basis of kappa number as follows:

$$\text{Total chlorine demand (O.D. basis)} = 0.35 \times \text{kappa number}$$

70 % of the total chlorine demand was given in the first D<sub>0</sub> stage. For D<sub>0</sub> stage 40 g (O.D. basis) unbleached pulp was used. Out of this 20 g was stored for measuring D<sub>0</sub> kappa number and remaining 20 g was used for subsequent E stage. D<sub>0</sub> and D<sub>0</sub>E kappa numbers of bleached pulps were measured as a function of time. For parametric calculation kinetics at four different temperatures was also studied. All the experiments were done twice and average values reported. The bleaching conditions for D<sub>0</sub> and E stages of D<sub>0</sub>ED<sub>1</sub> bleaching sequence are summarized in the Table 4.4.

##### 4.4.2.1 Chlorine dioxide bleaching Stage (D<sub>0</sub>)

Calculated amount of NaClO<sub>2</sub> solution and water was mixed with disintegrated pulp so that starting pH was between 3-4 and the pulp consistency was 10% at which the bleaching was performed for the desired time in polythene bags kept in water bath at desired temperature. The pulp was mixed from time to time. The polythene bag was removed and the pulp was washed. The end pH was measured after the bleaching.

##### 4.4.2.2 Alkaline extraction (E)

The required amount of alkali (NaOH) and water were mixed with the pulp suspension to give a pulp consistency of 10 % in polythene bag. The bag was placed in a water bath maintained at 70

<sup>0</sup>C. The pulp was kneaded from time to time for proper mixing. The end pH was recorded. After alkali extraction the pulp was washed with the plenty of water (distilled water) and stored in fridge at 4 <sup>0</sup>C for determining kappa number.

**Table 4.4 Bleaching conditions for D<sub>0</sub> and E stages of D<sub>0</sub>ED<sub>1</sub> bleaching sequence**

Parameter	D <sub>0</sub> ED <sub>1</sub> Bleaching Sequence	
	D <sub>0</sub> stage	E stage
Cl <sub>2</sub> , (% of total chemical charge)	70	-----
NaOH (% O.D. pulp)	-----	1
Temperature ( <sup>0</sup> C)	50, 60, 70 and 80	50, 60, 70 and 80
Consistency (%)	10	10
pH	3.5	11.3
Time (min)	180	90

#### 4.4.3. Standard test procedure

##### 4.4.3.1 Analysis of NaClO<sub>2</sub> bleach liquor

20 g/L solution of NaClO<sub>2</sub> was prepared. In 10 ml. of diluted bleach liquor, 10 ml of 10 % potassium iodide and 10 ml of 10 % acetic acid were added. This solution was titrated with 0.1N sodium thiosulphate solution by adding 0.5% starch as indicator. The end point was blue to colorless. The active chlorine (g/L) was calculated as

$$\text{Active chlorine (g/L)} = \text{Normality of bleach liquor} \times 35.5$$

##### (a) Disintegration of pulp

Before bleaching the air dried pulp was disintegrated to break the fiber bundles and lumps. Air dried pulp was soaked in water overnight and then disintegrated in laboratory disintegrator (maximum 20 g O.D. pulp in 1 run) for 3 minutes. Then the water was drained on a screen and the

pulp was squeezed and kept in refrigerator in polythene bags for not more than 7 days. This wet pulp was used for further bleaching experiments.

**(b) Preparation of Sheets for kappa number determination**

The consistency of the disintegrated pulp was adjusted to 1 %. The pulp suspension was transferred into a hand sheet former. Water was then drained from the hand sheet former, so as to give sheet of about 5 g O.D. weight. The pulp was picked with the help of 2 blotting papers and then pressed with metallic plate and air dried. The sheets were protected against dirt and dust. For kappa number determination the sheets were stored in polythene bags.

**Table 4.5 Standard test methods followed for analysis**

<b>Test Number</b>	<b>Description</b>
SCAN C 18: 65	Disintegration of chemical pulps for testing
SCAN C 26: 76	Forming of hand sheets for physical testing of pulp.
T-236	Kappa number of pulp
T 610 om-87	Preparation of indicators and standard solutions

**4.5 Experimental Results**

Experiment has been conducted for first chlorine dioxide stage at the same operating conditions by taking four samples at four different temperatures i.e. 50, 60, 70 and 80 °C. The data obtained only for kappa number reduction for D<sub>0</sub> stage are presented in the Table 4.6 and Table 4.7 for mix hardwood and bagasse and for E stage for bagasse pulp in Table 4.8 respectively.

**Table 4.6 Kappa number at different temperatures and times for D<sub>0</sub> stage for mix hardwood**

Time (min)	Kappa No. at 50 °C	Kappa No. at 60 °C	Kappa No. at 70 °C	Kappa No. at 80 °C
0	23	23	23	23
1.5	16.32	15.87	15.18	14.95
2.5	13.51	12.92	12.12	12.03
4	11.26	10.56	10.46	9.46
7	7.88	7.00	6.12	6.02
10	5.88	5.68	5.43	5.13
15	5.18	5.12	4.89	4.79
30	4.36	4.25	4.11	4.11
50	3.67	3.50	3.40	3.39
75	3.43	3.18	3.17	3.16

**Table 4.7 Kappa number at different temperatures and times for D<sub>0</sub> stage for bagasse pulp**

Time (min)	Kappa No. at 50 °C	Kappa No. at 60 °C	Kappa No. at 70 °C	Kappa No. at 80 °C
0	15	15	15	15
1.5	12.44	11.06	10.84	10.44
2.5	11.19	10.01	9.97	9.63
4	9.60	8.50	8.39	7.89
7	6.23	6.05	6.65	6.63
10	4.49	4.25	5.45	5.25
15	3.91	3.78	4.63	4.27
30	3.71	3.70	3.80	3.53
50	3.51	3.40	3.35	3.31
75	3.38	3.35	3.12	3.06

**Table 4.8 Kappa number at different temperatures and times for E<sub>0</sub> stage for Bagasse pulp**

Time (min)	Kappa No. at 50 °C	Kappa No. at 60 °C	Kappa No. at 70 °C	Kappa No. at 80 °C
0	15	15	15	15
1.5	12.65	11.65	10.37	9.87
2.5	10.32	9.32	8.01	7.90
4	7.37	6.87	5.69	5.55
7	5.28	4.88	4.35	4.18
10	4.28	3.98	3.86	3.32
15	3.88	3.32	3.04	2.87
30	3.51	3.02	2.97	2.56
50	3.15	2.97	2.81	2.36
75	3.01	2.87	2.80	2.15

#### 4.6. Solution of Kinetic Models

Solutions of the kinetic models are obtained for the same operating conditions as used in the experimental work (temperature, initial chlorine dioxide concentration and hydroxyl ion concentration) at different temperatures. For the solution of the models, D<sub>0</sub> stage kinetic parameters given by Tessier and Savoie (1997) [softwood] and Jain et al. (2009) [softwood & hardwood] and E stage kinetic parameters given by Axegard (1979) and Jain et al. (2009) are used. Solution of the kinetic models is obtained by using 'ode45' solver in MATLAB source code and presented from Figure 4.3 to Figure 4.10 for D<sub>0</sub> stage and Figure 4.11 to Figure 4.14 for E stage along with experimental data. It can be observed from the figures that models given by different researchers follow the similar trend. However models give different values of floor lignin and initial ratio of slow and fast kappa number for D<sub>0</sub> and E stage respectively. It is interesting to see that the models proposed by Jain et al. (2009) almost coincide for softwood and hardwood even though author has reported different values of kinetic parameters (activation energy) and floor lignin.



## 4.7. Results and Discussion

For the suitability of kinetic parameters for indigenous raw material namely (i) mixed hardwood (ii) bagasse, kinetic models for  $D_0$  stage at different temperatures along with the experimental data are presented from the Figure 4.3 to Figure 4.10. Similarly kinetic models for E stage along with experimental data are presented from Figure 4.11 to Figure 4.14.

### 4.7.1. Chlorine dioxide stage

Kinetics for mix hardwood presented from the Figure 4.3 to Figure 4.6 show that experimental data fitted more closely with the models given by Jain et al. (2009) than model given by Tessier and Savoie (1997). Value of floor lignin from the experiment is found 20.8 % of initial kappa which is very close to the value suggested by Jain et al. (2009) and while differ significantly with the value suggested by Tessier and Savoie (1997). It can be seen from the figures that slow reaction rate equation given by Jain et al. (2009) fitted very closely with the experimental data. However, fast reaction plot of experimental data is not as steep as the plot of model equations. Hence during the lab experiment fast reaction continued beyond till 8 minutes while Jain et al. (2009) and Tessier and Savoie (1997) suggested that it is completed in less than 1 min. This may be due the fact that laboratory experiments were conducted in polythene bags and which resulted in very slow mixing of chemical and pulp.

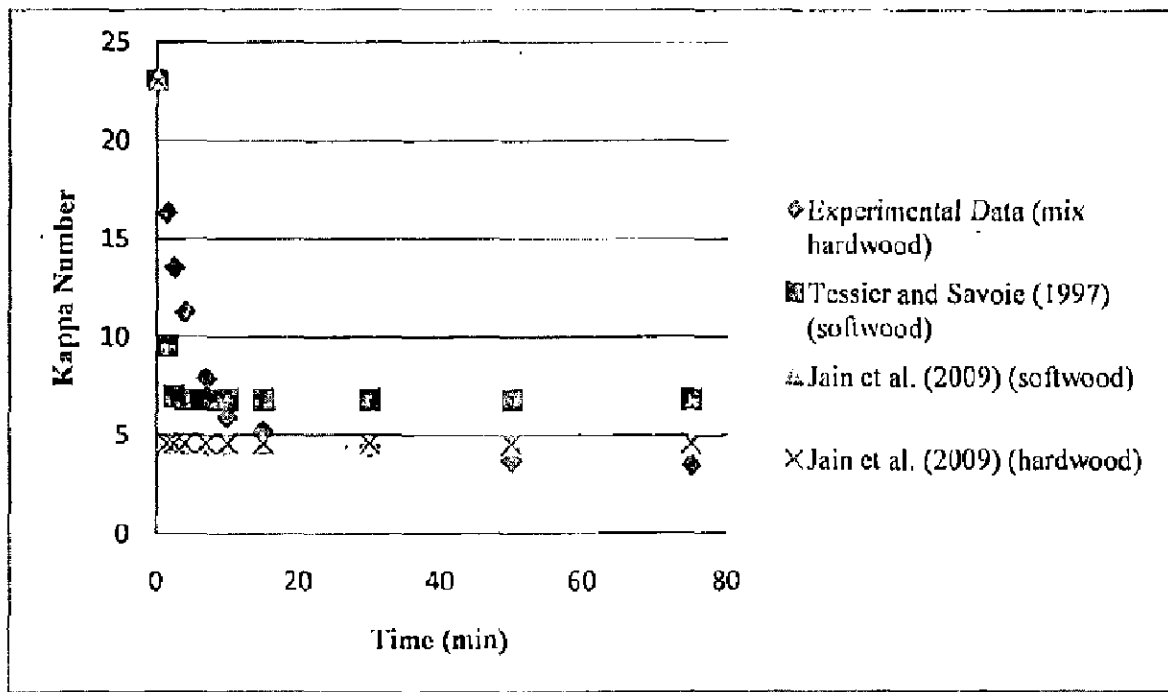


Figure 4.3 Experimental data ( $D_0$ ) and models prediction at 50 °C for mix hardwood

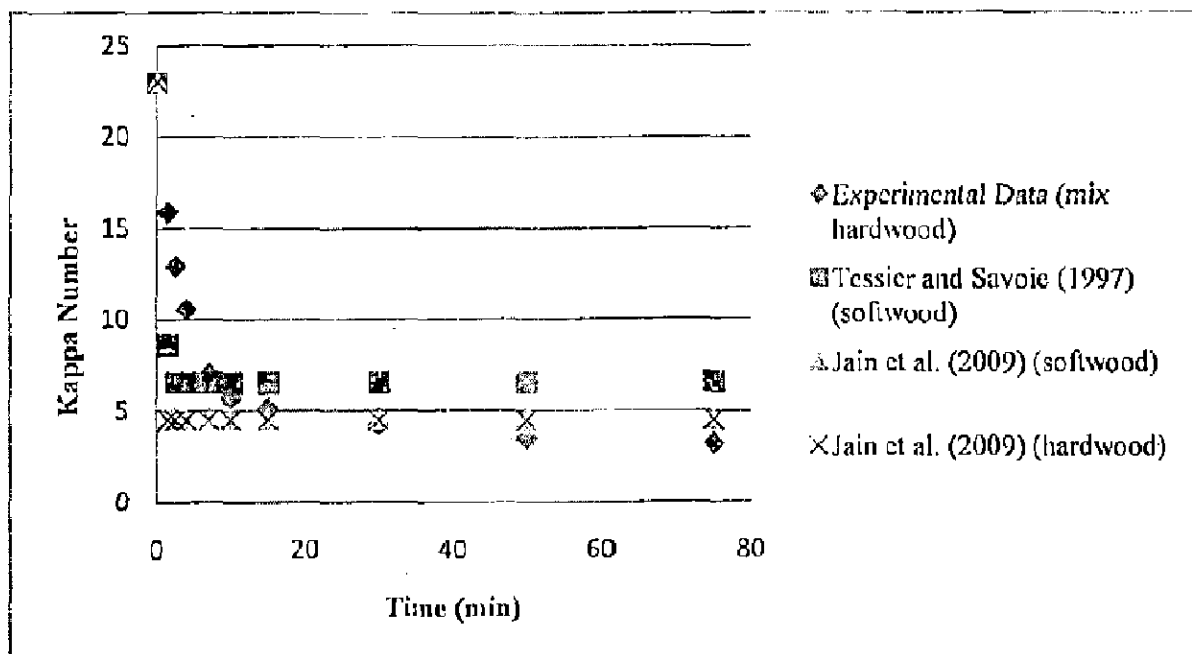


Figure 4.4 Experimental data ( $D_0$ ) and models prediction at 60 °C for mix hardwood

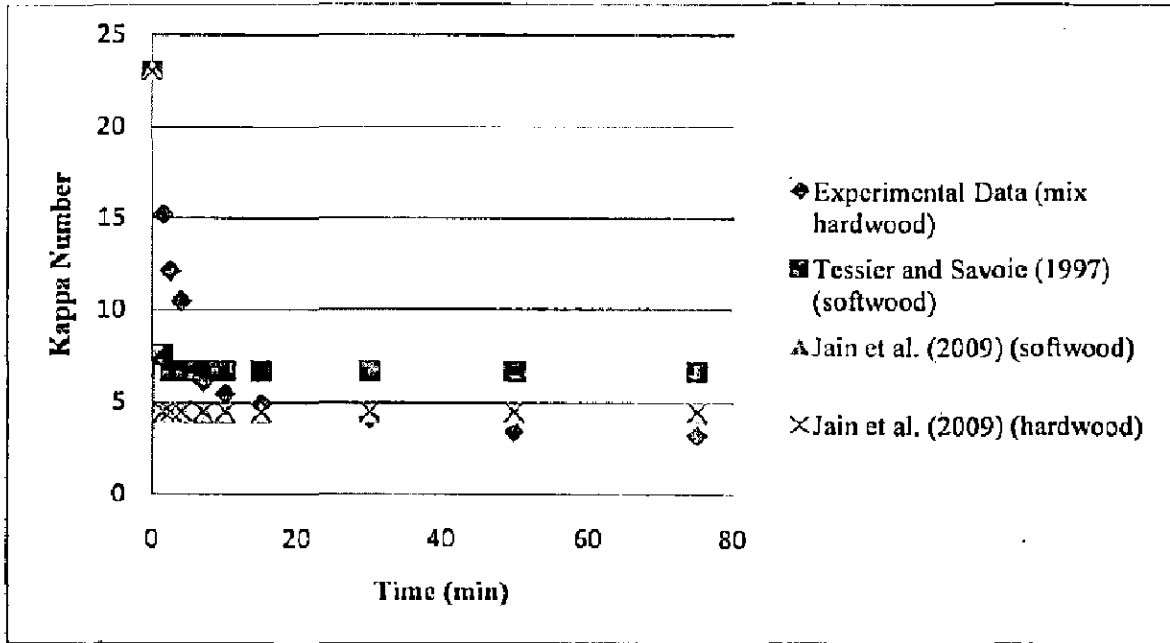


Figure 4.5 Experimental data ( $D_0$ ) and models prediction at 70 °C for mix hardwood

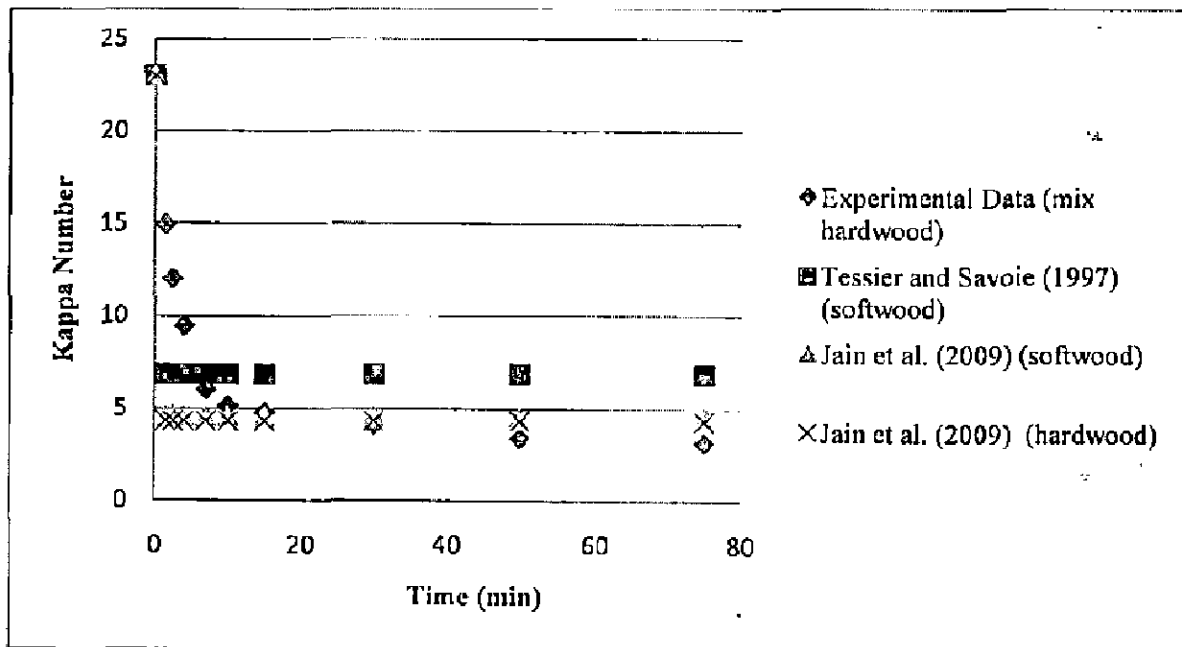


Figure 4.6 Experimental data ( $D_0$ ) and models prediction at 80 °C for mix hardwood

Kinetics for bagasse is presented from the Figure 4.7 to Figure 4.10. It can be seen that experimental data fitted more closely with the models given by Jain et al. (2009) than model given by Tessier and Savoie (1997). Value of floor lignin from the experiment is found 21% of initial kappa which is very close to the value suggested by Jain et al. (2009). For both the raw material it can be seen from the figures that slow reaction rate equation given by Jain et al. (2009) fitted very closely with the experimental data. However, fast reaction plot of experimental data is not as steep as the plot of model equations. Hence during the lab experiment fast reaction continues till approximately 10 minutes while Jain et al. (2009) and Tessier and Savoie (1997) suggested that it is completed in less than 1 min. This may be due the fact that laboratory experiments were conducted in polythene bags and which resulted in very slow mixing of chemical and pulp.

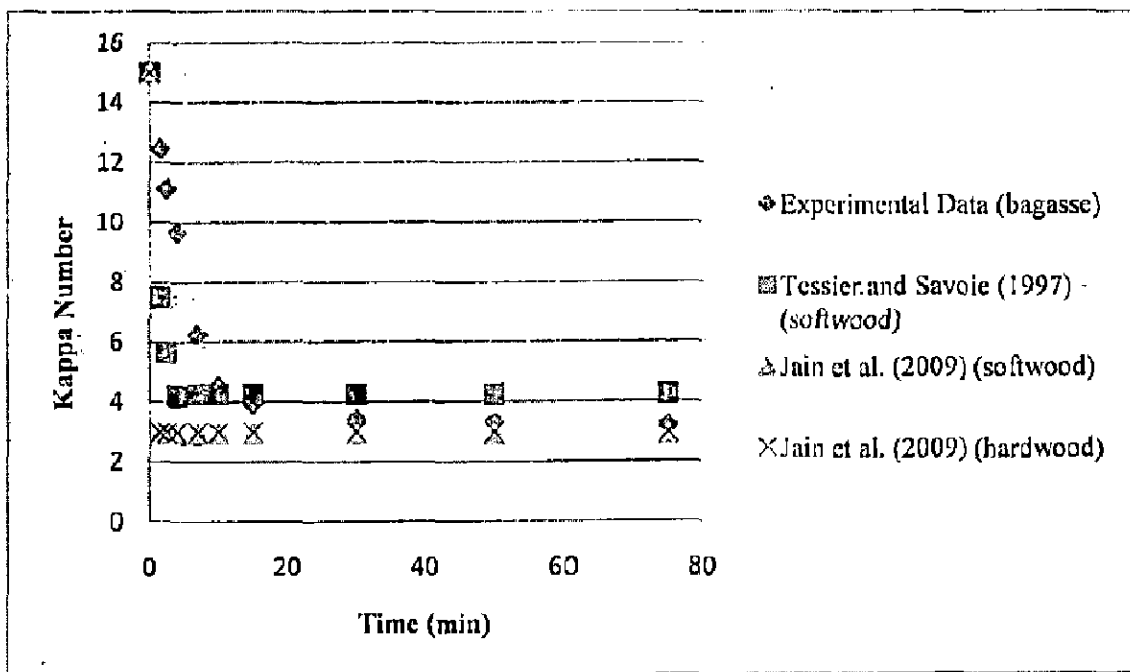


Figure 4.7 Experimental data ( $D_0$ ) and models prediction at 50 °C for bagasse

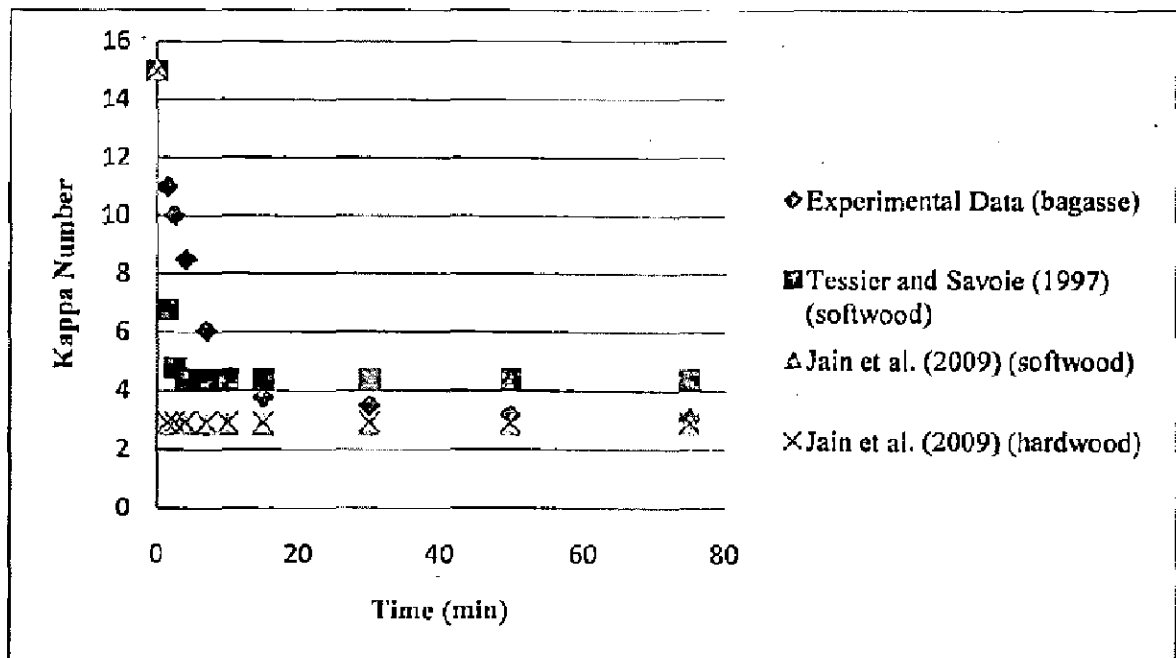


Figure 4.8 Experimental data ( $D_0$ ) and models prediction at 60 °C for bagasse

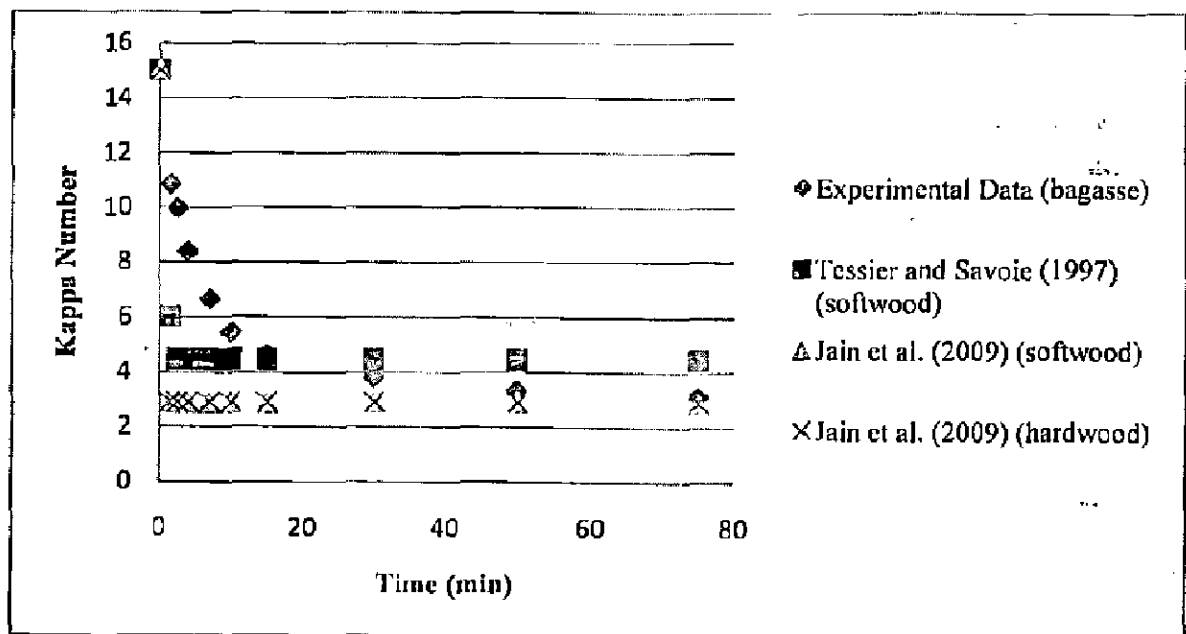


Figure 4.9 Experimental data ( $D_0$ ) and models prediction at 70 °C for bagasse

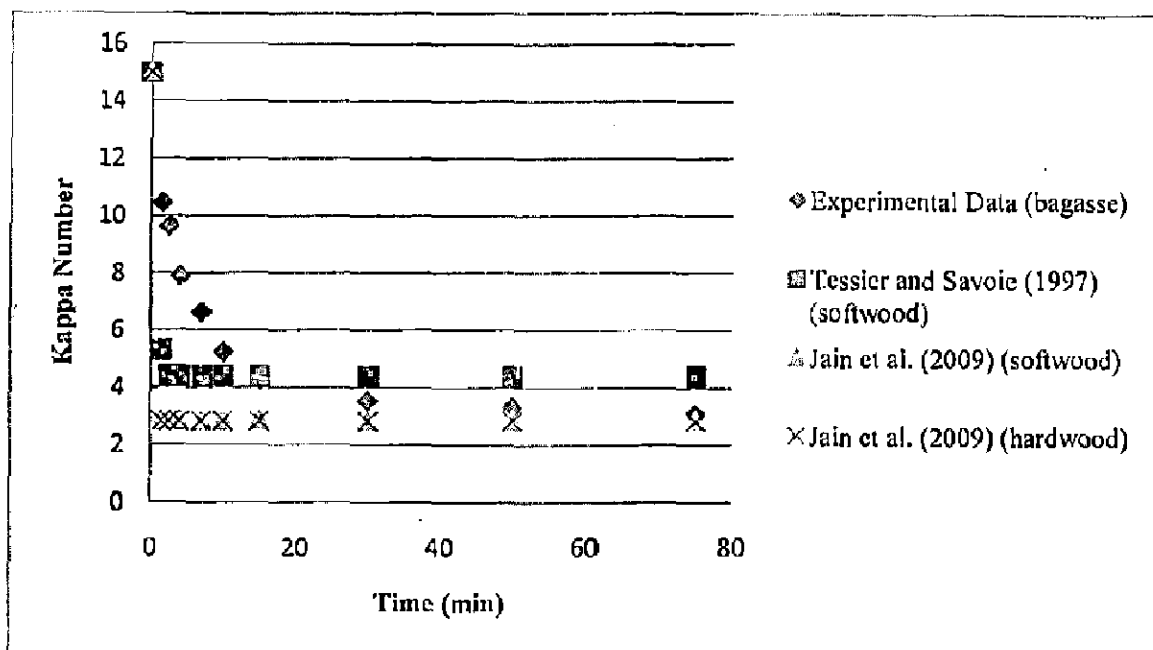


Figure 4.10 Experimental data ( $D_0$ ) and models prediction at  $80^{\circ}\text{C}$  for bagasse

#### 4.7.2. Extraction stage

The kinetics for the first extraction stage is very complicated since the reaction rate with respect to its effect on kappa number is high and variable. Furthermore, both the activation energy and frequency factor with respect to hydroxide ions are variable. Disregarding the very slow reaction dominating the rate after passage of several hours, the reaction may be described by a simple model which assumes that the rapid initial phase and the slow final phase are two separate first order reactions with respect to the kappa number.

Kinetics for bagasse are presented from the Figure 4.11 to Figure 4.14 show that experimental data fitted more closely with the models given by Jain et al. (2009) than model given by Tessier and Savoie (1997). It can be seen from the figures that slow reaction rate equation given by Jain et al. (2009) fitted very closely with the experimental data. However, fast reaction plot of experimental data is not as steep as the plot of model equations. Hence during the lab experiment fast reaction continued beyond 7 to 8 minutes while plot of model given by Jain et al. (2009) shows that it is completed in approximately in 2.5 minutes. This may be due the fact that laboratory experiments were conducted in polythene bags and which resulted in slow mixing of dissolved lignin in alkali.

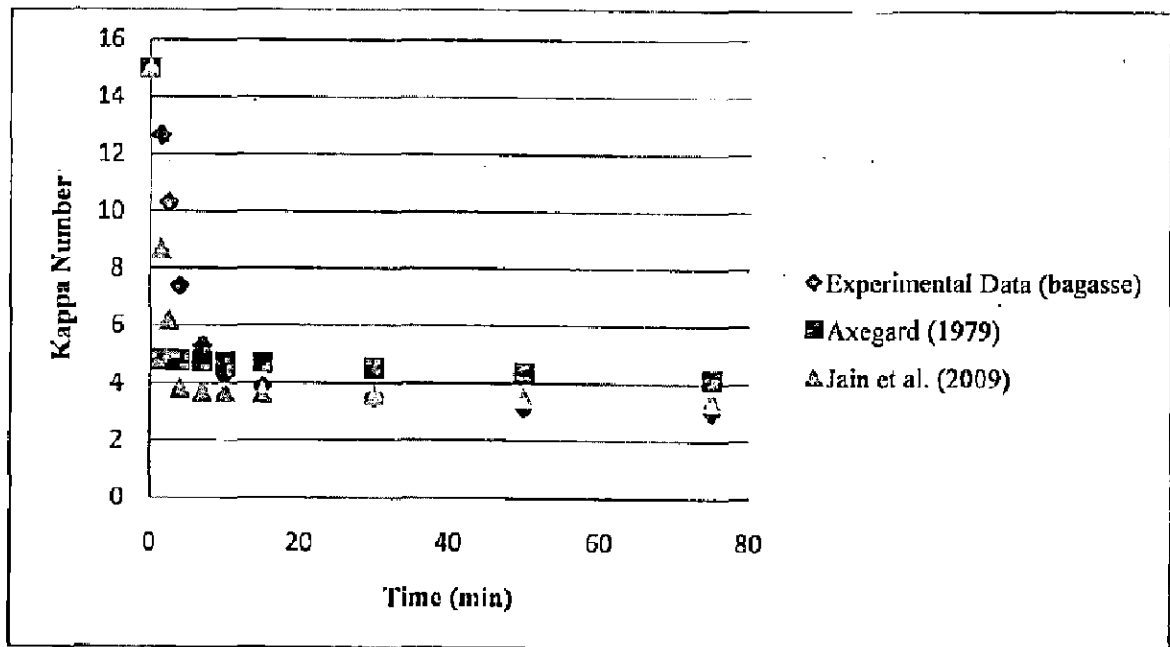


Figure 4.11 Experimental data ( $E_0$ ) and models prediction at 50 °C for bagasse

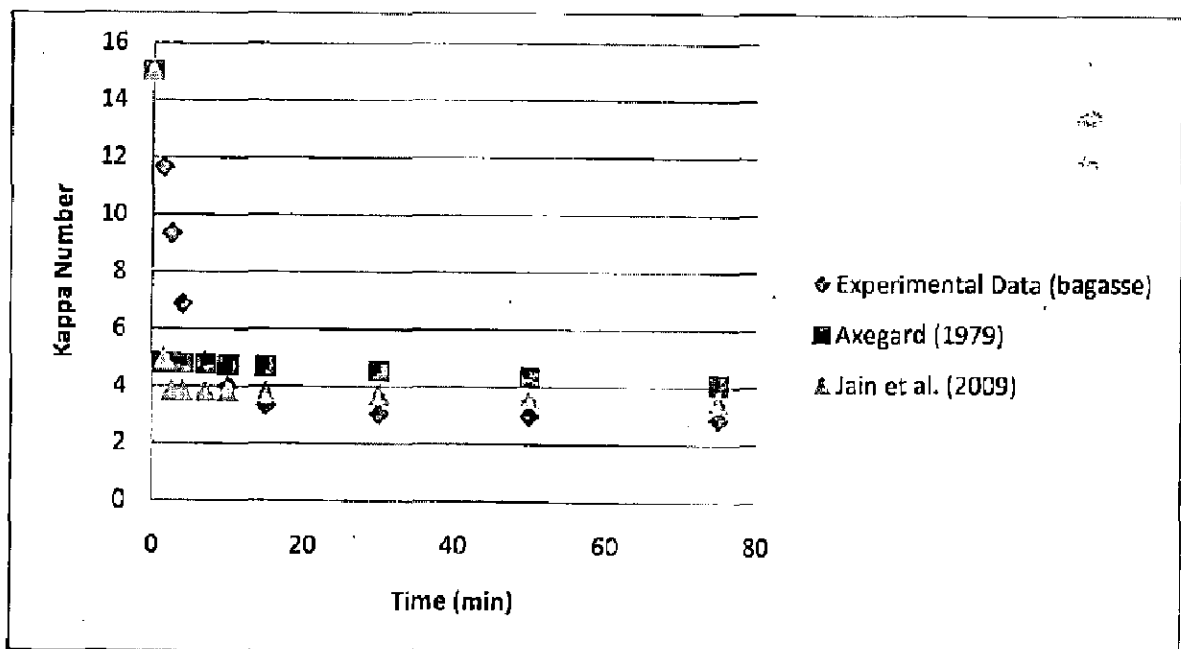


Figure 4.12 Experimental data ( $E_0$ ) and models prediction at 60 °C for bagasse

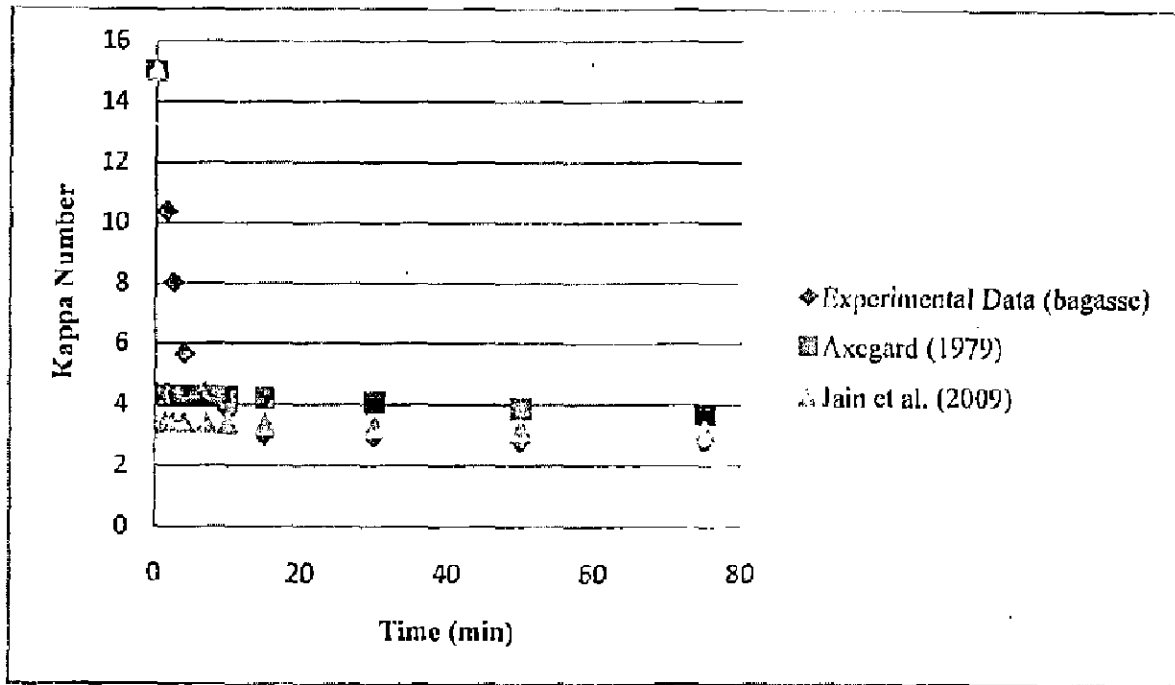


Figure 4.13 Experimental data ( $E_0$ ) and models prediction at 70 °C for bagasse

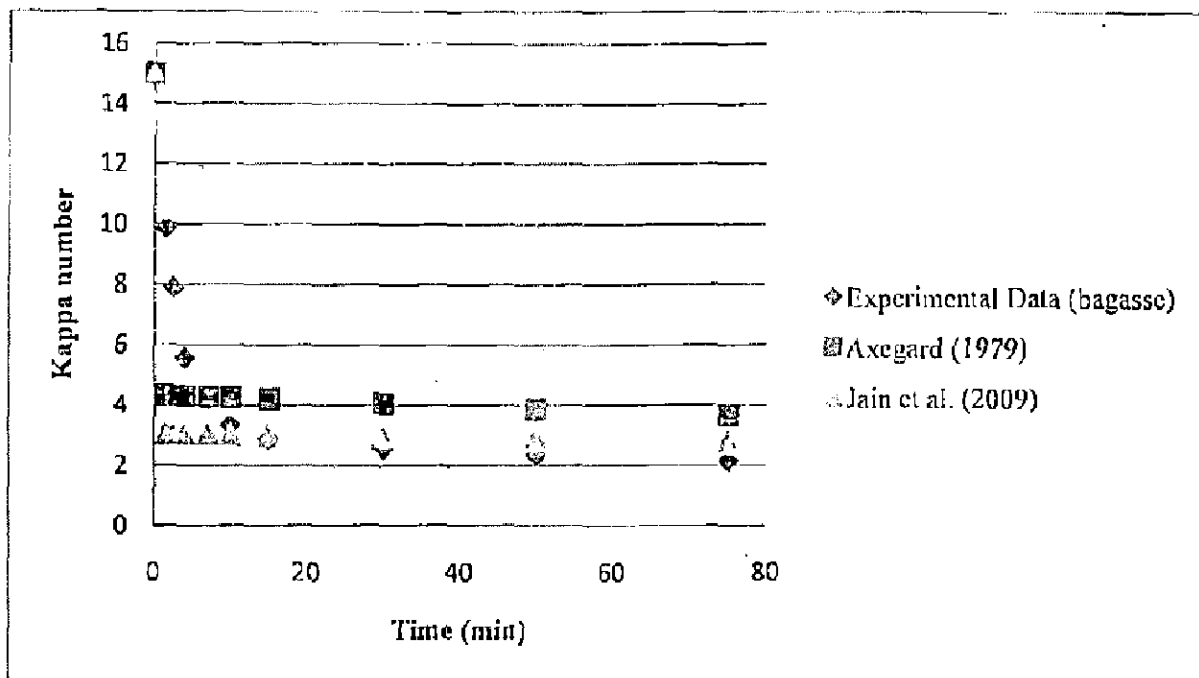


Figure 4.14 Experimental data ( $E_0$ ) and models prediction at 80 °C for bagasse



#### 4.8. Conclusion

In the present investigation an attempt has been made to find the suitable kinetic model for two different type of indigenous raw material. It may be concluded by the present study that for the indigenous raw material the model given by Jain et al. (2009) for the first chlorine dioxide and extraction stages may be used. However to find the accurate kinetic model for the indigenous raw material the complete experimental work is required to obtained the actual activation energy results in slower fast reaction than model given by Jain et al. (2009). This prompts in concluding that the activation energy and frequency factor for bagasse and indigenous hardwood are quite different. But same results obtained by hardwood and softwood models of Jain et al. (2009) and similar trend shown by experimental data shows that this difference in the values is more due to experimental methodology rather than the nature of raw material. This is substantiated with the fact that temperature does not have impact on the reaction time of fast reaction as shown by the data. This is possible only when the reaction slow down due to poor mixing. Hence it can be concluded that the models given by Jain can be used for modelling purpose. However the experiment should be carried out to get the exact value of the kinetic parameters.

In the present work simulation studies of different sections of an integrated pulp mill namely pulp washing, multi-effect evaporation and pulp bleaching is carried out. Mathematical modelling and Simulation of these sections is very typical task. In order to achieve this goal, available models in the literature are inspected in terms of their limitations. After the analysis necessary modifications and some useful assumptions are taken to resolve these limitations. Further these models are extended and solved to describe more complicated issues such as dynamics of multistage washing and multi-effect evaporator system. The present work utilizes MATLAB as a solution technique for solving these highly complex model equations.

### 5.1 Pulp Washing

In the present work model for counter current four stage brown stock washing has been described in the same manner as has been done by different workers [Kuo (1960), Brenner (1962), Sherman (1964), Pellett (1966), Neretnieks (1972), Grahs (1975), Perron and Lebeau (1977), Han and Edwards (1988), Kukreja (1996), Kumar (2002) and Arora et al. (2006a, b)] for pulp washing system along with the effect of dispersion-diffusion as used by some workers [Lapidus and Amundson (1952), Brenner (1962), Sherman (1964), Neretnieks (1972)]. It may be mentioned that some workers [Brenner (1962), Wong and Reeve (1990), Tervola (2006)] neglected adsorption desorption isotherms. Some other school of thoughts have neglected dispersion effects [Kuo (1960), Perron and Lebeau (1977)]. Even in adsorption isotherms investigators used different types of equations [Grahs (1975), Kukreja (1996), Kumar (2002), Arora et al (2006a, b)] and some [Tervola and Rasanen (2005)] used the Donnan equilibrium. The solution techniques used by different worker are also remarkably different. No investigator studied the multistage washing system by using *linear or nonlinear adsorption isotherm*.

In the present investigation multistage counter current washing system based on mathematical model derived for displacement washing with axial dispersion and particle diffusion with different boundary conditions is proposed. Non linear Langmuir adsorption isotherm is used to describe the relationship between the concentration of the solute in the liquor and concentration of the solute on the fibers. The numerical solutions are obtained for four stages in counter current manner by using

“pdepe” solver in MATLAB source code. Peclet number for the first washer was taken from the literature and for second and subsequent washers is obtained by using the algorithm given by Kumar (2002). For each stage of a series of four washers, the variations in the dimensionless solute concentration with respect to dimensionless time as well as dimensionless cake thickness are shown by 3-D graphs. Parametric effect of the various parameters is also studied for varying range of parameters for each washer individually of the four stage washing system.

The major conclusions of the study are as follows

- An unsteady-state mathematical model was described for a pulp washing system using material balance equations. The model for single stage washing system is further extended for multistage washing system.
- The solution of single stage washing is obtained by using different adsorption-desorption isotherms to show the suitability of the isotherm coupling with the washing model.
- Rate of mass accumulation in the solid phase due to adsorption-desorption is taken into consideration for evaluation of the solute concentration in the fiber by the linear isotherms given by [Lapidus and Amundson (1952), Perron and Lebeau (1977) and Sherman (1964)] and non linear Langmuir isotherm.
- Linear isotherm based model gives satisfactory profile, although the model with isotherm given by Sherman (1964) gives the erratic values of the solute concentration. However, non linear Langmuir isotherm is the best suitable for the satisfactory model performance.
- Boundary conditions do not influence significantly the washing performance results.
- The ‘pdepe’ solver used in the present investigation is simple, elegant and convenient for solving two point boundary value problems with varying range of parameters and show a comparable performance with average numerical errors.
- The use of MATLAB for the simulation of such type of complex system is a good alternative to the available techniques.
- The parametric effects of peclet number, kappa number and porosity are shown by the C vs. T graphical representations for constant bed depth at  $Z = 1.0$  and the effects of dimensionless cake thickness and dimensionless time are shown by C vs. Z & T profiles (3-D graphs) for the various values of parameters for sodium ion species for four stage counter current brown stock washing.

- For Peclet number below 20 (say 10 to 19) more deviation in the profile is observed. Higher Peclet number shows the little deviation in the shape of breakthrough curves as shown in the C-T profiles of washer 1. The deviation for  $Pe = 20$  is maximum for  $T = 0.5$  to  $T = 1.0$ , which continually decreases for higher Peclet numbers.
- The effect of Peclet number on dynamic behavior of solute concentration decreases continuously for washer 1 to 4. This is due to the fact that the range of variation in Peclet number for first washer is from 20 to 120, which narrow significantly from washer 2 to 4. For example for second washer the range of paclet number calculated is from 19 to 22 and for third and fourth washer is from 19 to 20.
- Varying the kappa number from 22 to 73 in the first washer, a very small deviation observed in the C-T profiles for all washers which is negligible in the engineering practice.
- The variation in the porosity is also applied on first washer and then the influence in C vs. T profile is observed for all washers. The C vs T profiles for different porosity at the bed exit i.e at  $Z = 1.0$ , are shown for sodium ion species of black liquor. The deviation in the breakthrough curve start after  $T = 0.5$ . For the porosity values below 0.40 (say 0.10 to 0.30) significant deviations in the profile is observed, and while for the higher porosity values show the practically no deviation in the shape of breakthrough curves.

## 5.2 Multi-effect Evaporation

Vast literature has been reported in last five decades on mathematical models and design of single as well as multi-stage evaporation for the steady state analysis [Rao and Kumar (1985), Lambert et al. (1987), Ray et al. (1992), Ray (1995), Patel and Babu (1996), Ugrin and Urbicain (1999), El-Dessouky et al. (1998), Cadet et al. (1999), El-Dessouky et al. (2000), Ray and Singh (2000), Al-Ansari et al (2001), Ray and Sharma (2004), Bakker et al. (2006), Karimi et al. (2007), Kaya and Sarac (2007), Bhargava et al. (2008a, b), Johansson et al. (2009), Khademi et al. (2009), and Khanam and Mohanty (2010)].

Many investigator [Andre and Ritter (1968), Bolmstedt and Jernquist (1976), Bolmstedt (1977), El-Nashar and Qamhiyeh (1990), Tonelli et al. (1990), Hanbury (1995), Aly and Marwan (1997), Cadet et al. (1999), Winchester and Marsh (1999), Miranda and Simpson (2005), Svandova et al. (2006), Gonzalez-Bustamante et al. (2007)] studied the dynamic behavior together with steady state analysis for various process industries.

Scanty literature [Stefanov and Hoo (2003, 2004)] is available on the dynamic response of MEE system in paper industry. Stefanov and Hoo (2003, 2004) used a distributor parameter model (System of partial differential equations) based on first principles knowledge about the fluid dynamics and heat transfer processes for a falling film lamella type evaporator. Stefanov and Hoo (2004) studied the dynamic responses for backward feed sequence and neglecting the effect of boiling point rise. No work presented on the dynamic response of MEE system in paper industry by using lumped parameter model (System of ordinary differential equations).

In the present investigation an attempt has been made for study of dynamic responses for tubular type falling film MEE system. The lumped parameter model of sextuple effect falling film evaporator system of a paper industry is developed by using unsteady state material and energy balance equations and physico-thermal properties of black liquor including the effect of boiling point rise for backward as well as mixed and split feed sequences. The transient behavior of the system is studied by disturbing the input parameters like feed flow rate, feed concentration, feed temperature and steam temperature.

The major conclusions of the study are as follows

- An unsteady-state mathematical model was developed for a sextuple effect backward, mixed and split feed evaporator by using material and energy balance equations with physico-chemical and thermal properties of the black liquor.
- In the present work for the steady state and dynamic simulation the 'fsolve' and 'ode45' solvers in MATLAB source code are used respectively. The solution is obtained for a range of input parameters taken from the literature.
- Simulations results obtained using MATLAB source code shows a comparable performance and so it may concluded that with the use of MATLAB it is possible to have better control of such complex system.
- Based on the steady state solution of the model the effect of variation of various input parameters on steam economy is studied. It may be concluded that mixed feed is always optimal for entire range of each parameters.
- The dynamic response on system variables of MEE is studied by creating four types of disturbances namely (i) in feed flow rate, (ii) in feed concentration, (iii) in live steam

temperature and (iv) in feed temperature as step input function. System variables selected were (i) temperature of each effect and (ii) output concentration of each effect.

- The disturbance is taken as a step input of  $\pm 10\%$ . Responses to the disturbance for the last (6<sup>th</sup>) and first (1<sup>st</sup>) effects are presented in graphical form for backward, mixed and split feed.
- For each response curve times constant ( $\tau$ ) is also calculated.
- The temperature and concentration of both the effects (6<sup>th</sup> and 1<sup>st</sup>) show an increase or decrease with decrease or increase in the feed flow rate. It is obvious as fresh steam supply rate is constant and water to be evaporates and decreases per unit time.
- The dynamic behavior of effect's temperature with respect to disturbances in feed concentration shows slight but insignificant change in temperature. However the change, it observed is unidirectional i.e. the temperature increases irrespective of increase or decrease in feed concentration.
- The changes in product concentration of both the effect show increase or decrease according as the feed concentration is increase or decrease. This may be due to the fact that  $\Delta T$  across the evaporator system remains constant and vapor-liquid equilibrium of each effect remains almost unchanged for the optimum performance.
- The change in steam temperature results in increase or decrease in the temperature of both the effects before obtaining the steady state for increase or decrease respectively. However the disturbance in steam temperature does not result in any noticeable change in the product concentration of both the effects. Although after scaling down Y-axis value it is observed that product concentration increase and then decrease or decrease and then increase for increase or decrease in the steam temperature respectively.
- It is evident from the figures that disturbance in feed temperature does not bring noticeable change in the temperature and product concentration each effect. However after scaling down Y-axis, it is observed that temperature of the both the effect increases and decreases to obtain the steady state with an increase and decrease in feed temperature and the product concentration of each effect first decreases and then increases to obtain the steady state with a very small fluctuations about the steady state up to four to five decimal places in the value of concentrations of both the effect and conversely for increase in feed temperature.
- Dynamic behavior of each effect's temperature and product concentration while disturbing the liquor flow rate, feed concentration, steam and feed temperatures by  $\pm 10\%$  shows that

the steady state is reached more quickly in temperature in comparison of the solid concentration and all of the responses converge in a smooth fashion.

### **5.3 Pulp Bleaching**

In a modern pulp mill that produces elementally chlorine-free (ECF) pulp, the  $D_0$  stage plays a critical role in determining the end results such as final brightness and pulp strength. It is very important to have accurate and robust models that can be used in controlling and optimizing the process. As more and more pulp mills in India are switching to 100% chlorine dioxide in the first bleaching stage to respond to environmental regulations, there is a need for a kinetic model for chlorine dioxide bleaching of indigenous raw material so that it can be used for process optimization or model based control strategies.

Scanty literature is available on the 100% chlorine dioxide bleaching. In the present investigation the possible applicability of the earlier kinetic models in reproducing the experimental findings was tested. An attempt has been made to investigate the suitability of the kinetic model's parameters taken by earlier researchers for indigenous raw materials namely (i) mix hardwood and (ii) bagasse pulp for first chlorine dioxide stage and using only bagasse pulp for the extraction stage. For this purpose the experiments of first chlorine dioxide stage with the first extraction stage have done on laboratory scale. For this purpose the kinetic models given by Tessier and Savoie (1997) and Jain et al. (2009) is selected. Solution of these kinetic models is obtained by using 'ode45' solver in MATLAB source code. For the suitability of the kinetic models, the model predicted results were fitted with the experimental data.

It may be concluded by the present study that the model given by Tessier and Savoie (1997) and Jain et al. (2009) can be used for the bagasse indigenous raw material but for the hardwood there is a need of some modifications in the values of frequency factor and the values of the activation energy may be used as usual.

### **5.4 Recommendations for future work**

Based on the entire investigations the following recommendations can be made for future work in these areas

#### **5.4.1 Pulp washing**

- Model should be further extended for the other washers like pressure, horizontal washer, belt washer, screw press etc.
- Reverse trend of N-T profile can be obtained for the multistage washing system.
- The solutions of the washing model with or without using adsorption-desorption isotherms are available in the literature by various techniques. Thus to obtain the best suitable technique there is need of comparison of all the available solution techniques reported in the literature. Comparison may be based on closeness with analytic solution along with the convergence of the solution techniques or CPU time.
- Experiment should be conducted to find out the data for simulation for  $\text{Na}^+$  and lignin species of indigenous raw material.
- Nonlinear multi-variate statistical analysis of the effects of the operating variables can be attempted to examine the effect of temperature, thickness and consistency of the mat (at inlet and discharge conditions), and superficial velocity of liquor/wash water on washing efficiency.
- Elaborate experiment should be conducted in an industrial BSW with various kinds of pulp obtained from hardwood, bamboo, non woods like bagasse and straw which are the main raw material for pulp and paper industry. It may be mentioned that the this present work is based on the softwood (pine) sulphate pulp.
- Experiments need to be carried out to find the displacement ratio for different number of stages of BSW for accurate estimation of parameters for evaporator and bleach plant, particularly soda loss, and COD loss.

#### **5.4.2 Multi-effect evaporation**

- Evaporator should be optimized with various feed sequence or PFR with all possible economy measures like utilization of condensate and product flash in order to reduce both electrical and thermal energy consumption.
- With unsteady-state simulation, the economic influence of the optimized time of operation can be analyzed.
- In the present investigation optimum feed sequence is obtained using steam economy. However a cost optimization function should be obtained including pumping and man power cost.



- The recent trend in the design of evaporator is to use unequal heating surface areas in evaporator bodies. Therefore it will be importance to consider this aspects for concentration of black liquor in MEE.
- Detailed study on the modelling of physico-chemical propertise of black liquor based on experimental measurements of different Indian pulp mill liquor from varieties of raw materials and their blends followed by simulation needs careful attention.

#### 5.4.3 Pulp bleaching

- Simulation of the steady state model for DED bleach plant is required for waste minimization and to calculate the pollution load in terms of COD.
- In the preesent work only kappa number measurmmment was done. Detailed laboratory experiment of chlorine dioxide and extraction stage bleach is required including pH measurment,  $\text{ClO}_2$  cosumption and resudual chemical measurement to develop kinetic model for indigenous raw material.
- Present work is carried in the laboratory at flask level. More accurate results can be obtained by performing experiments on lab scale reactors.
- The laboratory based experiment should be carried out to establish the relation among AOX, COD, soda loss and TOCL for various bleaching sequences like ECF with various chlorine di oxide substitution and also for TCF bleaching sequence.
- Cost optimization of multistage bleach plant using non- linear techniques shoul be carried out.

1. Ackert, J.E., "Kraft Pulp Kinetics", Ph.D. Thesis, Univ. Idaho, (1973).
2. Ackert, J.E., Koch D.D. and Edwards, L.L., "Displacement chlorination of kraft pulps - an experimental study and comparison of models," Tappi Journal, 58(10), 141-145, (1975).
3. Akanksha., Pant, K.K. and Srivastava, V.K., "Modelling of sulphonation of tridecylbenzene in a falling film reactor", Mathematical and Computer Modelling, 46, 1332-1344, (2007).
4. Ala-Kaila, K., "Washing efficiency in fractional post-O2 washing", Paperi ja Puu -Paper and Timber, 79, 489-495, (1997).
5. Al-Ansari, A., Ettouney, H. and El-Dessouky, H.M., "Water-zeolite adsorption heat pump combined with single effect evaporation desalination process", Renewable Energy, 24, 91-111, (2001).
6. Algehed, J. and Berntsson, T., "Evaporation of black liquor and wastewater using medium-pressure steam: Simulation and economic evaluation of novel designs", Applied Thermal Engineering, 23, 481-495, (2003).
7. Alhumaizi, K., "A moving collocation method for the solution of transient convection-diffusion-reaction problems", Journal of Computational and Applied Mathematics, 193, 484-496, (2006).
8. Alhousseini, A.A., Tuzla, K., and Chen, J.C., "Falling film evaporation of single component liquids", Int. J. Heat Mass Transfer, 41(12), 1623-1632, (1998).
9. Al-Jabari, M., van Heiningen, A.R.P. and van De Ven, T.G.M., "Modelling the flow and the deposition of fillers in packed beds of pulp fibers", Journal of Pulp Paper Science, 20 (9), J249-J253, (1994).
10. Aly, N.H and Marwan, M.A., "Dynamic response of multi-effect evaporators", Desalination, 114, 189-196, (1997).
11. Andersen, J.E., Glasson, L.W. and Lees, F.P., "The control of single concentration evaporator", Transactions of the Society of Instrument Technology, 13(1), 121, (1961).
12. Andre, H. and Ritter, R.A., "Dynamic Response of a Double Effect Evaporator", The Canadian Journal of Chemical Engineering, 46, 259-264, (1968).
13. Anttila, J.R., Rousu, P.P. and Tanskanen., "Modelling of multistage washing systems-application in the design of pulping processes based on organic acids", Paperi ja Puu-Paper and Timber, 89(2), 95-101, (2007).

14. Arora, S., Dhaliwal, S.S. and Kukreja, V.K., "Modelling of the displacement washing of pulp fiber bed", *Indian Journal of Chemical Technology*, 13, 1-6, (2006b).
15. Arora, S., Dhaliwal, S.S. and Kukreja, V.K., "Simulation of washing of packed bed of porous particles by orthogonal collocation on finite elements", *Computers and Chemical Engineering*, 30, 1054-1060, (2006a).
16. Axegard, P., "Kinetics of alkaline bleaching for the kraft CE sequence", *Svensk Papperstidning*, (12), 361-367, (1979).
17. Babu, B.V. and Gupta, S., "Modelling and simulation for dynamics of packed bed adsorption", *Proceedings of International Symposium & 57th Annual Session of IChE in association with AIChE (CHEMCON-2004)*, Mumbai, December 27-30, (2004).
18. Bakker Huub, H.C., Marsh, C., Paramalingam, S. and Chen, H., "Cascade controller design for concentration control in a falling-film evaporator", *Food Control*, 17, 325-330, (2006).
19. Barroca, M.J.M.C. and Castro, J.A.A.M, "Kinetics of the first chlorine dioxide bleaching stage (D1) of a hardwood kraft pulp", *Ind.Eng.Chem.Res.*, 42, 4156-4161, (2003).
20. Barroca, M.J.M.C., Simoes, R.M.S. and Castro, J.A.A.M, "Effect of unbleached kappa number on the kinetics of chlorine dioxide delignification", *Appita Journal*, 54(6), 532-535, (2001).
21. Bender, G., Richard, L. and Dorn, W., "Advanced control of brown-stock washers", *Tappi Journal*, Dec, 115-118, (1988).
22. Berry, R.M. and Fleming, B.I., "Why does chlorination and extraction fail to delignify unbleached kraft pulp completely", *Holzforschung*, 41(3), 1977-1981, (1987).
23. Bhargava, R., Khanam S., Mohanty, B. and Ray A.K., "Selection of optimal feed flow sequence for a multiple effect evaporator system", *Computers and Chemical Engineering*, 32, 2203-2216, (2008 a).
24. Bhargava, R., Khanam S., Mohanty, B. and Ray A.K., "Simulation of flat falling film evaporator system for concentration of black liquor", *Computers and Chemical Engineering*, 32, 3213-3223, (2008 b).
25. Bilmez, Y.G., Tosun, I. and Yilmaz, L., "Optimization of the locations of side streams in a filter cake washing process", *Chemical Engineering Communications*, 182, 49-67, (2000).
26. Bolmstedt, U. and Jernquist, A., "Simulation of the steady-state and dynamic behaviour of multiple effect evaporator plants", *AIChE Journal*, 17(5), 1080, (1976).
27. Bolmstedt, U., "Simulation of the steady-state and dynamic behaviour of multiple effect evaporator plants, Part: 2 Dynamic Behaviour", *Computer-aided Design*, 9(1), 29-40, (1977).

28. Brenner, H., "The diffusion model of longitudinal mixing in beds of finite length", *Chemical Engineering Science*, 17, 229-243, (1962).
29. Brooks, T.R., Edwards, L.L., Nepate, J.C. and Caldwell, M.R., "Bleach plant closeup and conversion to TCF: a case study using mill data and computer simulation", *Tappi Journal*, 77, 83-92, (1994).
30. Cadet, C., Toure, Y., Gilles, G. and Chabriat, J.P., "Knowledge modelling and non-linear predictive control of evaporators in cane sugar production plants", *Journal of Food Engineering*, 40 (1/2), 59-70, (1999).
31. Chandranupap, P. and Nguyen, K.L., "Effect of pH on kinetics and bleaching efficiency of chlorine dioxide delignification", *Appita Journal*, 53(2), 108-110, (2000).
32. Chapnerkar, V.D, "A kinetic study of the chlorination of unbleached kraft pulp," Ph. D. thesis, University of Florida, Gainesville, Fla. (1961).
33. Crotagino, R.H., Poirier, N.A. and Trinh, D.T., "The principles of pulp washing". *Tappi Journal*, 70, 95-103, (1987).
34. Cullinan (Jr.), H.T., "A unified treatment of brown stock washing on rotary filters", *Tappi Journal*, 69(8), 90-94, (1986).
35. Cullinan, H.T., "The efficiency of pulp washing with regard to lignin removal", *Appita Journal*, 44(2), 91-94, (1991).
36. Dence, C.W. and Reeve, D.W., "Pulp bleaching principles and practice", Tappi Press, Technology park/Atlanta, (1996).
37. Dogan, I. and Guruz, A.G., "Waste minimization in a bleach plant". *Advances in Environmental Research*, 8, 359-369, (2004).
38. Dumont, G., VanFleet, R. and Stewart, G., "A setpoint generation tool for optimal distribution of chemical load between bleaching stages", *Control Systems 2004 Conference* 95-97, (2004).
39. Dutta, B.K. "Heat transfer Principles and Applications", Prentice Hall of India Pvt.Ltd, New Delhi, (2005).
40. Edwards, L., Jamieson, A., Norberg, S.E. and Pettersson, B., "Material balance for brown stock washing, screening, and oxygen bleaching in closed-mill systems", *Tappi Journal*, 59, 83-87, (1976).
41. Edwards, L., Peyron, M. and Minton, M., "Models for cross flow-pulp washing calculation", *Pulp and Paper Canada*, 87(1), T17-T21, (1986).
42. El-Dessouky, H.T., Alatiqi, I., Bingulac, S. and Ettouney, H.M, "Steady-State analysis of the multiple effect evaporation desalination process", *Chem. Eng. Technol.*, 21(5), 437-451, (1998).

43. El-Dessouky, H.T., Ettouney, H.M. and Mandani, F., "Performance of parallel feed multiple effect evaporation system for seawater desalination", *Applied Thermal Engineering*, 20, 1679-1706, (2000).
44. El-Nashar, A.M. and Qamhiyeh, A., "Simulation of the performance of MES evaporators under unsteady state operating conditions", *Desalination*, 79, 65-83, (1990).
45. Eriksson, G. and Gren, U., "Pulp washing: sorption equilibria of metal ions on kraft pulps", *Nordic Pulp and Paper Research Journal*, 11, 164-170, (1996).
46. Fang, C.C. and Zhiming, G., "An analysis of black liquor falling film evaporation", *International Journal of Heat and Mass Transfer*, 47, 1657-1671, (2004).
47. Farooq, S. and Karimi, I.A., "Dispersed plug flow model for steady state laminar flow in a tube with a first order sink at the wall", *Chemical Engineering Science*, 58, 71-80, (2003).
48. Fogelberg, B.C. and Fugleberg, S., "A study of factors influencing the amount of residual alkali in sulphate pulp". *Papri ja Puu - Papper och Tra*, 45, 675-680, (1963).
49. Freedman, B.G., "Bleach plant optimization", *Tappi Journal*, 57 (10), 92-95, (1974).
50. Gallagher, B.J., "Two stage counter current drum washer", United States Patent, No. 6006554, Dec 28, (1999).
51. Germgard, U. and Lindberg, H., "A Mathematical model for (D+C) - prebleaching", *Svensk Papperstidning*, 85(18), R172-R176, (1982).
52. Germgard, U., "Stoichiometry of prebleaching of softwood kraft pulp with chlorinic dioxide and small fractions of chlorine", *Cellulose Chem. Technology*, 48(17), 35-48, (1983).
53. Germgard, U., Teder, A. and Tormund, D., "Mathematical Models for Simulation and Control of Bleaching Stages", *Nordic Pulp Paper Research*, 2(1), 16-22, (1987).
54. Germgard, U. and Karlsson, R.M., "Kinetics and stoichiometry of CE-prebleaching of softwood kraft pulp", *Svensk Papperstidning*, 88(85), R146-R150, (1985).
55. Gonzalez-Bustamantea, J.A., Salaa, J.M., Lopez-Gonzalez, L.M., Miguez, J.L. and Flores, I., "Modelling and dynamic simulation of processes with 'MATLAB'. An application of a natural gas installation in a power plant", *Energy*, 32, 1271-1282, (2007).
56. Grahs, L.E., "Displacement washing of packed beds of cellulose fibers part-1: Mathematical model", *Svensk Papperstidning*, 78(12), 446-450, (1975).
57. Grahs, L.E., "Displacement washing of packed beds of cellulose fibers, part-2: Analysis of laboratory experiments", *Svensk Papperstidning*, 79(3), 84-89, (1976).

58. Grahs, L.E., "Washing of cellulose fibers, analysis of displacement washing operation", PhD. Thesis, Chalmers University of Technology, Goteborg, Sweden, (1974).
59. Gren, U. and Grahs, L.E., "Washing of cellulose fibre beds", *Svensk Papperstidning*, 76(16), 597-601, (1973).
60. Gren, U.B. and Storm, K.H.U., "Displacement washing of packed beds of cellulose fibers", *Pulp and Paper Canada*, 86(9), T261-264, (1985).
61. Gu, Y. and Edwards, L., "Virtual bleach plants, Part 2: Unified  $\text{ClO}_2$  and  $\text{Cl}_2$  bleaching model", *Tappi Journal*, 2(7), 3-8, (2003).
62. Gudmundson, C., "Heat transfer in industrial black liquor evaporator plants, part II", *Svensk Papperstidning*, 75(22), 901-908, (1972).
63. Gullichsen, J. and Fogelholm, C.J., "Chemical Pulping", *Paper Making Science and Technology a series of 19 books*, 6B, B18-20, (2000).
64. Gullichsen, J. and Ostman, H., "Sorption and diffusion phenomena in pulp washing", *Tappi Journal*, 59, 140-143, (1976).
65. Gupta, A., "Mathematical modeling and analysis of pulp washing problems", Ph.D Thesis, Indian Institute of Technology Roorkee, Roorkee, (2001).
66. Han, Y. and Edwards, L., "Optimization of filter washer operation and control", *Tappi Journal*, 71(6), 101-104, (1988).
67. Hanbury, W.T., Proc., IDA World Congress on Desalination and Water Sciences, Abu Dhabi, UAE, 4, 375, (1995).
68. Hartler, N. and Rydin, S., "Washing of pulps, part-I: Equilibrium studies", *Svensk Papperstidning*, 78(10), 367-372, (1975).
69. Haywood, S., "Modeling brown stock washing systems using PCGEMS", *Pulp and Paper Canada*, 96(1), T5-T7, (1995).
70. Hindmarsh, A.C., "ODEPACK, a systemized collection of ode solvers", *Scientific Computing; 1 of IMACS Transactions on Scientific Computing; IMACS*, 55-64, (1982).
71. Hultin, S.O., "Physical Properties of Finish Sulphite Liquors and Black Liquors", *IUPAC-EUCEPA Symposium on Recovery of Pulping Chemicals, Helsinki*, 167-182, (1968).
72. Jain, S., Mortha, G. and Calais, C., "Kinetic models for all chlorine dioxide and extraction stages in full ECF bleaching sequences of softwoods and hardwoods", *Tappi Journal*, Nov, 12-21, (2009).

73. Jain, S., Mortha, G., Benattar, N. and Calais, C., "Critical assessment on modelling of elemental chlorine free bleaching sequence", 14<sup>th</sup> ISWFPC conference proceeding, 172, TAPPSA, Kloof, Durban, South Afrika, 1-17, (2007).
74. Jameel, H., Chang, Hou-min. and Geng, Z.P., "Modifying existing bleach plants for ECF sequences with low chlorine dioxide", TAPPI, Pulping conference, Book-2, 651-661, (1996).
75. Johnson, D.E., "Simulation and analysis improve evaporator control", ISA Journal, 7(7), 46, (1960).
76. Karimi, M., Jahanmiri, A. and Azarmi, M., "Inferential cascade control of multi-effect falling-film evaporator", Food Control, 18, 1036-1042, (2007).
77. Karmeshu., and Lara-Rasano, F., "Modelling data uncertainty in growth forecasts" Applied Mathematical Modelling, 11, 62-68, (1987).
78. Karter, E.M., "The role of physio-chemical rate phenomena in wood pulp chlorination", Ph.D thesis, University of Maine, Orono, Maine, (1968).
79. Kaya, D. and Sarac, I.H., "Mathematical modelling of multiple-effect evaporators and energy economy", Energy, 32, 1536-1542, (2007).
80. Khademi, M.H., Rahimpour, M.R. and Jahanmiri, A., "Simulation and optimization of a six-effect evaporator in a desalination process", Chemical Engineering and Processing, 48, 339-347, (2009).
81. Khanam, S. and Mohanty, B., "Energy reduction schemes for multiple effect evaporator systems", Applied Energy, 87, 1102-1111, (2010).
82. Koko, F.W. and Joye, D.D., "Design calculations for multiple effect evaporators 2. Comparison of linear and non linear method methods", Industrial & Engineering Chemistry Research, 26, 104-107, (1987).
83. Kropholler, H. and Spikins, D., "Principles of control for chemical engineers, Part 3", Chemical Process Engineering, 558-567, (1965).
84. Kukreja, V.K., "Modelling of washing of brown stock on rotary vacuum washer", PhD. Thesis, University of Roorkee, Roorkee, India, (1996).
85. Kukreja, V.K., Ray A.K. and Singh V.P., "Mathematical models for washing and dewatering zones of a rotary vacuum filter", Indian J. Chem. Tech., 5, 276-280, (1998).
86. Kukreja, V.K., Ray A.K., Singh V.P. and Rao N.J., "A mathematical model for pulp washing in different zones of a rotary vacuum filter", Indian Chem. Engr. Section a., 37(3), 113-124, (1995).

87. Kukreja, V.K., Ray, A.K., Singh, V.P. and Rao, N.J., "Some rotary vacuum washer performance parameters and their correlations", TAPPI Proceedings, Pulping conference, 837-847, (1996).
88. Kumana, J.D., "The impact of excess boiling point rise on evaporators and crystallizers", Chemical Engineering Progress, 86(5), 10-14, (1990).
89. Kumar, D., Kumar, V. and Singh, V.P., "Analysis of parametric effect on efficiency of the brown stock washer in Paper Industry using MATLAB", American Institute of Physics Conference Proceeding, 1146, 390-399, (2009b).
90. Kumar, D., Kumar, V. and Singh, V.P., "Mathematical modeling of brown stock washing problems and their numerical solution using MATLAB", Computers and Chemical Engineering, 34, 9-16, (2010b).
91. Kumar, D., Kumar, V. and Singh, V.P., "Mathematical modeling of pulp washing on rotary drums and their numerical solution for various adsorption isotherms", World Journal of Modeling and Simulation, 6 (3), 214-222, (2010a).
92. Kumar, D., Kumar, V. and Singh, V.P., "To study the parametric effects on the performance of brown stock washer in Paper Industry using MATLAB", World Journal of Modeling and Simulation, 5(1), 30-37, (2009a).
93. Kumar, M., "Mathematical modeling of pulp washing systems and solutions", Ph.D Thesis, Indian Institute of Technology Roorkee, Roorkee, India, (2002).
94. Kuo, M.T., "Filter cake washing performance", AIChE Journal, 6(4), 566-568, (1960).
95. Lambert, R.N., Joye, D.D. and Koko, F.W., "Design calculations for multiple effect evaporators I. Linear methods", Industrial & Engineering Chemistry Research, 26, 100-104, (1987).
96. Lapidus, L. and Amundson, N.R., "Mathematics of Adsorption in beds, part-vi: The effect of longitudinal diffusion in ion exchange and chromatographic columns", Journal of Physical Chemistry, 56, 984-988, (1952).
97. Leddy, J.E., "Evaluating the performance of rotary drum vacuum washers", Appita Journal, 51(6), 408-411, (1998).
98. Liao, H.T. and Shiau, C.Y., "Analytical solution to an axial dispersion model for the fixed bed adsorber", AIChE Journal, 46 (6), 1168-1176, (2000).
99. Lindsay, J.D., "Relative flow porosity in fibrous media: Measurements and analysis, including dispersion effects", Tappi Journal, 77(6), 225-239, (1994).
100. Liu, F. and Bhatia, S.K., "Application of Petrov-Galerkin methods to transient boundary value problems in chemical engineering: adsorption with steep gradients in bidisperse solids", Chemical Engineering Science, 56, 3727-3735, (2001).



101. Luthi, O., "Different approaches to modeling displacement ratio", *Pulp and Paper Canada*, 86(7), T201-T205, (1985).
102. Luthi, O., "Equivalent displacement ratio - Evaluating washer efficiency by comparison", *Tappi Journal*, 66(4), 82-84, (1983).
103. Mackinnon, J.C., Crotogino, R.H. and van Heiningen, A. R. P., "A Kinetic Model for the C (D) E/O stages of a Softwood Kraft Bleach Plant", *Journal of Pulp Paper Science*, 19(2), 571-579, (1993).
104. Miranda, V. and Simpson, R., "Modelling and simulation of an industrial multiple effect evaporator: tomato concentrate", *Journal of Food Engineering*, 66, 203-210, (2005).
105. Mohan. C. and Deep Kusum, "Optimization Techniques", Indian Edition: New Age, New Delhi, 2009.
106. Myers, M., Edwards, L. and Haynes, J., "Oxygen delignification systems: synthesizing the optimum design", *Tappi Journal*, 72, 131-135, (1989).
107. Nase, T and Sjoberg, K-E., "Advanced control of a drum washing plant", *Pulp and Paper Canada*, 90(9), T345-T348, (1989).
108. Neretnieks, I., "Analysis of some washing experiment of cooked chips", *Svensk Papperstidning*, 75(20), 819-825, (1972).
109. Neretnieks, I., "Mathematical model for continuous counter current adsorption", *Svensk Papperstidning*, 77(11), 407-411, (1974).
110. Newell, R.B. and Lee, P.L., "Applied process control: A case study", Australia Prentice-Hall, (1989).
111. Ni, Y., Kubes, G.J. and Van Heiningen, A.R.P., "A new mechanism for pulp delignification during chlorination", *Journal of Pulp-Paper Science*, 16(1), J13-J19, (1990).
112. Ni, Y., Kubes, G.J. and van Heiningen, A.R.P., "Chlorination kinetics of kraft pulp", *Journal of Pulp and paper Science*, 21(1), J30-J36, (1995).
113. Ni, Y., Kubes, G.J. and Van Heiningen, A.R.P., "Reduction of formation of organically bound chlorine during ClO<sub>2</sub> bleaching", *Journal of Pulp-Paper Science*, 20(4), J103-J19, (1990).
114. Nierman, H.H., "More on data adjustment on counter current washer efficiency calculations", *Tappi Journal*, 69(8), 85-89, (1986).
115. Norden, H.V. and Pekkanen, M., "General calculation method for stage wise models of pulp washing and other mass and heat transfer", *Symposium on Pulp Washing, Marieham, Finland: CPPA*, 237 (1987).

116. Norden, H.V. and Viljakainen, E., "Calculation of pulp washing by Z method", *Paperi ja Puu*, 65(4), 281-285, (1983).
117. Norden, H.V. and Viljakainen, E., "The calculation of pulp washing processes influenced by adsorption", *Svensk Papperstidning*, 83(2), 50-56, (1980).
118. Norden, H.V., "Analysis of a pulp washing filter". *Kemian Teollisuus*, 23, 344-35, (1966).
119. Norden, H.V., Pohjola, V.H. and Seppanen, R., "Statistical analysis of pulp washing on an industrial rotary drum", *Pulp and Paper Magazine of Canada*, 74(10), 83-91, (1973).
120. Norden, H.V., Viljakainen, E. and Nousiainen, H., "Calculation of the efficiency of the multizone pulp washers using a mass transfer model and superposition principle", *Pulp and Paper Canada*, 83(6), TR21-TR26, (1982).
121. Ohlsson, A. and Rydin, S., "Washing of pulps. Part 2. The sorption of Na, Mg and Ca on kraft pulp", *Svensk Papperstidning*, 78, 549-552, (1975).
122. Oxby, P.W., Sandry, T.D. and Kirkealdy, D.M., "A method for quantifying pulp washer performance that does not use flow rate measurements", *Tappi Journal*, 69(8), 118-119, (1986).
123. Pacheco, C.R.F., Paiva, J.L.de., Reynol, J.R. and Antonio, S., "Operational evaluation of rotary drum vacuum filters for brownstock washing using basic filtration parameters", *Tappi Journal*, 5(3), 15-20, (2006).
124. Parsad, B., Kirkman, A., Jamcel, H., Gratzl, J. and Magnotta, V., "Mill closure with high-kappa pulping and extended oxygen delignification", *Tappi Journal*, 79, 144-152, 1996.
125. Patel, N.L. and Babu, B.V., "Design of single and multiple-effect evaporators: A computer program", *Proceedings of International Symposium & 49th Annual session of IChE (CHEMCON-96)*, GIDC, Ankleshwar (Gujarat), December 18-21, (1996).
126. Pellett, G.L., "Longitudinal dispersion, intra particle diffusion and liquid-phase mass transfer during flow through multi particle systems", *Tappi Journal*, 49(2), 75-82, (1966).
127. Penttila, M., Laxen T. and Virkola, N.E., "Laboratory simulation of Kraft pulp washing", *Pulp and Paper Canada*, 87(1), T31-T37, (1986).
128. Perron, M. and Lebeau, B., "A mathematical model of pulp washing on rotary drums", *Pulp and Paper Canada*, 78(3), TR1-TR5, (1977).
129. Perry, R.H., Chilton, C.H. and Kirkpatrick, S.D., "Chemical Engineers Handbook", 4<sup>th</sup> edition, McGraw Hill, New York, (1963).
130. Perry, R.H., Green, D.W. and Maloney, I.O., "Perry's Chemical Engineers Handbook", 6<sup>th</sup> edition, McGraw Hill, New York, (1984).

131. Phillips, J.R. and Nelson, J., "Diffusion washing system performance", *Pulp and Paper Canada*, 78(6), T123-T127, (1977).
132. Pollard J.F., Broussard M.R., Garisson D.B. and San K.Y., "Process identification neural networks", *Computers Chem. Engineering*, 16(4), 253-270, (1992).
133. Potucek, F. and Pulcer, M., "Displacement of black liquor from pulp bed", *Chem Pap.*, 58 (6), 377-381, (2004).
134. Potucek, F. and Pulcer, M., "Displacement washing of pulp with urea solutions", *Chem Pap.*, 60 (5), 365-370, (2006).
135. Potucek, F. and Skotnicova, I., "Influence of wash liquid properties on the efficiency of pulp washing", *Chem. Pap.*, 56 (6), 369-373, (2002).
136. Potucek, F., "Chemical Engineering view of pulp washes", *Papir a celuloza*, 60(4), 114-117, (2005).
137. Potucek, F., "Displacement of washing of pulp I. Dispersion model for non imaginary flow", *Papir a celuloza*, 56(1), 8-11, (2001a).
138. Potucek, F., "Displacement of washing of pulp II. Analysis of laboratory data", *Papir a celuloza*, 56(2), 49-53, (2001b).
139. Potucek, F., "Miscible liquid flow through a pulp fiber bed", *Cellulose Chem. and Technology*, 37(5-6), 391-404, (2003).
140. Potucek, F., "Washing of pulp fiber bed", *Collect. Czech. Chem. Commun*, 62, 626-644, (1997).
141. Prasad, R.C., "Analytical solution for a double-pipe heat exchanger with a non-adiabatic condition at the outer surface", *Int. Comm. Heat Mass Transf.*, 14, 665-672, (1987).
142. Prasad, R.C., Karmeshu., and Bharadwaj, K.K., "Stochastic modelling of heat exchanger response to data uncertainties, *Applied Mathematical Modelling*, 26, 715-726, (2002).
143. Pugliese, S.C. and McDonough, T.J., "Kraft Pulp Chlorination: A New Mechanistic Description", *Tappi Journal*, 71(3), 159-167, (1989).
144. Rao, N.J. and Kumar, R., "Energy conservation approaches in a paper mill with special reference to the evaporator plant", *Proceedings of the IPPTA international seminar on energy conservation in pulp and paper industry*, 58-70, (1985).
145. Ray, A. K., "Lecture Notes in Human Resources Development Program for the Phonix's Paper Mill, Thailand, (1995).
146. Ray, A.K. and Sharma, N.K., "Simulation of multi-effect evaporator for paper mill-effect of flash and product utilization for mixed feeds sequences", *IPPTA*, 16(4), 55-64, (2004).

147. Ray, A.K. and Singh, P., "Simulation of multiple effect evaporator for black liquor concentration", *IPPTA*, 12(3), 35-45, (2000).
148. Ray, A.K., Sharma, N.K. and Singh, P., "Estimation of energy gains through modelling and simulation of multiple effect evaporator system in a paper mill", *IPPTA*, 16(2), 35-45, (2004).
149. Regestad, S.O., "Fundamental Studies of Black Liquor Combustion", *Svensk Papperstidning*, 54(2), 36, (1951).
150. Russel, P and Freiberg, J., "Modelling the chlorination stage in a pulp bleach plant" *Tappi*, 6, 151-156, (1989).
151. Saltin, G. and Edwards, L., "A New Kinetic Model of Chlorine and Chlorine Dioxide Bleaching", *Tappi Pulping Conference*, Atlanta, GA, Nov. 1-3, 951-962, (1993).
152. Sherman, W.R., "The movement of a soluble material during the washing of a bed of packed solids", *AIChE Journal*, 10(6), 855-860, (1964).
153. Singh, S.V., Goyal, R.P. and Guha, S.R.D., "Kinetics of each stage of the bleaching sequence CEHD", *Indian Pulp and Paper*, 1, 25-34, (1975).
154. Singh, V.P., Kumar, V. and Kumar, D., "Numerical solution of diffusion model of brown stock washing beds of finite length using MATLAB". *Proceeding of "Second UKSIM European Symposium on Computer Modeling and Simulation"*, IEEE Digital Library, 295-300, (2008).
155. Smith, R.J. and Duffy, G.G., "Pulp washing by dilution-thickening without remixing", *Appita Journal*, 44(4), 265-269, (1991).
156. Smook, G.A., "Hand book for pulp and paper technologists", Angus wilde publication, fifth printing, (2001).
157. Sridhar, P., "Design of affinity membrane bio separations", *Chem. Eng. Tech.*, 19, 398-404, (1996a).
158. Sridhar, P., "Implementation of one point orthogonal collocation method to an affinity packed bed model", *Indian chem. Engr. Section a*, 41(1), 39-46, (1999).
159. Sridhar, P., "Modelling of affinity separation by batch and fixed bed adsorption-A comparative study", *Chem. Eng. Tech.*, 19, 357-363, (1996b).
160. Sridhar, P., Sastri, N.V.S., Modak, J.M. and Mukherjee, A.K., "Mathematical simulation of bio separation in an affinity packed column", *Chem. Eng. Tech.*, 17, 422-429, (1994).
161. Stefanov, Z.I. and Hoo, K.A., "A distributed parameter model of black liquor falling-film evaporators. 1. Modelling of a single plant", *Ind. Eng. Chem. Res.*, 42, 1925-1937, (2003).

162. Stefanov, Z.I. and Hoo, K.A., "Distributed parameter model of black liquor falling-film evaporators. 2. Modelling of a multiple-effect evaporator plant", *Ind. Eng. Chem. Res.*, 43, 8117-8132, (2004).
163. Svandova, Z., Katora, M., Markos, J. and Jelemensky, L., "Dynamic behaviour of a CSTR with reactive distillation", *Chemical Engineering Journal*, 119, 113-120, (2006).
164. Szukiewicz, M.K., "New approximate model for diffusion and reaction in a porous catalyst", *AIChE Journal*, 46(3), 661-665, (2000).
165. Tervola, P. and Rasanen, E., "A cake washing model with an overall cation transfer in kraft pulp washing", *Chemical Engineering Science*, 60, 6899-6908, (2005).
166. Tervola, P., "Fourier series solution for multistage countercurrent cake washing and segregated wash effluent circulation", *Chemical Engineering Science*, 61, 3268-3277, (2006).
167. Tessier, P. and Savoie, M., "Chlorine dioxide delignification kinetics and Eop extraction of softwood kraft pulp", *The Canadian Journal of Chemical Engineering*, 75(2), 23-30, (1997).
168. Tomiak, A., "Predict performance of belt-filter washing", *Chemical Engineering*, 86, 143-146, (1979a).
169. Tomiak, A., "Predicting performance of countercurrent filtration washing systems", *Filtration and Separation*, 16, 354-360, (1979b).
170. Tomiak, A., "Theoretical recoveries in filter cake reslurrying and washing", *AIChE Journal*, 19, 76-84, (1973).
171. Tonelli, S., Romagnoli, J.A. and Porras, J.A., "Computer package for transient analysis of industrial multiple effect evaporators", *Journal of Food Engineering*, 12, 267-281, (1990).
172. Turner, P.A. and Livingstone L., "A method to monitor cleanliness of washed pulp directly", *Pulp and Paper Canada*, 96(6), T218- T222, (1995).
173. Turner, P.A., Roche, A.A., McDonald J.D. and van Heiningen, A.R.P., "Dynamic behavior of a brownstock washing system", *Pulp and Paper Canada*, 94(9), T263-T268, (1993).
174. Ugrin, E. and Urbicain, M.J., "Design and Simulation of Multi-effect Evaporators", *Heat Transfer Engineering*, 20(4), 38-44, (1999).
175. Veeramani, H. and Koorse, G.M., "Engineering properties of black liquor in process design and development of kraft chemical recovery units", *Indian Pulp and Paper*, Oct-Nov. (1975).
176. Viljakainen, E., "Mass transfer models and multizone washing efficiency calculations", *Pulp and Paper Canada*, 86(10), T301-305, (1985).

177. Wakeman, R.J. and Tarleton, E.S., "Filtration-Equipment Selection, Modelling and Process Simulation", Elsevier Advanced Technology, Oxford, (1999).
178. Wang, R.X., "Dynamic simulation of brown stock washers and bleach plants", Master's Thesis, University of British Columbia, Vancouver, BC, (1993).
179. Winchester, J.A. and Marsh, C., "Dynamics and control of falling film Evaporators with mechanical Vapor recompression", Institution of Chemical Engineers Trans IChemE, 77, Part A, 357-371, (1999).
180. Wong, B.M. and Reeve, D.W., "Diffusion in fiber beds", Journal of Pulp and Paper Science, 16(2), 172-176, (1990).
181. Yoon, B.H., Wang, L.J. and Lee, M.K., "Empirical modeling of chlorine dioxide delignification of oxygen-delignified hardwood kraft pulp", J. Wood Sci., 50, 524-529, (2004).